# The Legacy of *Planck*

*Carlo Burigana*
*INAF-IASF Bologna*
*burigana@iasfbo.inaf.it*

**On behalf of the**
***Planck* Collaboration**
**& with contributions from**
**the CORE Collaboration**
**for related aspects**

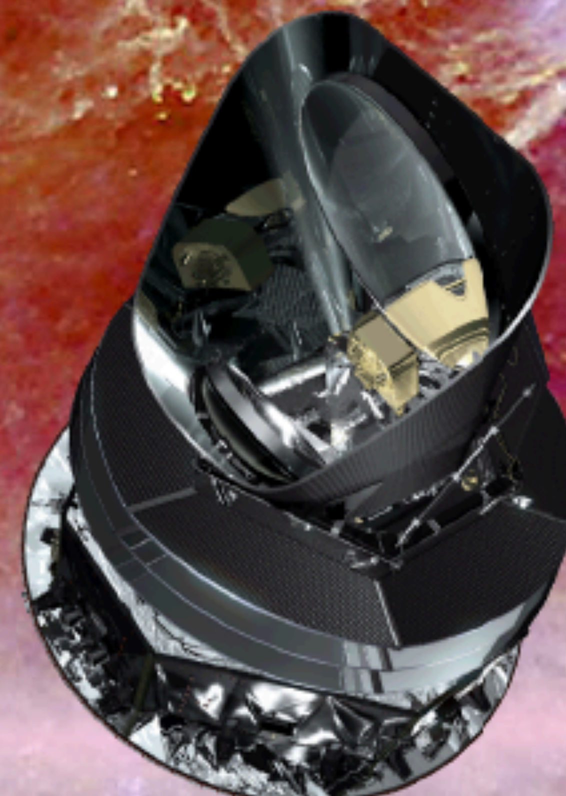

**International School of Physics "Enrico Fermi"**
**Varenna, Lake Como, Italy - Course 200**
**Gravitational Waves and Cosmology**
**3 - 12 July 2017**

# Outline

- Brief introduction to CMB
- *Planck* mission main aspects and products
- Extragalactic astrophysics … and using them for cosmology
- Methods - an example: sky pixelization
- Methods: separating CMB from foregrounds
- CMB maps and power spectrum from *Planck*
- Cosmological parameters & DM, DE, neutrinos …
- Polarization with *Planck* & B-modes
- Microwave sky complexity
- Future of CMB anisotropy missions
- Future of CMB spectrum

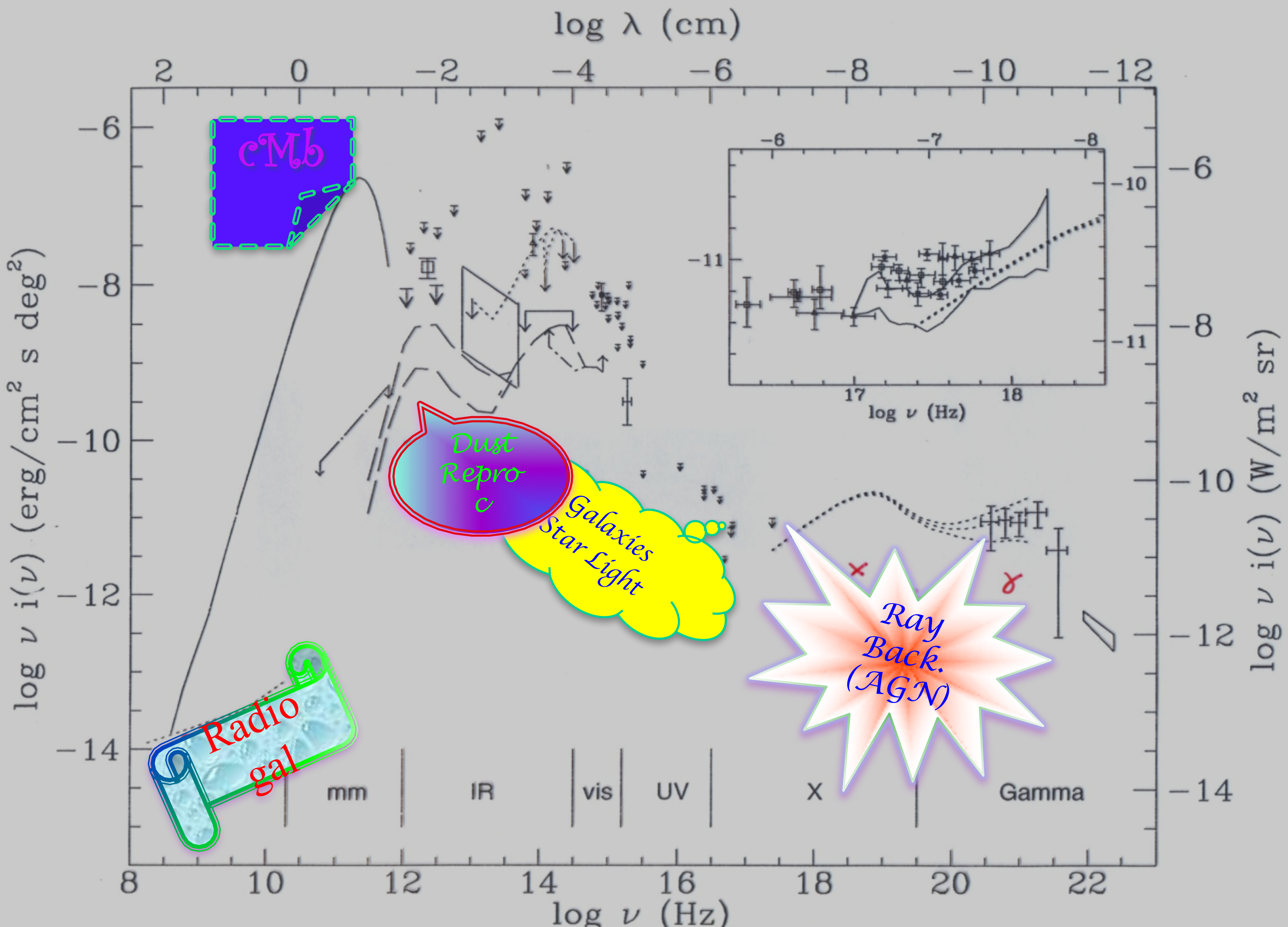


Adapted from de Zotti & Burigana 1992, Highlights of Astronomy, 9, 265

**Multifrequency view of cosmic backgrounds**

# Cosmic Microwave Background Radiation

## *Anisotropies*

- $\frac{\Delta T}{T}(\hat{\mathbf{n}})$ → Map of CMB anisotropies; Angular power spectrum

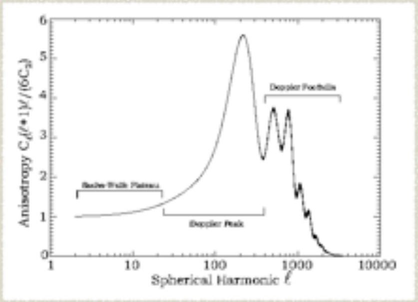


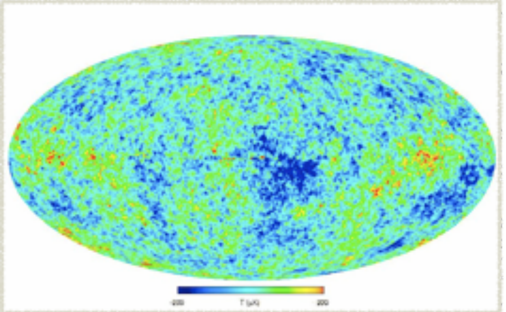

## Polarization

- $P^2 = Q^2 + U^2$ →

**Main contribution:**

**Thomson Scattering of radiation with quadrupole anisotropy generates linear polarization**

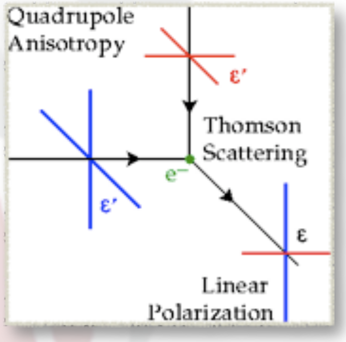


## Spectrum

- **Photon distribution function** →

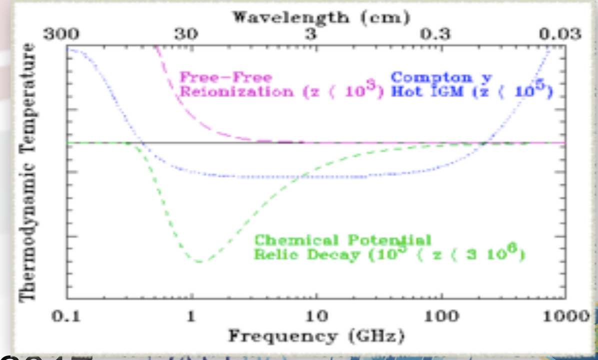

# CMB space mission experiments overview

1965 — Penzias and Wilson

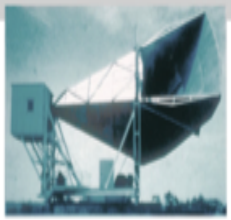

1992 — COBE

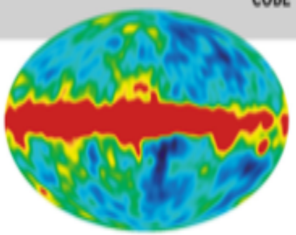

2003 — WMAP

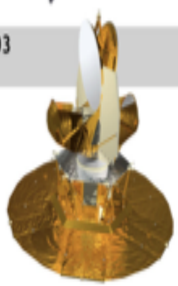

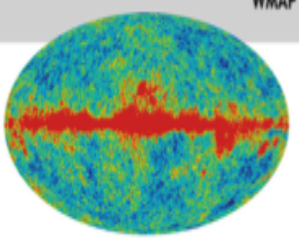

2009 — Planck

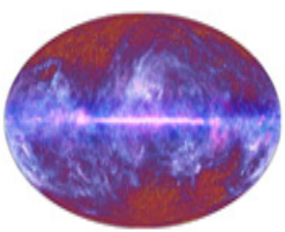

**The oldest light or the first light of the Universe**

Discovered the remnant afterglow from the **Big Bang**.
→ **2.7 K**

**Blackbody radiation,**
Discovered the patterns (**anisotropy**) in the afterglow.
→ **angular scale ~ 7°** at a level $\Delta T/T$ of $10^{-5}$

(Wilkinson Microwave Anisotropy Probe):
→ **angular scale ~ 15'**

→ **angular scale ~ 5',**
$\Delta T/T \sim 2 \times 10^{-6}$, 30~857 GHz

# Evolution of CMB space missions since discovery

The scientific results that we present today are a product of the Planck Collaboration, including individuals from more than 100 scientific institutes in Europe, the USA and Canada

Planck is a project of the European Space Agency, with instruments provided by two scientific Consortia funded by ESA member states (in particular the lead countries: France and Italy) with contributions from NASA (USA), and telescope reflectors provided in a collaboration between ESA and a scientific Consortium led and funded by Denmark.

LFI PI N. Mandolesi, HFI PI J.L. Puget

# The ESA mission to map the Cosmic Microwave Background

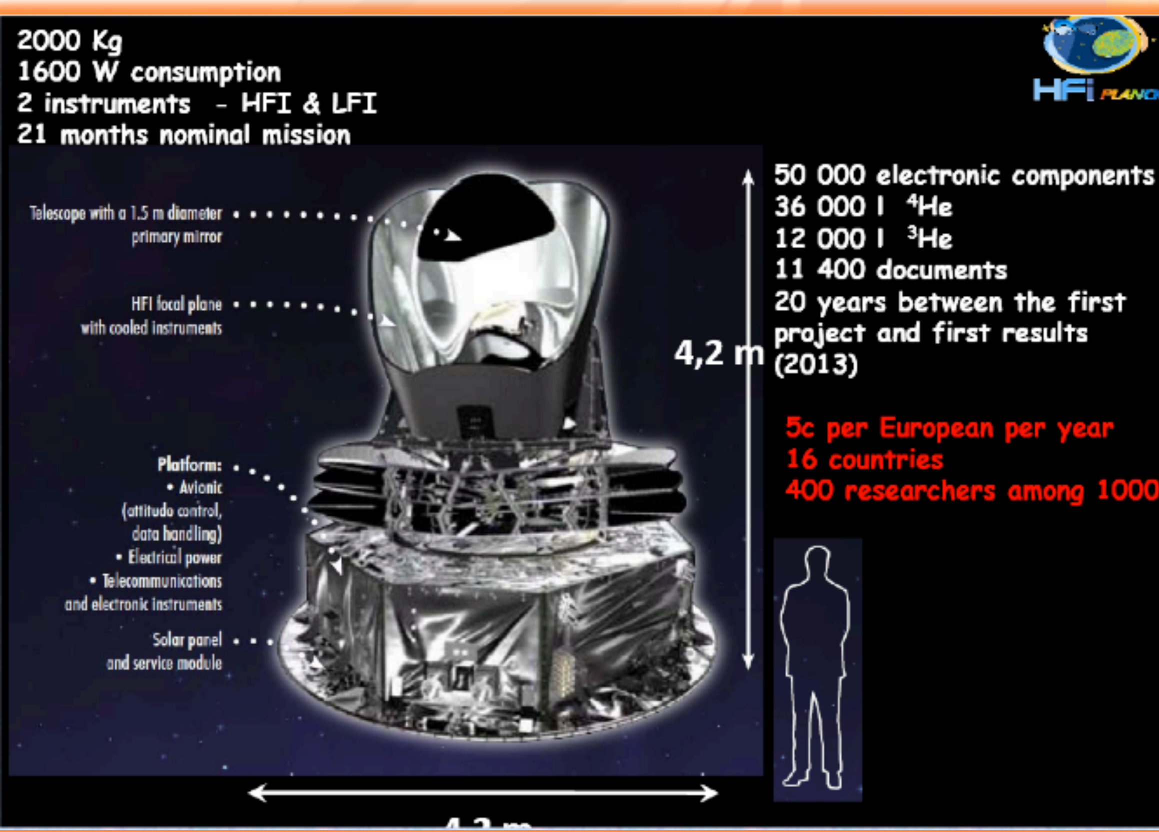


To image the temperature and polarisation anisotropies of the Cosmic Microwave Background (CMB), over the whole sky, with an uncertainty on the temperature limited by "natural causes" (foreground fluctuations, cosmic variance) rather than intrinsic or systematic detector noises, and an angular r

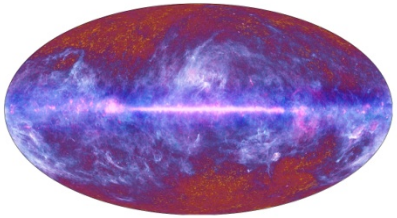

arcmin.

*Planck* is composed by two instruments:

- ❖The Low Frequency Instrument (LFI) based on EMT receivers and
- ❖The High Frequency Instrument (HFI) based on bolometers

@ focal plane of a1.5 m Gregorian telescope


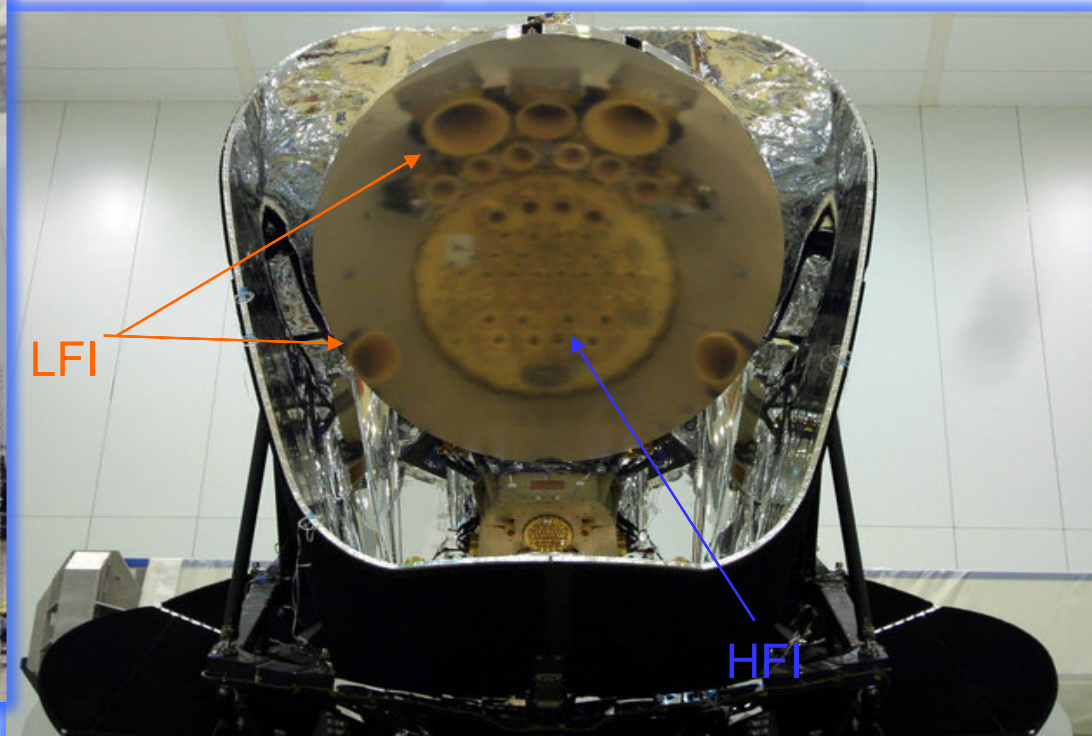

*PLANCK* HAS BEEN SUCCESSFULLY LAUNCHED ON THE 14 OF MAY 2009, TOGETHER WITH HERSCHEL, ON ARIANE 5 VECTOR

Is acquired data since the 15 August 2009,

In January 2012 HFI was switched off and since then *Planck* was in LFI only mode

*Planck* switch-off: 23 October 2013


| Survey | Instrument | Beginning | End | Coverage[a] |
|---|---|---|---|---|
| 1 . . . . . . . . . . | LFI & HFI | 12 August 2009 (14:16:51 UT) | 2 February 2010 (20:51:04 UT) | 93.1 % |
| 2 . . . . . . . . . . | LFI & HFI | 2 February 2010 (20:54:43) | 12 August 2010 (19:27:20 UT) | 93.1 % |
| 3[b] . . . . . . . . . | LFI & HFI | 12 August 2010 (19:30:44) | 8 February 2011 (20:55:55 UT) | 93.1 % |
| 4 . . . . . . . . . . | LFI & HFI | 8 February 2011 (20:59:10) | 29 July 2011 (17:13:32) | 86.6 % |
| 5[c] . . . . . . . . . | LFI & HFI | 29 July 2011 (18:04:49) | 1 February 2012 (05:26:29 UT) | 80.1 % |
| 6 . . . . . . . . . . | LFI | 14 January 2012 | July 2012 | |
| 7 . . . . . . . . . . | LFI | July 2012 | Jan 2013 | |
| 8 . . . . . . . . . . | LFI | Jan 2013 | August 2013 | |

[a] Fraction of the sky covered by all frequencies
[b] End of Nominal period = 28 November 2010 (12:00:53 UT)
[c] End of data acquisition with HFI = 13 January 2012 (14:54:07 UT)

# *Planck* Scanning Strategy

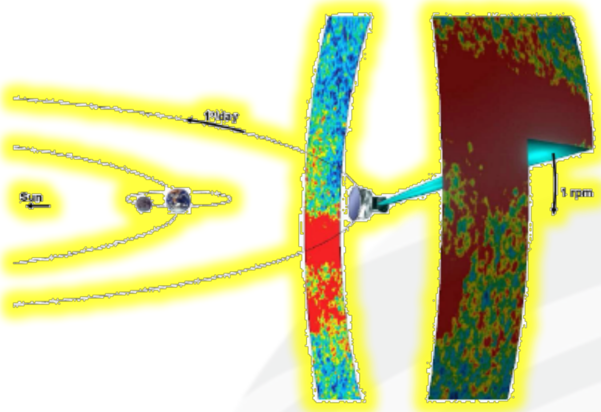


Planck is a survey mission

About 6 months are needed to cover ~95% of the sky.

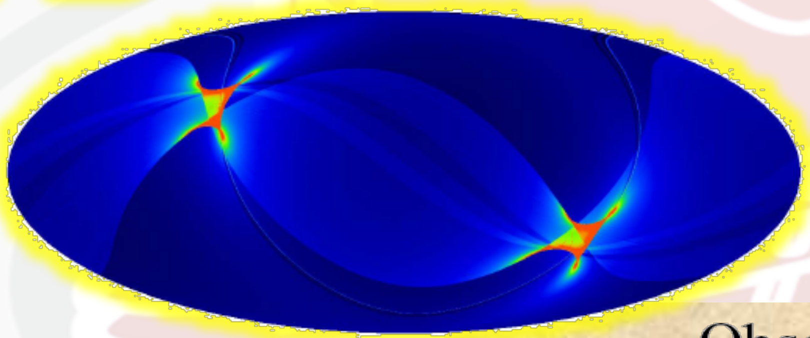

**Survey ≥ 5:**
**cycloid phase shifted by 90 deg.**

**During LFI only phase (surveys 6-8): scanning strategy combines standard mode with deep annuli on calibration sources to improve the quality of calibration and systematic effect control.**

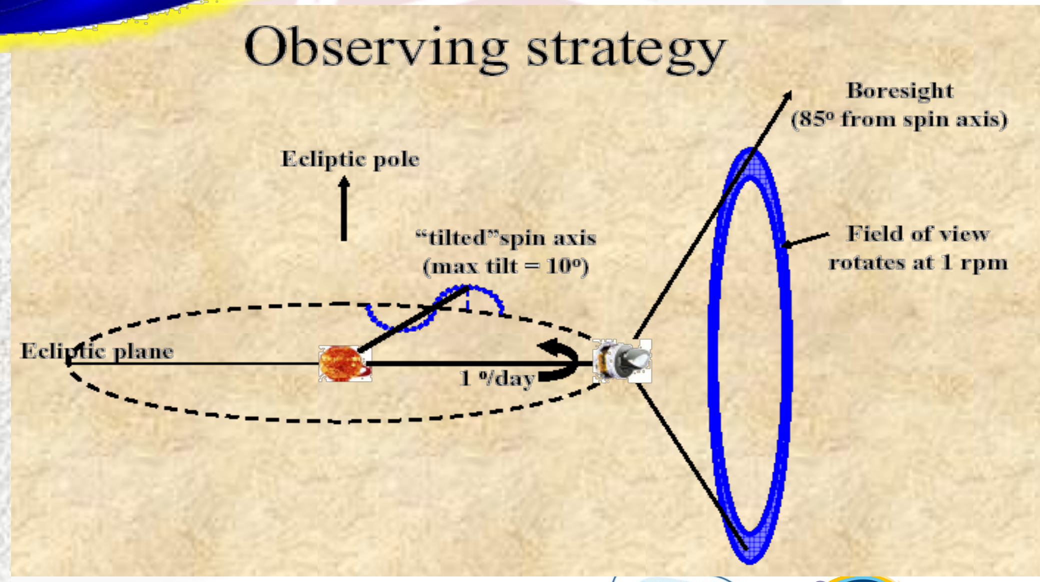

# *Planck* final performance in temperature & polarization

Average sensitivity, δT/T, per FWHM$^2$ resolution element (FWHM in arcmin) and white noise (per frequency channel for LFI and per detector for HFI) in 1 sec of integration (NET, in μK ·√s) in CMB temperature units. Acronyms: DT = detector technology, N of R (or B) = number of radiometers (or bolometers), EB = effective bandwidth (in GHz). At 100 GHz all bolometers are polarized, thus the temperature measure is derived combining data from polarized bolometers.

| HFI | $\simeq$ 29.5 months | of integration | ($\simeq$ 5 surveys) | |
|---|---|---|---|---|
| Frequency (GHz) | 100 | 143 | 217 | 353 |
| FWHM in $T$ ($P$) | 9.6 (9.6) | 7.1 (6.9) | 4.6 (4.6) | 4.7 (4.6) |
| N of B in $T$ ($P$) | (8) | 4 (8) | 4 (8) | 4 (8) |
| EB in $T$ ($P$) | 33 (33) | 43 (46) | 72 (63) | 99 (102) |
| NET in $T$ ($P$) | 100 (100) | 62 (82) | 91 (132) | 277 (404) |
| $\delta$T/T [$\mu$K/K] in $T$ ($P$) | 2.04 (3.31) | 1.56 (2.83) | 3.31 (6.24) | 13.7 (26.2) |

| HFI | | |
|---|---|---|
| Frequency (GHz) | 545 | 857 |
| FWHM in $T$ | 4.7 | 4.3 |
| N of B in $T$ | 4 | 4 |
| EB in $T$ | 169 | 257 |
| NET in $T$ | 2000 | 91000 |
| $\delta$T/T [$\mu$K/K] in $T$ | 103 | 4134 |

| LFI | $\simeq$ 29.5 + 21 months | of integration | ($\simeq$ 8 surveys) |
|---|---|---|---|
| Frequency (GHz) | 30 | 44 | 70 |
| InP DT | MIC | MIC | MMIC |
| FWHM | 33.34 | 26.81 | 13.03 |
| N of R (or feeds) | 4 (2) | 6 (3) | 12 (6) |
| EB | 6 | 8.8 | 14 |
| NET | 159 | 197 | 158 |
| $\delta$T/T [$\mu$K/K] (in $T$) | 1.85 | 2.85 | 4.69 |
| $\delta$T/T [$\mu$K/K] (in $P$) | 2.61 | 4.02 | 6.64 |

# HOW TO EXTRACT INFORMATION FROM THE MEASUREMENTS

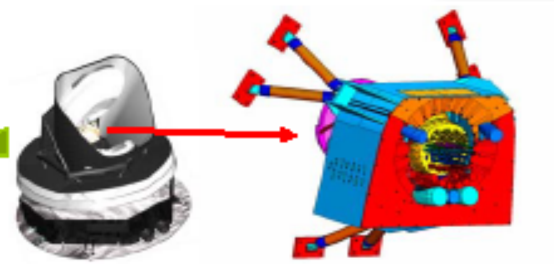

Acquiring and processing time-ordered information

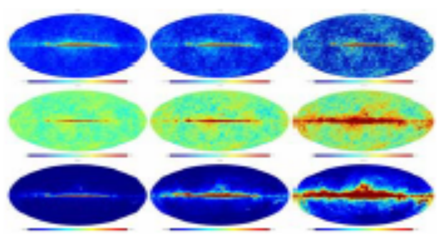

Converting time-ordered data to maps of the sky emission at many frequencies

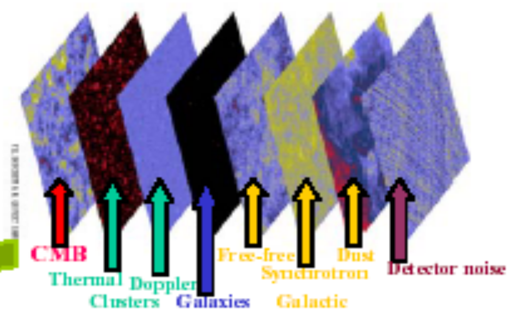


Converting frequency maps to component maps, e.g. the Cosmic Microwave Background

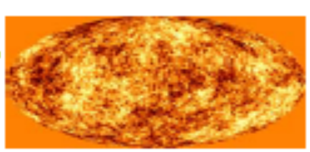

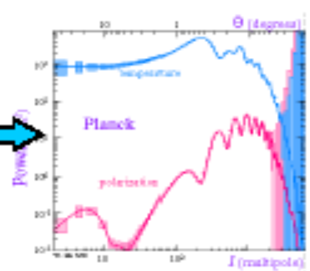


Estimating the CMB angular power spectrum and cosmological parameters

PLANCK

esa ASTROPHYSICS

# Classical ZLE:

**Separated in "time domain", for now simply exploiting differences in surveys**

## Zodiacal emission

...measured by IRAS (it's the white 'S', not the Galaxy)

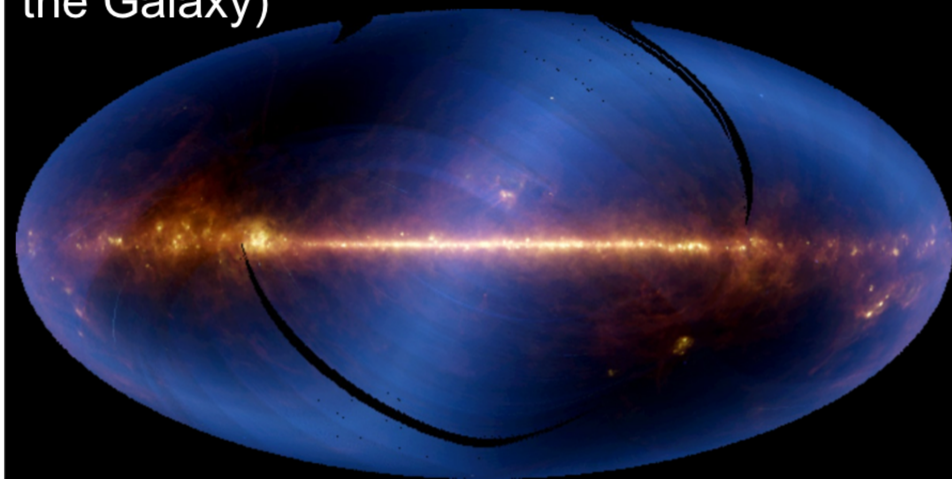

http://coolcosmos.ipac.caltech.edu/image_galleries/IRAS/allsky.html

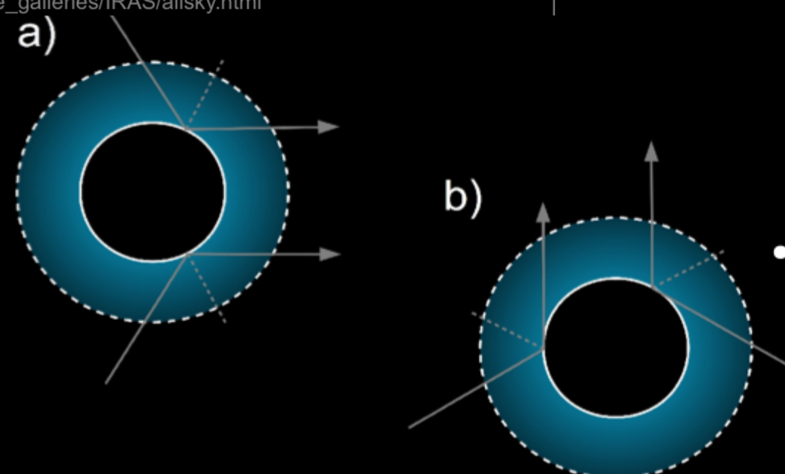


- In successive surveys we observe similar, but different total columns of interplanetary (local) dust (IPD)
- Making differences of successive surveys allows us to remove "contamination", but still be sensitive to the IPD

# The Diffuse Cloud

- This is what we usually think about when we talk about the IDP
- It varies with our “cycloid” scanning strategy
- The difference is about what we will use to detect it.
- Top: Survey 1;
  Middle: Survey 2;
  Bottom: Survey Difference
  (Survey 2 minus Survey 1)

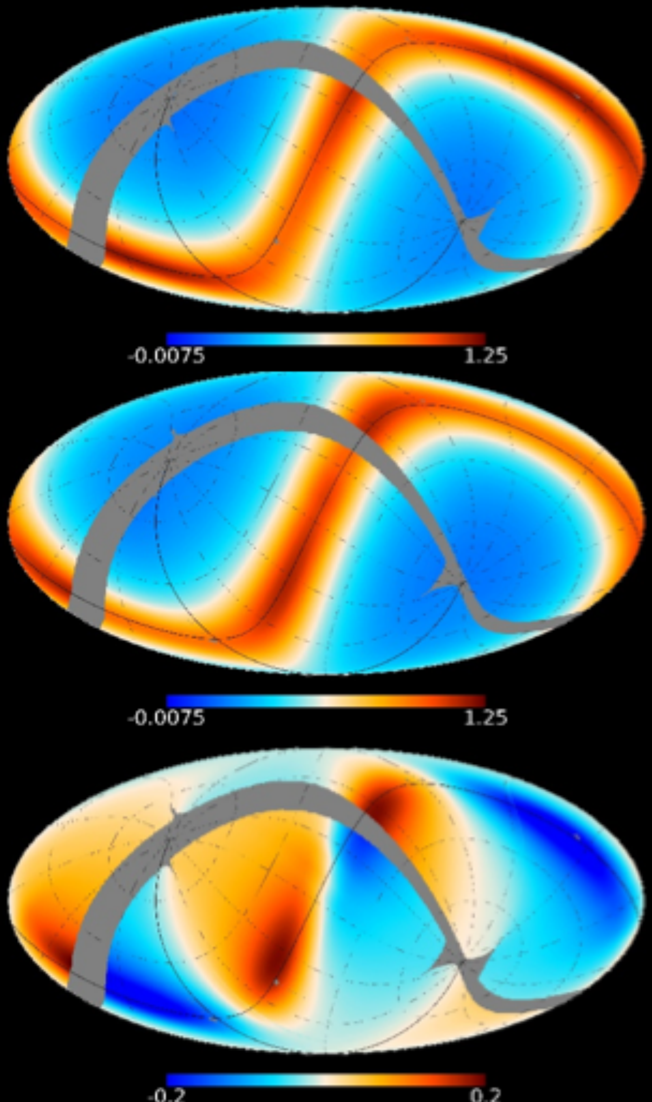

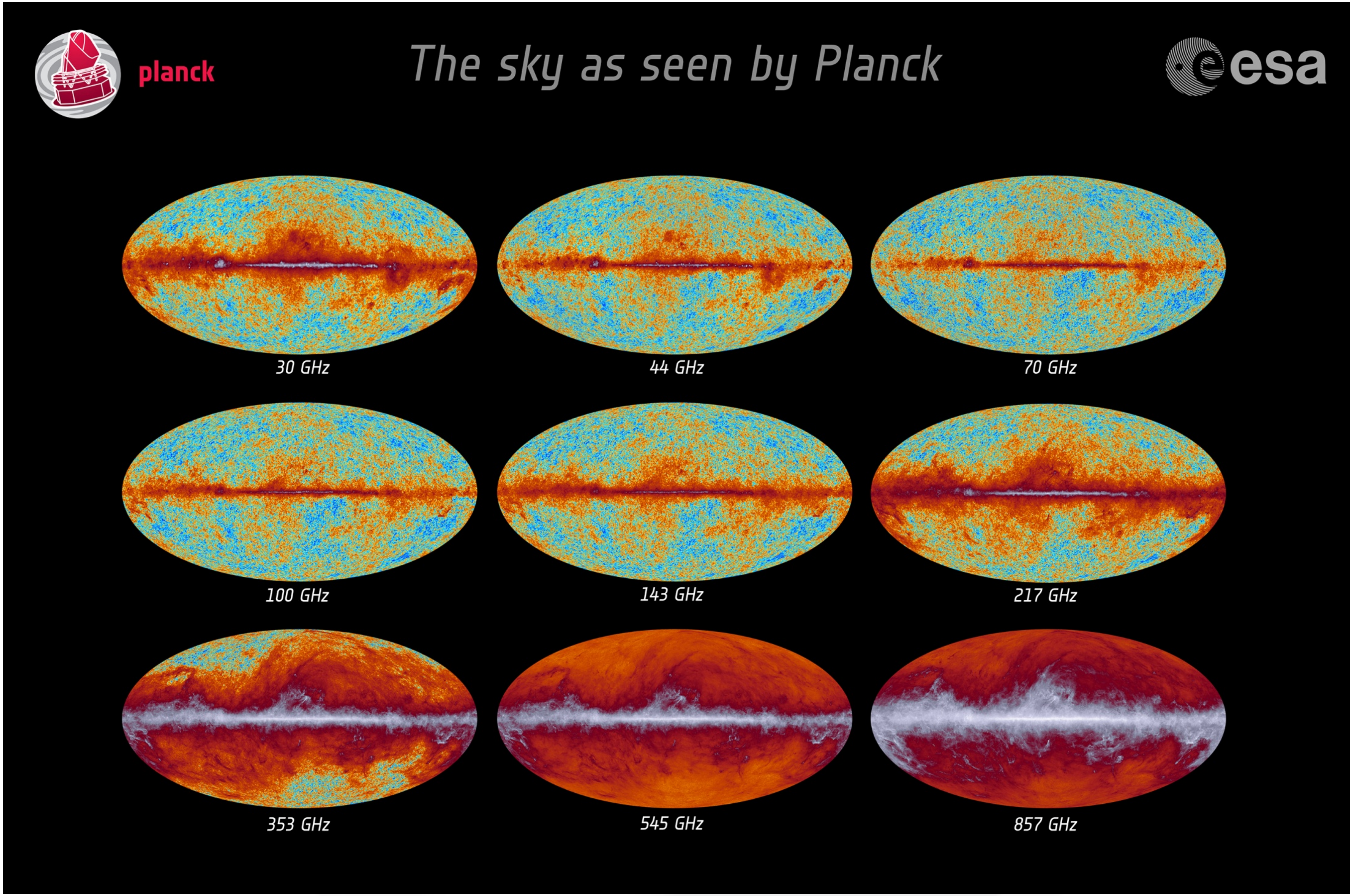


**Frequency maps! Real and fundamental measure / product of *Planck***

# *Planck* polarization frequency maps: synchrotron & dust components

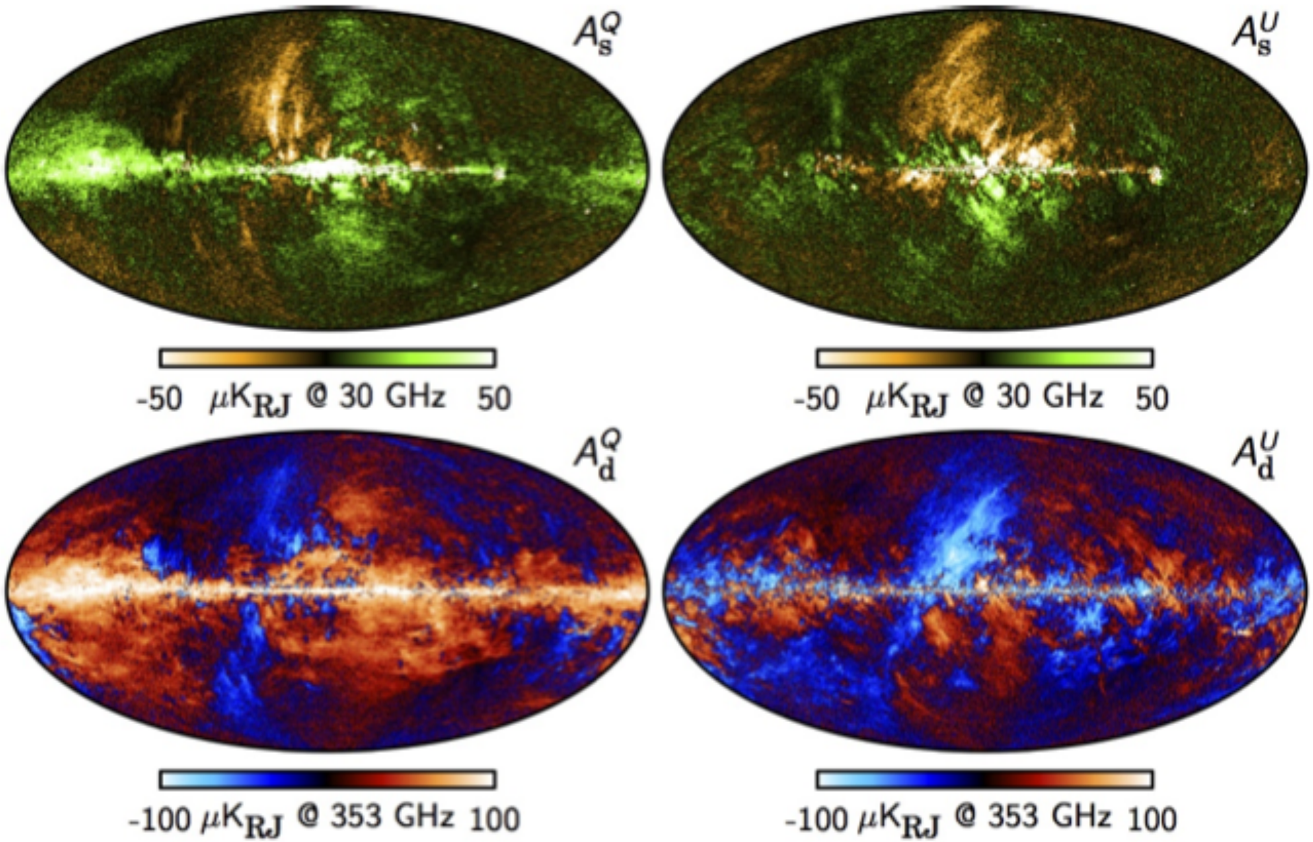


**Fig. 15.** Maximum posterior amplitude polarization maps derived from the *Planck* observations between 30 and 353 GHz (Planck Collaboration X 2015). The left and right columns show the Stokes $Q$ and $U$ parameters, respectively. Rows show, from top to bottom: CMB; synchrotron polarization at 30 GHz; and thermal dust polarization at 353 GHz. The CMB map has been highpass-filtered with a cosine-apodized filter between $\ell = 20$ and 40, and the Galactic plane (defined by the 17 % CPM83 mask) has been replaced with a constrained Gaussian realization (Planck Collaboration IX 2015).

# Planck 2015 data release

- Timelines for each detector at 30, 44, 70, 353, 545 and 858 GHz and for the unpolarized bolometers at 100, 143, 217 GHz
- Maps of the sky at 9 freqs in temp, and at 30, 44, 70, 353 GHz in pol
- Four high-res maps of the CMB sky in T (Commander, NILC, SEVEM, SMICA)
- Four high-pass filtered maps of the CMB sky in pol
- A low-res CMB T map (Commander)
- Maps of thermal dust, CIB, CO, synchrotron, free-free, spinning dust temperature emission
- Maps of synchrotron and dust polarized emission
- Map of the estimated lensing potential
- Map of the SZ Compton parameter
- MC chains used for cosmological parameter estimation
- Planck catalogue of compact sources
- Planck catalogue of SZ sources
- Planck catalogue of galactic cold clumps

# *Planck* Products → PLA

http://pla.esac.esa.int/pla/

## PLANCK LEGACY ARCHIVE CONTENTS

**MAPS**
Search through all maps stored in the Planck Legacy Archive.

**CATALOGUES**
Perform queries on all catalogues in the Planck Legacy Archive.

**COSMOLOGY**
Browse cosmology products of the Planck Legacy Archive.

**TIMELINES**
Perform coordinate-based and time-based queries on all Planck time-ordered data.

**INSTRUMENT MODELS & SOFTWARE**
Browse instrument models and software of the Planck Legacy Archive.

**OPERATIONAL DATA**
Spacecraft and instrument house-keeping data acquired during Planck operations.

## USEFUL INFORMATION

**EXPLANATORY SUPPLEMENT**
Detailed information on all Planck Legacy Archive products.

**EXTERNAL DATA & SOFTWARE**
Links to external data related to Planck products.

**PLANCK COLLABORATION PAPERS**
List of scientific publications by the Planck consortium.

**USE OF PLANCK DATA**
How to acknowledge the use of Planck products.

**PLANCK LEGACY ARCHIVE UPDATE HISTORY**
Changes to Planck Legacy Archive products and functionalities.

**PLANCK SCIENCE TEAM HOME**
General information on Planck directed to the astronomical community.

**PR2 - 2015 MAPS**

Frequency maps | CMB maps | Foreground maps | Ancillary maps

Beams | ES

| Frequency maps | 30GHz NS1024 | 44GHz NS1024 | 70GHz NS1024 | 70GHz NS2048 | 100GHz NS2048 | 143GHz NS2048 | 217GHz NS2048 | 353GHz NS2048 | 545GHz NS2048 | 857GHz NS2048 |
|---|---|---|---|---|---|---|---|---|---|---|
| FULL | (480 MB) | (480 MB) | (480 MB) | (1.9 GB) | (576 MB) | (576 MB) | (576 MB) | (1.9 GB) | (576 MB) | (576 MB) |

# *Planck* Products → PLA

PR2 - 2015 MAPS

Frequency maps | **CMB maps** | Foreground maps | Ancillary maps

→ ES

| METHOD | DESCRIPTION |
|---|---|
| SMICA | *Maps of the Cosmic Microwave Background fluctuations built with the Spectral-Matching Independent Component Analysis method* |
| COMMANDER | *Maps of the Cosmic Microwave Background fluctuations made with the Commander software* |
| SEVEM | *Maps of the Cosmic Microwave Background fluctuations built with the Spectral Estimation Via Expectation Maximisation method* |
| NILC | *Maps of the Cosmic Microwave Background fluctuations built with the Needlet Internal Linear Combination method* |
| COMMON | *Masks of the common field used for CMB analysis* |

Frequency maps | CMB maps | **Foreground maps** | Ancillary maps

→ ES

| COMPONENT | DESCRIPTION |
|---|---|
| AME | *Maps of the foreground Anomalous Microwave Emission* |
| CMB | *Map of the Cosmic Microwave Background fluctuations from foreground analysis* |
| CO | *Maps of the carbon monoxide emission* |
| DUST | *Maps of the diffuse thermal dust emission* |
| FREEFREE | *Maps of the foreground free-free emission* |
| SYNCHROTRON | *Maps of the foreground synchrotron emission* |
| SZ | *Maps of the SZ contamination* |
| XLINE | *Map of line emissions common to the WMAP W-band (94 GHz) and the HFI 100 GHz band (including the HCN line)* |

# *PCCS: Characteristics*

30 GHz
143 GHz
857 GHz

Distribution of the sources from the PCCS2.

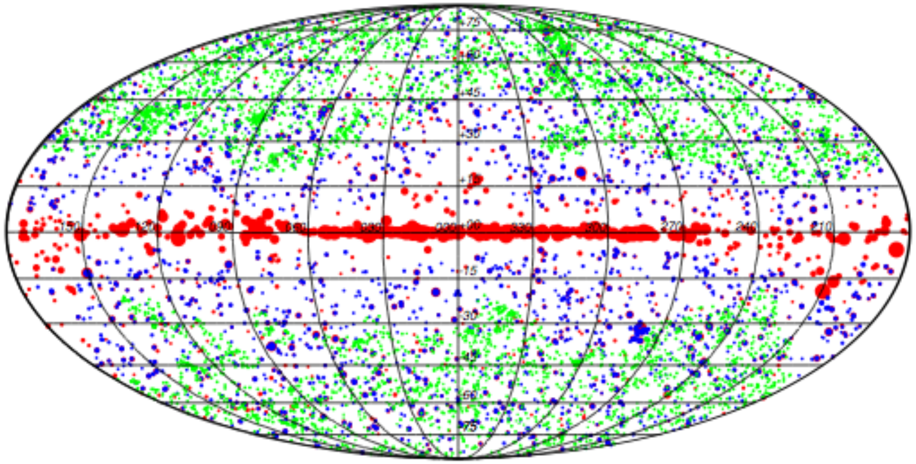

Distribution of the sources in the 143 and 857 PCCS2E.

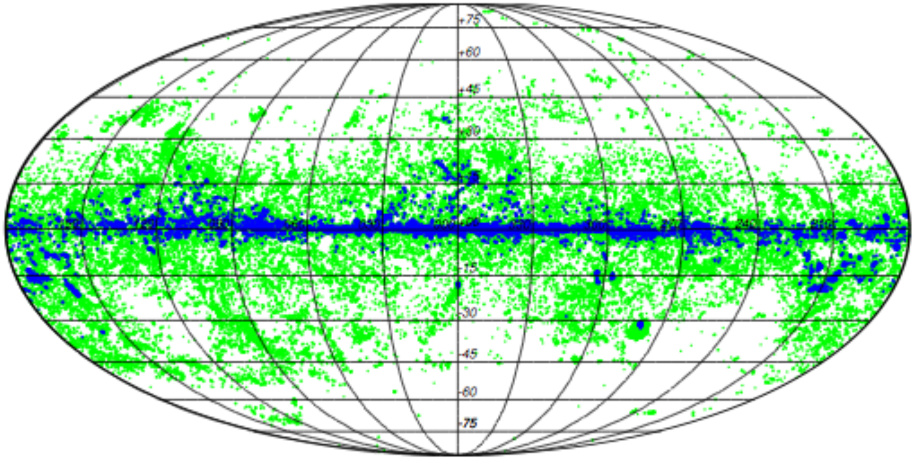

Many of the *Planck* PCCS sources can be associated with stars with dust shells, stellar cores, radio galaxies, blazars, infrared luminous galaxies and Galactic interstellar medium features.
As expected, the high frequency channels (545 and 857 GHz) are dominated (> 90 %) by dusty galaxies and the low frequency ones are dominated (> 95 %) by synchrotron sources.

# Galaxies and AGN evolution: *Planck* observations → models

Microwave/mm/sub-mm surveys are crucial because in these bands we can study:

- Transition between radio (synchrotron/free-free) and dust emission occurrs
- break ($\nu_M$) of emission of jets related to compactness ($r_M \approx$pc) of emission region:

FSRQs: $\nu_M \cong$ 10–100 GHz – BL Lacs : $\nu_M$>100 GHz

→ Multifrequency studies can not miss information in this range

**The *Planck* Catalogue (PCCS)**: the most complete all-sky catalog in the microwaves

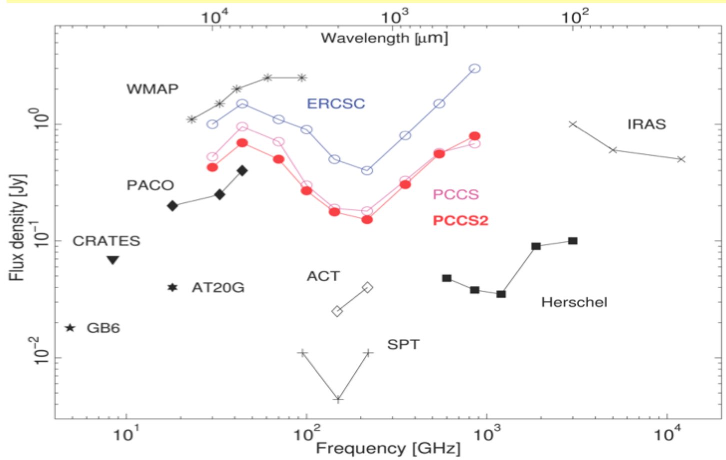



**Planck, Swift Fermi observations of Radio and high-energy selected blazars**

Planck Collaboration 2011, A&A 563, A16 and Giommi et al. A&A 2012, 514, 160

- **Large number of sources**: **175 blazars** observed by Swift when they were in the FOV of Planck: ~160 Swift ToOs
- **Simultaneous** Planck Swift Fermi + ground based telescopes
- **Multi-selection approach.** Four flux-limited samples.

Radio (100 brightest northern sources)
Soft X-ray (RASS, sample)
Hard X-ray (Swift-BAT sample)
γ-ray (Fermi sample)

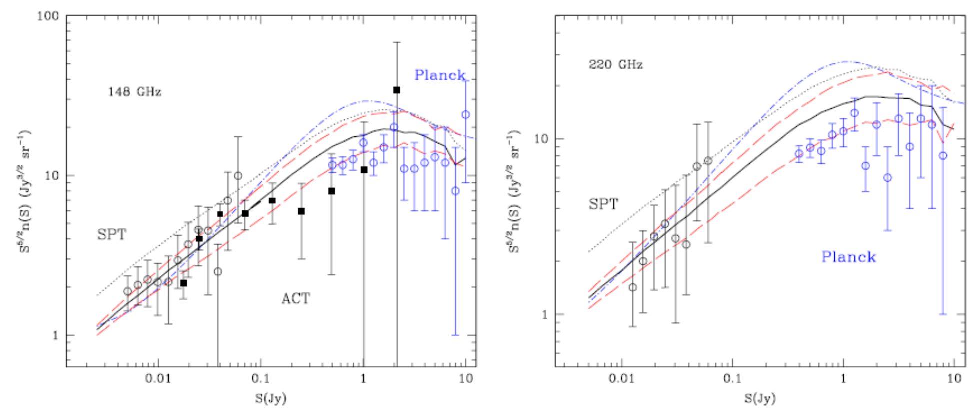


⟹ **Best model (C2Ex)**: BL Lacs more compact than FSRQs. Break frequency is typically

$$10 \lesssim \nu_M \lesssim 100\,\mathrm{GHz\ for\ FSRQs}$$
$$\nu_M \gtrsim 100\,\mathrm{GHz\ for\ BL\,Lacs}$$

Tucci et al. 2001 model

# Extragalactic sources in polarization

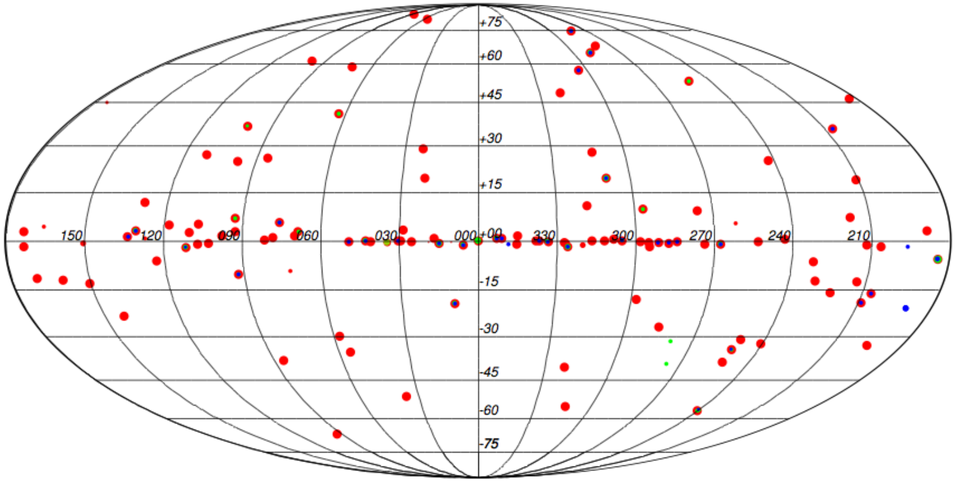


30 GHz
44 GHz
70 GHz

Distribution of the polarized sources in the lowest channels of the PCCS2.

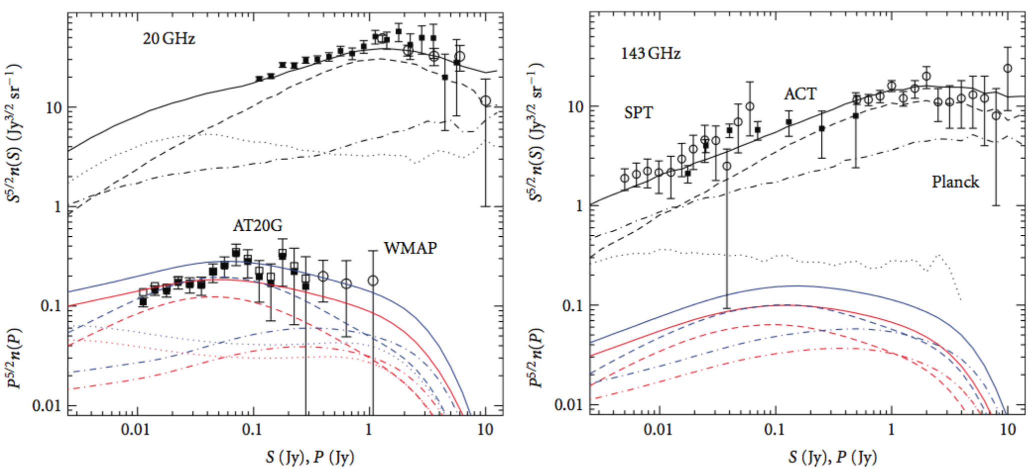


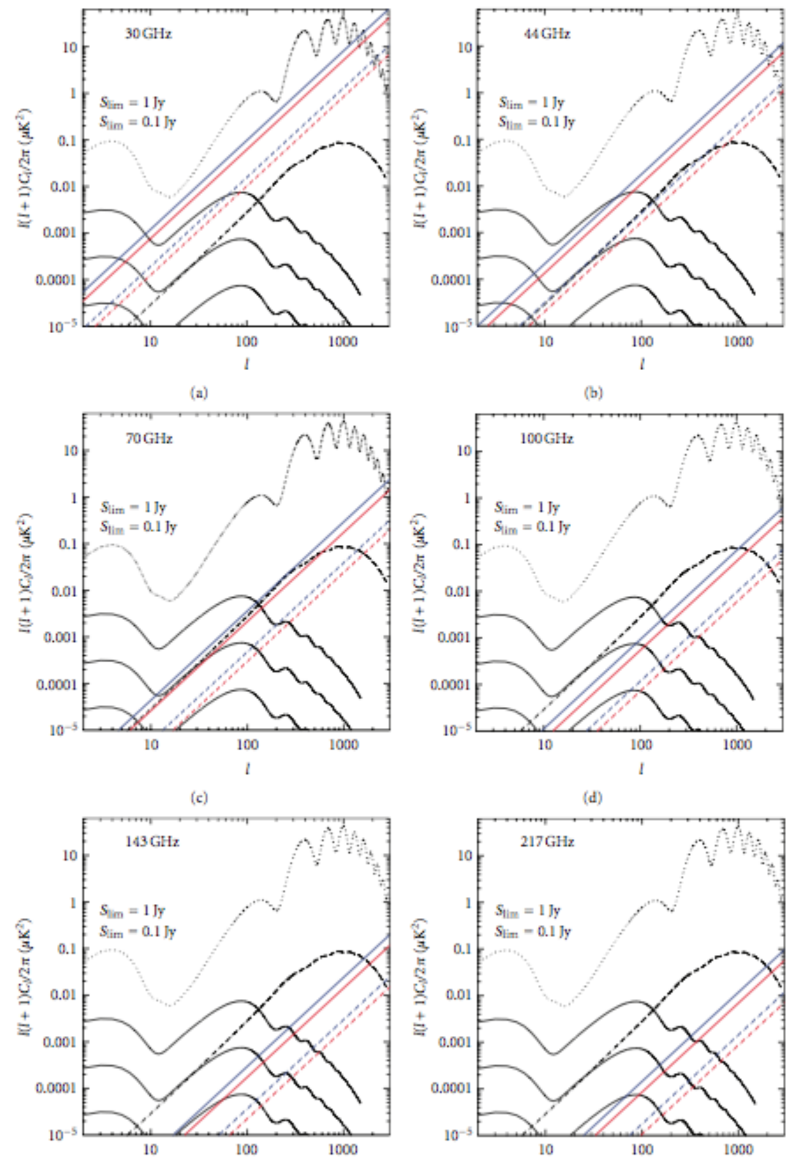


From Tucci & Toffolatti 2012

C. Burigana – Varenna 6/7/2017

The analysis of the sub-mm/far-IR background provides integrated information on star formation even where/when optical/UV signals are masked by dust

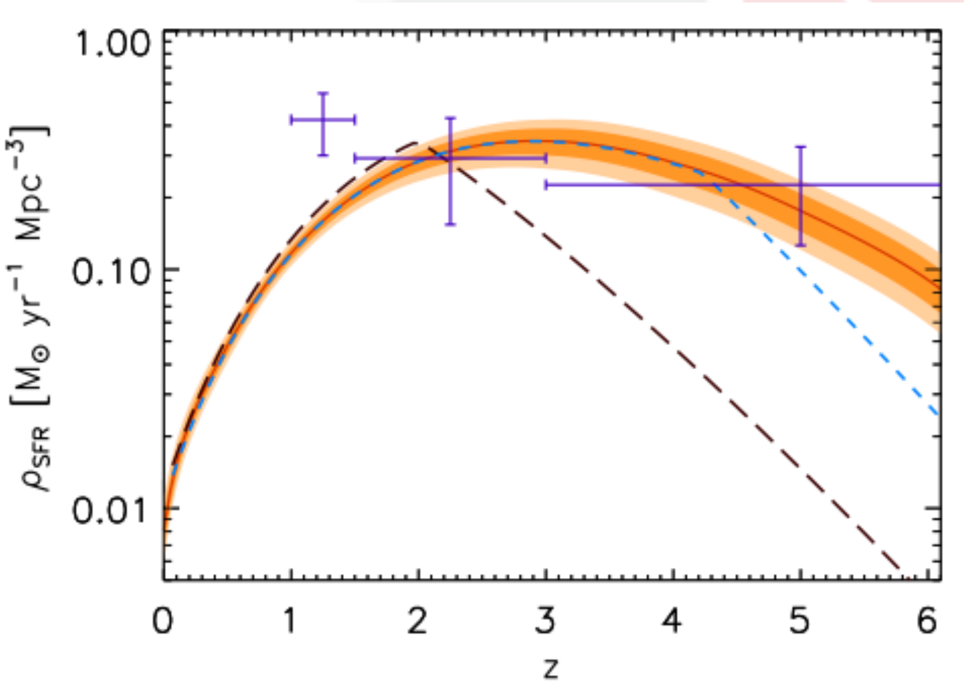


***Planck* 2013 results. XXX. Cosmic infrared background measurements and implications for star formation**

Marginalized constraints to the rate of star formation (SFR) obtained from the extended halo model In *Planck* 2013 results. XXX (solid red line; limits at ±1σ & ±2σ: orange regions).

Comparison with averaged values computed from two different break (dashed lines).
Violet values: density of obtained from the model of cross-correlation of CIB with CMB lensing

(from *Planck* 2013 results. XVIII. The gravitational lensing-infrared background correlation).

**Mollweide projection with the Galactic plane horizontal and the Milky Way centre in the middle, of the 1653 *Planck clusters and candidates across the sky, 1203 confirmed by external data.* Planck 2015 results. XXVII.**

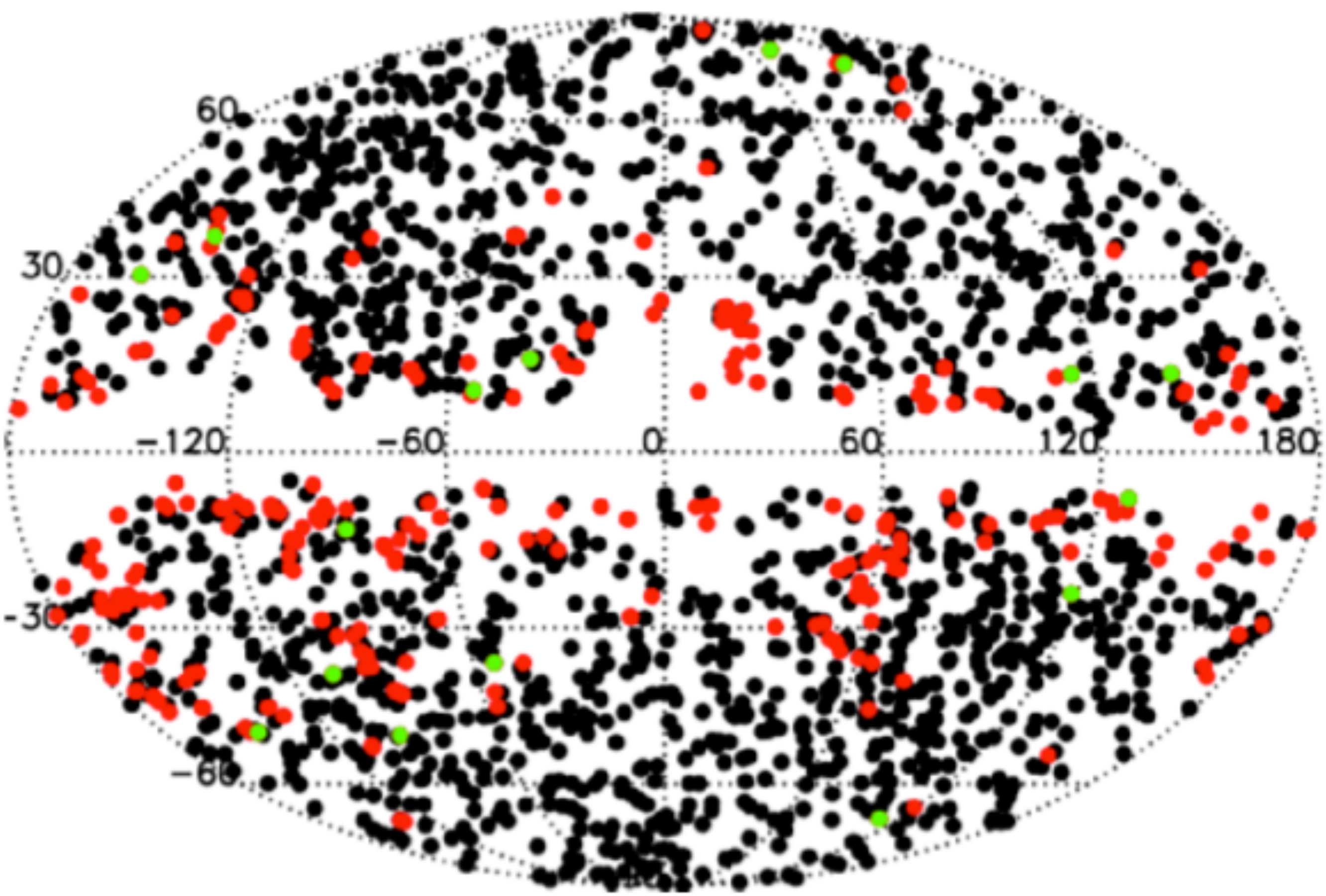


Distribution of raw detections of clusters with SZ effect from Planck (deleted IR flagged candidates in red and retained IR flagged detections in green)

# A secondary anisotropy: the thermal Sunyaev-Zel'dovich effect

30 GHz

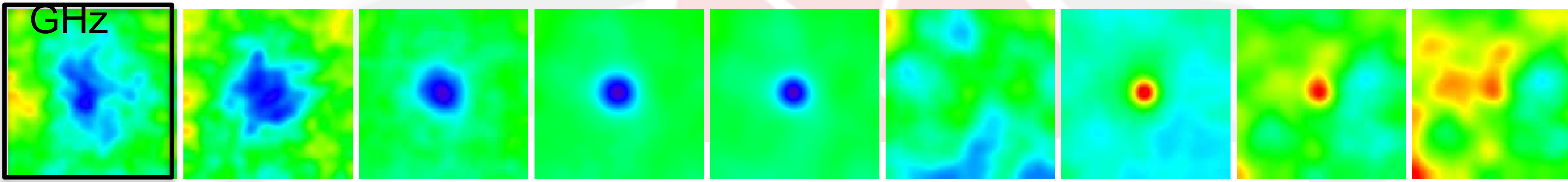

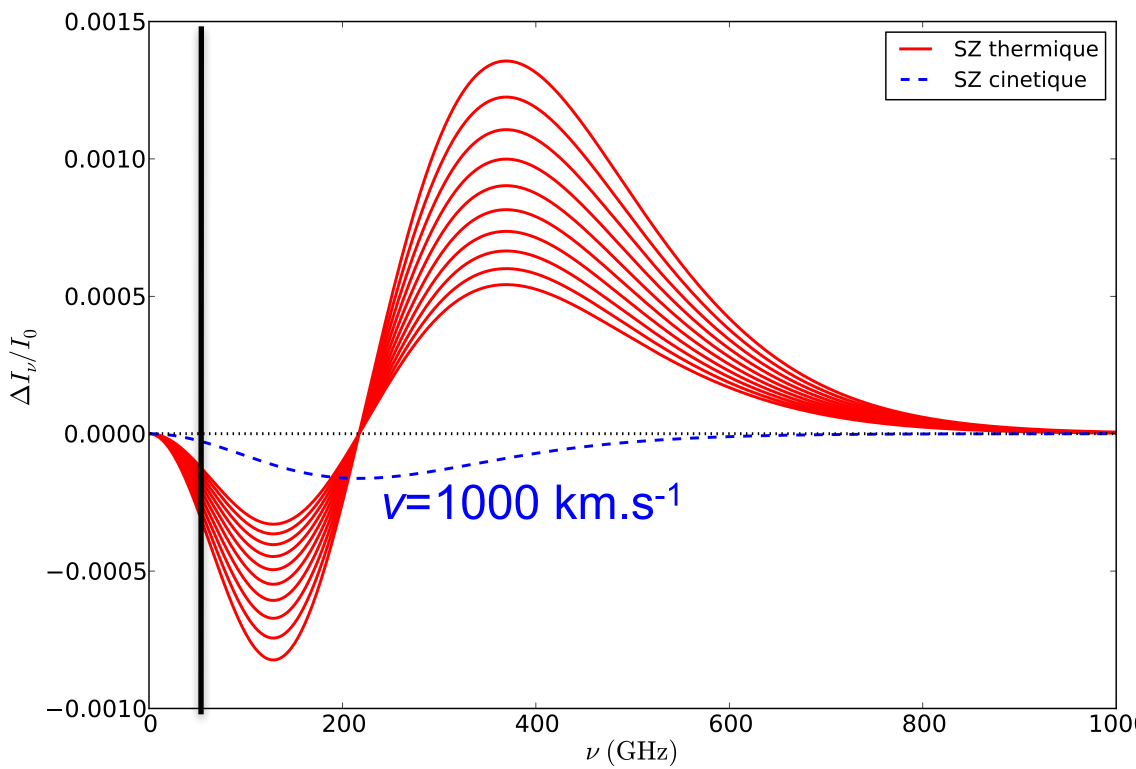


[Planck Collaboration. Planck 2013 results. *XXIX. The Planck catalogue of Sunyaev-Zeldovich sources.* A&A 571, A29, 2014]

$y$=2x10$^{-4}$

$y$=8x10$^{-5}$

Courtesy M. Roman

# A secondary anisotropy: the thermal Sunyaev-Zel'dovich effect

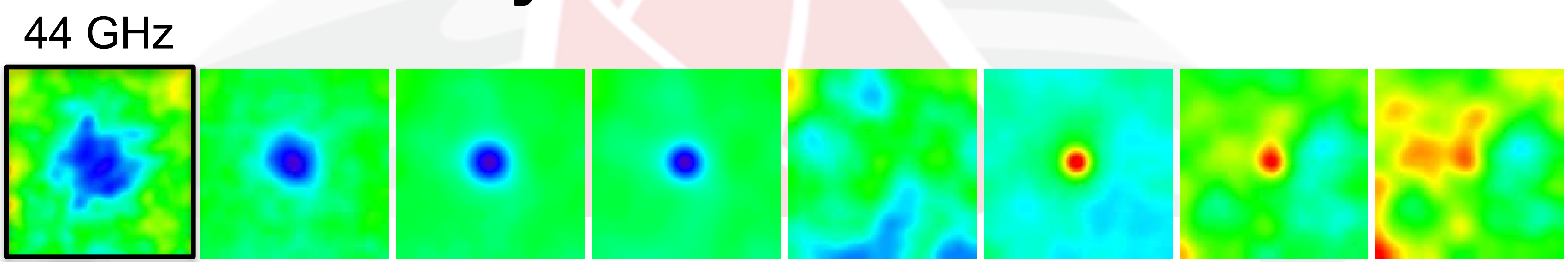


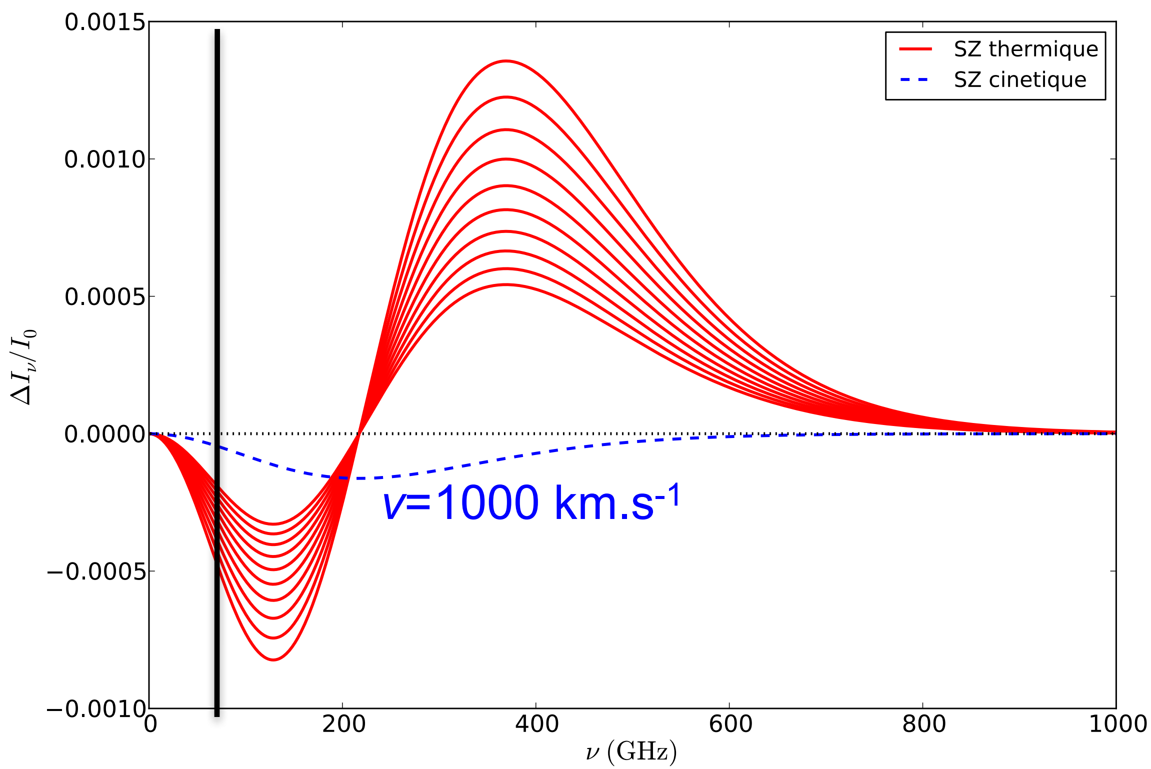


[Planck Collaboration. Planck 2013 results. *XXIX. The Planck catalogue of Sunyaev-Zeldovich sources.* A&A 571, A29, 2014]

$y$=2x10$^{-4}$

$y$=8x10$^{-5}$

# A secondary anisotropy: the thermal Sunyaev-Zel'dovich effect

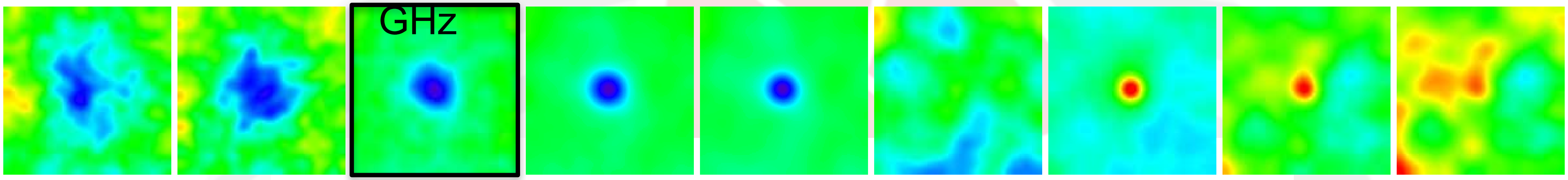


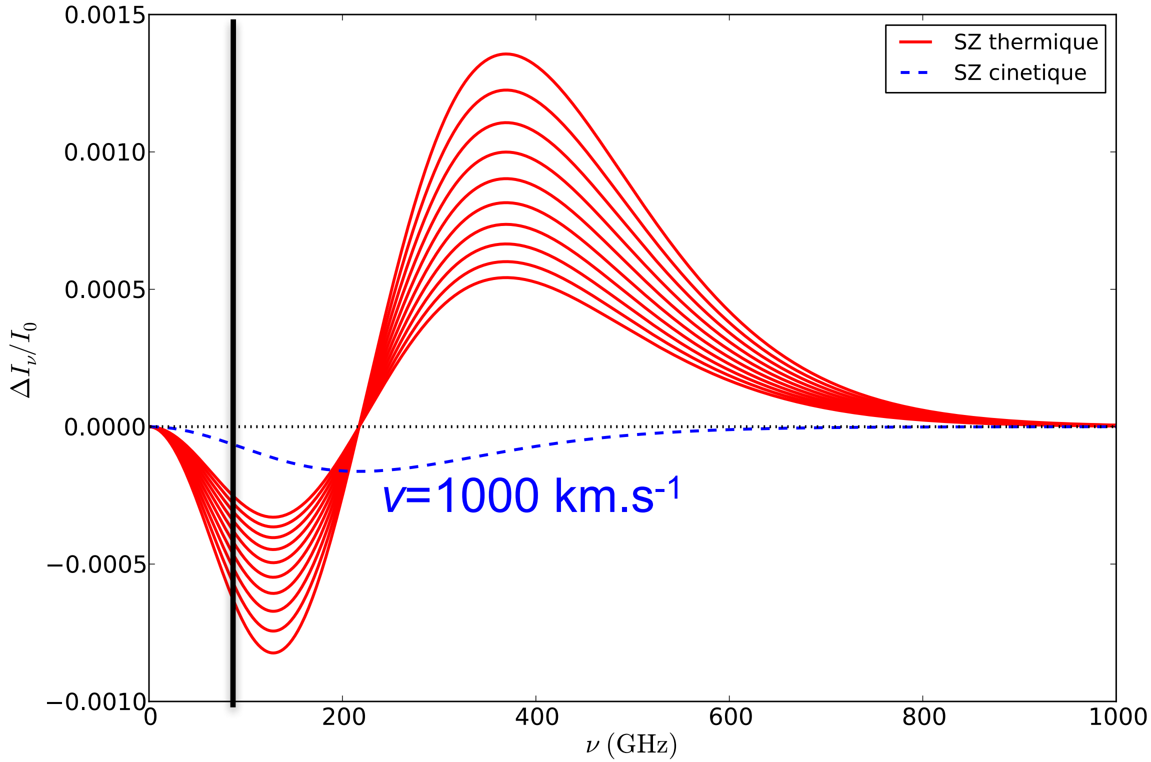


[Planck Collaboration. Planck 2013 results. *XXIX. The Planck catalogue of Sunyaev-Zeldovich sources.* A&A 571, A29, 2014]

$y$=2x10$^{-4}$

$y$=8x10$^{-5}$

# A secondary anisotropy: the thermal Sunyaev-Zel'dovich effect

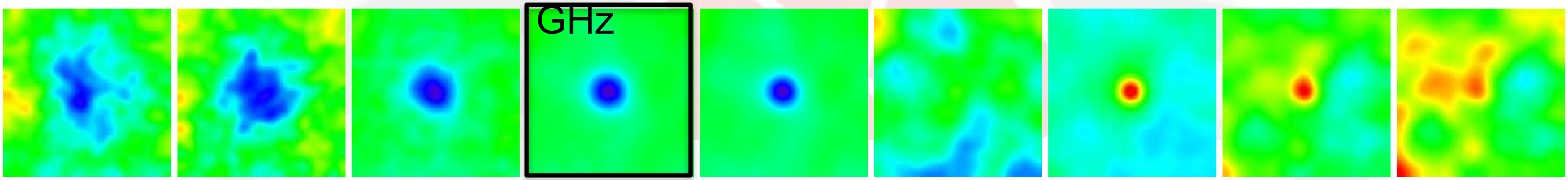


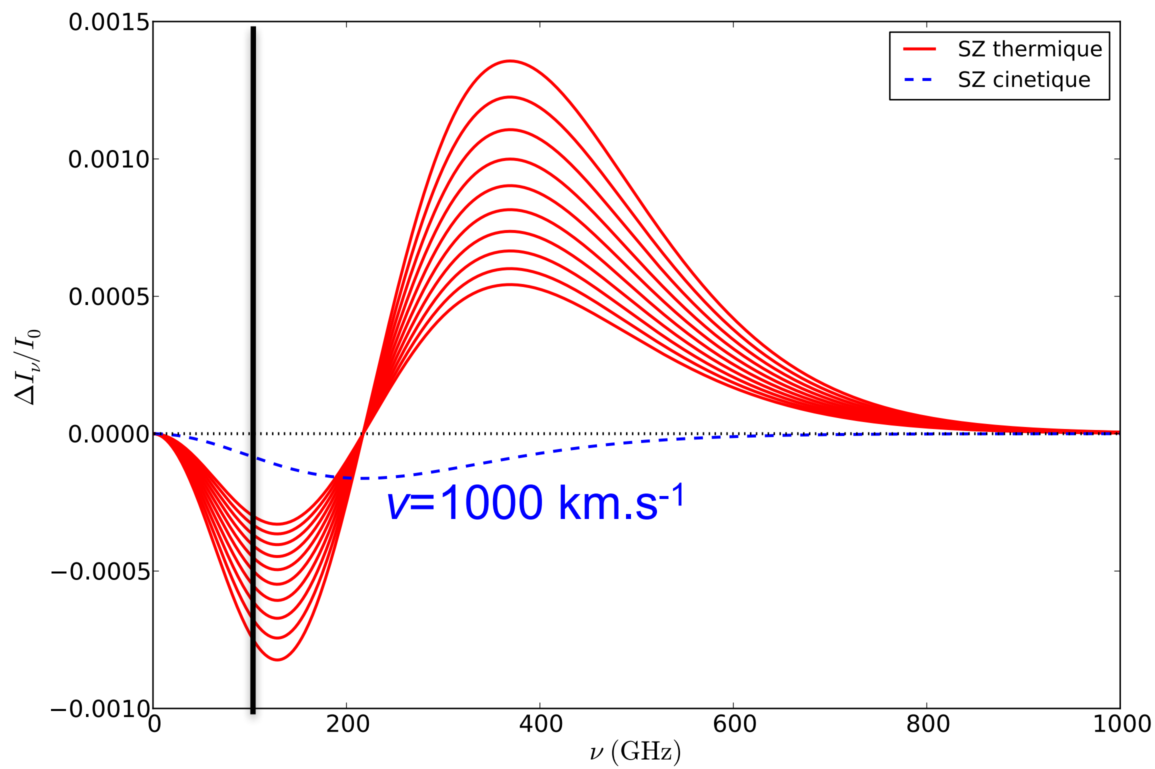


[Planck Collaboration. Planck 2013 results. *XXIX. The Planck catalogue of Sunyaev-Zeldovich sources.* A&A 571, A29, 2014]

$y$=2x10$^{-4}$

$y$=8x10$^{-5}$

# A secondary anisotropy: the thermal Sunyaev-Zel'dovich effect

143 GHz

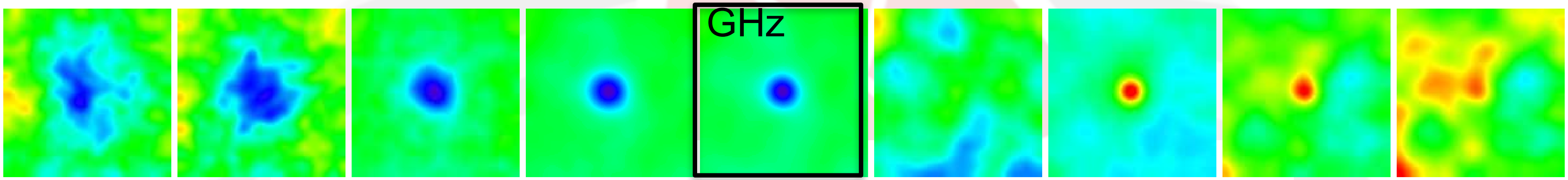

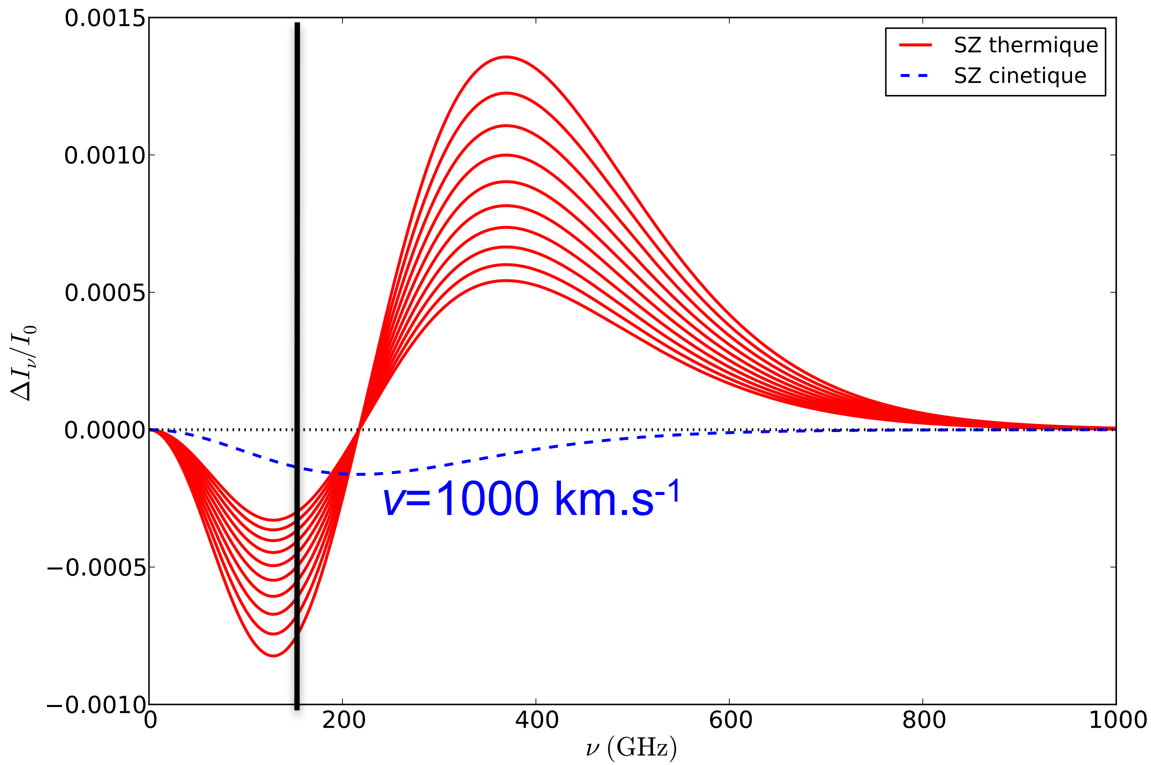


[Planck Collaboration. Planck 2013 results. *XXIX. The Planck catalogue of Sunyaev-Zeldovich sources.* A&A 571, A29, 2014]

$y$=2x10$^{-4}$

$y$=8x10$^{-5}$

# A secondary anisotropy: the thermal Sunyaev-Zel'dovich effect

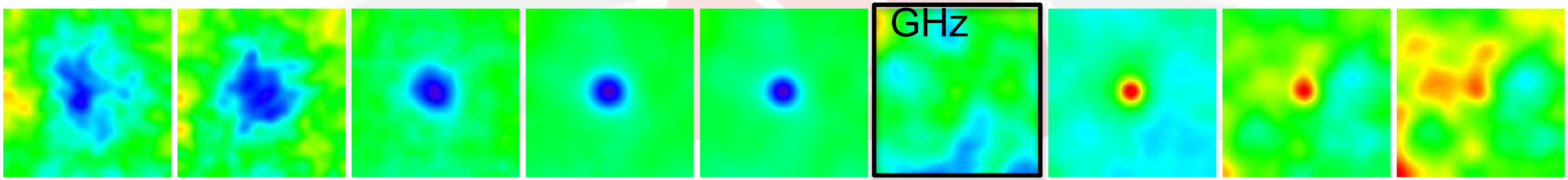


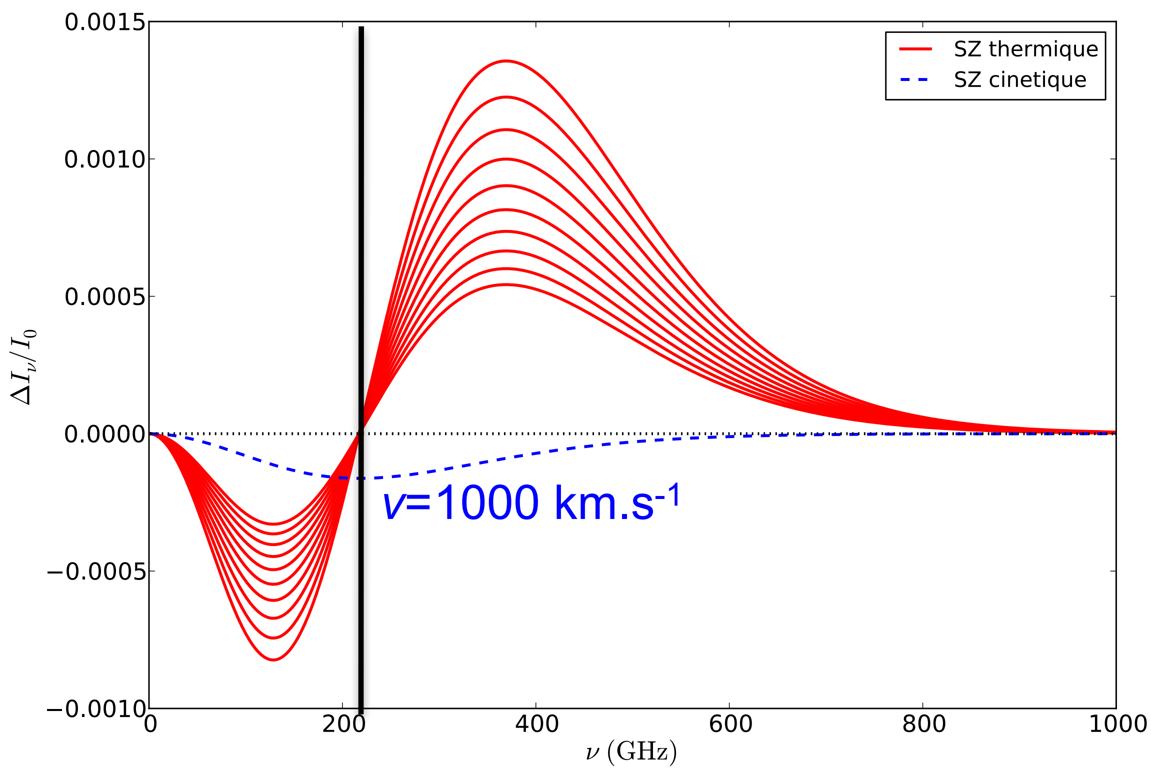


[Planck Collaboration. Planck 2013 results. *XXIX. The Planck catalogue of Sunyaev-Zeldovich sources.* A&A 571, A29, 2014]

$y=2\times10^{-4}$

$y=8\times10^{-5}$

# A secondary anisotropy: the thermal Sunyaev-Zel'dovich effect

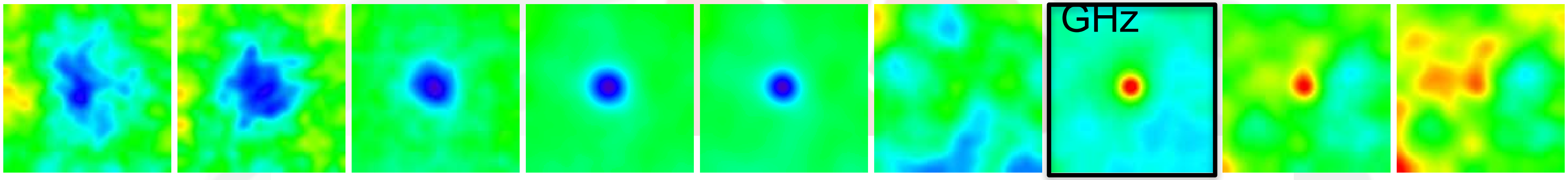


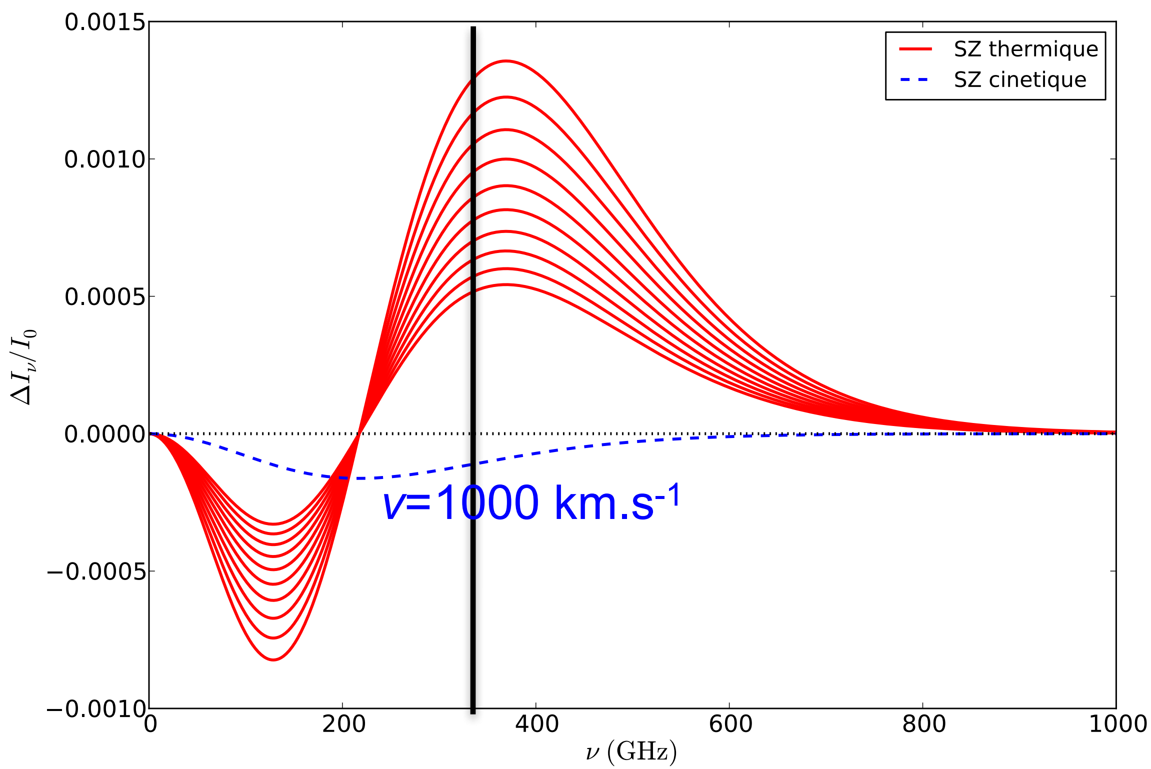


[Planck Collaboration. Planck 2013 results. *XXIX. The Planck catalogue of Sunyaev-Zeldovich sources.* A&A 571, A29, 2014]

$y$=2x10$^{-4}$

$y$=8x10$^{-5}$

# A secondary anisotropy: the thermal Sunyaev-Zel'dovich effect

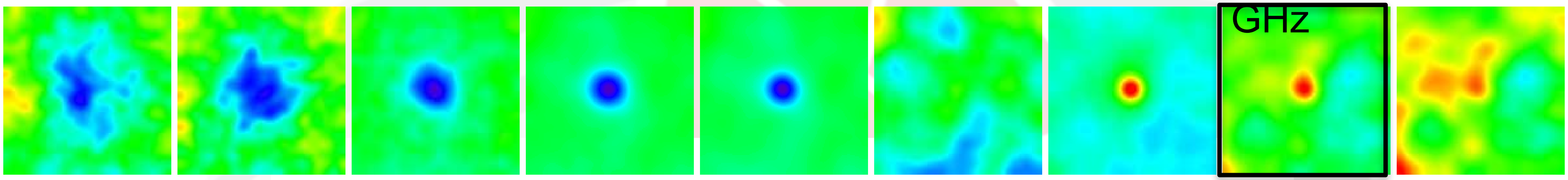


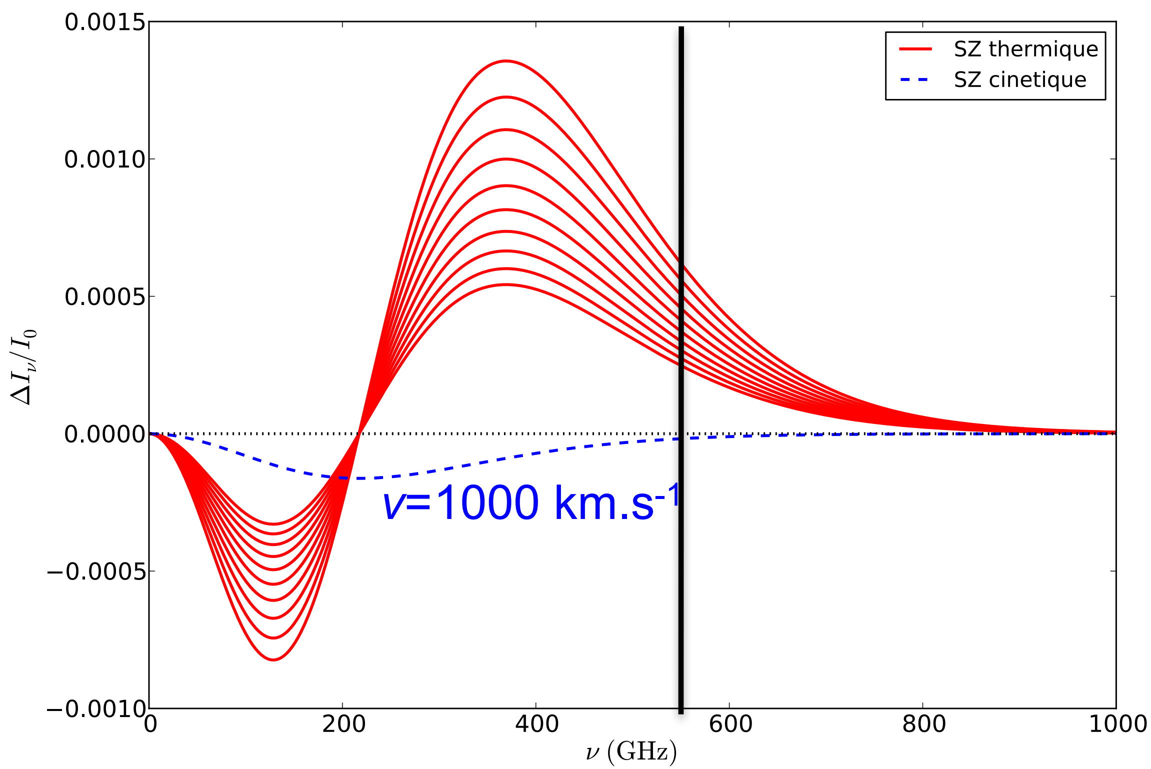


[Planck Collaboration. Planck 2013 results. *XXIX. The Planck catalogue of Sunyaev-Zeldovich sources.* A&A 571, A29, 2014]

$y=2\times10^{-4}$

$y=8\times10^{-5}$

# A secondary anisotropy: the thermal Sunyaev-Zel'dovich effect

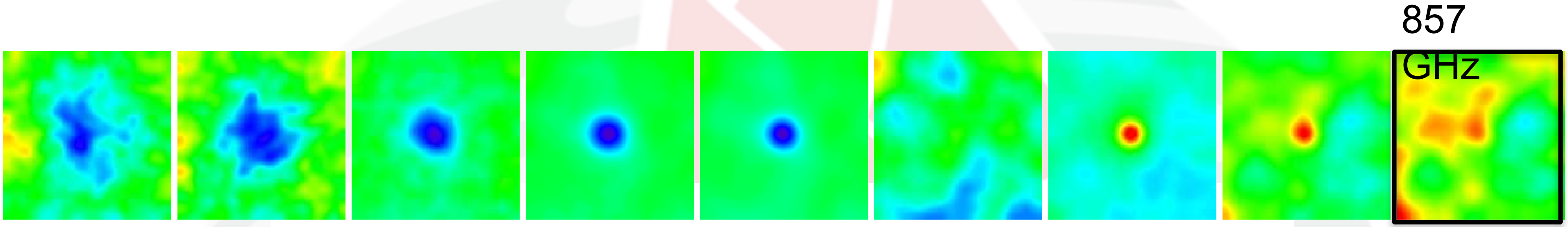


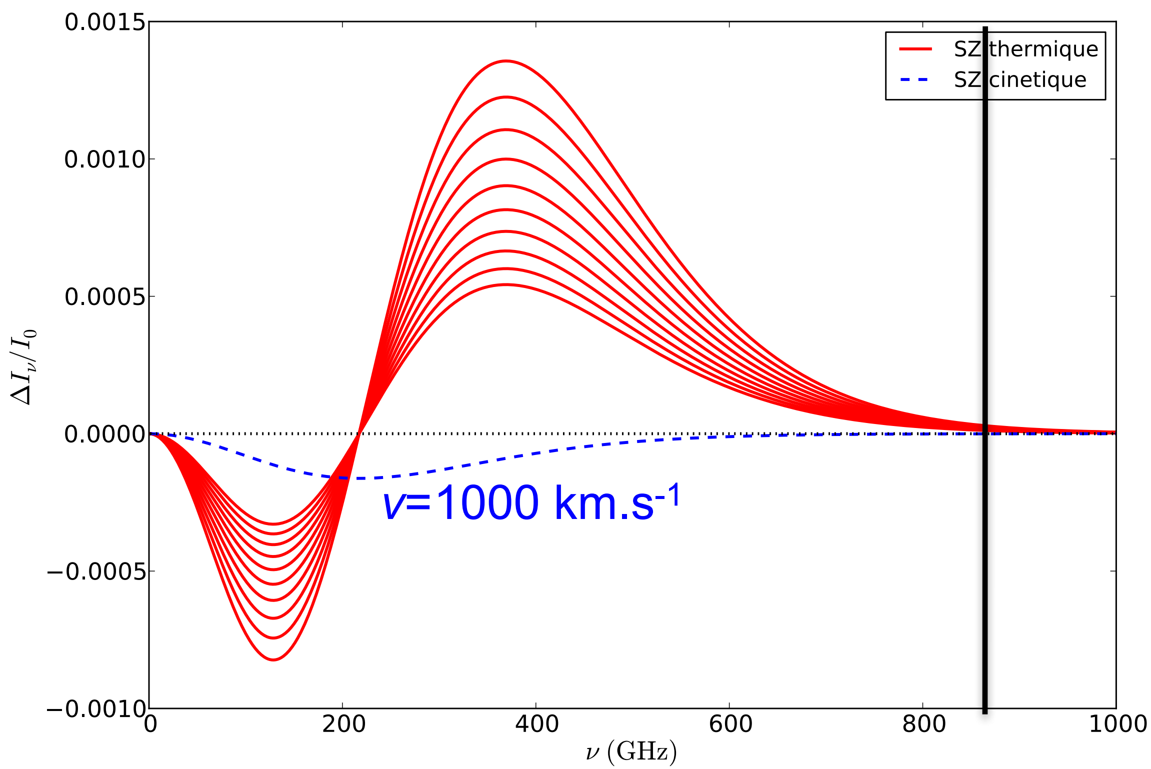


[Planck Collaboration. Planck 2013 results. *XXIX. The Planck catalogue of Sunyaev-Zeldovich sources.* A&A 571, A29, 2014]

*y*=2x10$^{-4}$

*y*=8x10$^{-5}$

# **The Sunyaev-Zeldovich effect** allows to study intergalactic medium gas at relatively lower densities than those accessible to X rays

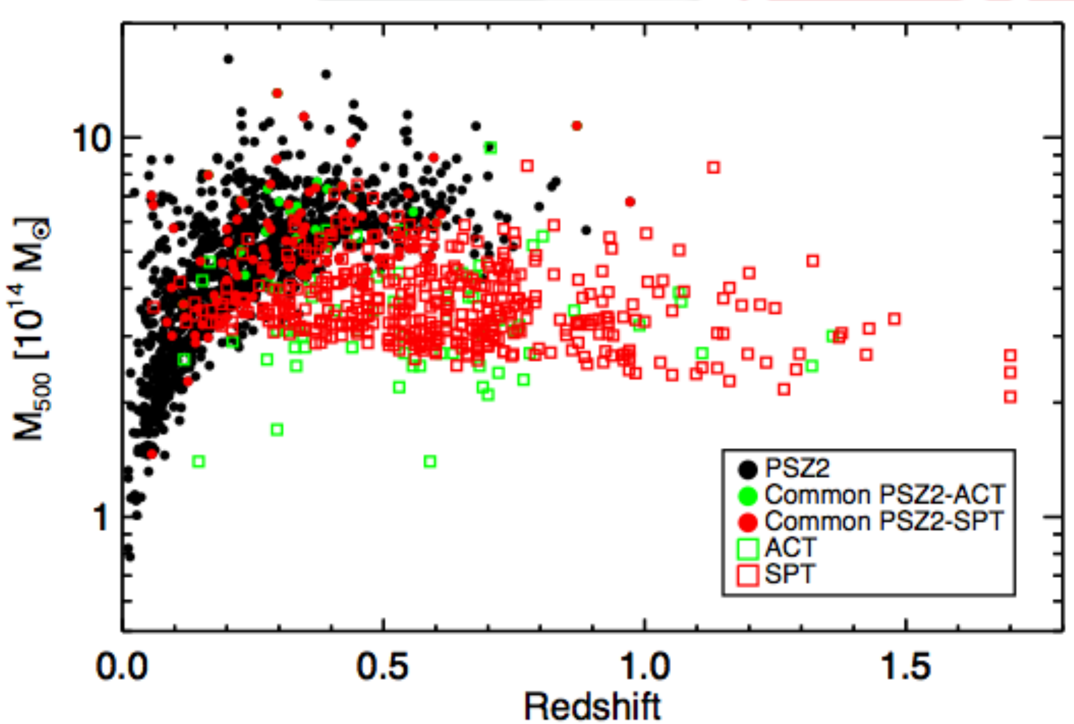


Distribution in z of clusters at different masses from various CMB experiments. From Planck 2015 results. XXVII. The Second Planck Catalogue of Sunyaev-Zeldovich Sources

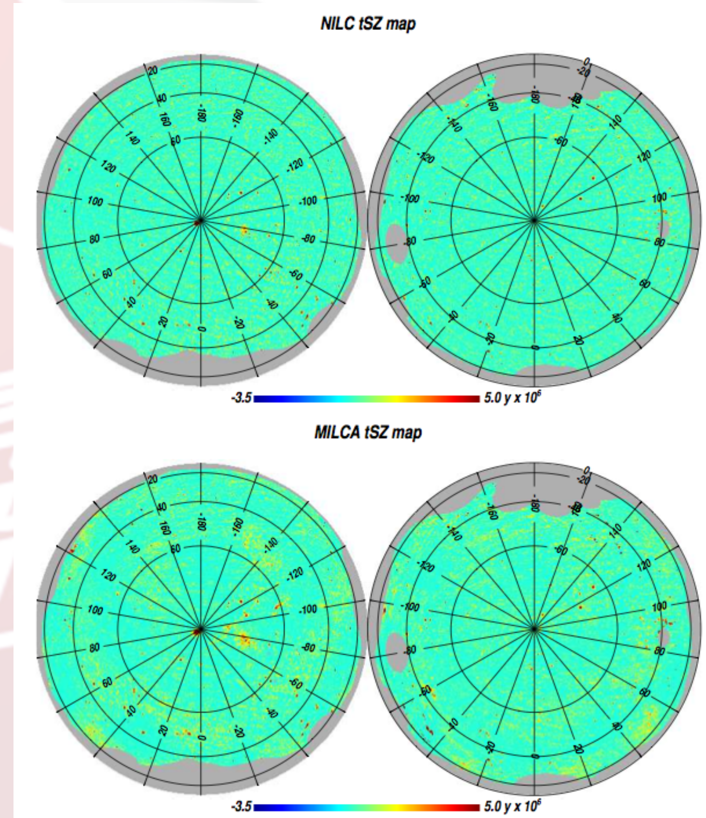


Planck all-sky maps of the Comptonization parameter derived with two different methods. From Planck 2015 results XXII. A map of the thermal Sunyaev-Zeldovich effect

# Cluster model

$P$ = distribution of $q$ given the mean predicted by the model for a cluster of mass $M_{500}$ and redshift $z$ located at Galactic coordinates ($l$,$b$).
$M_{500}$ mass within $r_{500}$ (where 500 times critical density)

Courtesy M. Roman

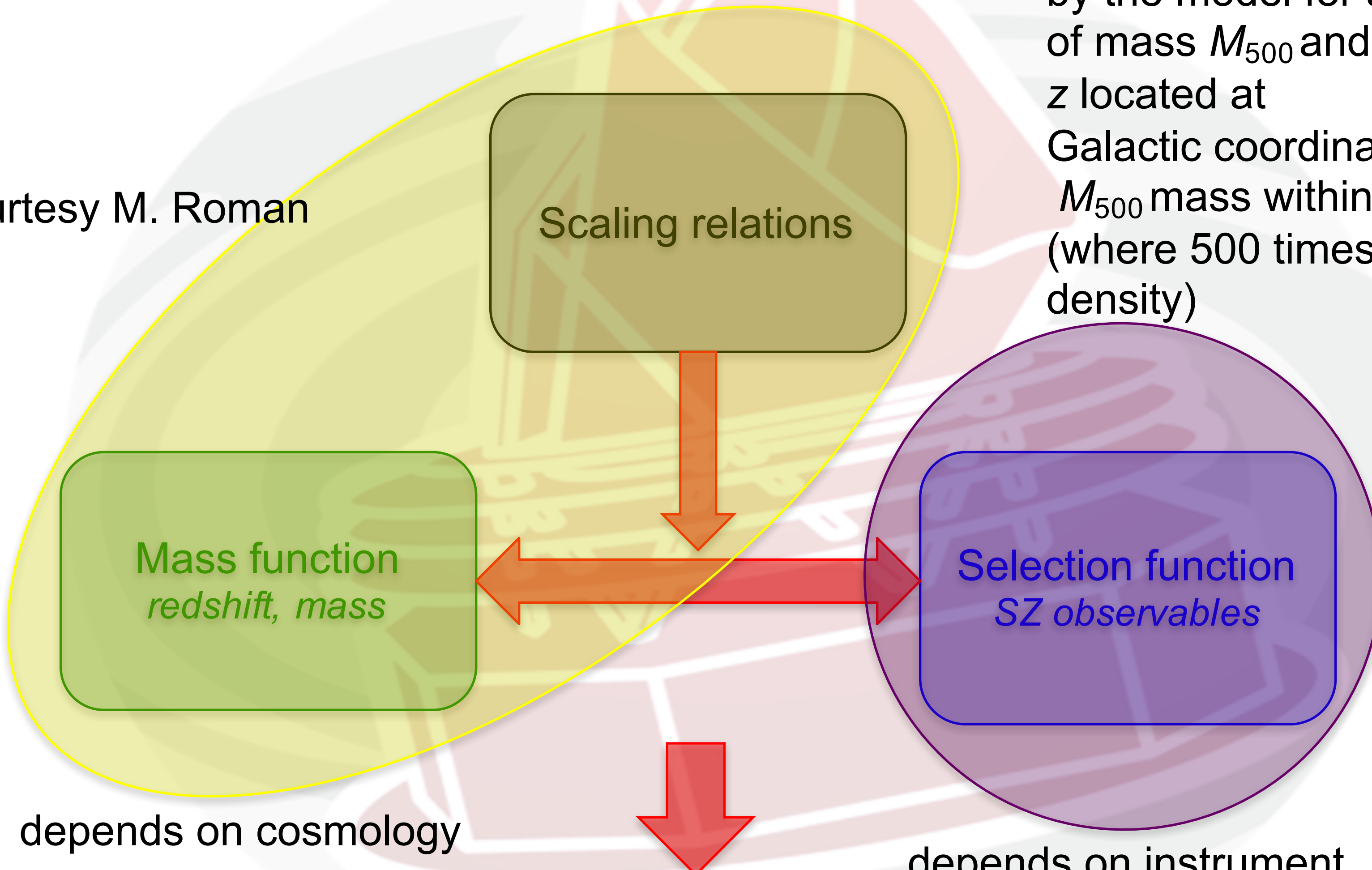


depends on cosmology

depends on instrument

$$\frac{dN}{dzdq} = \int d\Omega_{\rm mask} \int dM_{500} \, \frac{dN}{dzdM_{500}d\Omega} P[q|\bar{q}_{\rm m}(M_{500}, z, l, b)]$$

Distribution of clusters in redshift z and and q=S/N

# Some cosmological implications

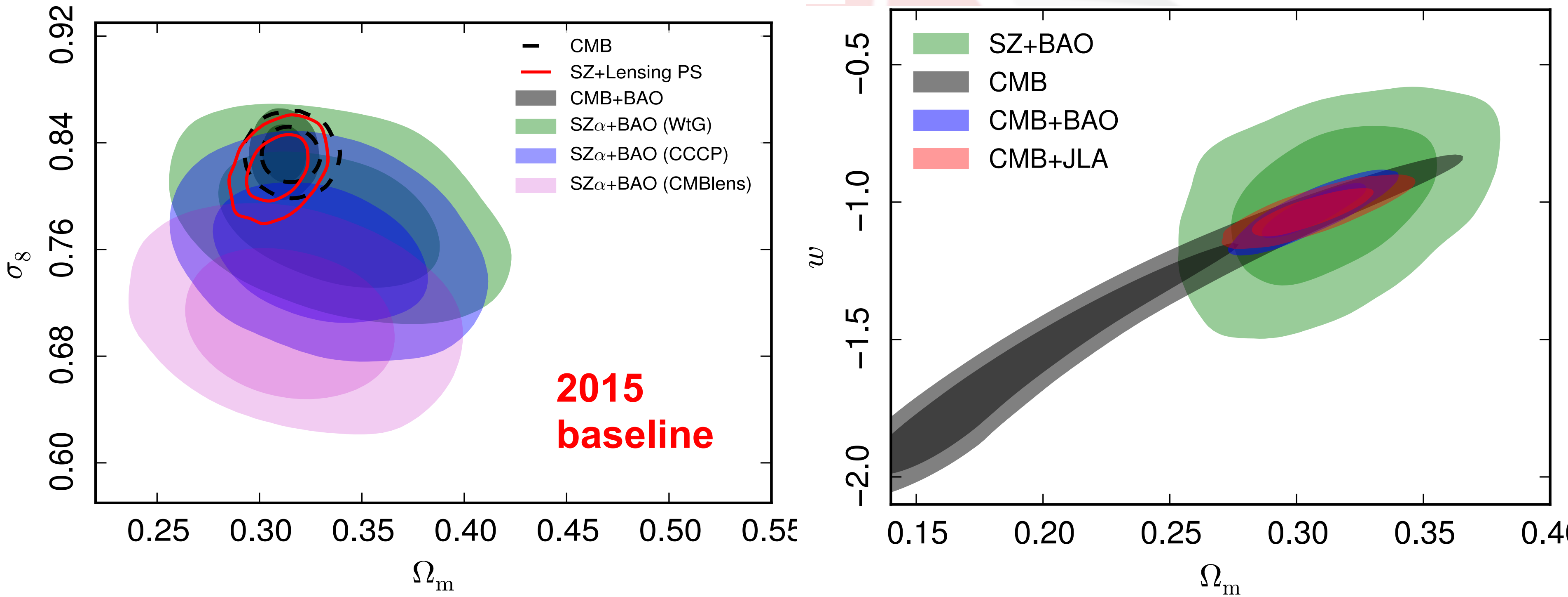


**From cluster counts** (Planck 2015 results. XXIV):

✓**cosmological parameters for ΛCDM model**

✓**extension from ΛCDM**

# Methods. Example I: sky pixelization

# COBE sky cube scheme

(Chan & O'Neill 1976; O'Neill & Laubsher 1976)

1. The sphere is inscribed in a cube, whose faces are pixelized with a regular square grid.
2. The points are mapped radially onto the sphere.
3. The points are shifted around slightly, to give all pixels approximately equal area.

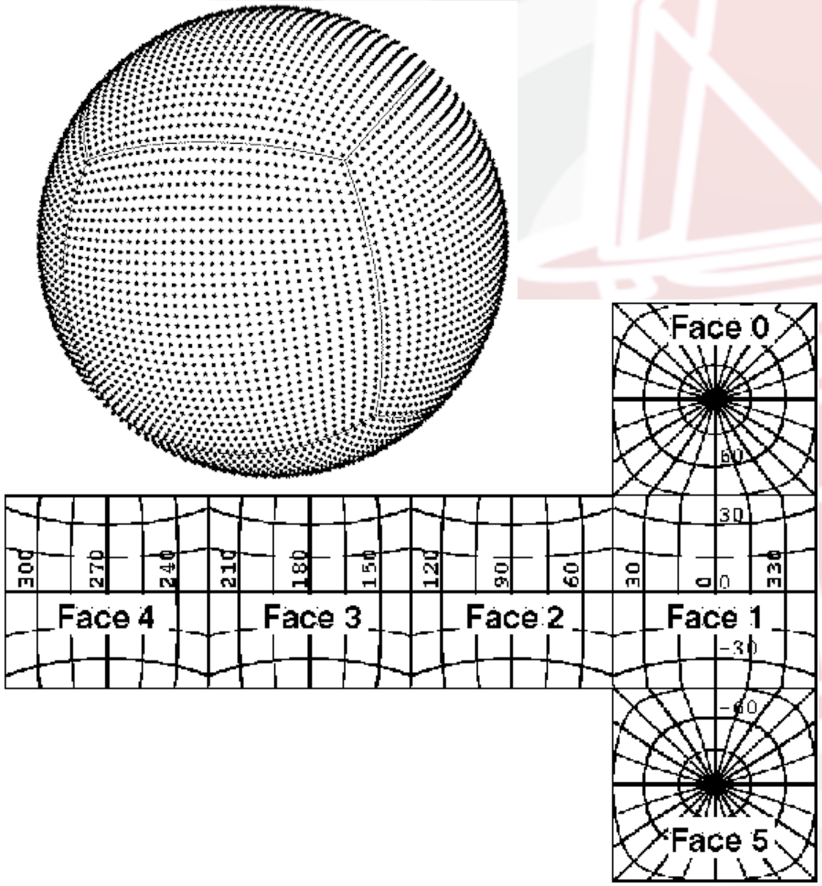


The "(ex)standard" COBE-cube pixelisation ("good" equal-area conditions, hierarchic) satisfies two simple symmetry properties:

1) if $\theta_k \in \{\theta_i\}$ , then also $-\theta_k \in \{\theta_i\}$
2) if $\varphi_k \in \{\varphi_j\}$ then also $(\varphi_k + \pi) \in \{\varphi_j\}$

→ It allows to divide by four the computational time for generating maps using spherical harmonic expansion, because the temperature anisotropy can be computed in four points of the sky at the same time.

In spite of this, generating maps was extremely time consuming!

# Icosahedron pixelization scheme

(M. Tegmark 1996)

1. The sphere is inscribed in an icosahedron (instead of a cube), whose faces are pixelized with a regular triangular (instead of a square) grid.
2. The points are mapped radially onto the sphere.
3. The points are shifted around slightly, to give all pixels approximately equal area.

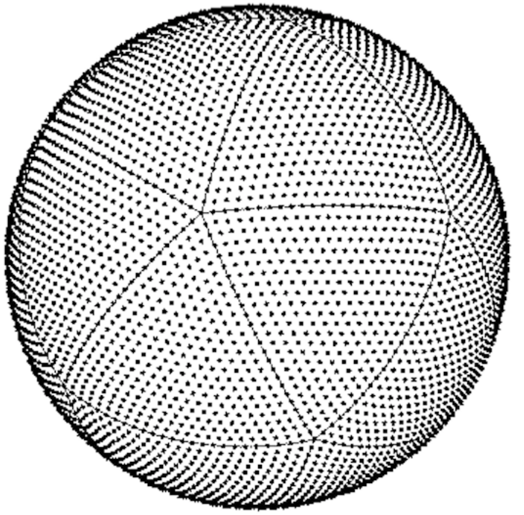

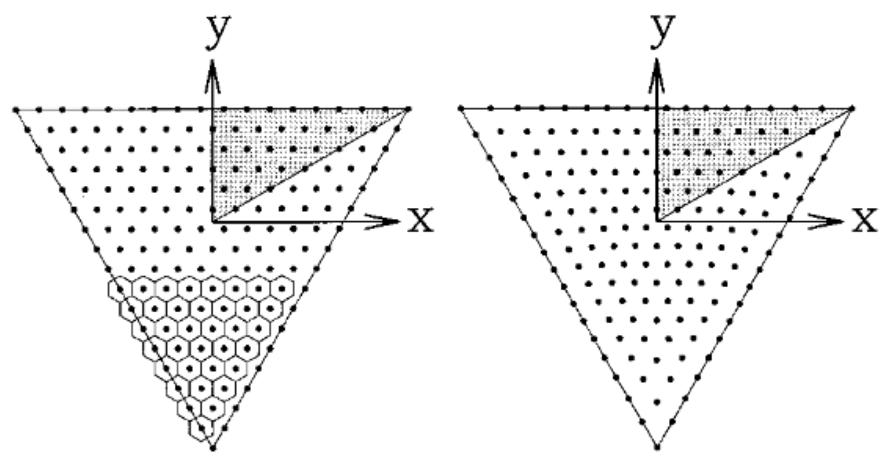


FIG. 2.—A regular triangular grid (*left*) is adjusted (*right*) to give all pixels the same area. As illustrated, the pixels have a hexagonal shape. A triangular icosahedron face can be symmetrically decomposed into six identical right triangles (one is shaded), and the area-equalization mapping is seen to respect this symmetry.

"Moment of inerzia" of pixels is minimum

→ Very good from the pixel geometry point of view

→ But again: generating maps was extremely time consuming!

# Link between spherical harmonic expansion and FFT

Muciaccia et al. (1997)

**A really huge change in map generation and analysis!**

$$Y_{lm}(\theta,\ \phi) = \lambda_l^m(\cos\theta)e^{im\phi}, \tag{2}$$

$$a_{lm} = \int d\Omega \frac{\Delta T}{T}(\hat{\gamma})Y_{lm}^*(\hat{\gamma}). \tag{7}$$

Fortunately, after substituting equation (2) in equation (7) we can write

$$a_{lm} = \int \sin\theta d\theta \lambda_l^m(\theta) b_m(\theta), \tag{8}$$

where

$$b_m(\theta) = \int_0^{2\pi} d\phi \Delta(\phi,\ \theta)\exp(-im\phi). \tag{9}$$

Thus, equation (8) is the conjugate of equation (4): the $b_m$ values are the Fourier antitransform of the anisotropy pattern along a parallel in the ECP of the sky and are easily computed at fixed $\theta$ with an FFT. In conclusion, inverting a map to obtain the $a_{lm}$ values requires $\approx l_{\max}^2 \propto N_\phi^2$ recurrence relations for evaluating the $\lambda_l^m$ values plus an FFT (which scales as $N_\phi \ln N_\phi$) to evaluate the $b_m$ values. All of this must be done $N_\theta$ ($\propto N_\phi$) times to be able to perform the integral in equation (8). Using these tricks, we can invert a full-sky, high-resolution map with a number of operations that are, in principle, comparable with those needed for generating a map, i.e., $N_{\rm pix}^2 \ln N_{\rm pix}$. As in that case, we can exploit the symmetries of the $\lambda_{lm}$ values evaluated at $\theta$ and $\pi - \theta$, respectively.

# HEALPix (K. Gorski 1997 → K. Gorski et al. 2005)

**Hierarchical, Equal Area, and iso-Latitude Pixelation of the sphere**

- **Great idea!**
- Combining/ ingesting link between spherical harmonic expansion and FFT into suitable sky pixelization
- **Implemented with many facilities/tools!**

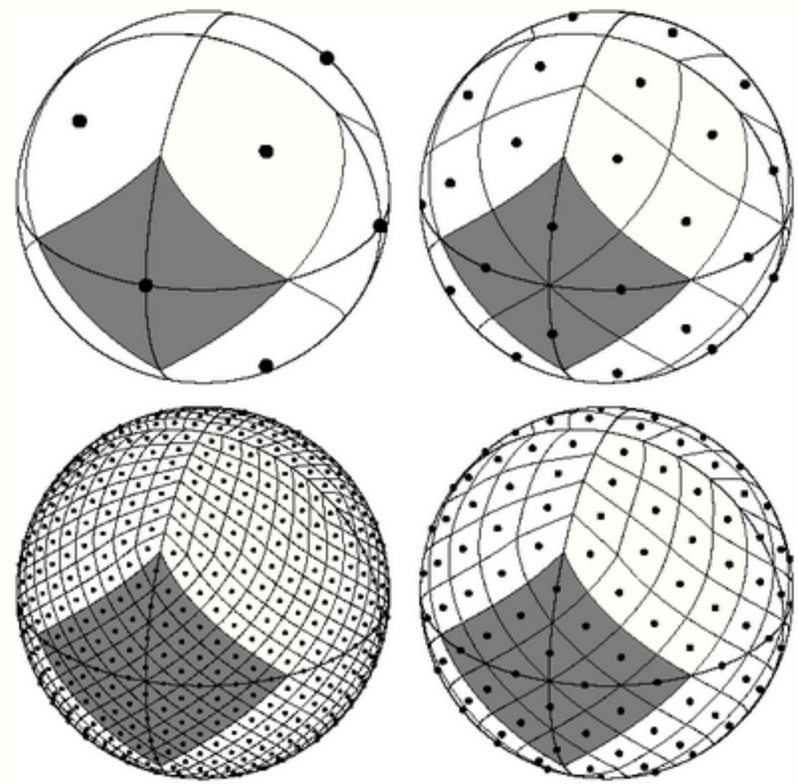

**Figure 2:** Orthographic view of **HEALPix** partition of the sphere. Overplot of equator and meridians illustrates the octahedral symmetry of **HEALPix**. Light-gray shading shows one of the eight (four north, and four south) identical polar base-resolution pixels. Dark-gray shading shows one of the four identical equatorial base-resolution pixels. Moving clockwise from the upper left panel the grid is hierarchically subdivided with the grid resolution parameter equal to $N_{\rm side} = 1, 2, 4, 8$, and the total number of pixels equal to

$N_{\rm pix} = 12 \times N_{\rm side}^2$ = 12, 48, 192, 768. All pixel centers are located on

$N_{\rm ring} = 4 \times N_{\rm side} - 1$ rings of constant latitude. Within each panel the areas of all pixels are identical.

# IGLOO; GLESP

R.G. Crittenden 1998; A.G. Doroshkevich et al. 2009-2011

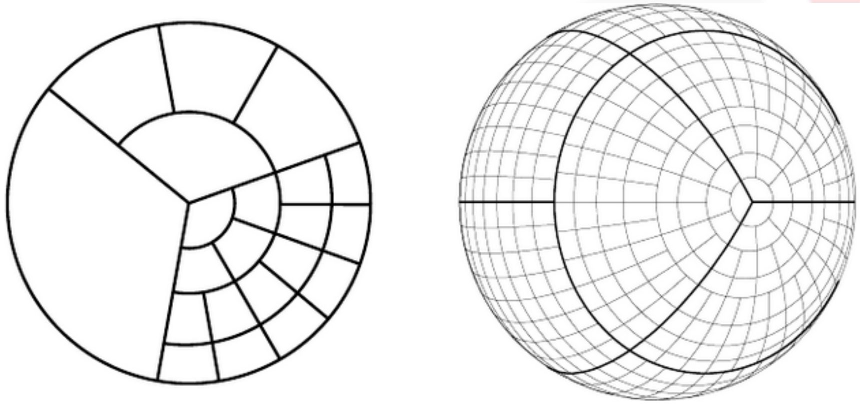

FIGURE 2. The left figure shows a polar cap division scheme which is hierarchical and causes little pixel distortion. This is implemented in the right figure, a 3:6:3 pixelization, with each of its twelve base pixels broken into 64 subpixels in an equal area way.

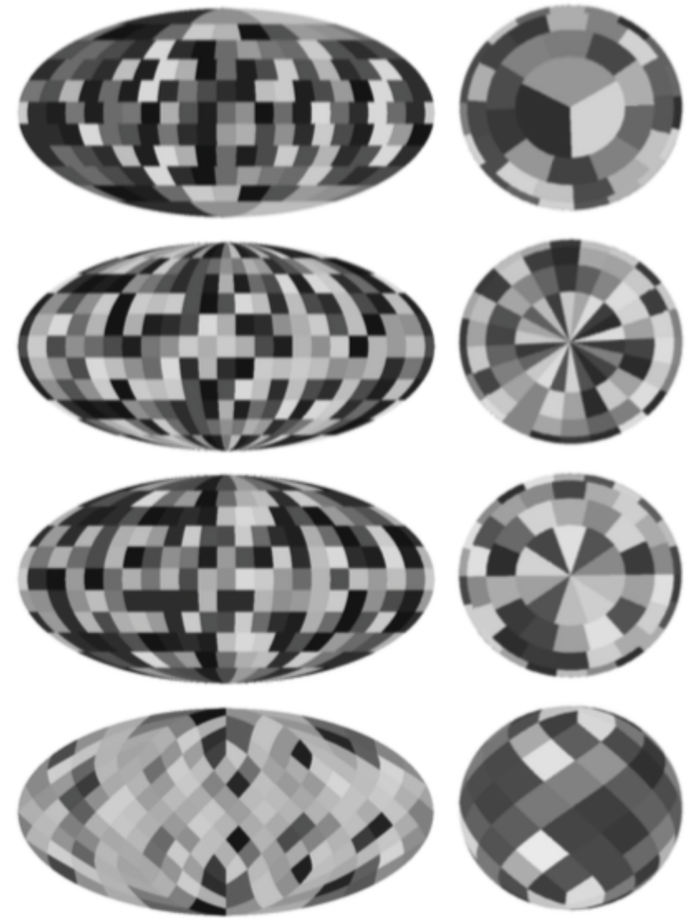

Fig. 1. Left column is the Molldweide projection of pixelization grids (from top to bottom): (a) the standard pixelization grid of the GLESP 1.0 (b) the GLESP-pol rectangular grid with the same number of pixels per each ring (the so called case 'grN'), (c) the GLESP-pol grid with an pixel number increment 4 (case 'grS') starting from 10 pixels near poles but not greater than a given resolution in the equator ring, (d) the HEALPix grid. The right column shows the corresponding pixelization in the vicinity of the polar cups.

# Euclid survey projection into HEALPix

Courtesy T. Trombetti & C.B. 2016

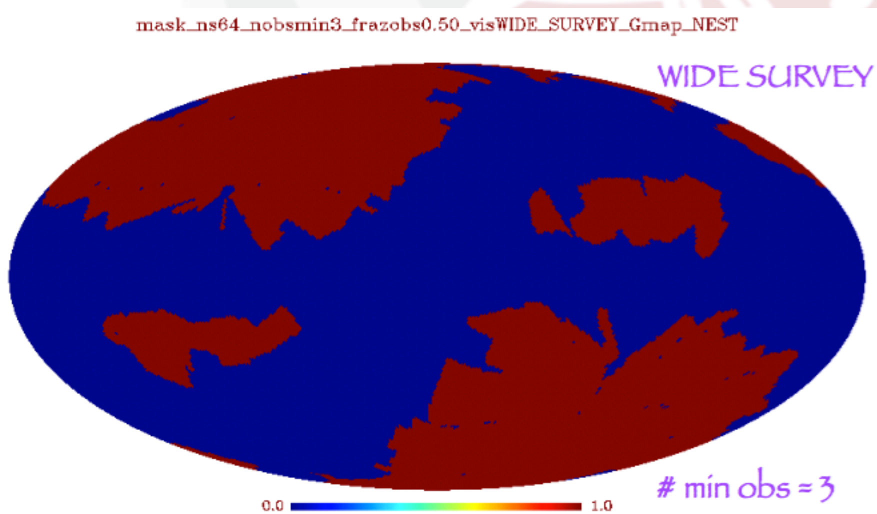

# Methods. Example II: separating CMB from foregrounds

# Separation of diffuse foreground in temperature - I

**4 methods applied to Planck maps:**

1. **SEVEM,** in real space. It is based construction foreground template typically based on of Planck maps at highest & lowest frequencies. They are subtracted to maps at central frequencies, where CMB dominates, through suitable coefficients minimizing the variance of each difference map in the considered. → cleaned maps of CMB at various frequencies → they are typicaly combined in pairs in harmonic space → final CMB cleaned.

2. **NILC** (Needlet Internal Linear Combination), data are first remapped in localized domains in both real and harmonic space, **needlets** → production of solutions of minimum variance in each space → recombination of them → CMB map in original domain. The methods allows localized and scale dependent, and improved the fit to space and angular size varying foregrouds.

# Separation of diffuse foreground in temperature - II

**3. Commander,** based on a-priori knowledge of foreground components characterized by parameters to be reconstructed with bayesian methods in real space independently for each resolution element.

2 steps: low resolution fit of parameters to describe foreground frequency scaling & high resolution fit of CMB & foreground amplitudes based on previous step output.→ control of space variations of foreground properties.

Also, noise full covariance matrix is propagated in the first step.

The method is also ingested in the construction of Planck likelihood.

**4. SMICA,** general parametrization of mixing coefficients of various components in the harmonic or needlet domain. CMB can be obtained under various assumptions, e.g. minimum variance, parametrization & fitting.

The first worked better on simulated data in temperature.

# Masks

From Planck Coll. 2015, Pap. IX
Diffuse component separation: CMB maps

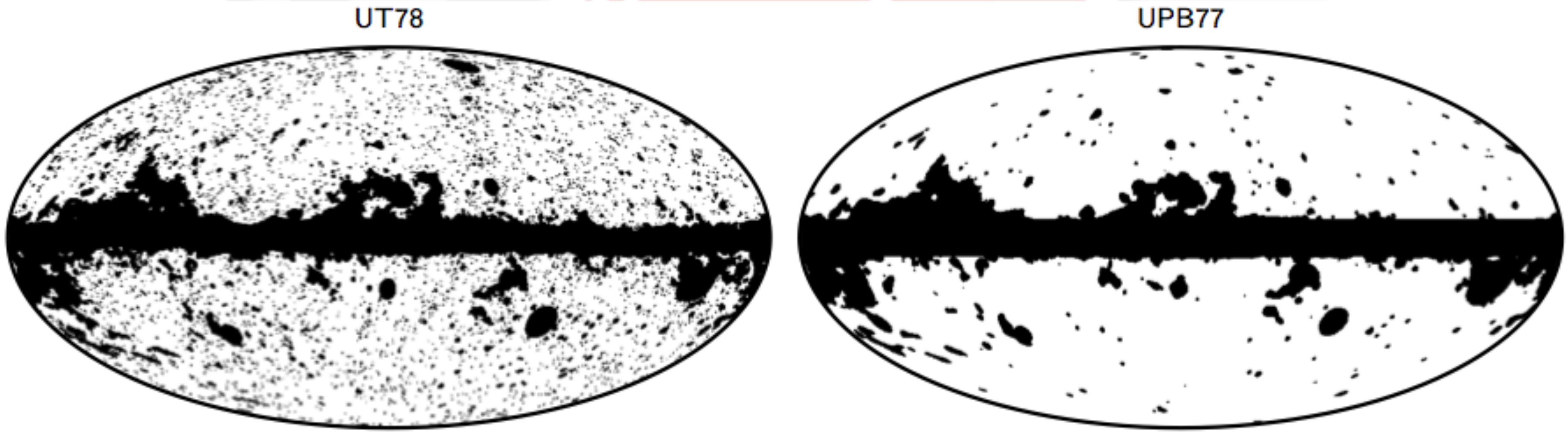


**Fig. 1.** Preferred masks for analysing component-separated CMB maps in temperature (*left*) and polarization (*right*).

Sky coverage 77.6 %

Sky coverage 77.4 %

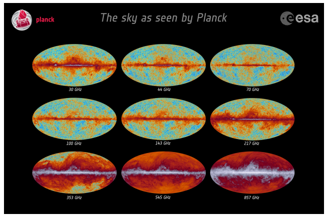


from freq. maps

# *Planck* Galactic foreground components in temperature

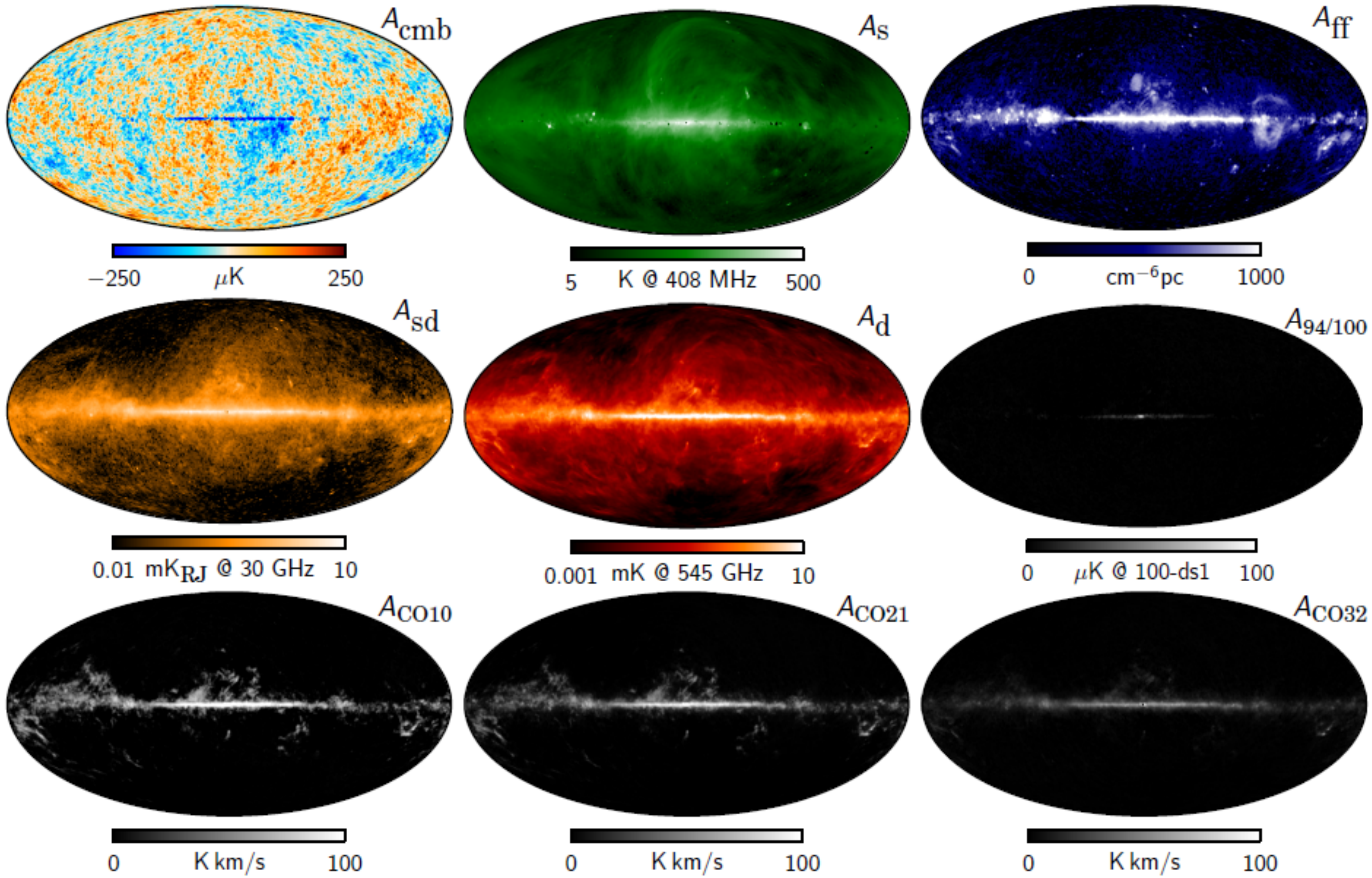

# Separation of diffuse foreground in polarization - I

CMB power very different in E & B modes → advantageous for separation to operate in harmonic domain (**NILC & SMICA**) to specialize methods to E & B modes separation indipendently.

input maps Q, U → maps of E & B

Differently, COMMANDER & SEVEM work in real space & perform separation directly & indipendently in Q & U.

**In Planck release 2014, E & B are official products.**

**COMMANDER & SEVEM** apply a post-processing to obtain E & B.

**Constrained impainting** is adopted to fill non relevant for CMB areas & E & B maps are reconstructed through all-sky decomposition.

# Galactic dust emission High polarization degree

Cumulative Histogram of P/I ratio
353 GHz and 1° resolution

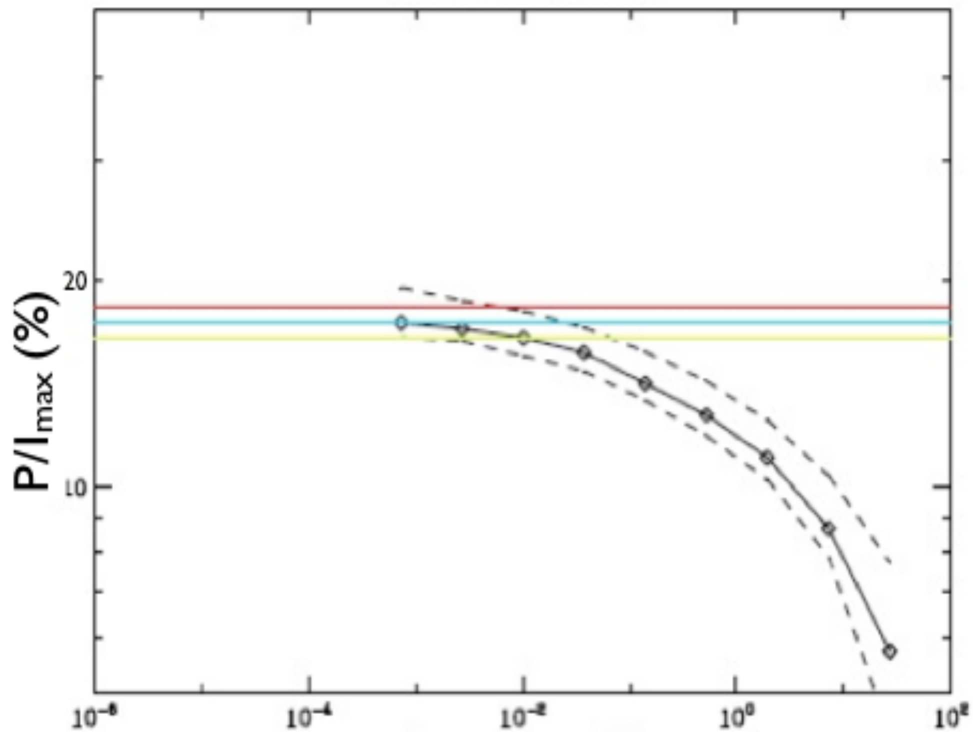


- The observed degree of polarization $(P/I)_{obs}$ is up to 18%.

➡**The intrinsic degree of dust polarization** $((P/I)_{dust} \geq (P/I)_{obs})$ **is high**

- This result is consistent with earlier results from the Archeops experiment (Benoit et al. 2004).

- $(P/I)_{dust}$ is likely to vary across the sky. Theory says alignment depends on the grain size distribution, the spectrum of the radiation field, and its orientation with respect to the B field. $H_2$ formation can also locally enhance $(P/I)_{dust}$ (Hoang & Lazarian 2008).

# CMB products & analysis - I

## CMB Stokes, T, Q & U maps with 4 methods

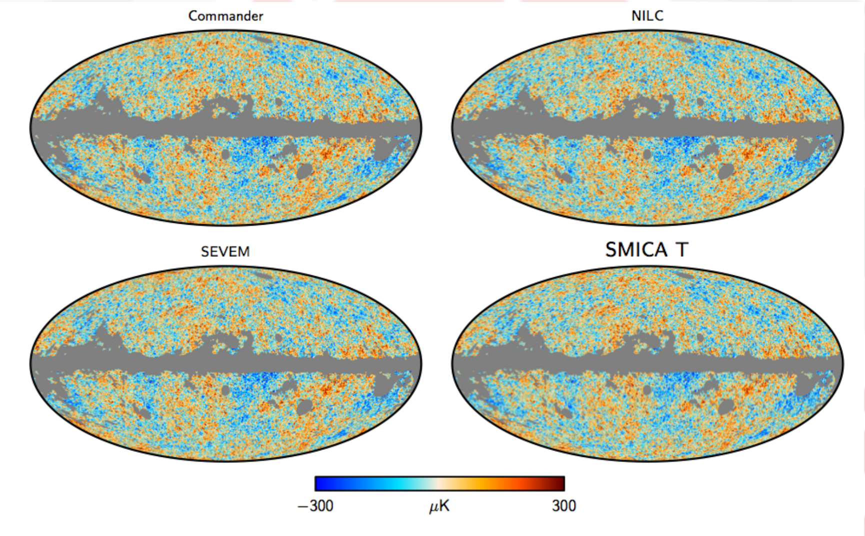


**Fig. 2.** Component-separated CMB temperature maps at full resolution, FWHM 5′, $N_{side}$ = 2048.

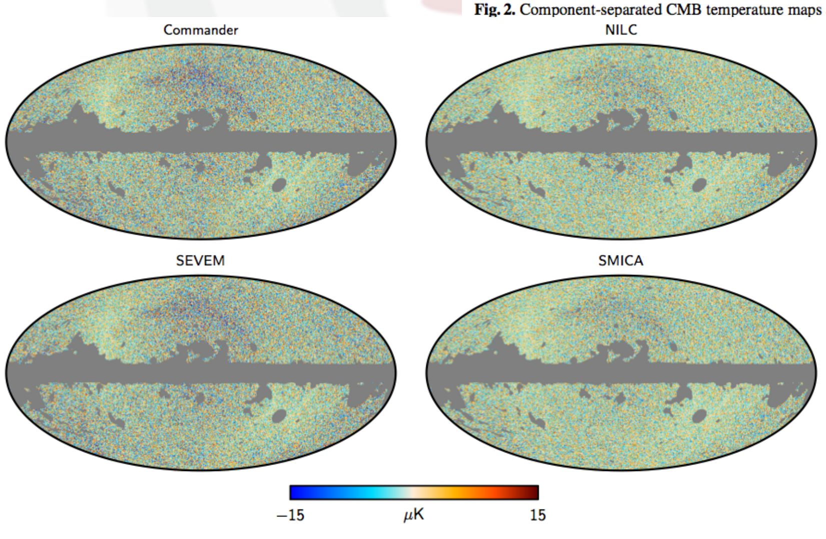


**Fig. 6.** Component-separated CMB $Q$ maps at resolution FWHM 10′, $N_{side}$ = 1024.

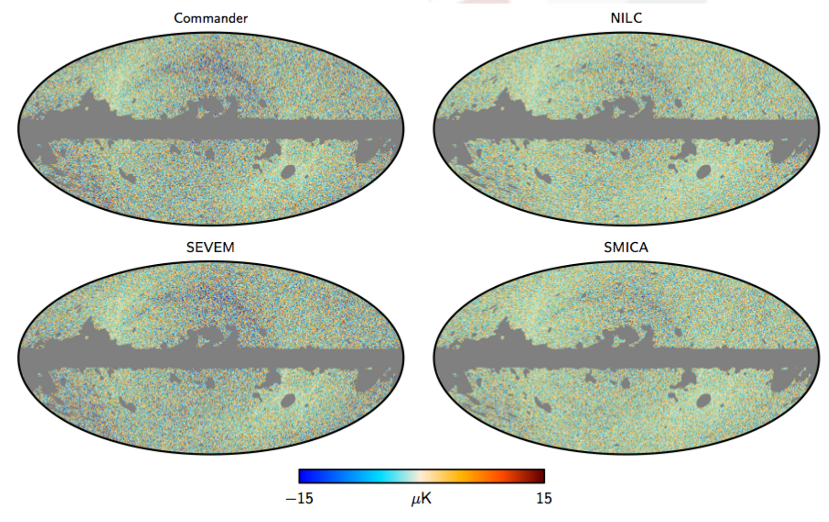


**Fig. 7.** Component-separated CMB $U$ maps at resolution FWHM 10′, $N_{side}$ = 1024.

# CMB products & analysis - II

**Consistency of CMB map from the 4 methods**

Cross-verifications also with cosmological parameter estimation, higher statistics (ex. for non-Gaussianity), cross-check on different masks & different fractions of satellite data

In T:

✧ Level of discrepancies & morphology similar to 2013

✧ Large differences on the Galactic plane

✧ @ high |b|, differences are due to strong, localized sources, or residal dipole differences betwen maps

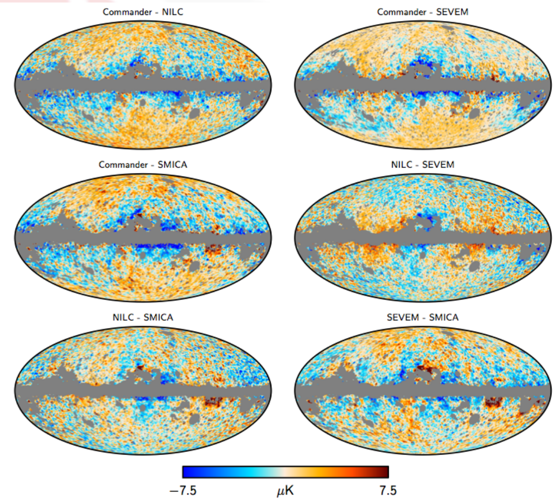


**Fig. 4.** Pairwise difference maps between CMB temperature maps. As in the previous Fig. 3, the maps have been smoothed to FWHM 80′ and downgraded to $N_{\rm side}$ = 128.

Q & U (Commander & SEVEM ) (NILC & SMICA) Solutions closest to each other

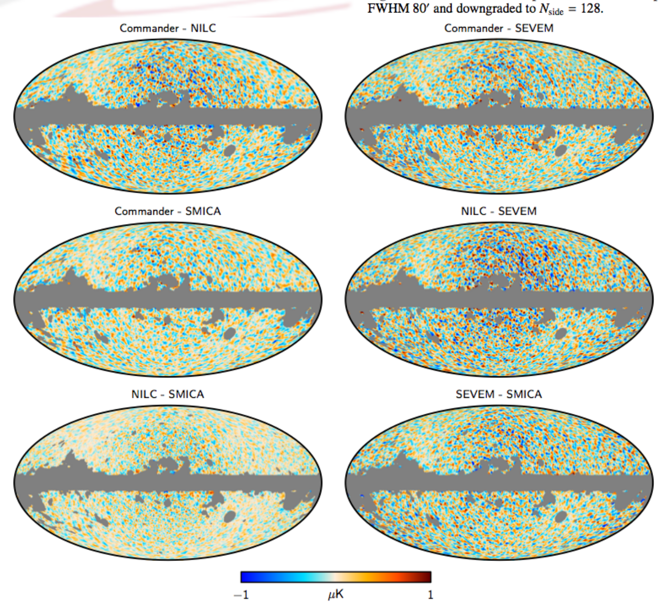


**Fig. 9.** Pairwise differences between CMB $Q$ maps, after smoothing to FWHM 80′ and downgrading to $N_{\rm side}$ = 128.

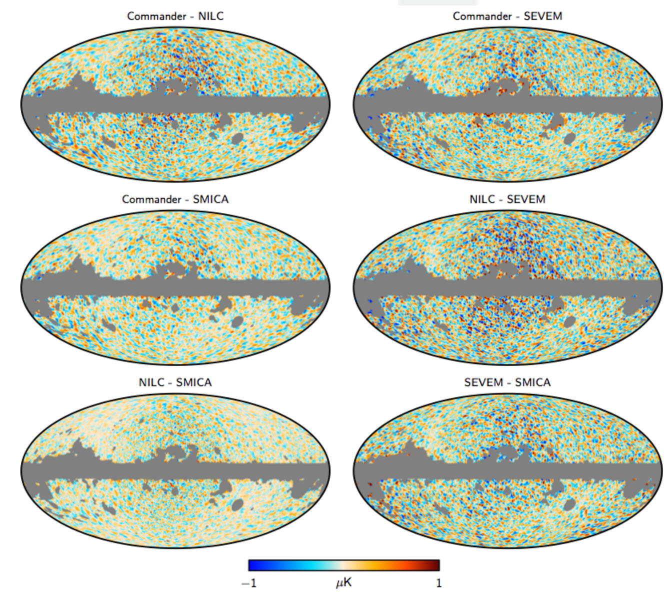


**Fig. 10.** Pairwise differences between CMB $U$ maps, after smoothing and downgrading as in Fig. 9.

# CMB maps and power spectrum from *Planck*
# Cosmological parameters & DM, DE, neutrinos …

# The CMB seen by *Planck* & its cosmological implications

2015

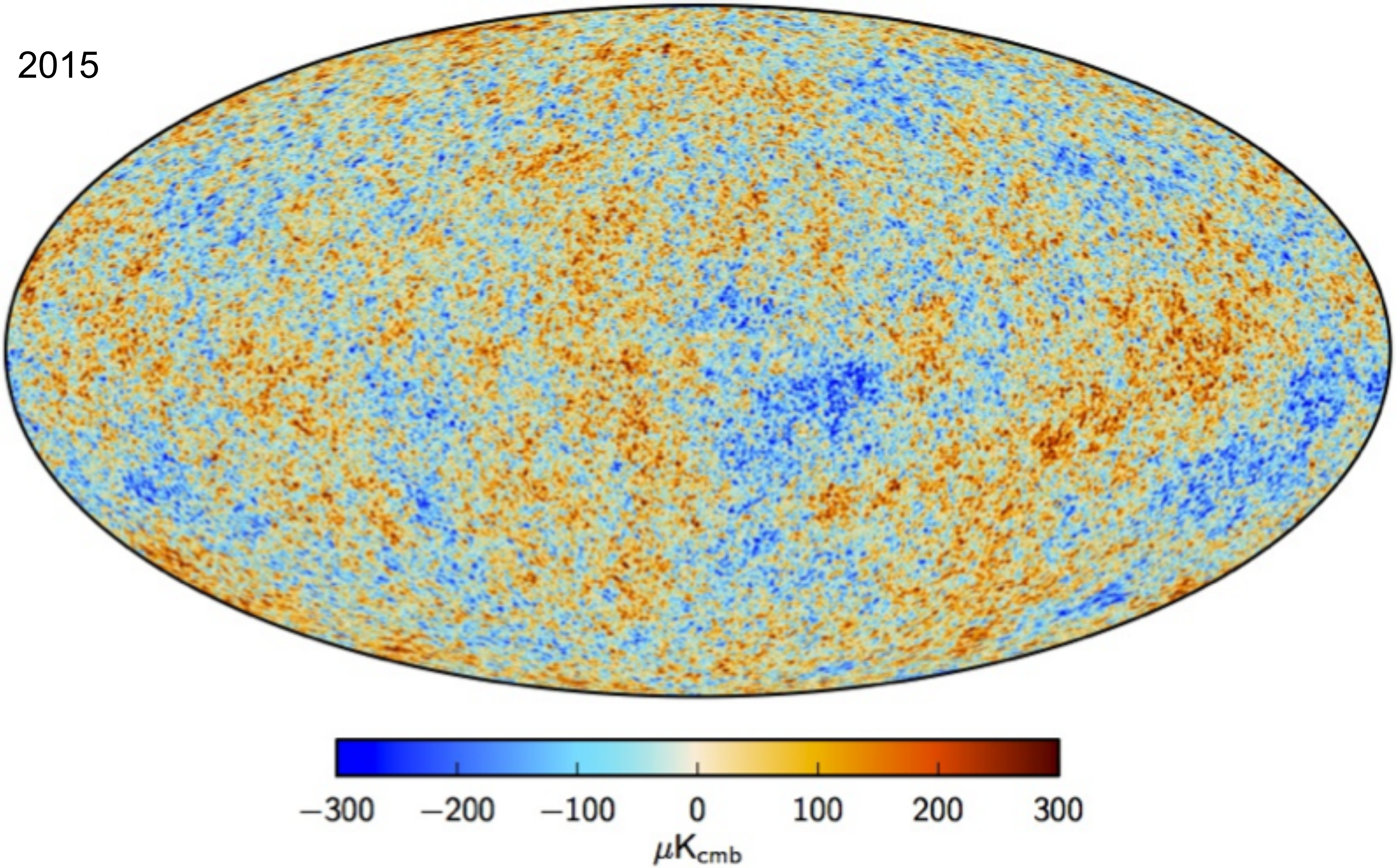

# CMB map in Q,U (2015)

***Planck* 2015**
**all-sky**
**CMB**
**polarization**
**maps**

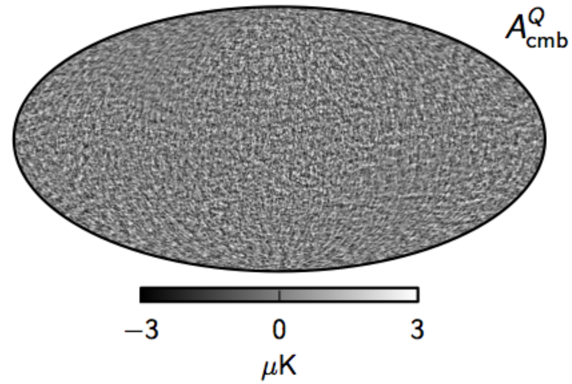


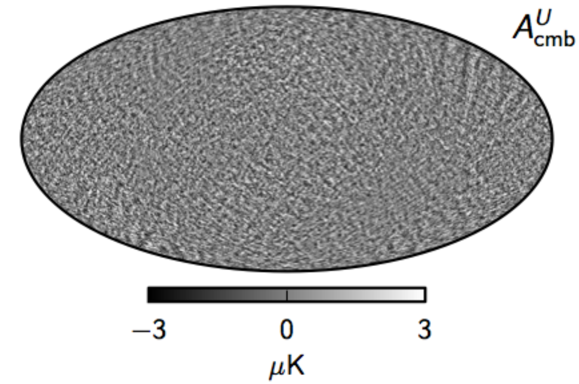


Maximum posterior amplitude Stokes Q (left) and U (right) maps derived from Planck observations between 30 and 353 GHz.
These maps have been high pass-filtered with a cosine-apodized filter between l= 20 and 40, and a 17% region of the Galactic plane has been replaced with a constrained Gaussian realization.

Planck 2015 Polarization map

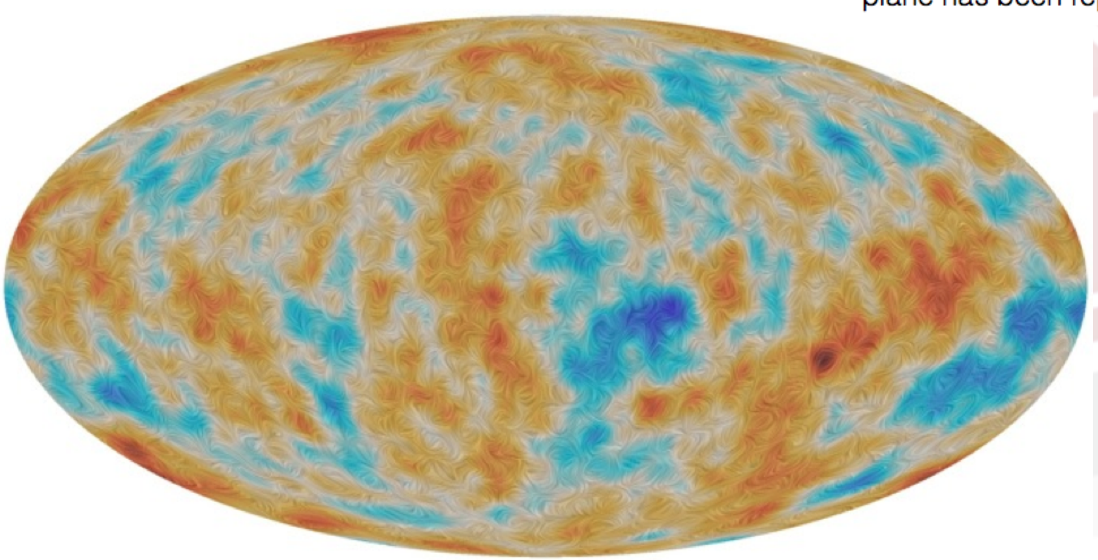

$$\Delta T(\vec{x}, \hat{n}, \tau) = \Sigma_{l=1}^{\infty} \Sigma_{m=-l}^{l} a_{lm}(\vec{x}, \tau) Y_{lm}(\hat{n})$$

# *Planck* CMB map & multipole components = 2, 3, 4

CMB_Tonly_G_ns256_K_nested.fits: UNKNOWN1

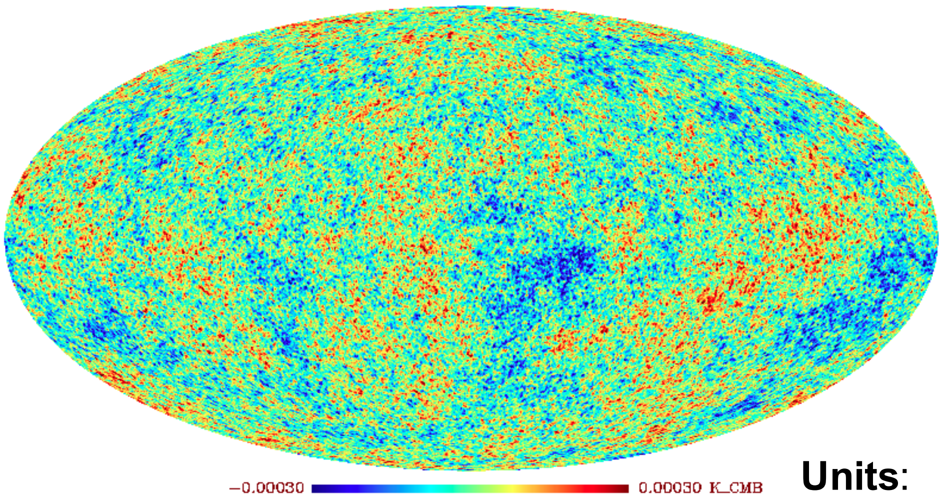


CMB_Tonly_G_ns256_K_nested_uptol_2.fits: TEMPERATURE

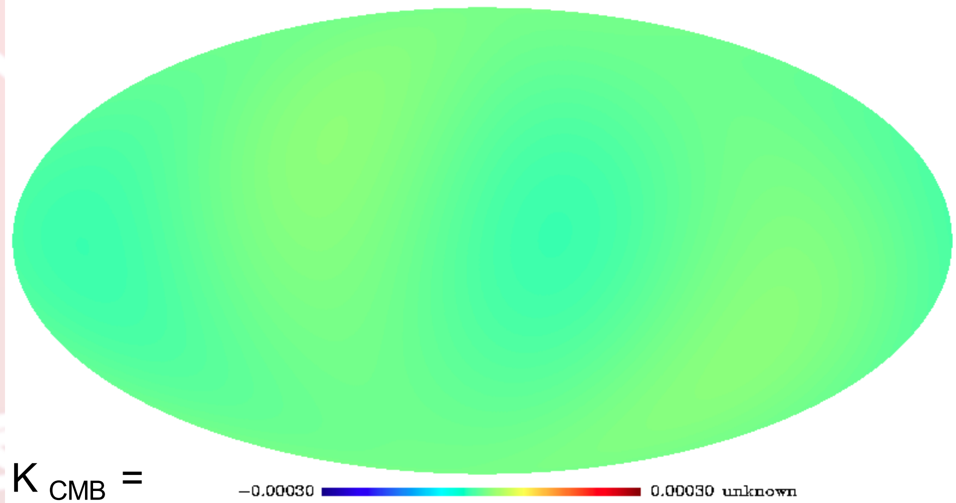


**Units**: K $_{CMB}$ = Eq. Therm.Temp.

CMB_Tonly_G_ns256_K_nested_uptol_3.fits: TEMPERATURE

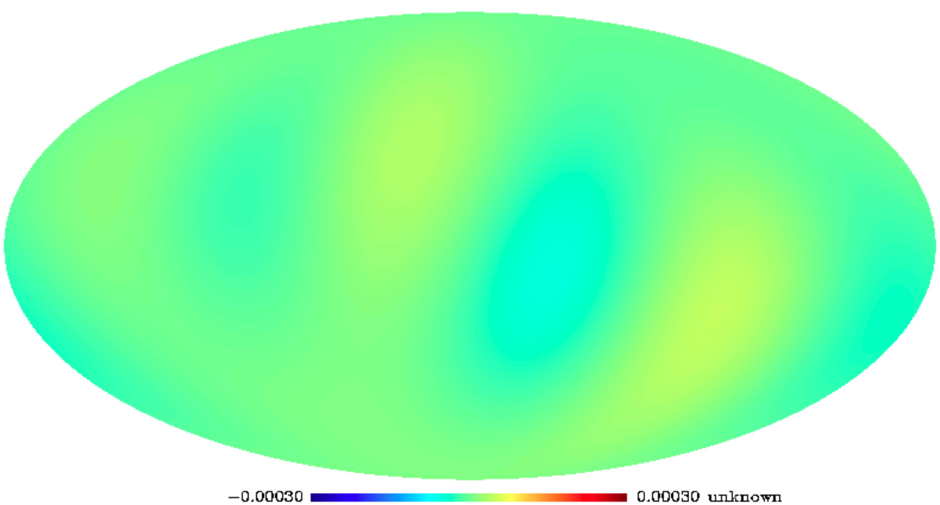


CMB_Tonly_G_ns256_K_nested_uptol_4.fits: TEMPERATURE

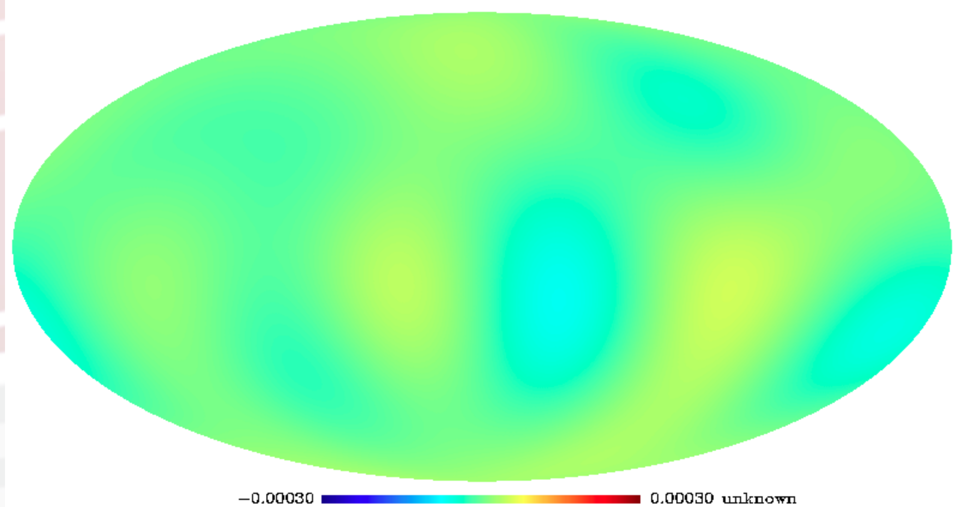

# multipole components = 5, 6, 7, 8

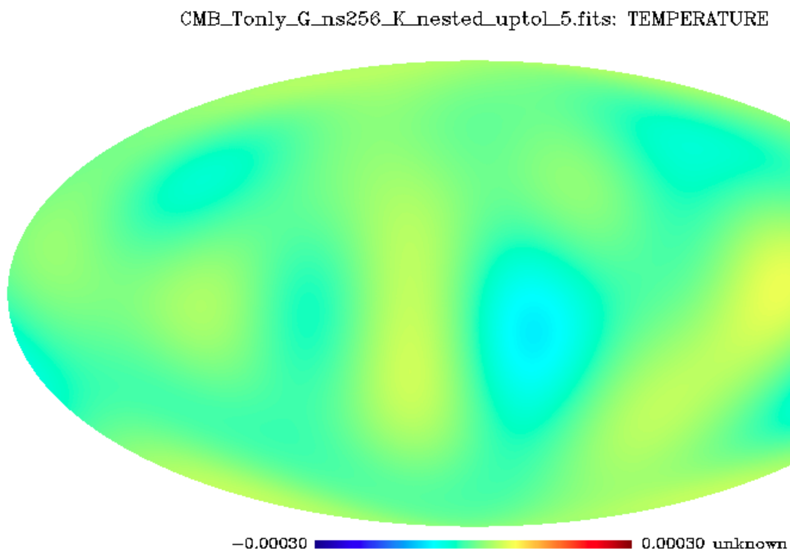


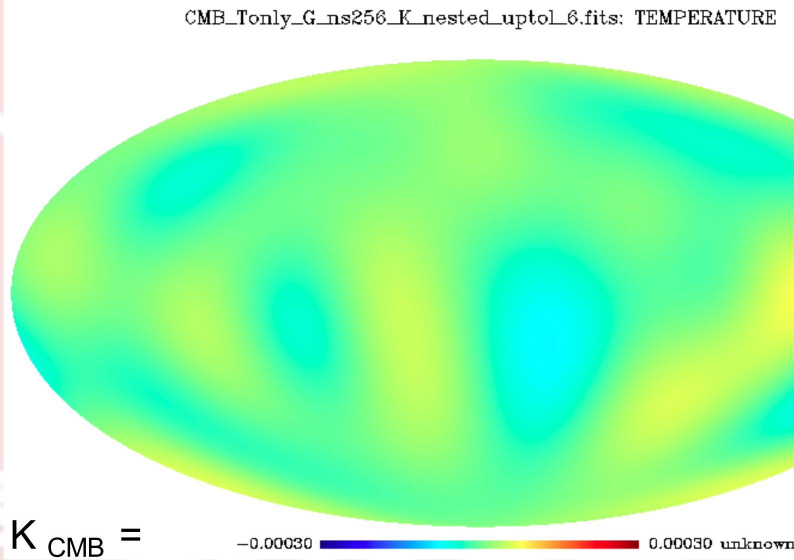


**Units**: K $_{CMB}$ =
Eq. Therm. Temp.

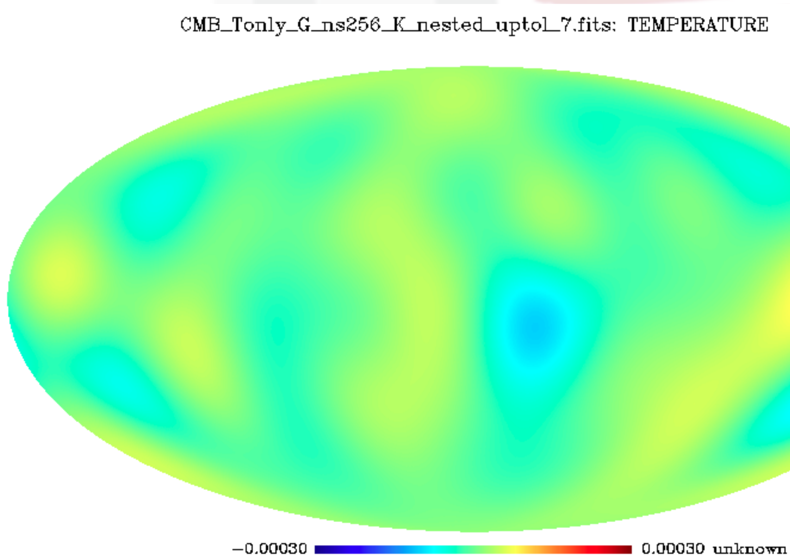


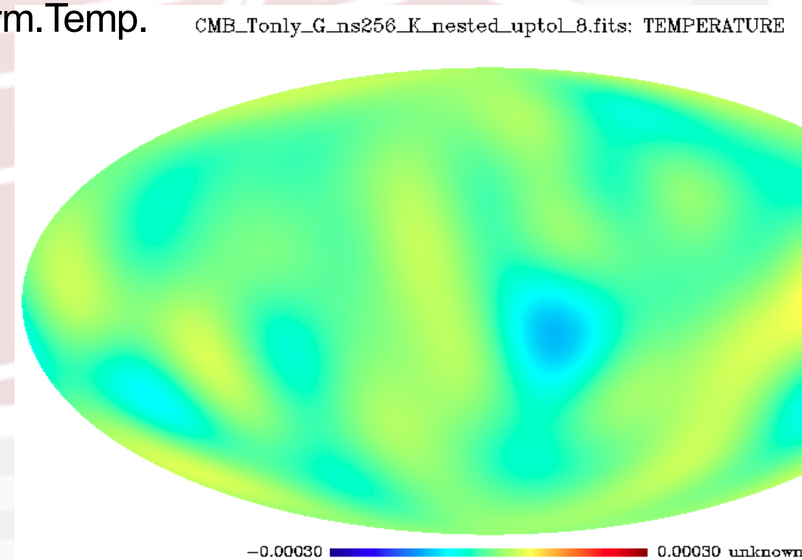

# multipole components = 9, 10, 11 & *Planck* CMB map

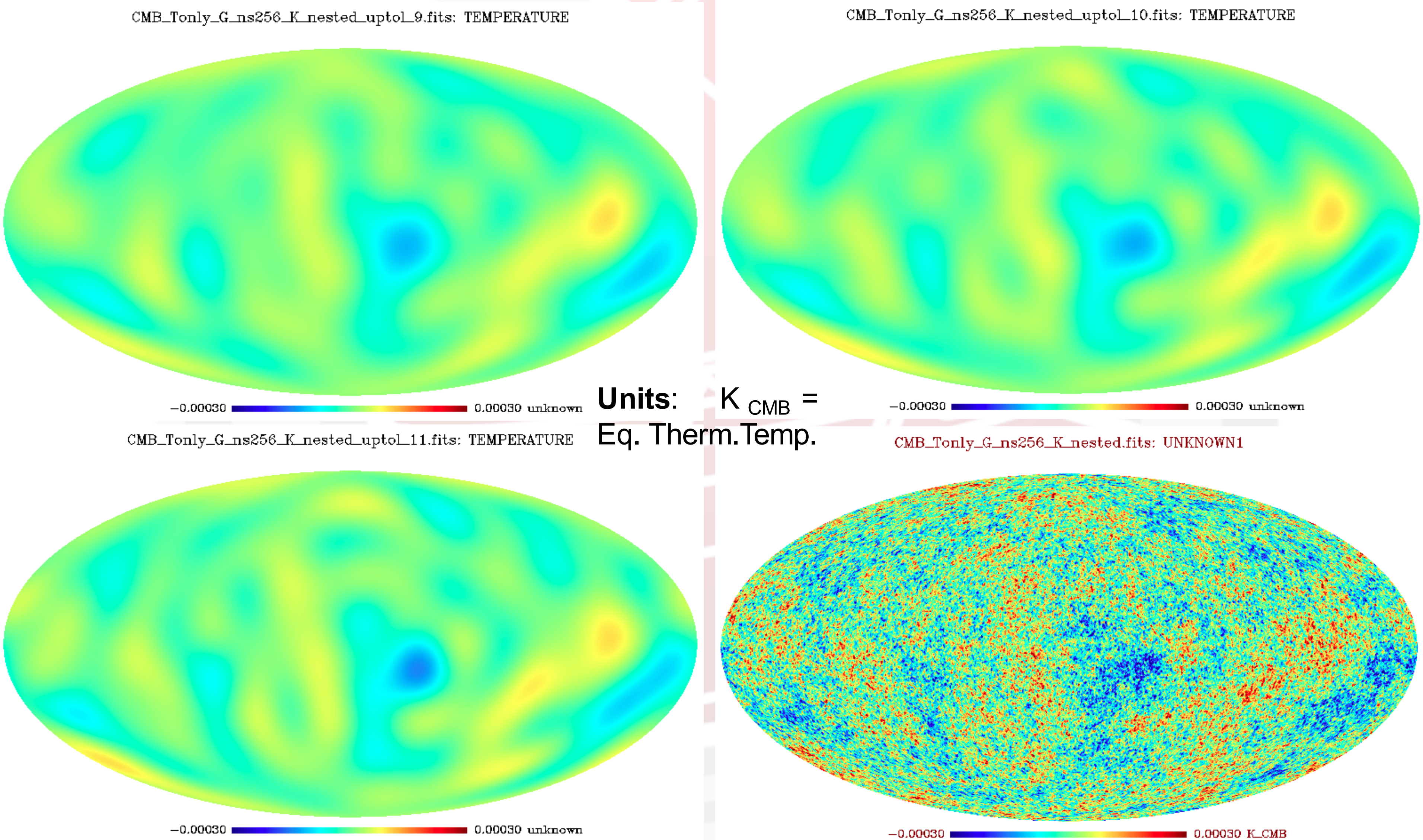


**Units**: $K_{CMB}$ = Eq. Therm.Temp.

# *Large scales*

# *Planck* results: flat-decoupled-Bianchi model?

There is an elephant in the room? ☺

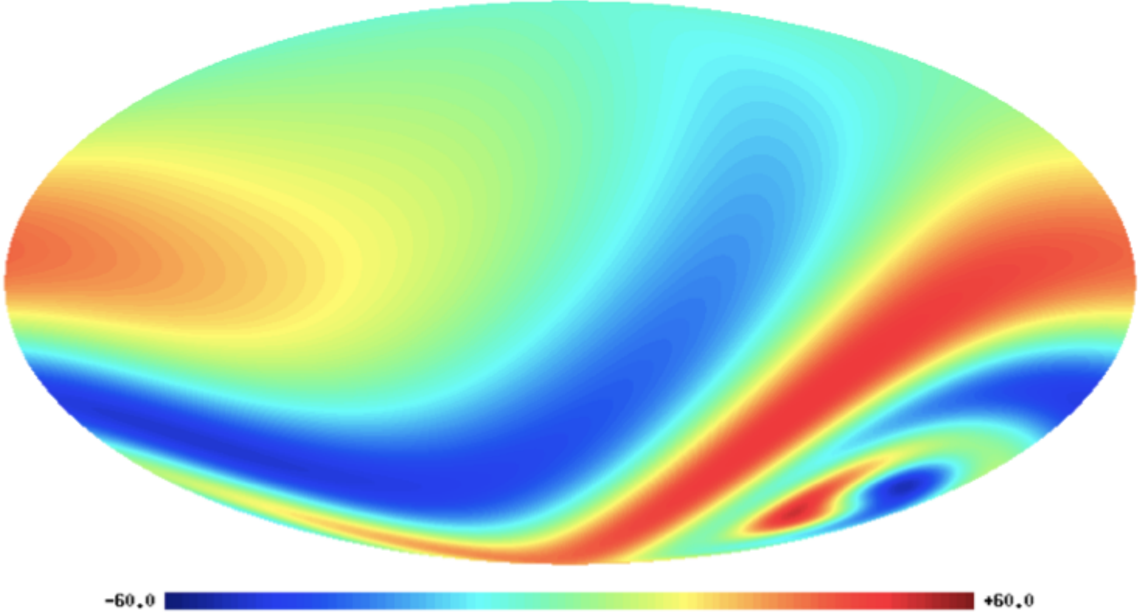


**Omogeneous but anisotropic**

**Generalization of the standard model generated by 3-parameter Lie groups: Bianchi IX (closed) vs Bianchi VIIh (open)**

**Biaxial symmetric Bianchi IX**

**→ "squashed 3-sphere" Universe**

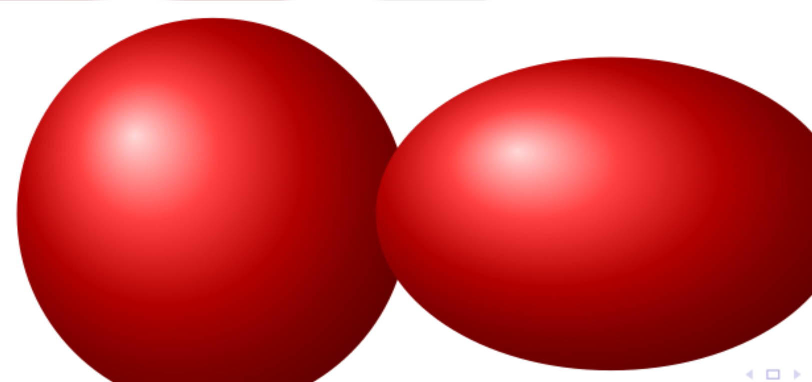

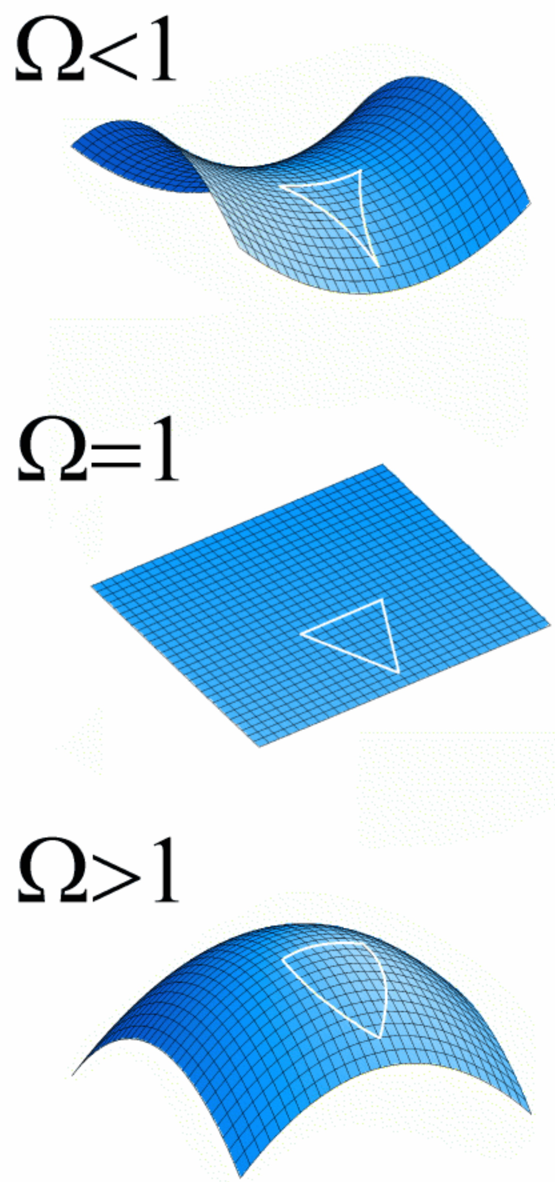


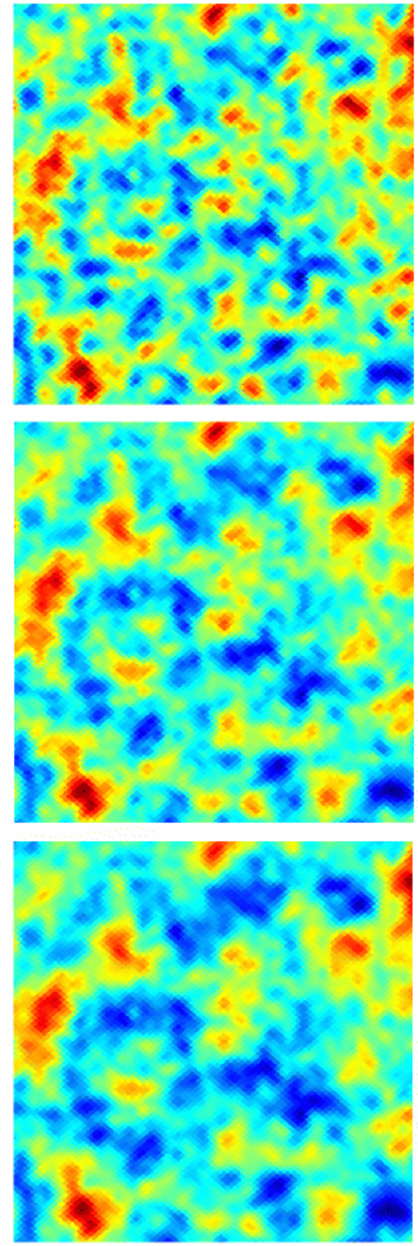

**Geometry of the Universe with CMB anisotropy at about 1 deg resolution**

# Gravitational lensing of CMB

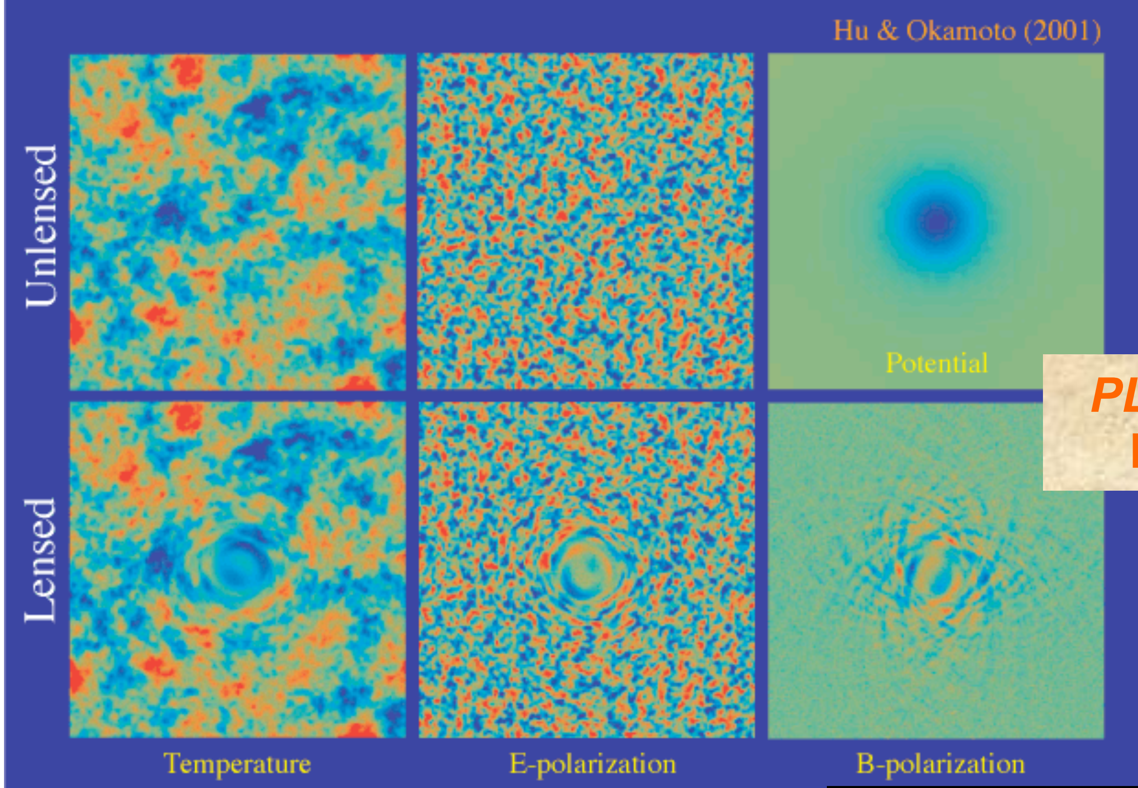


***PLANCK 2013-2015* HAS A 25-40 σ DETECTION OF CMB LENSING**

The effect is similar to a de-focusing of the maps

CMB photons are almost unperturbed in their journey from the last scattering surface … but not completely … **LENSING EFFECT**

MATTER DISTRIBUTION DEFLECTS THE LIGHT PATH LENSING THE CMB PHOTONS

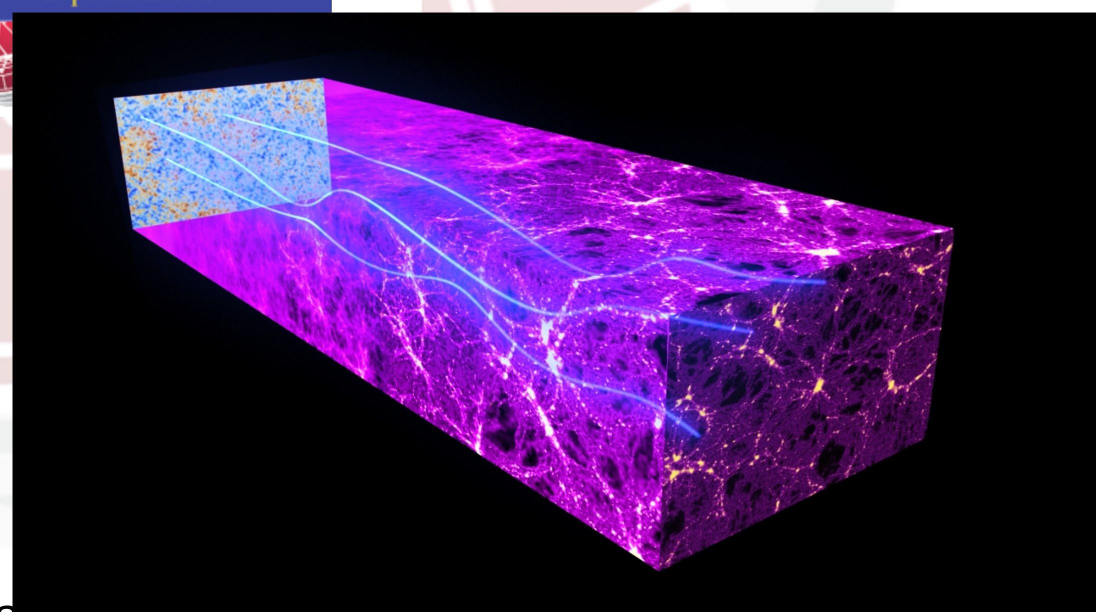

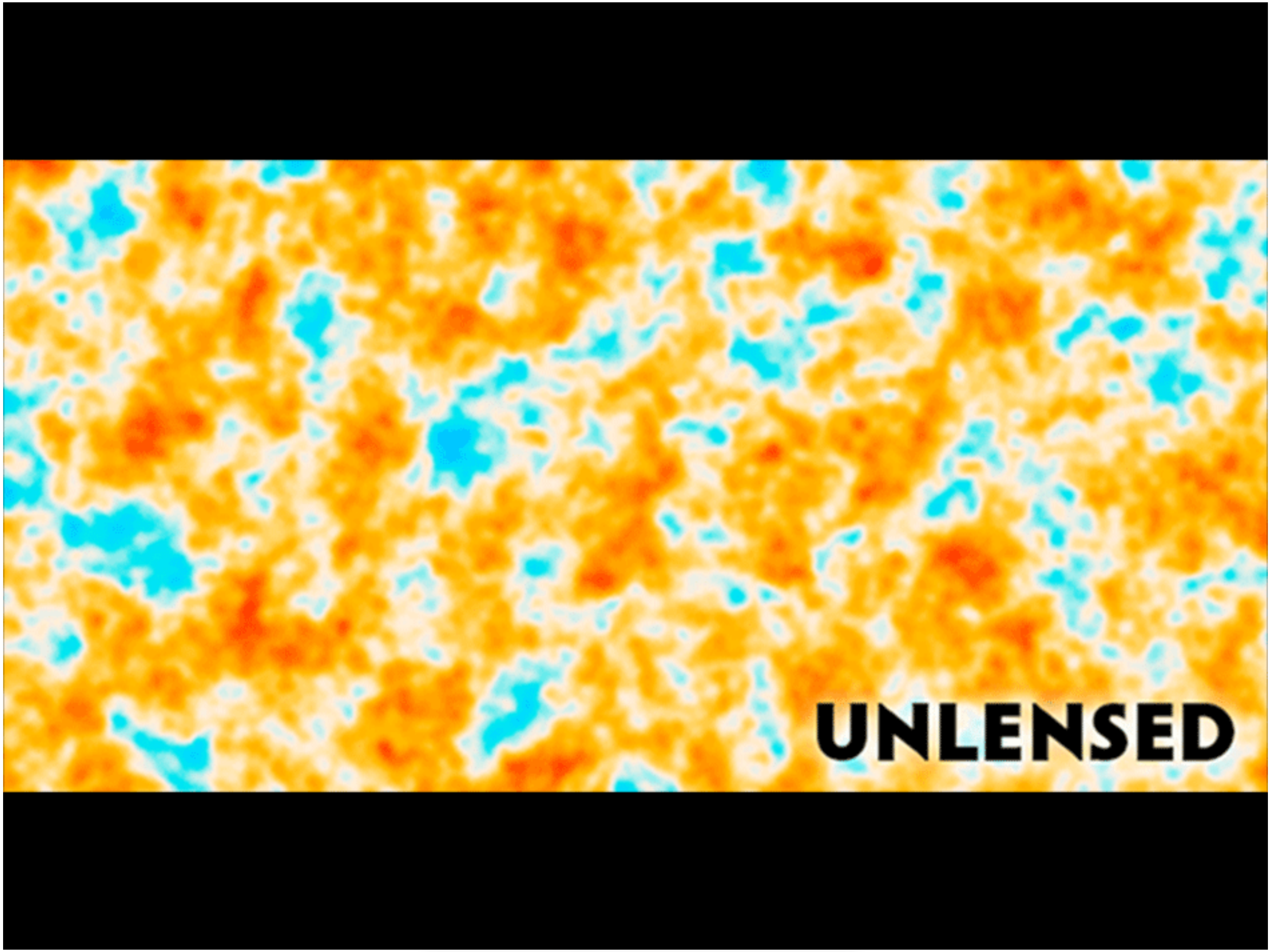
UNLENSED

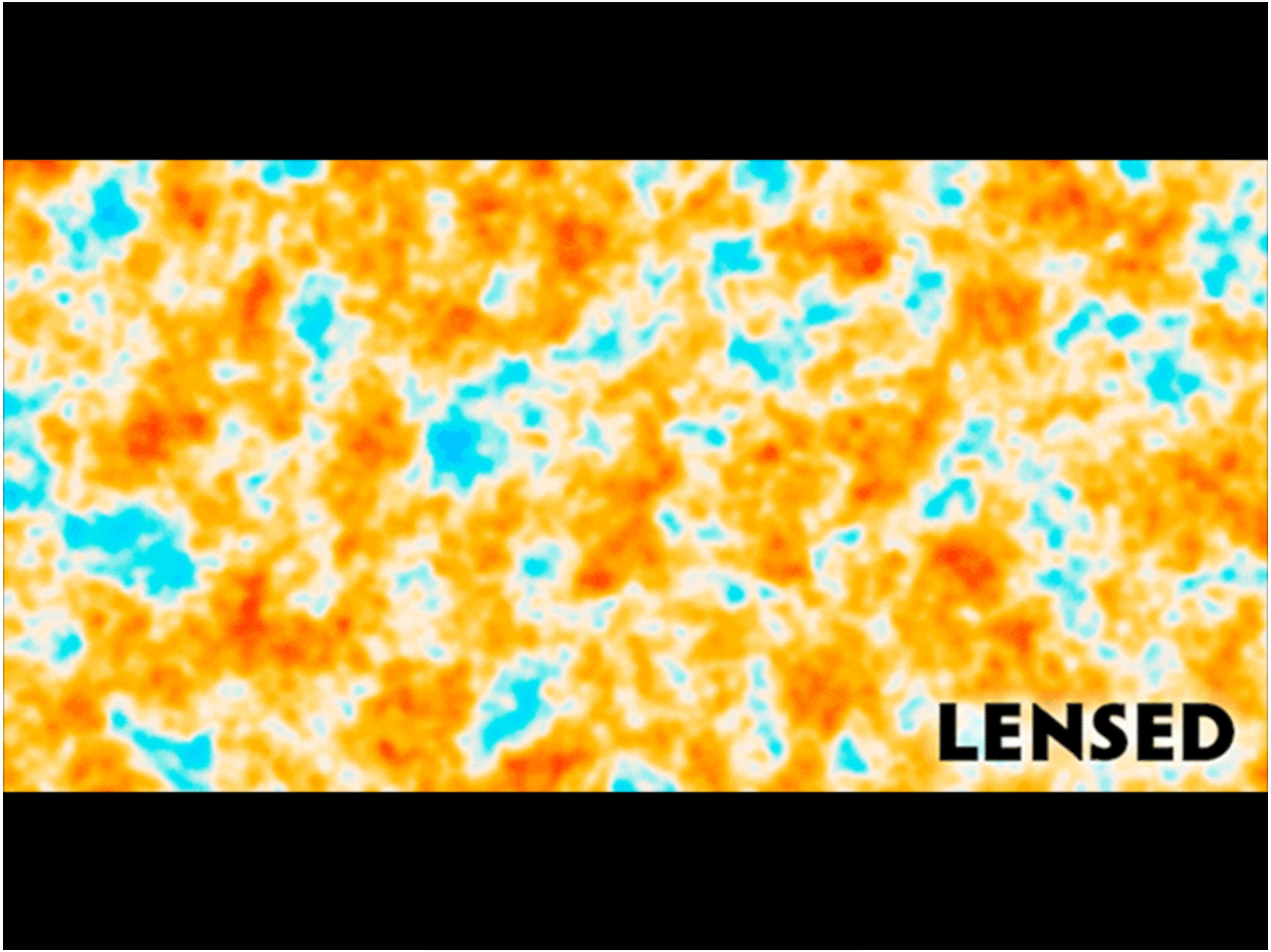
LENSED

# APS DEPENDENCE ON COSMOLOGICAL PARAMETERS

***Planck*: a single experiment spanning a wide multipole range!**

**Theta → first peak position**

**Baryon Density → height difference between even and odd peaks**

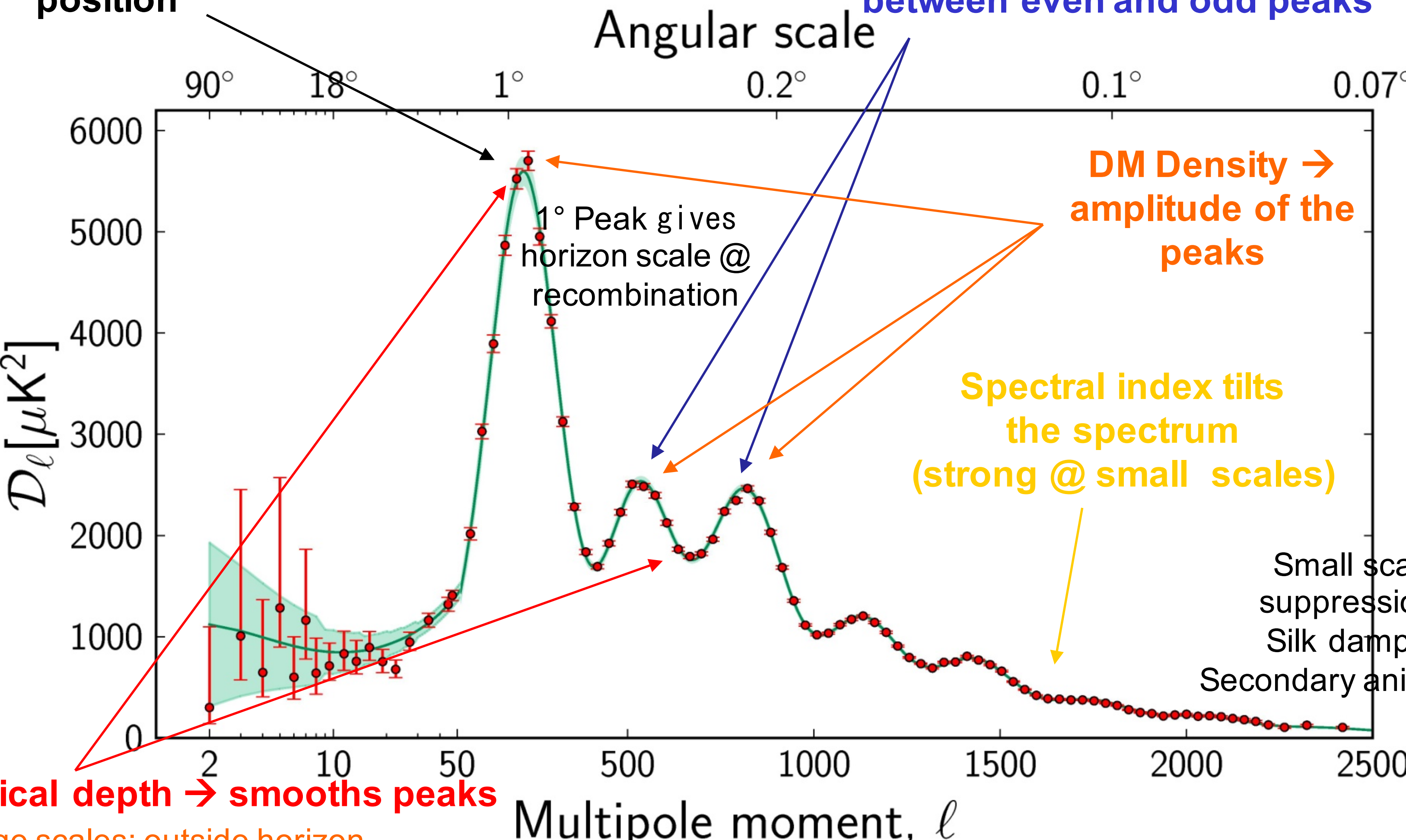


1° Peak gives horizon scale @ recombination

**DM Density → amplitude of the peaks**

**Spectral index tilts the spectrum (strong @ small scales)**

Small scales: suppression by Silk damping - Secondary anisotropies

**Optical depth → smooths peaks**

Large scales: outside horizon @ recombination – only gravity

Intermediate scales: photon-baryon fluid acoustic oscillations - DM potential well vs radiation pressure

# Planck 2015 APS

From Planck 2015 results. XX.

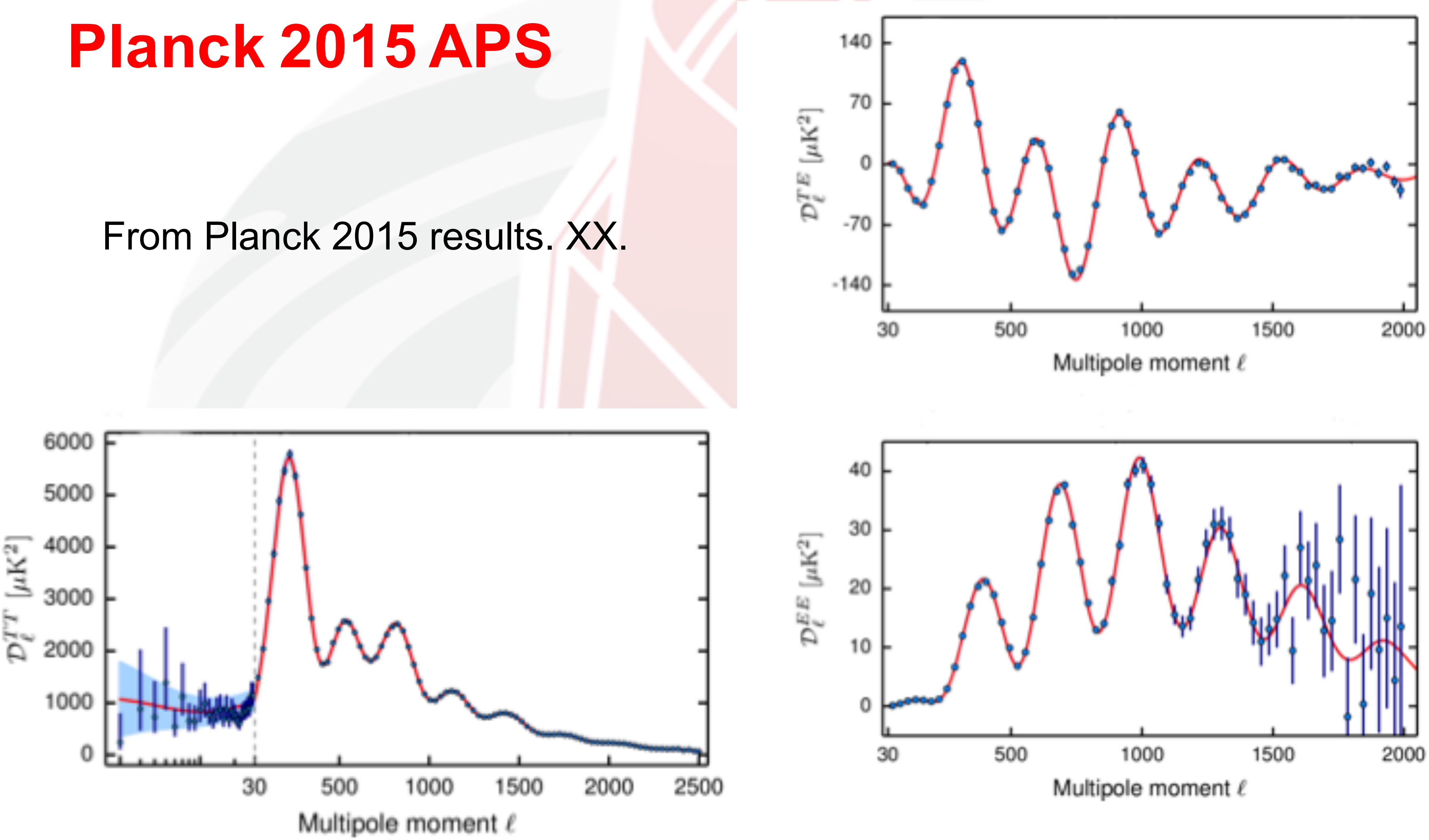


**Fig. 2.** *Planck* $TT$ (top), high-$\ell$ $TE$ (centre), and high-$\ell$ $EE$ (bottom) angular power spectra. Here $\mathcal{D}_\ell \equiv \ell(\ell+1)C_\ell/(2\pi)$.

# Current status: CMB & foregrounds in terms of APS

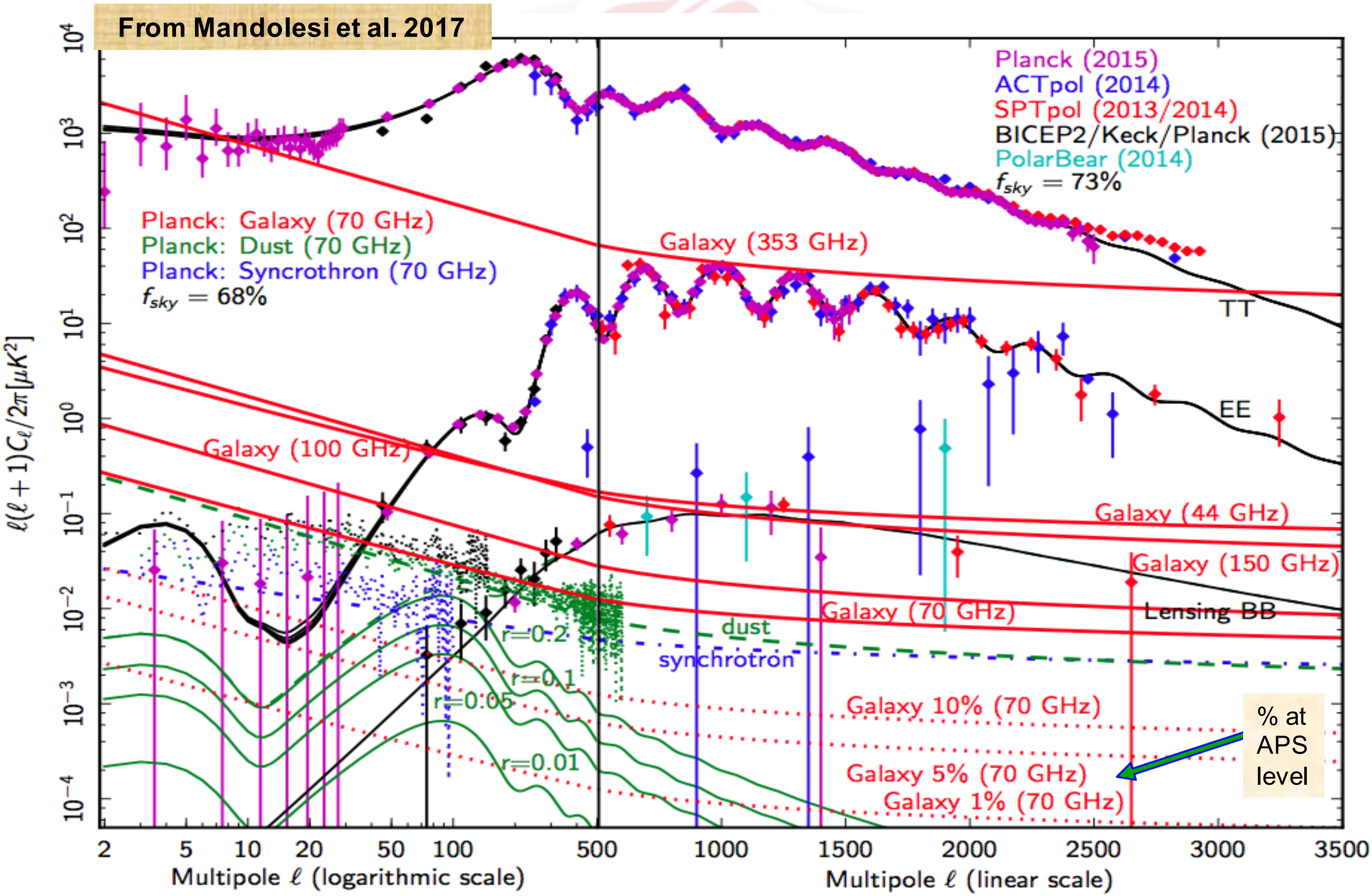


C. Burigana – Varenna 6/7/2017

# Non-Gaussianity … mainly through CMB bispectrum

$$B^{m_1 m_2 m_3}_{\ell_1 \ell_2 \ell_3} \equiv \langle a_{\ell_1 m_1} a_{\ell_2 m_2} a_{\ell_3 m_3} \rangle$$

$$= \mathcal{G}^{\ell_1 \ell_2 \ell_3}_{m_1 m_2 m_3} \, b_{\ell_1 \ell_2 \ell_3}$$

Gaunt integrals

$$\mathcal{G}^{\ell_1 \ell_2 \ell_3}_{m_1 m_2 m_3} \equiv \int Y_{\ell_1 m_1}(\hat{n}) \, Y_{\ell_2 m_2}(\hat{n}) \, Y_{\ell_3 m_3}(\hat{n}) \, d^2\hat{n}$$
$$= h_{\ell_1 \ell_2 \ell_3} \begin{pmatrix} \ell_1 & \ell_2 & \ell_3 \\ m_1 & m_2 & m_3 \end{pmatrix},$$

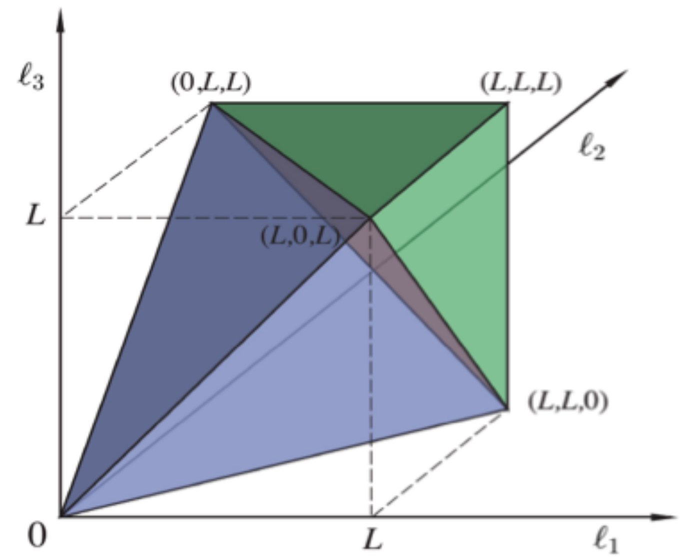


Triangle condition: $\ell_1 \le \ell_2 + \ell_3$ for $\ell_1 \ge \ell_2, \ell_3$, +perms.

Parity condition: $\ell_1 + \ell_2 + \ell_3 = 2n, \quad n \in \mathbb{N},$

Resolution: $\ell_1, \ell_2, \ell_3 \le \ell_{\max}, \quad \ell_1, \ell_2, \ell_3 \in \mathbb{N}.$

(1) Multiple fields (local models, non-linearities develop outside horizon)

(2) Non-canonical kinetic term of quantum fields (higher derivative interactions; Dirac-Born-Infeld, K-inflation)

(3) Non-vacuum initial conditions

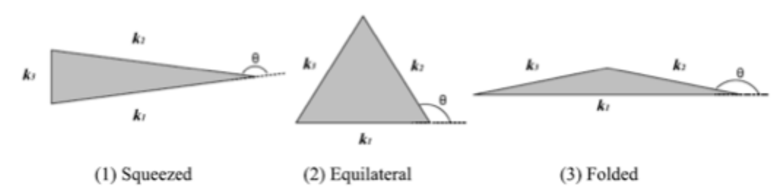


+ many more

# $f_{NL}$ from *Planck* data

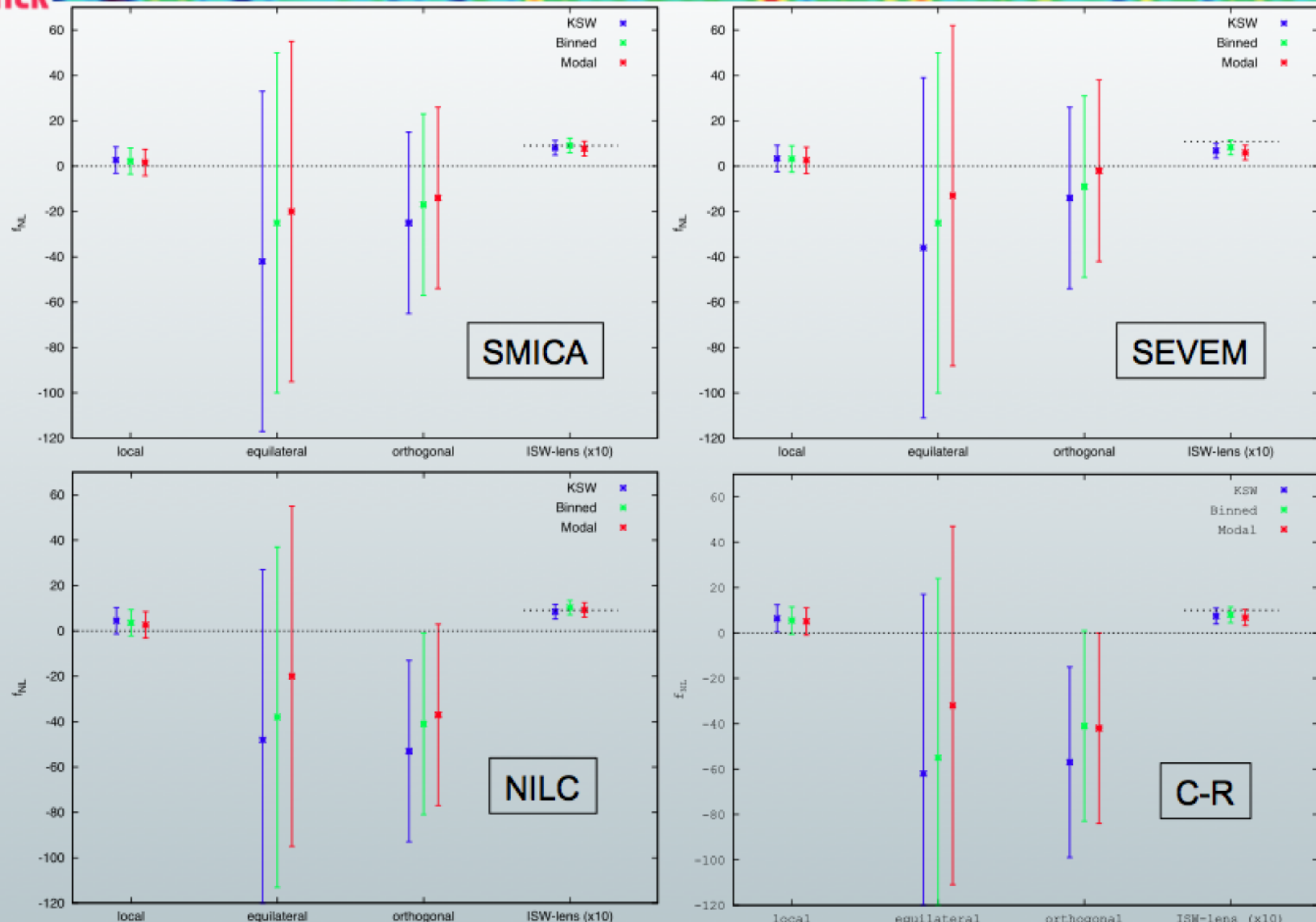


C. Burigana – Varenna 6/7/2017

# *PLANCK* COSMOLOGICAL PARAMETERS

The CMB anisotropy angular power spectrum shape and amplitude is strongly dependent on the underlying cosmological model.

Cosmological models are characterized by cosmological parameters

## STANDARD VANILLA MODEL PARAMETERS

- Baryon Density today $\omega_{\mathrm{b}} \equiv \Omega_{\mathrm{b}} h^2$
- Dark Matter Density today $\omega_{\mathrm{c}} \equiv \Omega_{\mathrm{c}} h^2$
- Horizon @REC Angular Diameter Distance $100\theta_{\mathrm{MC}}$
- Optical depth for reionization $\tau$
- Cosmological perturbation tilt $P(k) = A_s k^n$ $n_{\mathrm{s}}$
- Cosmological perturbation amplitude $\ln(10^{10} A_{\mathrm{s}})$

# Some more information on parameter definition - I

- Evolution of cosmic scale factor $a=1/(1+z)$

$$H^2 = [(da/dt)/a]^2 = [da / (a^2\, d\eta)]^2 = (8\pi G/3)\,[\rho_M/a^3 + \rho_R/a^4 + \rho_v(a) + \rho_\Lambda + \rho_K/a^2]$$

where $d\eta=dt/a$, $t$ =time, $\eta$=conformal time

- Ratio of energy densities relative to the total:

$\Omega_i=3\rho_i/(8\pi G H_0^2)$ ; $H_0 = H(@\ t=\text{today})$ = Hubble constant,

$h=H_0/[100 Km/s/Mpc]$ $1/H_0$ related to the age of the Universe

for example: $t_0= (2/3)/H_0$ for a simple Einstein-de Sitter model

- $\rho_\Lambda= 3\Lambda/(8\pi G)$ ; $\rho_K= 3K/(8\pi G)$ (K=0,+1,-1)

# Some more information on parameter definition - II

- Thomson optical depth due to reionization $\tau = \int \chi_e n_e \sigma_T c dt$
  (integral from the raising of ionization fraction after "quiescent phase" following recombination up to current epoch)

- Redshift of last-scattering, $z_\star$, such that optical depth to Thomson scattering from z = 0 to z = $z_\star$ is unity, assuming no reionization

- Angular scale of the sound horizon at last-scattering

$$\theta_* = r_s(z_*)/D_A(z_*)$$

where $r_s(z) = \int_0^{\eta(z)} \frac{d\eta'}{\sqrt{3(1+R)}},$ with $R \equiv 3\rho_b/(4\rho_\gamma)$

- Typically $100 \times \theta_\star$ is given

# *PLANCK* COSMOLOGICAL PARAMETERS: ΛCDM model

# 2015 Release

**Table 3.** Parameters of the base ΛCDM cosmology computed from the 2015 baseline *Planck* likelihoods illustrating the consistency of parameters determined from the temperature and polarization spectra at high multipoles. Column [1] uses the *TT* spectra at low and high multipoles and is the same as column [6] of Table 1. Columns [2] and [3] use only the *TE* and *EE* spectra at high multipoles, and only polarization at low multipoles. Column [4] uses the full likelihood. The last column lists the deviations of the cosmological parameters determined from the TT+lowP and TT,TE,EE+lowP likelihoods.

| Parameter | [1] *Planck* TT+lowP | [2] *Planck* TE+lowP | [3] *Planck* EE+lowP | [4] *Planck* TT,TE,EE+lowP | $([1]-[4])/\sigma_{[1]}$ |
|---|---|---|---|---|---|
| $\Omega_b h^2$ . . . . . . . . . . | $0.02222 \pm 0.00023$ | $0.02228 \pm 0.00025$ | $0.0240 \pm 0.0013$ | $0.02225 \pm 0.00016$ | $-0.1$ |
| $\Omega_c h^2$ . . . . . . . . . . | $0.1197 \pm 0.0022$ | $0.1187 \pm 0.0021$ | $0.1150^{+0.0048}_{-0.0055}$ | $0.1198 \pm 0.0015$ | $0.0$ |
| $100\theta_{MC}$ . . . . . . . . | $1.04085 \pm 0.00047$ | $1.04094 \pm 0.00051$ | $1.03988 \pm 0.00094$ | $1.04077 \pm 0.00032$ | $0.2$ |
| $\tau$ . . . . . . . . . . . . . | $0.078 \pm 0.019$ | $0.053 \pm 0.019$ | $0.059^{+0.022}_{-0.019}$ | $0.079 \pm 0.017$ | $-0.1$ |
| $\ln(10^{10} A_s)$ . . . . . . | $3.089 \pm 0.036$ | $3.031 \pm 0.041$ | $3.066^{+0.046}_{-0.041}$ | $3.094 \pm 0.034$ | $-0.1$ |
| $n_s$ . . . . . . . . . . . . | $0.9655 \pm 0.0062$ | $0.965 \pm 0.012$ | $0.973 \pm 0.016$ | $0.9645 \pm 0.0049$ | $0.2$ |
| $H_0$ . . . . . . . . . . . | $67.31 \pm 0.96$ | $67.73 \pm 0.92$ | $70.2 \pm 3.0$ | $67.27 \pm 0.66$ | $0.0$ |
| $\Omega_m$ . . . . . . . . . . . | $0.315 \pm 0.013$ | $0.300 \pm 0.012$ | $0.286^{+0.027}_{-0.038}$ | $0.3156 \pm 0.0091$ | $0.0$ |
| $\sigma_8$ . . . . . . . . . . . . | $0.829 \pm 0.014$ | $0.802 \pm 0.018$ | $0.796 \pm 0.024$ | $0.831 \pm 0.013$ | $0.0$ |
| $10^9 A_s e^{-2\tau}$ . . . . . . | $1.880 \pm 0.014$ | $1.865 \pm 0.019$ | $1.907 \pm 0.027$ | $1.882 \pm 0.012$ | $-0.1$ |

**Main difference with respect to previous release in τ**
**now polarization comes from *Planck***

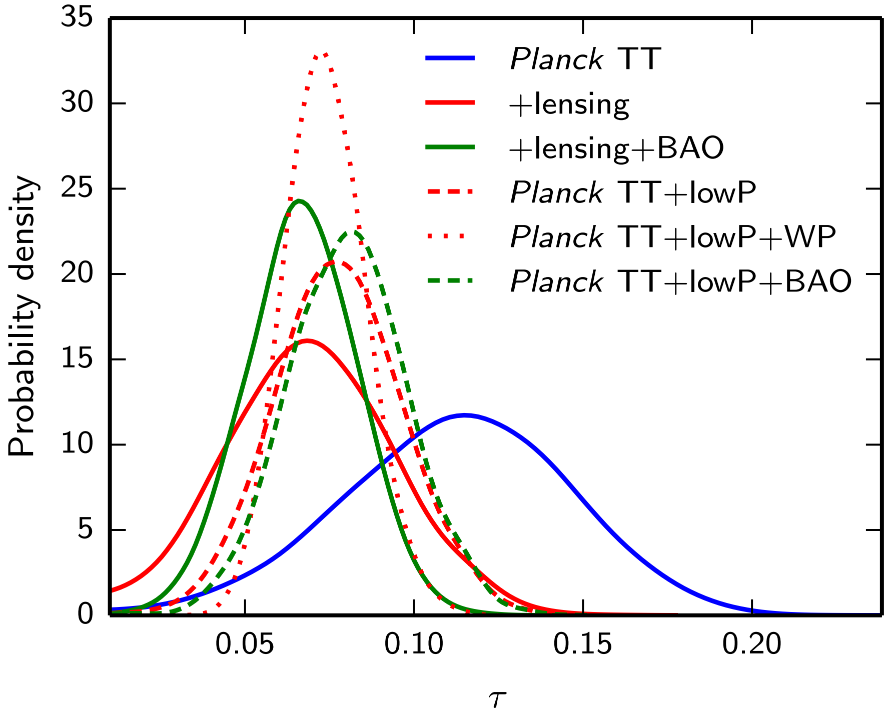


# First luminous sources in the Universe: cosmological reionization

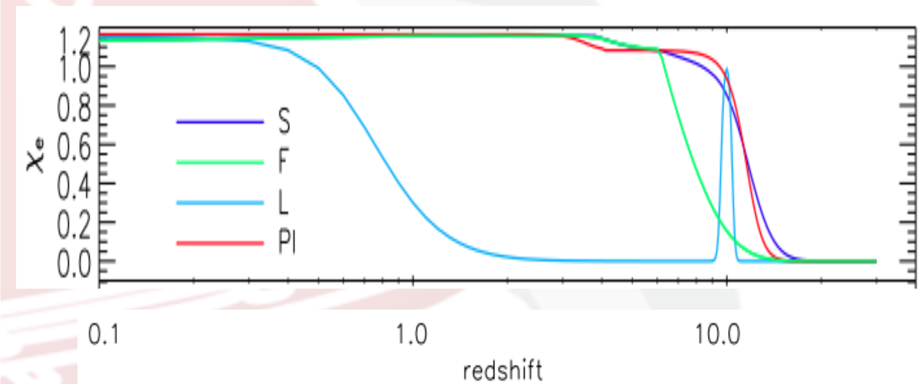


**WP (WMAP 9) reanalysed with *Planck* dust emission maps**

$$\tau = 0.066 \pm 0.0016 \quad z_{\rm re} = 8.8^{+1.7}_{-1.4} \quad (68\,\%\mathrm{CL}\,, \textit{Planck}\,\mathrm{TT} + \mathrm{lensing} + \mathrm{lowP})$$

$$\tau = 0.074^{+0.011}_{-0.013} \quad z_{\rm re} = 9.6 \pm 1.1 \quad (68\,\%\mathrm{CL}\,, \textit{Planck}\,\mathrm{TT} + \mathrm{lowP} + \mathrm{WP})$$

More accurate CMB polarization measurements will allow reionization history reconstruction **"beyond the τ approximation"** with both "blind" methods" (e.g. principal component method, reconstruction of $\chi_e$ in $z$ bins) and estimation (e.g. with MCMC methods) of physical / phenomenological reionization model parameters.

Before *Planck*

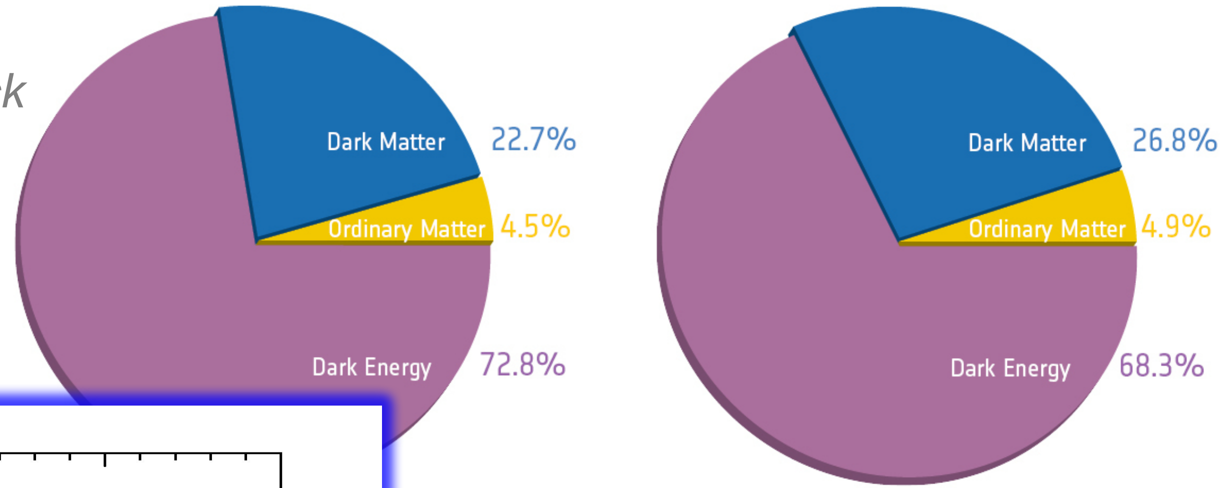


After Planck

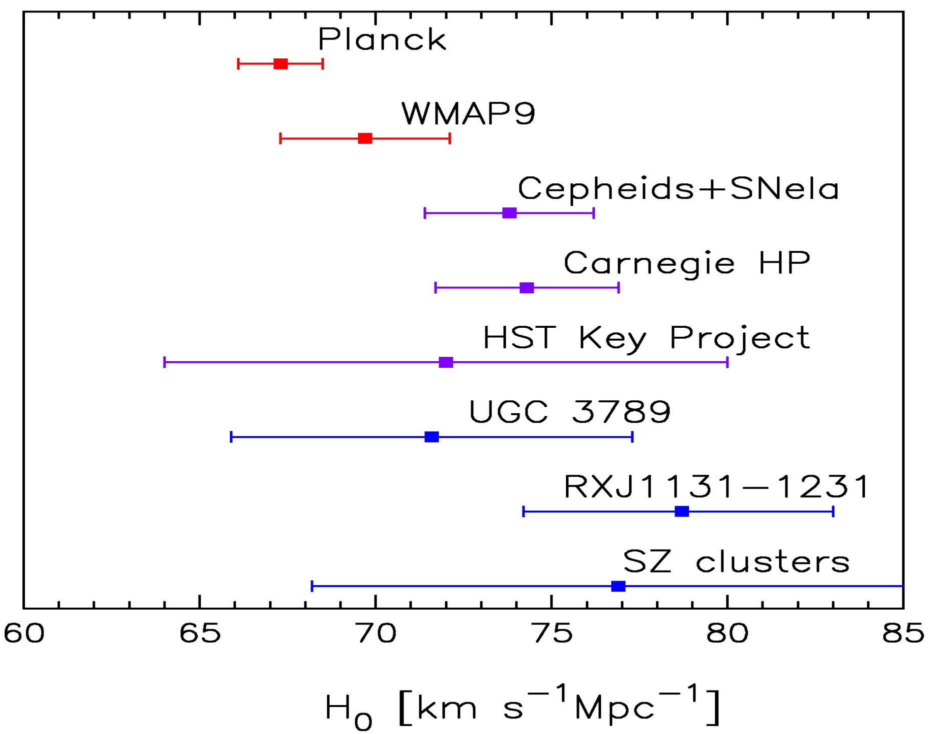


**Types of energy densities**
**&**
**Universe age**

# Robustness $n_s$ - r

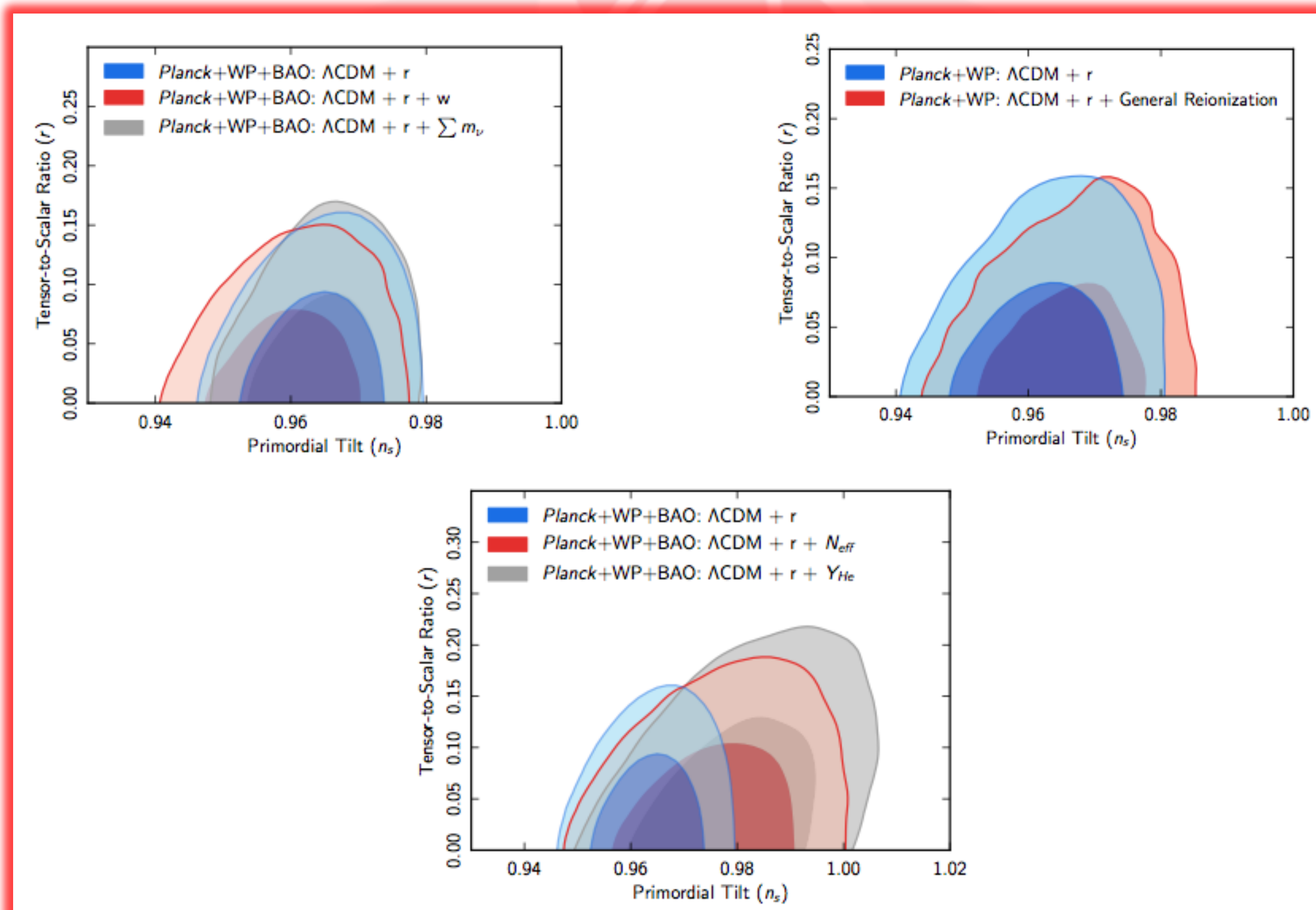

# Initial conditions of the Universe

***Planck* 2015 results XX: Constraints on inflation**

Euclidean geometry $\Omega_K = -0.005^{+0.016}_{-0.017}$ 68%CL

Primordial perturbations spectrum $n_s = 0.968 \pm 0.006$ 68%CL

Spectral index of primordial perturbation: limits on running $\frac{dn_s}{d\ln k} = -0.003 \pm 0.007$ 68%CL

$r_{0.002} < 0.11$ 95 %CL

$r_{0.002} < 0.09$ (incl. BICEP/KeckArray/Planck) 95 %CL

Isocurvature perturbations $\beta_{\rm iso} < 0.038$ 95%CL

Gaussian perturbations

$f_{\rm NL}^{\rm local} = 2.5 \pm 5.7$

$f_{\rm NL}^{\rm equil} = -16 \pm 70$ 68%CL

$f_{\rm NL}^{\rm ortho} = -34 \pm 33$

***Planck* 2015 results XVII: Constraints on primordial non-Gaussianity**

*Planck* TT + lensing + lowP

**N.B.: polarization still not fully explored → improvements expected for the last release**

# Neutrinos with CMB & Planck

- Neutrinos with a mass ≈ 0.001−1 eV contribute to the radiation density at the time of equality and to the non-relativistic matter density today → affect primary CMB spectrum

  → Integrated Sachs-Wolfe effect (@ early & late times) &/or change in angular diameter distance to the last scattering surface

  → constraints on neutrino mass from CMB data

- *With Planck:* precise analysis of intermediate/high multipoles → dominant effect is gravitational lensing.
  Increasing the neutrino mass suppresses clustering on scales smaller than the size of the horizon at the time of the NR transition, suppressing the lensing potential.

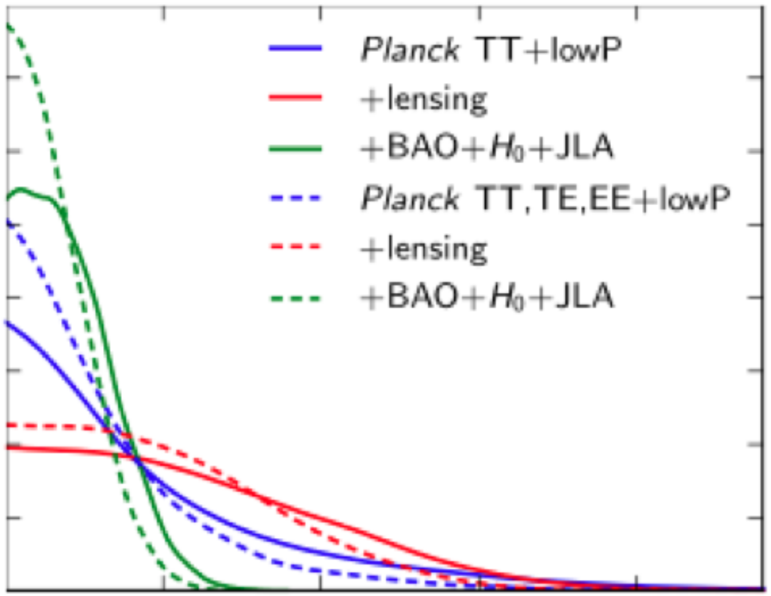


$\Sigma m_\nu < 0.72$ eV (PlanckTT+lowP)

$\Sigma m_\nu < 0.68$ eV (…. + lensing)

$\Sigma m_\nu < 0.23$ eV (… + ext)

$\Sigma m_\nu < 0.49$ eV (PlanckTT,TE,EE +lowP)

$\Sigma m_\nu < 0.59$ eV (…. + lensing)

$\Sigma m_\nu < 0.19$ eV (… + ext)

# *Planck* 2015 (95% CL) limits on neutrino masses

# &

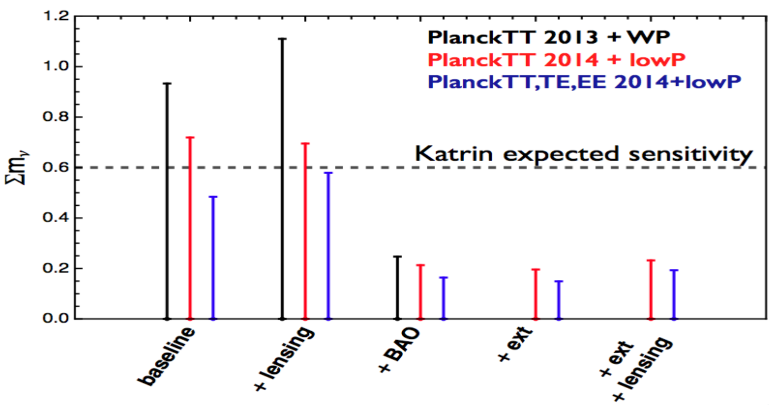


## Comparison with Katrin

$N_{eff} = 3.13 \pm 0.32$ (PlanckTT+lowP)

$N_{eff} = 3.15 \pm 0.23$ (PlanckTT+lowP+BAO)

$N_{eff} = 2.98 \pm 0.20$ (PlanckTT,TE,EE+lowP)

$N_{eff} = 3.04 \pm 0.18$ (PlanckTT,TE,EE+lowP+BAO)

(uncertainties are 68% CL)

# $N_{eff}$

$N_{eff} = 4$ (i.e., one extra thermalized neutrino) ***is excluded at between ~ 3 and 5 sigma.***

# Nature of Dark Energy

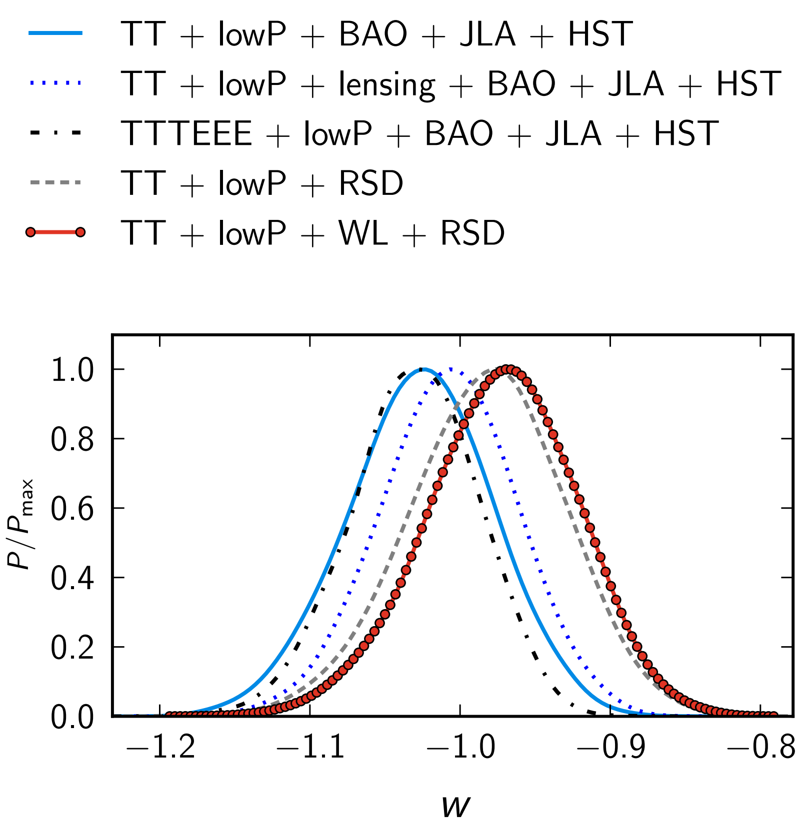


LambdaCDM compatible with data

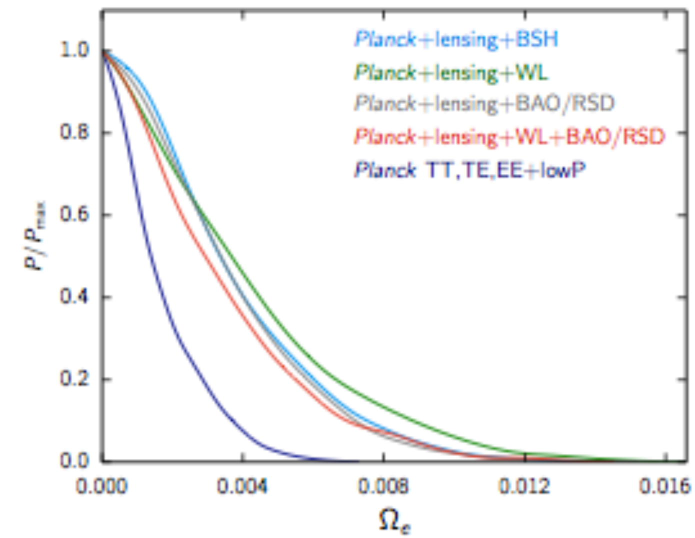


**"Early Dark Energy"**

$$\Omega_{\rm de}(a) = \frac{\Omega^0_{\rm de} - \Omega_{\rm e}(1 - a^{-3w_0})}{\Omega^0_{\rm de} + \Omega^0_{\rm m} a^{3w_0}} + \Omega_{\rm e}(1 - a^{-3w_0})$$

***Planck* 2015 results XIII: Cosmological parameters**

***Planck* 2015 results XIV:Dark Energy and Modified Gravity**

$\Omega_e < 0.007$ (95 %CL , *Planck* TT + lensing + lowP + BSH)

# Fundamental physics constants

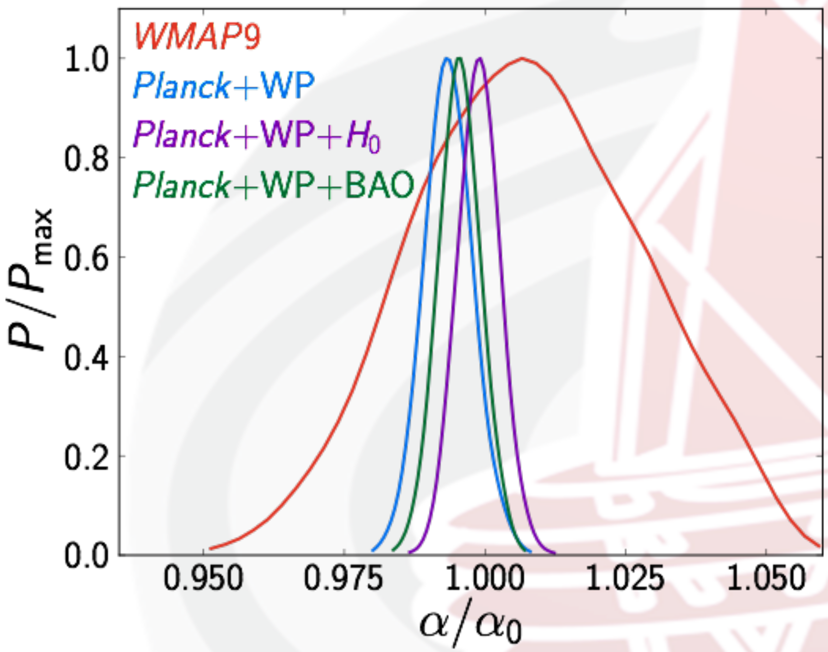


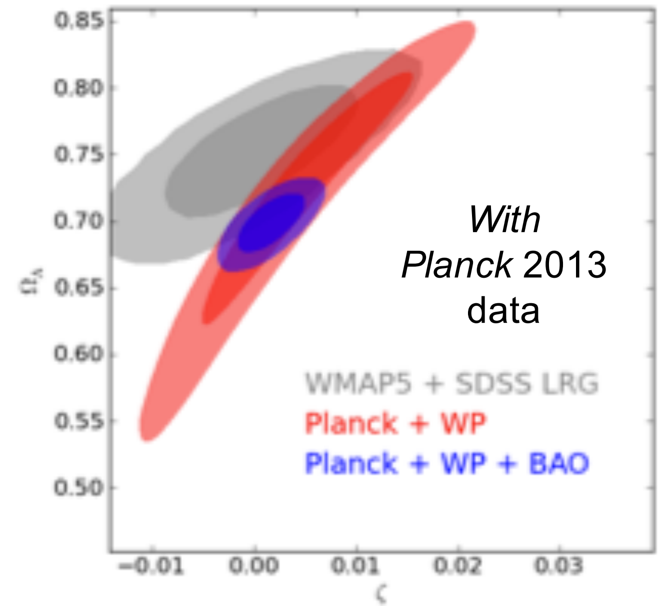


$\alpha/\alpha_0$=0.9936±0.0043

*(68%; Planck*+WP)

In laboratory on ground:

$\Delta\alpha/\alpha_0$ = 0.25 (0.32) $10^{-9}$

$$\xi = \ln\left(1+\frac{1}{\omega_{\rm BD}}\right)$$

$$\delta G/G = 0.010^{+0.019}_{-0.007} \quad 68\%\mathrm{CL}$$

**Li, Wu & Chen 2013, Phys Rev. D 88, 084053**

***Planck* 2013 results XXVI: Cosmological parameters**

***Planck* Intermediate results XXIV: Constraints on variation of fundamental constants**

# Polarization with *Planck* & B-modes

C. Burigana – Varenna 6/7/2017

# Polarization with *Planck*:

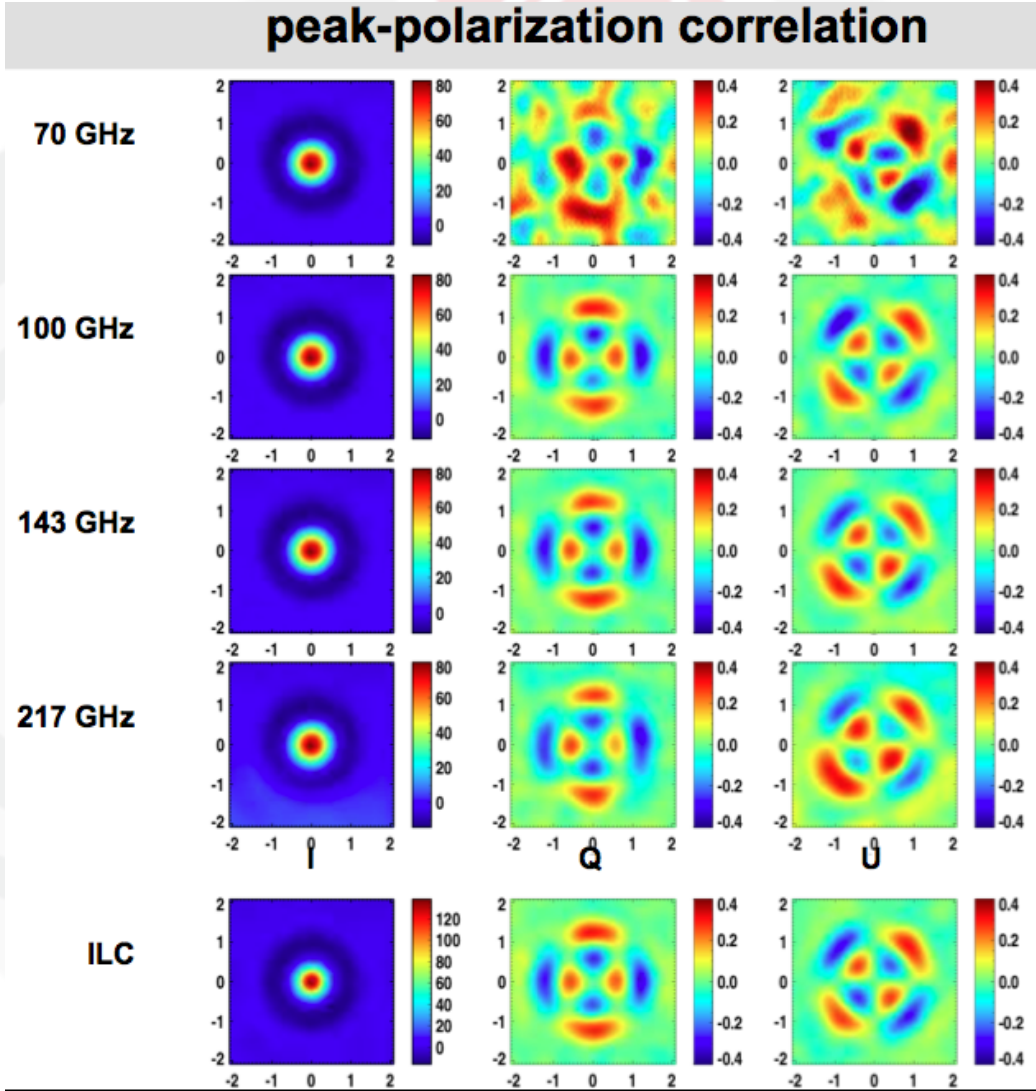

# CMB polarization with *Planck*
# E & B – 30% binning, $f_{sky}$=74%

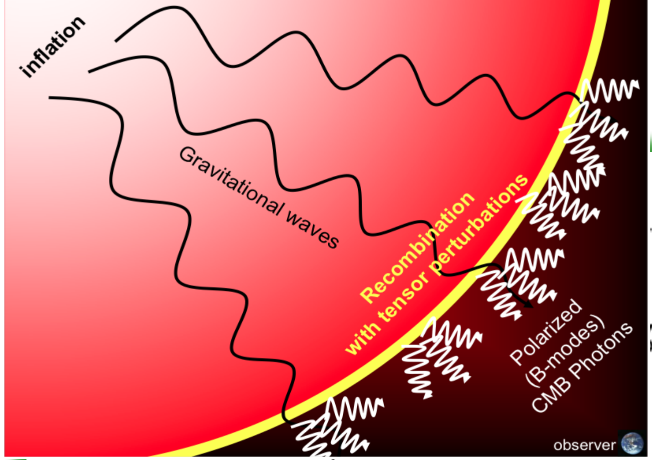


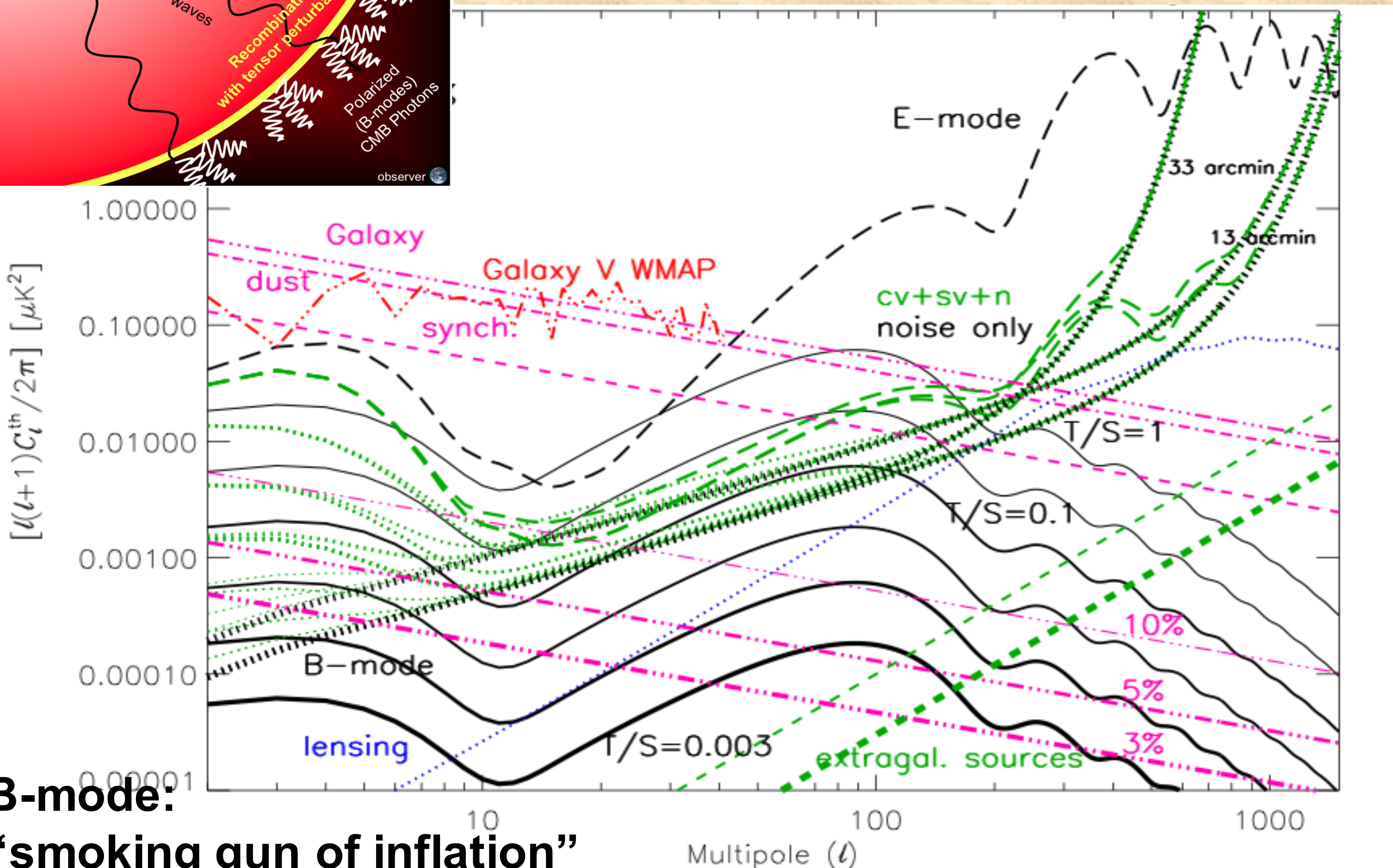


**B-mode:**
**"smoking gun of inflation"**
**energy scale**

# Planck 353 GHz full sky maps in polarization

- 353 GHz polarized maps are dominated by Galactic dust emission

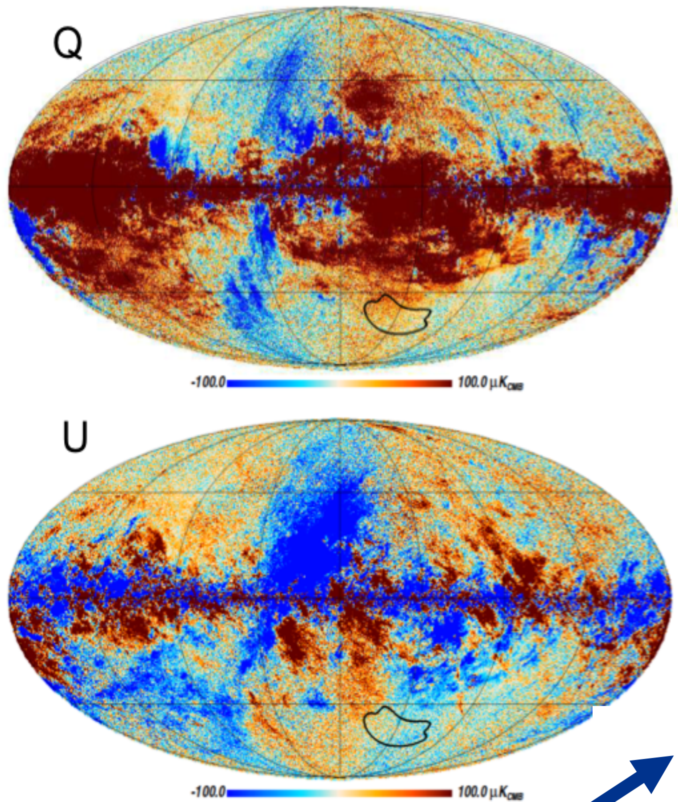


For comparison, Planck 70 GHz is close to the minimum of Galactic foreground emission

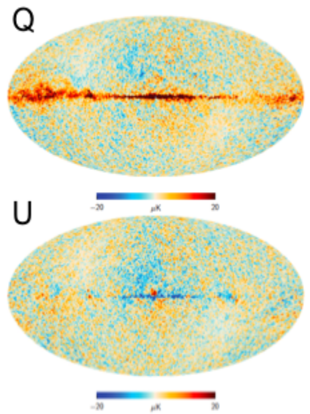


Bicep2, Keck Array and Planck Collaboration

**Dust essentially everywhere**

**Crucial for understanding the nature of B-mode polarization signal**

## *Planck* first results on dust polarized emission:

**High observed degree of polarization (P/I)obs up to 18%**

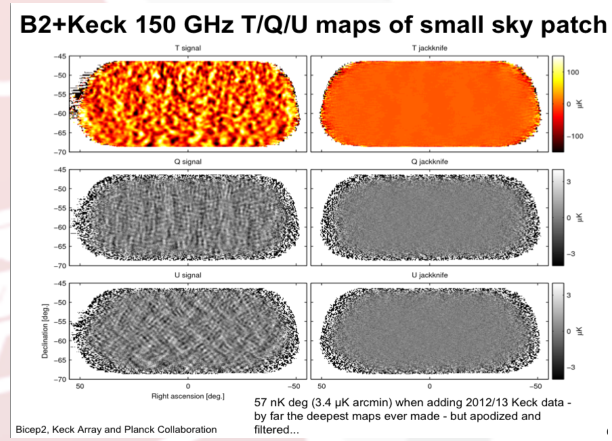


Planck Collaboration: Dust polarization at high latitudes

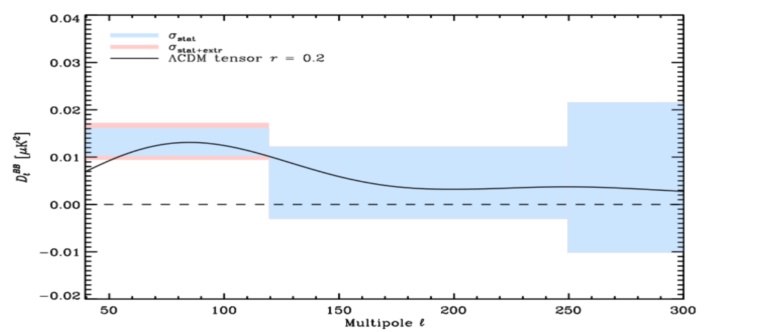


Fig. 9: *Planck* 353 GHz $\mathcal{D}_\ell^{BB}$ angular power spectrum computed on $M_{B2}$ defined in Sect. 6.1 and extrapolated to 150 GHz (box centres). The shaded boxes represent the $\pm 1\,\sigma$ uncertainties: blue for the statistical uncertainties from noise; and red adding in quadrature the uncertainty from the extrapolation to 150 GHz. The *Planck* 2013 best-fit ΛCDM $\mathcal{D}_\ell^{BB}$ CMB model based on temperature anisotropies, with a tensor amplitude fixed at $r = 0.2$, is overplotted as a black line.

# Compare BK 150 GHz (left) with Planck 353 GHz (right)

Dominated by LCDM E-modes

Dominated by noise & dust

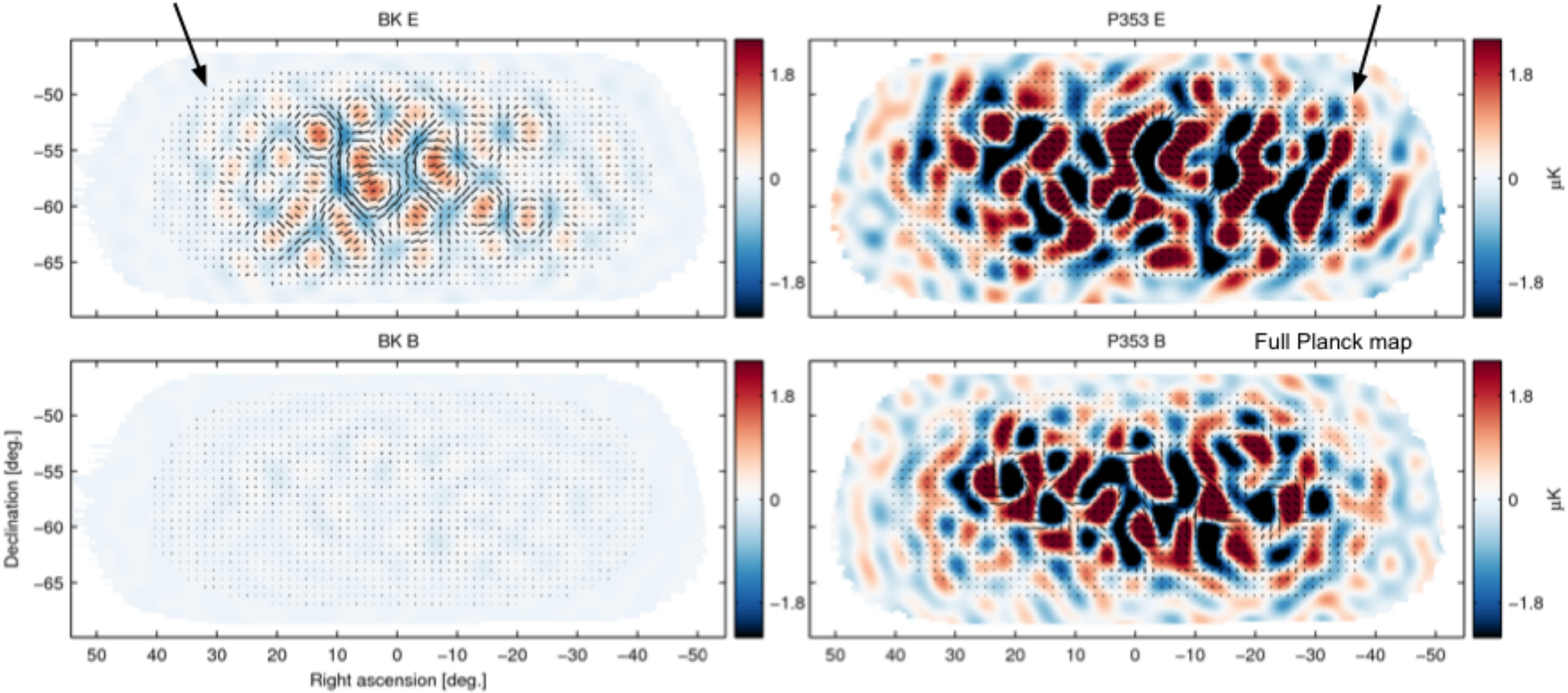


E-modes and B-modes filtered to range l=50-120

all maps shown with the same color stretch

## The Real Data

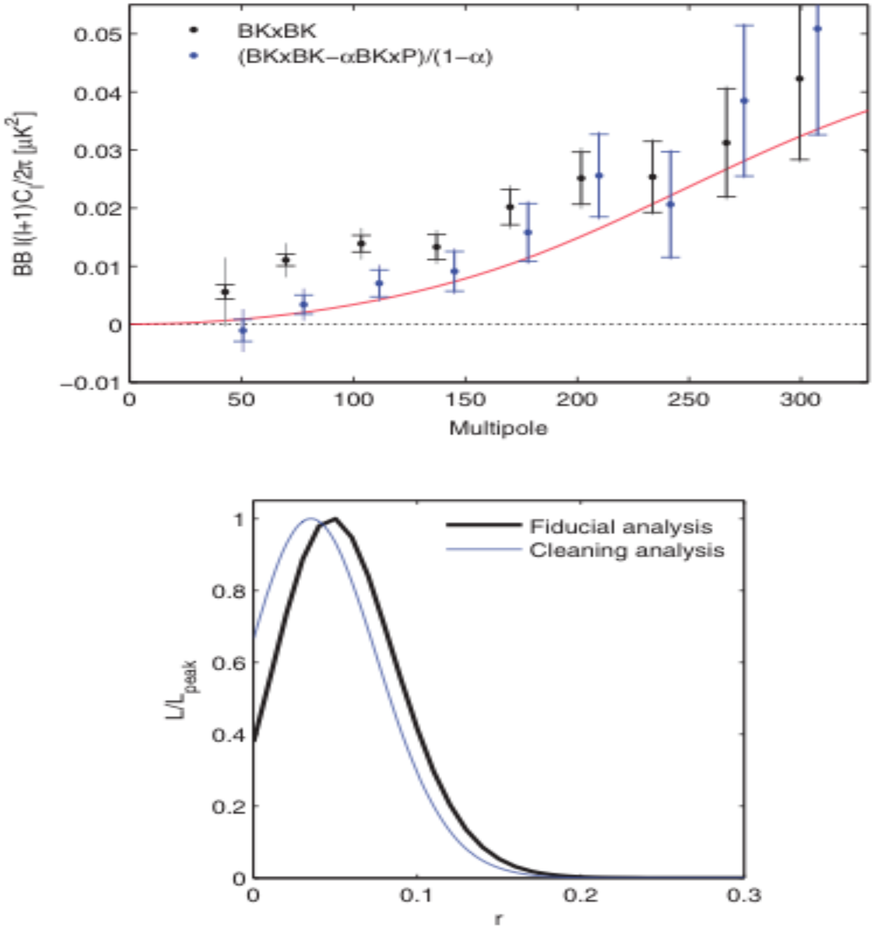


FIG. 12 (color). (Upper) *BB* spectrum of the BICEP2/*Keck* maps before and after subtraction of the dust contribution, estimated from the cross spectrum with *Planck* 353 GHz. The error bars are the standard deviations of simulations, which, in the latter case, have been scaled and combined in the same way. The inner error bars are from lensed-ΛCDM + noise simulations as in the previous plots, while the outer error bars are from the lensed-ΛCDM + noise + dust simulations. The red curve shows the lensed-ΛCDM expectation. (Lower) Constraint on $r$ derived from the cleaned spectrum compared to the fiducial analysis shown in Fig. 6.

❖ **Fundamental conclusion: dust is detected at high significance, $r < 0.12$ at 95% CL.**

○ **Multi-component likelihood gives $\sigma(r) \sim 0.035$ → very direct constraint on tensors!**

○ **No significant evidence for $r > 0$. Currently $r = 0$ and $r = 0.1$ are at equal likelihood.**

○ **There may yet be a gravitational wave signal, but if there is it must be considerably smaller than the full signal.**

❖ **We have checked the stability of the analysis under variations of the data selection and other details.**

○ **Most variations make little difference. There is some difference in the results depending onwhether BICEP2 or Keck data is used but this is shown to be within noise fluctuation.**

**BICEP2 / Keck Array VI: … Adding 95 GHz Data From Keck Array, arXiv:1510.09217: combining with *Planck* analysis of CMB temperature and other evidence yields $r_{0.05} < 0.07$ at 95% CL.**

# Microwave sky complexity

# rms fluctuations in T & P: CMB vs foregrounds
# Change of paradigm from *Planck* maps

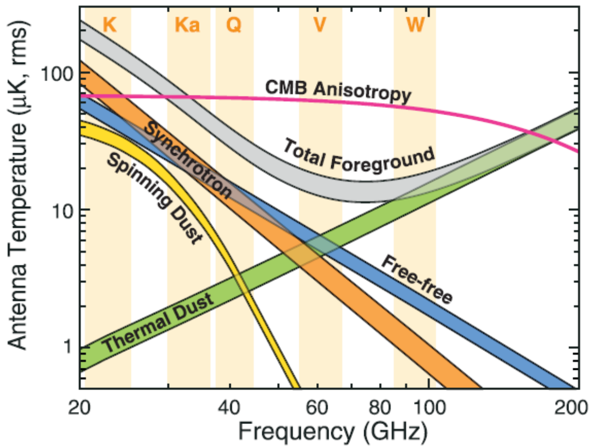


**WMAP 9**

75-85% sky coverage

***Planck* in T:** 81-93% sky coverage - 1° FWHM

c.f. common mask 78%

**Microwave sky complexity:** more relevant components!

**Many parameters!**

Synch: 2 +

Dust: 3 (* 2 ?)

FF: 2 (EM,$T_e$)

Spinning dust: 3loc+1glob

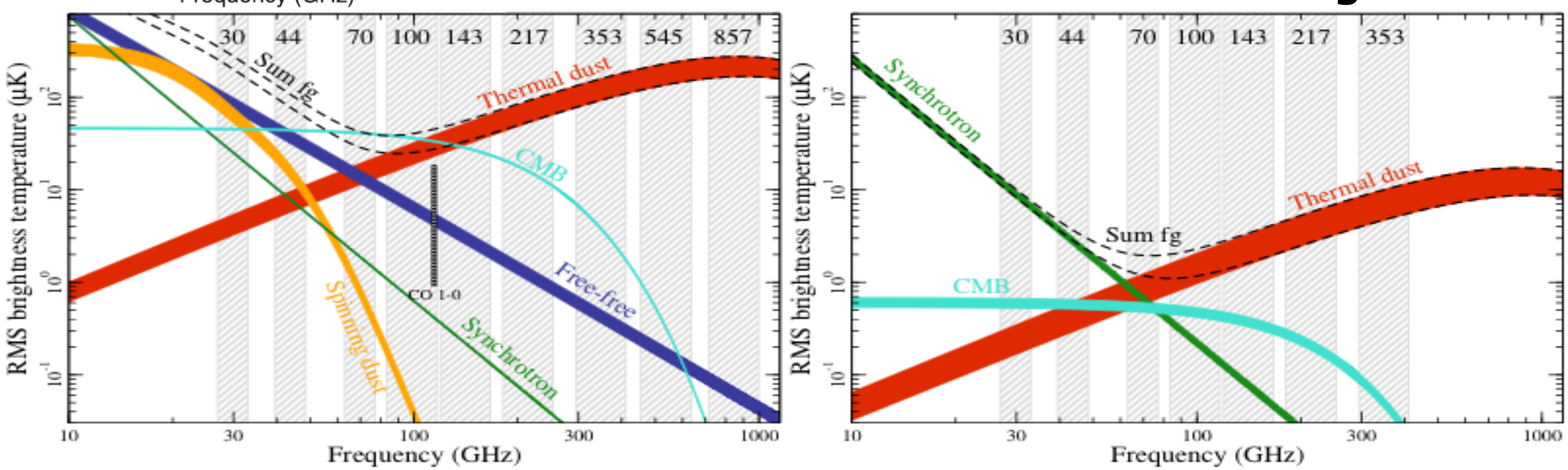


**Fig. 16.** Brightness temperature rms as a function of frequency and astrophysical component for temperature (*left*) and polarization (*right*). For temperature, each component is smoothed to an angular resolution of 1° FWHM, and the lower and upper edges of each line are defined by masks covering 81 and 93 % of the sky, respectively. For polarization, the corresponding smoothing scale is 40′, and the sky fractions are 73 and 93 %.

## *Classical ZLE* - Separated in "time domain", for now simply exploiting differences in surveys

## & Secondary components? KBOE?

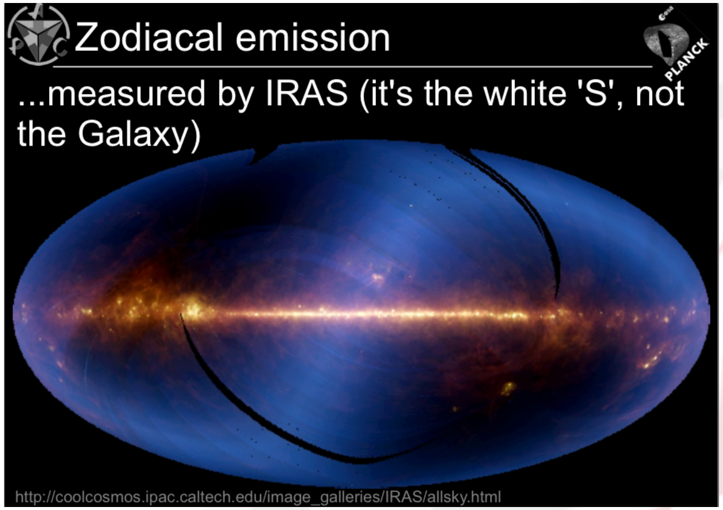


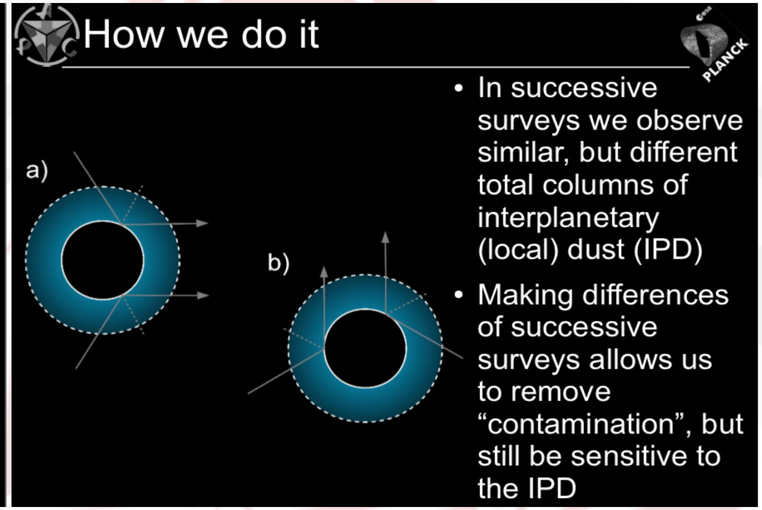


ZLE: first piece of the game

**KBOE ?**
far, cold, large dust grains

**Imprints @ large scales?**

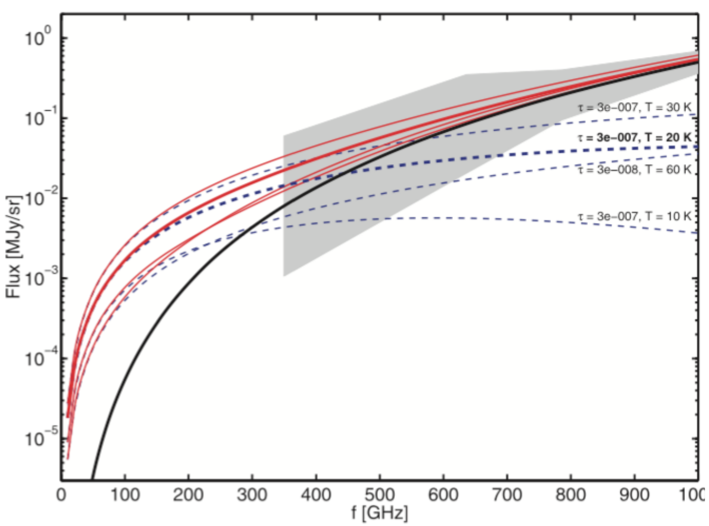


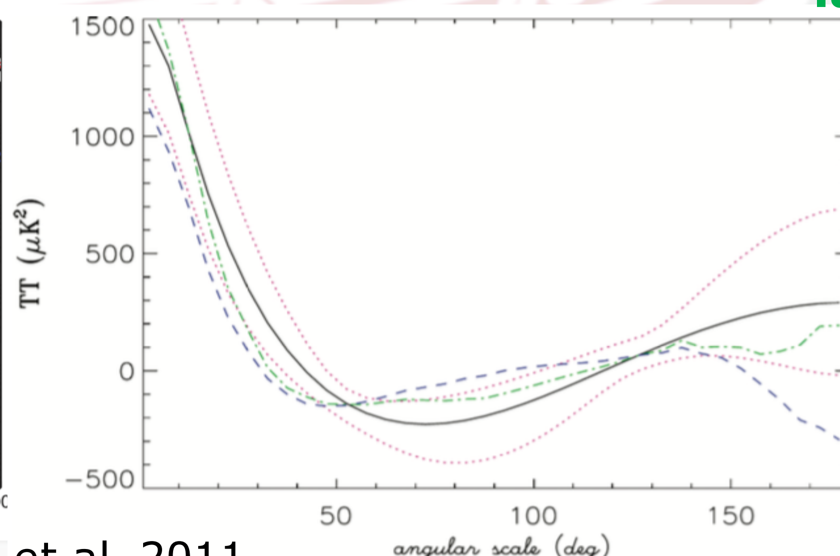


Maris et al. 2011

**mm signal from KBOE?**

**Low quadrupole?**

**Correlation function?**

# Synchrotron emission in polarization: radio vs mm

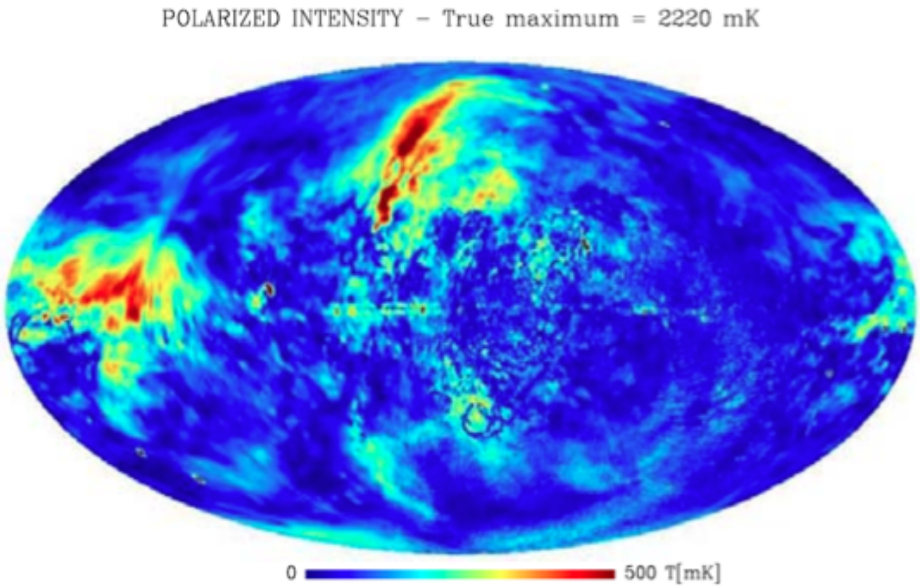


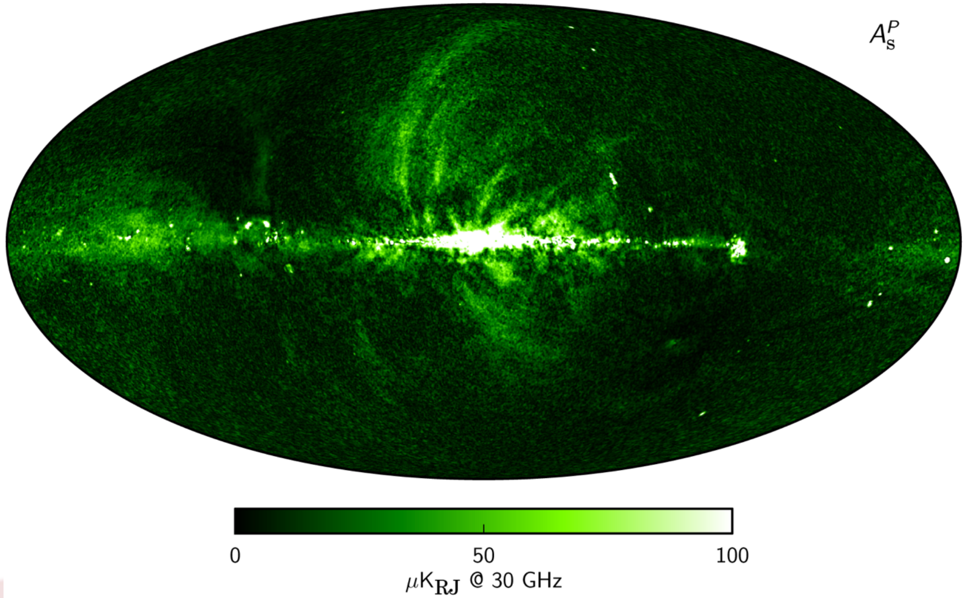


All-sky maps of Galactic polarized synchrotron emission
at radio (1.4 GHz; from Burigana et al. '06) & mm (30 GHz) from *Planck*

**Relativistic cosmic ray electrons spiralling in the Galactic magnetic field → Galactic synchrotron emission**

**Significant depolarization appearing in a wide region around the Galactic center in the radio, much less relevant in the microwaves**

# Synchrotron emission characterization

Relevance for e.g.:

- **cosmic ray physics**
- **Galaxy 3D models**
- **Galactic magnetic fields**

**In frequency SED**

From Planck Coll. 2015, XXV

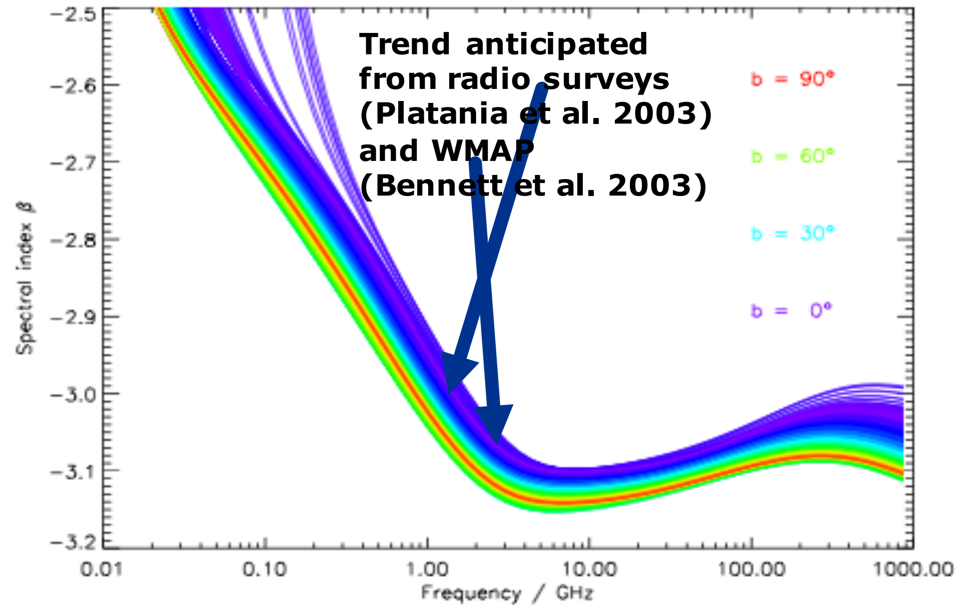


**Fig. 15.** Local spectral index of the synchrotron emission $\beta(\nu) = d\ln T/d\ln\nu$ vs. frequency for a sample of pixels (one per $N_{\rm side} = 8$ super-pixel), in the GALPROP z10LMPD_SUNfE model from Orlando & Strong (2013). The spectra are colour-coded by Galactic latitude: spectra at low latitudes show strong low-frequency curvature due to free-free absorption.

From Planck Coll. 2015, X

| | Synchrotron | |
|---|---|---|
| | $q$ [$\mu K^2_{\rm CMB}$] | $\alpha$ |
| **Common mask; apod = 1° FWHM; $f^{\rm eff}_{\rm sky}$ = 0.73** | | |
| $EE$ . . . . . . . . . | $3.7 \pm 0.2$ | $-0.44 \pm 0.07$ |
| $BB$ . . . . . . . . . | $1.3 \pm 0.2$ | $-0.31 \pm 0.13$ |
| $BB/EE$ . . . . . | $0.36 \pm 0.06$ | |
| **Common mask; apod = 2° FWHM; $f^{\rm eff}_{\rm sky}$ = 0.68** | | |
| $EE$ . . . . . . . . . | $3.2 \pm 0.2$ | $-0.49 \pm 0.08$ |
| $BB$ . . . . . . . . . | $1.1 \pm 0.2$ | $-0.02 \pm 0.17$ |
| $BB/EE$ . . . . . | $0.34 \pm 0.07$ | |

**In angular correlation**

**EE & BB ← APS**

# AME – spinning dust *all-sky* diffuse component

Planck Int. XV (2014)

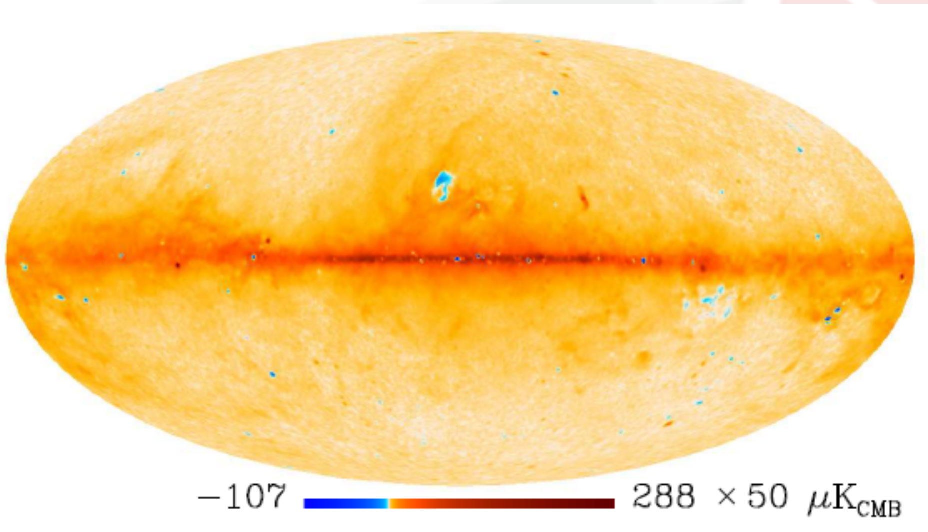


**CMB, dust and free-free killed ILC combination**

**Rising spectrum between 30 & 44 GHz**

**AME with high-frequency peak**

QUIJOTE (10-18 GHz), C-BASS (5 GHz)
S-PASS (2.3 GHz)
GMIMS (300 -1800 MHz) for synchrotron

# *Planck* Commander model has 2 AME components:

- ✓ **Main component has variable peak with prior centred on 19 GHz**
- ✓ **"High frequency" component with peak 30 GHz**
  - ➢ **Still too low for some regions (Oph, California Nebula)**

- ❑ **AME flexibility forces us to use fixed template for synchrotron spectrum, despite plausible evidence for spectral variability**

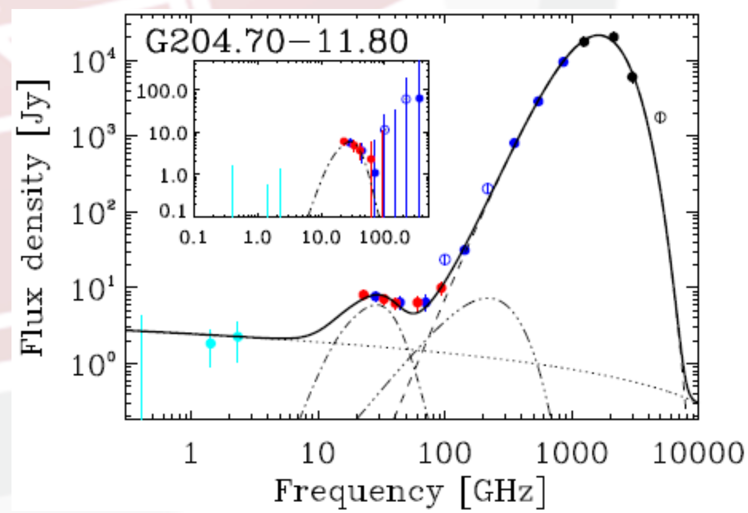

# Haze with *Planck*

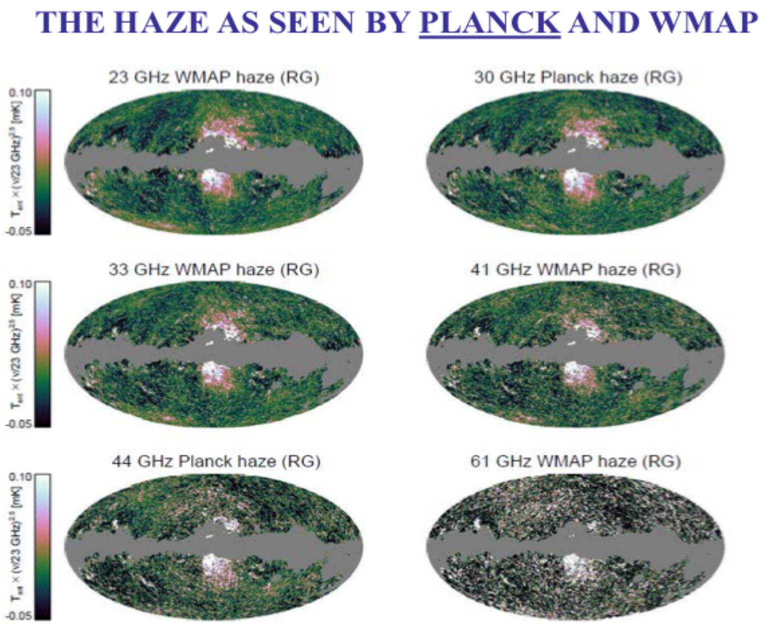


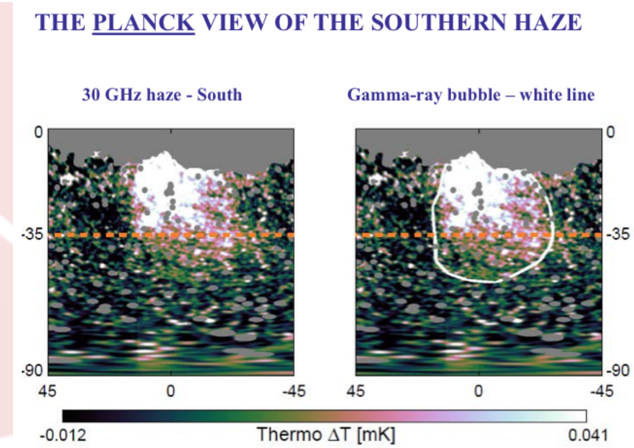


**Galactic Haze at 30 and 44 GHz, from *Planck***

❖ The **Galactic Haze** is seen to be distributed **around the Galactic Centre**

❖ Its **spectrum is similar to that of synchrotron emission**

❖ However, compared to the synchrotron emission seen elsewhere in the Milky Way, the Galactic **Haze has a 'harder' spectrum**, meaning that its emission **does not decline as rapidly with increasing frequency**

❖ Diffuse synchrotron emission is interpreted as **radiation from highly energetic electrons** that have been accelerated in shocks created by supernova explosions

❖ **Several explanations:** ***enhanced supernova rates, galactic winds and even annihilation of dark-matter particles … but*** **none** of them have been **confirmed**

# Impact of residuals & subdominant components / features complexity in dominant components

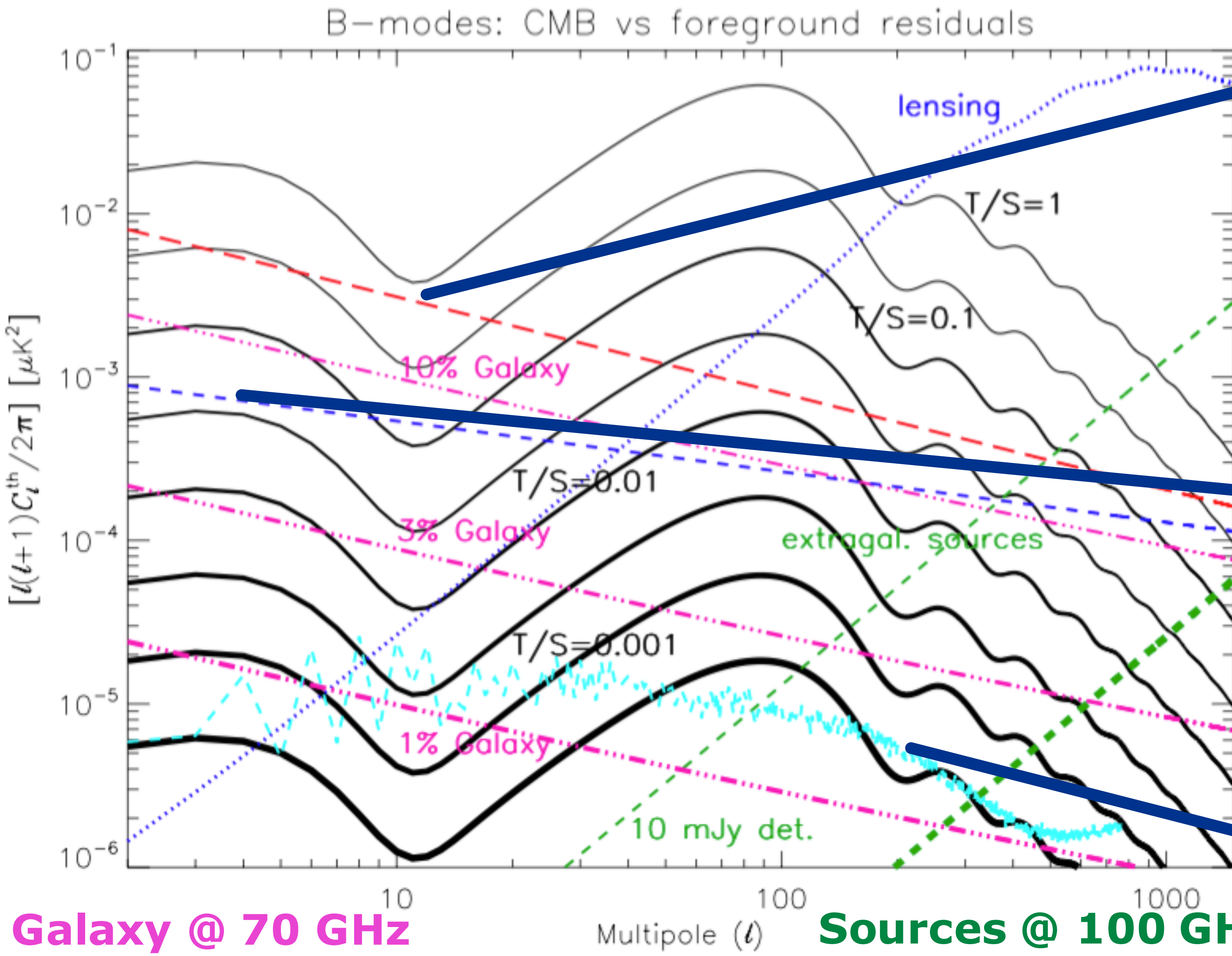


**Residual from dust starting from 353 GHz for an error in beta_dust of 0.01**

**Residual from synch starting from 30 GHz for an error in slope of 0.02**

**Estimate of AME, assuming pol. degree of 2%**

**Galaxy @ 70 GHz**

**Sources @ 100 GHz**

# General remarks

- The analysis of the *Planck* nine frequency channels reveals the complexity of the mm sky
- At the sensitivity level of *Planck*, only two astrophysical diffuse components are significantly polarized, namely the synchrotron and thermal dust emissions
- On the other hand, the recent limits set on primordial B-modes derived combining data from *Planck* and BICEP2-Keck array call for

  → a new generation of precise polarization measurements for detecting and *characterizing* primordial B-modes
- Particularly for low values of the tensor-to-scalar ratio, r, they
  - a very large number of receivers
  - frequency channels necessary for the accurate treatment of (even subdominant) foreground emissions

# Future of CMB anisotropy missions

C. Burigana – Varenna 6/7/2017

**National coordinators:**
P de Bernardis (IT), F Bouchet (FR), E Kreysa (GE), L Piccirillo (UK), R Rebolo (SP)

**Instrument working group:**
P de Bernardis, L Piccirillo, P Ade, M Bersanelli, FX Desert, E Kreysa, L Kuzmin, B Maffei, N Mandolesi, S Masi, P Mauskopf, T Peacocke, F Piacentini, M Piat, G Pisano, R Rebolo, G Savini, R Tascone, F Villa, S Withington, G Yassin

**Science working group:**
M Bucher, J Bartlett, F Bouchet, C Caprini, A Challinor, R Battye, G Efstathiou, F Finelli, K Ganga, J Garcia-Bellido, F Hansen, K Land, A Jaffe, S Matarrese, A Melchiorri, P Natoli, L Popa, R Stompor, B van Tent, L Verde

**Foregrounds working group:**
C Burigana, T Arshakian, C Baccigalupi, A Banday, D Barbosa, R Beck, JP Bernard, G Bernardi, A Bonaldi, E Carretti, D Clements, P Coles, G de Zotti, R Fabbri, P Fosalba Vela, J Gonzales-Nuevo, M Hobson, L La Porta, P Leahy, JF Macias-Perez, E Martinez-Gonzalez, M Massardi, P Naselsky, N Ponthieu, W Reich, S Ricciardi, F Stivoli, L Toffolatti, M Tucci, P Vielva

Here is a list of the institutions presently involved in B-pol:

**Canada:** Dept. of Physics and Astronomy, Univ. of British Columbia, Vancouver; Canadian Institute for Theoretical Astrophysics (CITA), University of Toronto.

**Denmark:** Neils Bohr Institute

**France:** Laboratoire AstroParticule et Cosmologie (APC), Univ. Paris VII; Institut d'Astrophysique Spatiale (IAS), Univ. Paris-Sud, Orsay; Centre d'Etude Spatiale des Rayonnements (CESR), Toulouse; Commissariat à l'Energie Atomique (CEA), Saclay; Institut d'Astrophysique de Paris (IAP); Institut Néel - Matière Condensée et Basses Températures (IN-MCBT), Grenoble; Laboratoire de l'Accélérateur Linéaire (LAL), Univ. Paris-Sud, Orsay; Laboratoire d'Astrophysique de l'Observatoire de Grenoble (LAOG); Laboratoire de Physique Théorique (LPT), Univ. Paris-Sud, Orsay; Laboratoire de Physique Subatomique et de Cosmologie (LPSC), Grenoble.

**Germany:** Argelander-Institut für Astronomie (AIfA), Bonn Univ.; Institut für Photonische Technologien (IPHT), Jena; Max-Planck-Institut für Astrophysik (MPA), Garching; Max-Planck-Institut für Radioastronomie (MPIfR), Bonn.

**Ireland:** Maynooth.

**Italy:** Istituto di Elettronica e di Ingegneria dell'Informazione e delle Telecomunicazioni (CNR-IEIIT), Torino; Istituto di Astrofisica Spaziale e Fisica cosmica (INAF-IASF), Bologna; Istituto di RadioAstronomia (INAF-IRA), Bologna; Istituto Nazionale di Fisica Nucleare (INFN) - Sezioni di Genova, Perugia, Roma1; Scuola Internazionale Superiore di Studi Avanzati (SISSA), Trieste; Univ. di Firenze, Dip. di Fisica; Univ. di Genova, Dip. di Fisica; Univ. di Milano Bicocca, Dip. di Fisica; Univ. di Milano, Dip. di Fisica; Univ. di Padova, Dip. di Fisica; Univ. di Perugia, Dip. di Fisica; Univ. di Roma La Sapienza, Dip. di Fisica; Univ. di Roma Tor Vergata, Dip. di Fisica.

**Norway:** Institute of Theoretical Astrophysics, University of Oslo

**Portugal:** Instituto de Telecomunicações (IT), Lisbon; Instituto de Telecomunicações (IT), Aveiro; Instituto Superior Técnico (IST), Lisbon.

**Romania:** Institute for Space Sciences (ISS), Bucharest.

**Spain:** Instituto de Astrofísica de Canarias (IAC), La Laguna; Instituto de Física de Cantabria (IFCA), Santander; Instituto de Ciencias del Espacio (ICE), Barcelona; Universidad Autonoma de Madrid (UAM), Madrid.

**Sweden:** Chalmers Univ. of Technology, Dept. of Microtechnology and Nanoscience.

**Switzerland:** U. Genève

**United Kingdom:** Univ. of Manchester, Physics Dept.; Jodrell Bank; Univ. of Cardiff, Physics and Astronomy Dept.; Univ. of Oxford, Physics and Astronomy Dept.; Univ. of Cambridge, Physics and Astronomy Dept.; Imperial College, London; Univ. of Edinburgh.

**USA:** Caltech; NASA Goddard Space Flight Center (GSFC); NASA Jet Propulsion Laboratory (JPL); Univ. of Wisconsin, Madison, Dept. of Physics.

Contact for proposal:
Paolo de Bernardis, University of Rome – La Sapienza, paolo.debernardis@roma1.infn.it, +390649914271

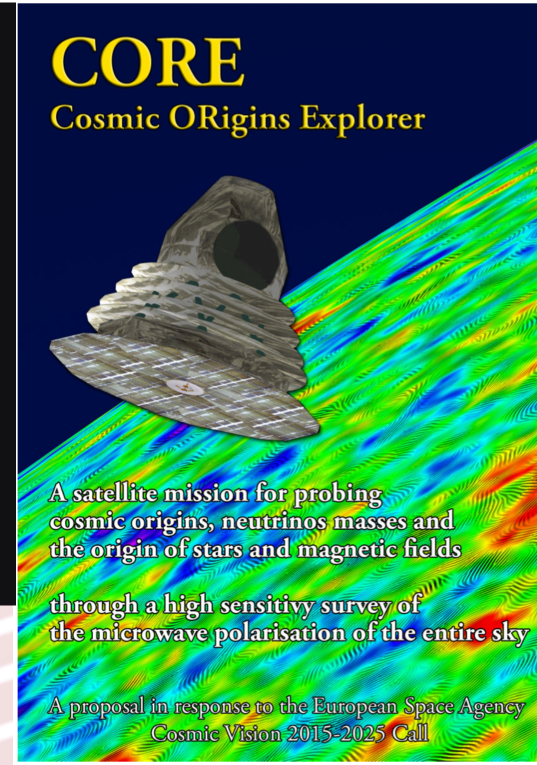


# CMB missions proposals to ESA – I: B-Pol, COrE (medium-size (M) missions)

**National coordinators:**
F. R. Bouchet (FR), P. de Bernardis (IT), B. Maffei (UK), E. Martinez-Gonzalez (SP)

**Mission & programmatics working group**
F. R. Bouchet, P. de Bernardis, B. Maffei, M. Piat, N. Ponthieu, R. Stompor

**Instrument working group:**
B. Maffei, M. Bersanelli, P. Bielewicz, P. Camus, P. de Bernardis, M. De Petris, S. Masi, F. Nati, F. Piacentini, L. Piccirillo, M. Piat, G. Pisano, M. Salatino, R. Stompor, S. Withington, T. Peacocke

**Science working group:**
M. Bucher, D. Barbosa, N. Bartolo, R. Battye, J.-P. Bernard, F. Boulanger, A. Challinor, S. Chongchitnan, S. Colafrancesco, T. Ensslin, J. Fergusson, P. Ferreira, K. Ferriere, F. Finelli, J. Garcia-Bellido, S. Galli, M. Haverkorn, M. Hindmarsh, A. Jaffe, M. Kunz, J. Lesgourgues, A. Liddle, M. Liguori, S. Matarrese, A. Melchiorri, P. Mukherjee, L. Pagano, D. Paoletti, H. Peiris, L. Perroto, C. Rath, J. Rubino Martin, C. Rath, P. Shellard, J. Urrestilla, B. Van Tent, L. Verde, B. Wandelt

**Foregrounds working group:**
C. Burigana, J. Delabrouille, C. Armitage-Caplan, A. Banday, A. Bonaldi, S. Basak, D. Clements, G. De Zotti, C. Dickinson, J. Dunkley, M. Lopez-Caniego, E. Martinez-Gonzalez, M. Negrello, S. Ricciardi, L. Toffolatti

# The Polarized Radiation Imaging and Spectroscopy Mission

An Extended White Paper

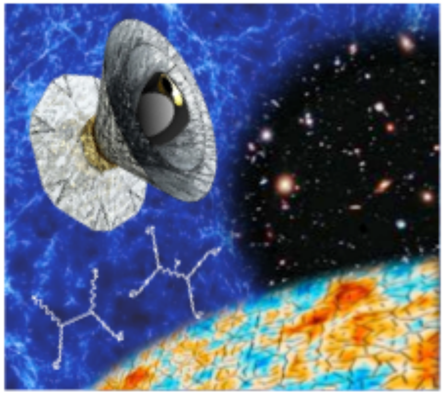

# CMB missions proposals to ESA – II: PRISM (Large mission ideas) COrE+ (M mission)

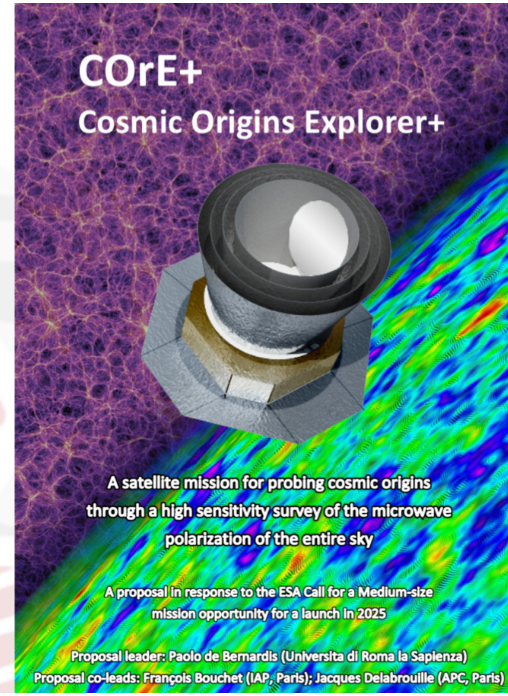


## Authors

Philippe André, Carlo Baccigalupi, Anthony Banday, Domingos Barbosa, Belen Barreiro, James Bartlett, Nicola Bartolo, Elia Battistelli, Richard Battye, George Bendo, Alain Benoît, Jean-Philippe Bernard, Marco Bersanelli, Matthieu Béthermin, Pawel Bielewicz, Anna Bonaldi, François Bouchet, François Boulanger, Jan Brand, Martin Bucher, Carlo Burigana, Zhen-Yi Cai, Philippe Camus, Francisco Casas, Viviana Casasola, Guillaume Castex, Anthony Challinor, Jens Chluba, Gayoung Chon, Sergio Colafrancesco, Barbara Comis, Francesco Cuttaia, Giuseppe D'Alessandro, Antonio Da Silva, Richard Davis, Miguel de Avillez, Paolo de Bernardis, Marco de Petris, Adriano de Rosa, Gianfranco de Zotti, Jacques Delabrouille, François-Xavier Désert, Clive Dickinson, Jose Maria Diego, Joanna Dunkley, Torsten Enßlin, Josquin Errard, Edith Falgarone, Pedro Ferreira, Katia Ferrière, Fabio Finelli, Andrew Fletcher, Pablo Fosalba, Gary Fuller, Silvia Galli, Ken Ganga, Juan García-Bellido, Adnan Ghribi, Martin Giard, Yannick Giraud-Héraud, Joaquin Gonzalez-Nuevo, Keith Grainge, Alessandro Gruppuso, Alex Hall, Jean-Christophe Hamilton, Marijke Haverkorn, Carlos Hernandez-Monteagudo, Diego Herranz, Mark Jackson, Andrew Jaffe, Rishi Khatri, Martin Kunz, Luca Lamagna, Massimiliano Lattanzi, Paddy Leahy, Julien Lesgourgues, Michele Liguori, Elisabetta Liuzzo, Marcos Lopez-Caniego, Juan Macias-Perez, Bruno Maffei, Davide Maino, Anna Mangilli, Enrique Martinez-Gonzalez, Carlos Martins, Silvia Masi, Marcella Massardi, Sabino Matarrese, Alessandro Melchiorri, Jean-Baptiste Melin, Aniello Mennella, Arturo Mignano, Marc-Antoine Miville-Deschênes, Alessandro Monfardini, Anthony Murphy, Pavel Naselsky, Federico Nati, Paolo Natoli, Mattia Negrello, Fabio Noviello, Créidhe O'Sullivan, Francesco Paci, Luca Pagano, Rosita Paladino, Nathalie Palanque-Delabrouille, Daniela Paoletti, Hiranya Peiris, Francesca Perrotta, Francesco Piacentini, Michel Piat, Lucio Piccirillo, Giampaolo Pisano, Gianluca Polenta, Agnieszka Pollo, Nicolas Ponthieu, Sara Ricciardi, Matthieu Roman, Cyrille Rosset, Jose-Alberto Rubino-Martin, Maria Salatino, Alessandro Schillaci, Paul Shellard, Joseph Silk, Radek Stompor, Rashid Sunyaev, Andrea Tartari, Luca Terenzi, Luigi Toffolatti, Maurizio Tomasi, Neil Trappe, Matthieu Tristram, Tiziana Trombetti, Marco Tucci, Rien Van de Weijgaert, Bartjan Van Tent, Licia Verde, Patricio Vielva, Ben Wandelt, Robert Watson, Stafford Withington

**Proposal leader:** Paolo de Bernardis

Dipartimento di Fisica, Sapienza Università di Roma, P.le A. Moro 2, Roma, Italy
tel.: +390649914271, fax: +39064957697, mail: paolo.debernardis@roma1.infn.it.

*The Lead Proposer is committed to support the study activities by making available more than 20% of his time throughout the study period.*

**Proposal co-leads**: François Bouchet (IAP, Paris); Jacques Delabrouille (APC, Paris)

**Steering Committee:**

**Austria:** J. Alves; **Denmark:** P. Naselsky; **Finland:** H. Kurki-Suonio; **France:** F. Bouchet, M. Bucher, J. Delabrouille, M. Giard; **Germany:** E. Komatsu, R. Sunyaev; **Ireland:** N. Trappe; **Italy:** M. Bersanelli, C. Burigana, P. de Bernardis; **Netherlands:** R. van de Weygaert; **Norway:** H.K. Eriksen; **Poland:** A. Pollo; **Portugal:** C. Martins; **Spain:** E. Martínez-González, J.A. Rubiño-Martín, L. Verde; **Switzerland:** M. Kunz; **United Kingdom:** A. Challinor, B. Maffei, G. Pisano; **USA:** S. Hanany.

**Main contributors to proposal writing:**

*Coordinators*:
**Mission**: Paolo de Bernardis; François Bouchet; Jacques Delabrouille;
**CMB Science**: Martin Bucher (proposal writeup coordinator); Anthony Challinor; Eiichiro Komatsu;
**Non-CMB Science**: Gianfranco de Zotti; François Boulanger; Jean-Baptiste Melin;
**Instrument and Payload**: Bruno Maffei; Michel Piat.

Ph. André, P. Andreani, M. Ashdown, C. Baccigalupi, A. Baryshev, J. Bartlett, S. Basak, J. Baselmans, J.-P. Bernard, M. Bersanelli, P. Bielewicz, M. Bilicki, J. Bock, L. Bonavera, J. Borrill, F.R. Bouchet, F. Boulanger, T. Bradshaw, M. Bucher, C. Burigana, Z-Y. Cai, Ph. Camus, G. Castex, A. Catalano, A. Challinor, I. Charles, M. Clemens, D.L. Clements, B. Comis, M. Crook, P. de Bernardis, A. De Rosa, G. de Zotti, T. Decourcelle, J. Delabrouille, F.-X. Désert, C. Dickinson, J.M. Diego, S. Dodelson, J.-M. Duval, H.-K. Eriksen, J. Errard, G. Fabbian, P. Ferreira, F. Finelli, M. Gervasi, J. García-Bellido, A. Ghribi, J. Gonzalez-Nuevo, M. Griffin, A. Gruppuso, S. Golwala, R. Guesten, S. Hanany, A. Heavens, F. Helmich, D. Herranz, J. Hubmayr, K. Irwin, D. Johnson, A. Karakci, T. Kitching, L. Knox, A. Kogut, E. Komatsu, N. Krachmalnicoff, M. Kunz, M. Lattanzi, C. Lawrence, A. Lee, J. Lesgourgues, F. Levrier, A. Lewis, Y. Longval, M. Lopez-Caniego, J.F. Macias-Perez, B. Maffei, J. Martin, C. Martins, J. Martino, S. Masi, S. Matarrese, D. McCarthy, J.-B. Melin, A. Melchiorri, A. Mennella, M.-A. Miville-Deschênes, J. Mohr, A. Monfardini, L. Montier, G. Morgante, H. Moseley, P. Natoli, M. Negrello, F. Noviello, L. Pagano, L. Page, D. Paoletti, G. Patanchon, L. Perotto, F. Piacentini, M. Piat, G. Pisano, G. Polenta, N. Ponthieu, G. Pratten, D. Prêle, G. Puglisi, M. Remazeilles, V. Revéret, C. Ringeval, I. Ristorcelli, J. Rodriguez, L. Rodriguez, J.-A. Rubiño-Martín, S. Serjeant, P. Shirron, D. Spergel, R. Stompor, R. Sunyaev, A. Tartari, L. Toffolatti, N. Trappe, T. Trombetti, M. Tucci, R. van de Weygaert, V. Vennin, L. Verde, N. Vittorio, F. Voisin, B. Wandelt, K. Young, A. Zacchei, F. Zandanel, M. Zannoni.

CMB missions proposals
to ESA – III:

now:
ESA M5 → CORE

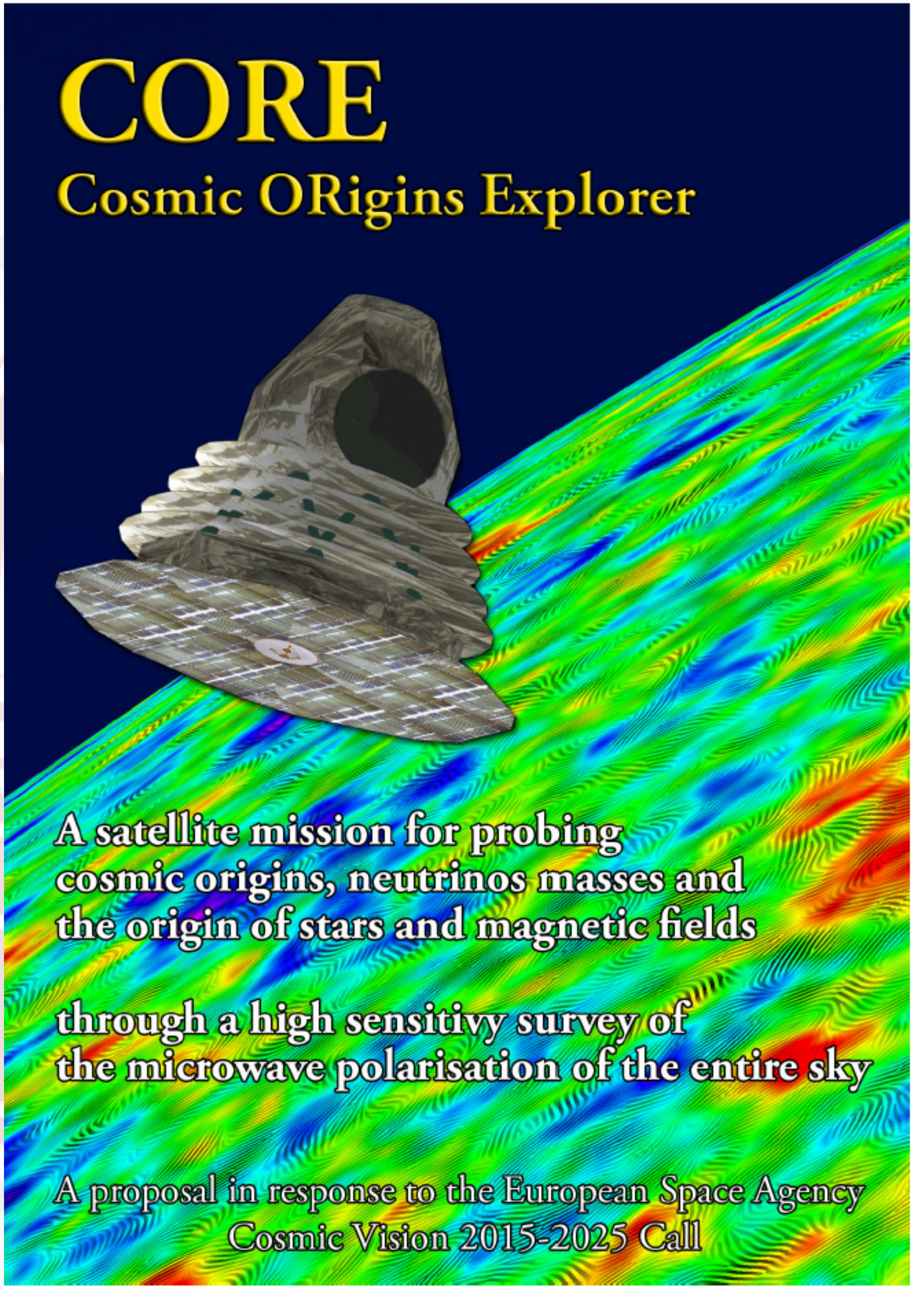

- Ground-Based building on SII & SIII
- Complementary, but not dependant on balloons/satellites
- US universities, DOE, Natl. Labs, HEP comm.
  - International Encouraged

| Years | Stage | Sensitivity ($\mu K^2$) | $r_{u.lim}$ | $\sigma(N_{eff})$ | $\sigma(\Sigma m_\nu)$ | D.E. F.O.M |
|---|---|---|---|---|---|---|
| 2015–2016 | Stage 2, 1000 detectors | $\gtrsim 10^{-5}$ | $r \lesssim 0.1$ | 0.14 | 0.15eV (Boss BAO prior) | ~180 (DES+BOSS SZ clusters) |
| 2017–2020 | Stage 3, 10,000 detectors | $10^{-6}$ | $r \lesssim 0.01$ | 0.06 | 0.06eV (Boss BAO prior) | ~300-600 (DES + DESI SZ Clusters) |
| 2021–2024 | Stage 4 CMB-S4, ~500,000 detectors | $10^{-8}$ | $r \lesssim 0.001$ | 0.02 | 0.015eV (DESI BAO prior) | ~1250 (DESI +LSST S4 Clusters) |

From John Carlstrom@UMich



Courtesy K.Ganga

# S4 Meeting Notes from Radek Stompor

- Huge and there seems to be a strong commitment to go ahead;
- Broad canvass of potential science goals: from primordial B-modes to lensing to cross-correlations to SZ effects (both thermal and kinematic);
- Cost now on order of 200-300 M$ (up a factor of 2-3 from the initial 100 M$);
- All major US CMB experimentation group represented;
- Still many differences and no common vision, but seems difficult to avoid multiple observatories in many (at least two ?!) sites with different, complementary characteristics.
- Stress on it being self contained and complementary to other probes (balloons, satellites) but the unanswered question is to what extent this is possible.
- Stress on need for continuing support for CMB-S3 projects as the necessary pathfinders for S4;
- General interest in the international collaboration -- very general and vague;
- Some seem to be interested in a Norther Hemisphere observatory (Greenland ?!)
- Real beginning (money!) anticipated for around 2018 (coinciding with the end of the LSST construction);
- But organizationally is already moving:
  - science paper in the next 6-12 months;
  - regular face-to-face meetings (next in Berkeley in January 2016), some of which may be more focused;
  - working groups, telecons, wiki, git etc in the weeks to come.
- Major questions for us:
  - is there a place for a significant external contribution ?!
  - how can we be visible given the anticipated size and cost of the overall effort ?

CMB-S4 Ann Arbor Meeting Update

Courtesy K.Ganga

# Ex.: CLASS @ Chile

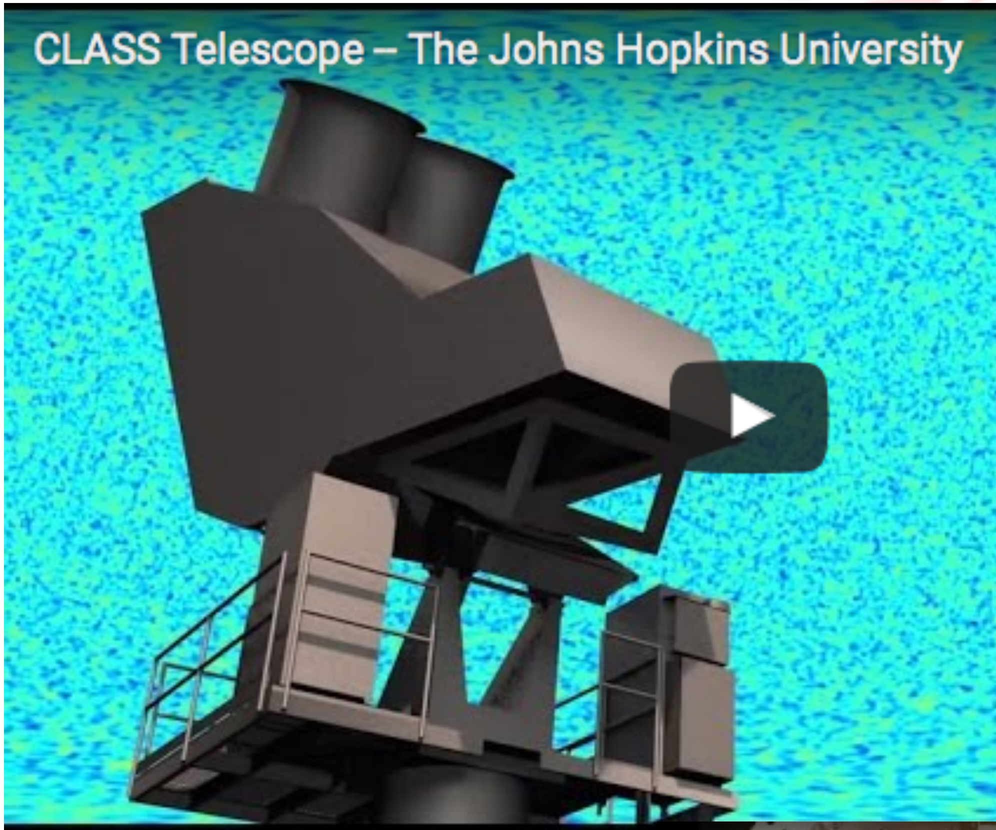


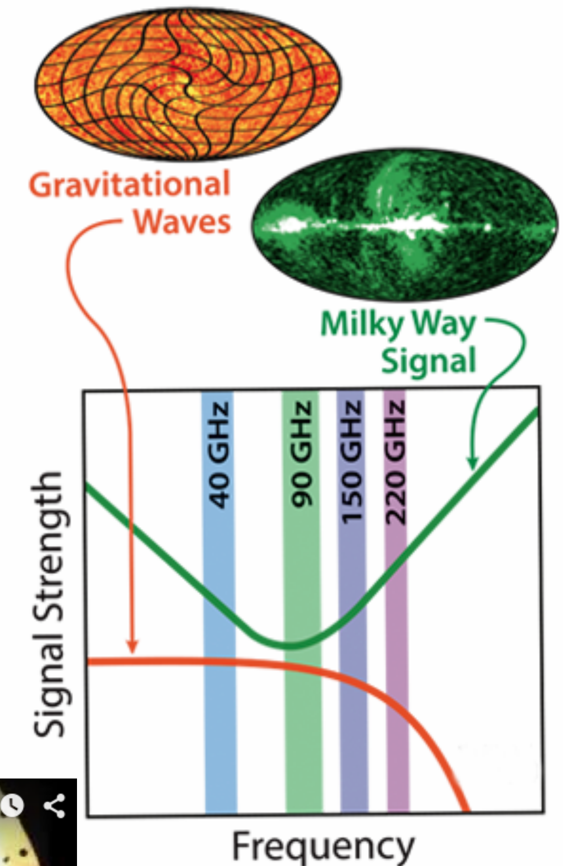


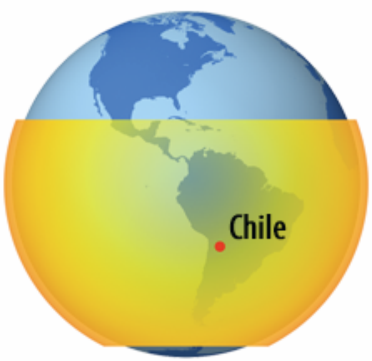


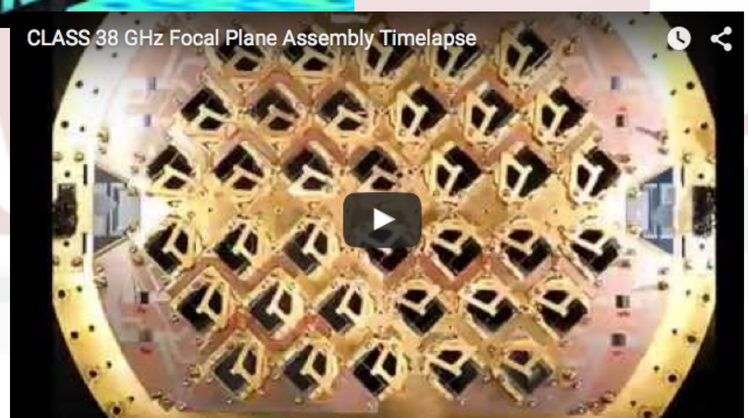

# LiteBIRD Overview

**Lite (Light) Satellite for the Studies of B-mode Polarization and Inflation from Cosmic Background Radiation Detection**

- CMB B-mode satellite proposed to JAXA and NASA
- Proposed launch year: JFY 2022
- Success criteria
  - Total uncertainty on r: $\sigma(r) < 0.001$*
  - Multipole coverage: $2 \leq \ell \leq 200$
    - Each bump (reionization, recombination) with >5sigma if $r > 0.01$
- Orbit: L2
- Observing time: ≥3 years

*Our current studies yield $\sigma(r) = 2 \times 10^{-4}$ for 3 year observation

# Why targeting σ(r) < 0.001 ?

- Many models predict r>0.01 → >10σ discovery.
- What if we do not see the signal ?
  - Focus on the simplest models based on Occam's razor principle.
  - Single field models that satisfy slow-roll conditions give

$$\boxed{r \simeq 0.002\left(\frac{60}{N}\right)^2\left(\frac{\Delta\phi}{m_{pl}}\right)^2}$$

Lyth relation

N: e-folding, $m_{pl}$: reduced Planck mass

  - Establishing a bound r < 0.002 (95%C.L.) will rule out large field models that satisfy the Lyth relation. Setting this limit is a very significant contribution to cosmology and fundamental physics.

- GUT-scale physics

$$\boxed{V^{1/4} = 1.06 \times 10^{16} \times \left(\frac{r}{0.01}\right)^{1/4} [\mathrm{GeV}]}$$

V: Inflaton potential, r: tensor-to-scalar ratio



Courtesy
M. Hazumi



PLANCK

# 15 frequency bands

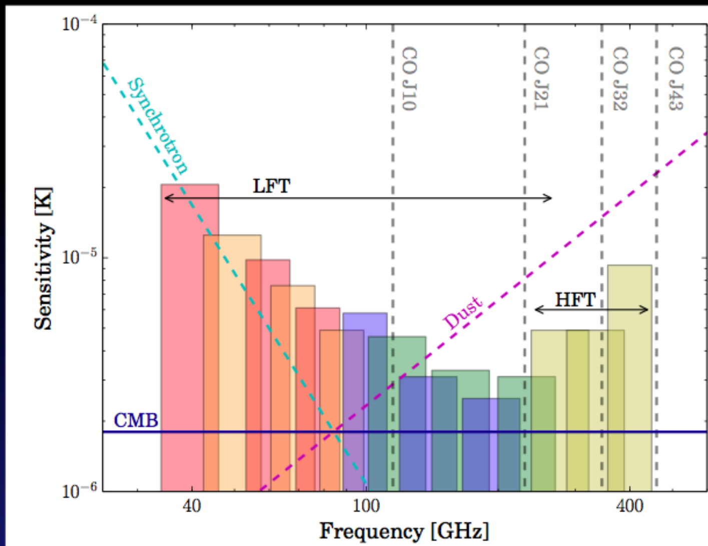


<u>Polarization sensitivity</u>

2.4 μKarcmin

(3 year operation, including margin)

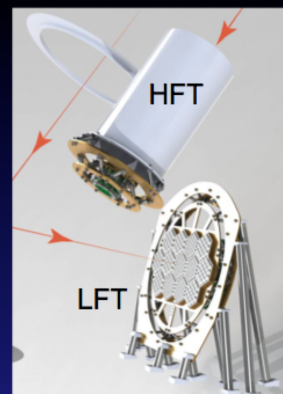


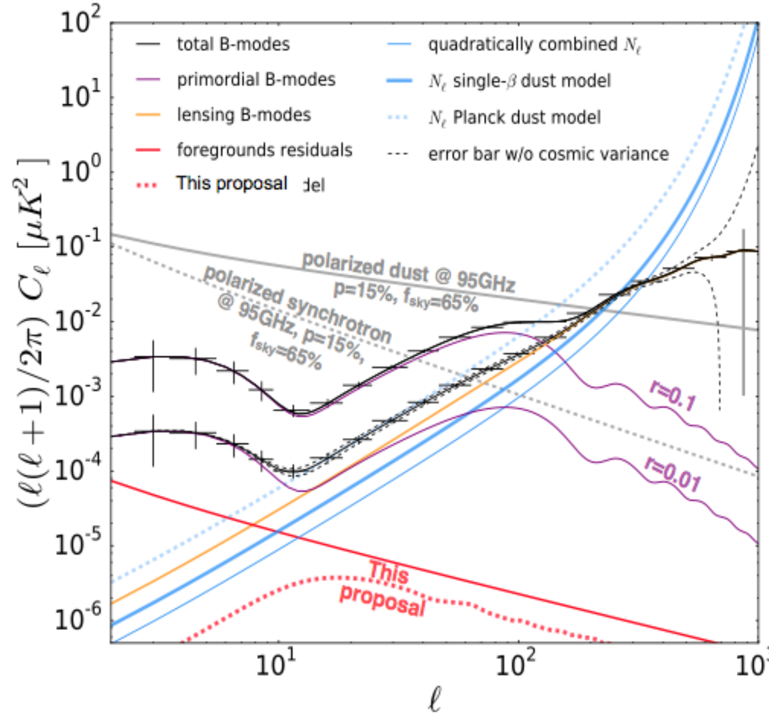


**Courtesy M. Hazumi**

$\sigma(r) = 0.45 \times 10^{-3}$

for r = 0.01, including foreground removal*, cosmic variance and delensing w/ CIB**

$r < 0.4 \times 10^{-3}$ (95% C.L.)

for undetectably small r

**N.B.: success of delensing largely depends on combination of LiteBIRD & CMB-S4**

**The European view to future CMB mission: selfconsistent experiment, B-modes … but not only ☺ → scientific return even for extremely low r**

# In a nutshell: New science with a polarimetric and spectral survey of the **Hubble volume** from the $\mu$–wave to the far-IR

5 — Ultimate measurement of CMB polarization, Gaussianity, and absolute spectrum. Search for the gravitational waves produced during inflation.

1 — **Ultimate galaxy cluster survey** via Sunyaev-Zeldovich effect (SZ): ($>10^6$ : all clusters with $M>10^{14}M_{\odot}$ within our horizon )

**Legacy archive of hundreds of full-sky intensity and polarization maps from tens of GHz to few THz with extreme precision and resolution :**
$1\mu K_{CMB}$arcmin
1'FWHM@$\lambda$1mm

"All" goals

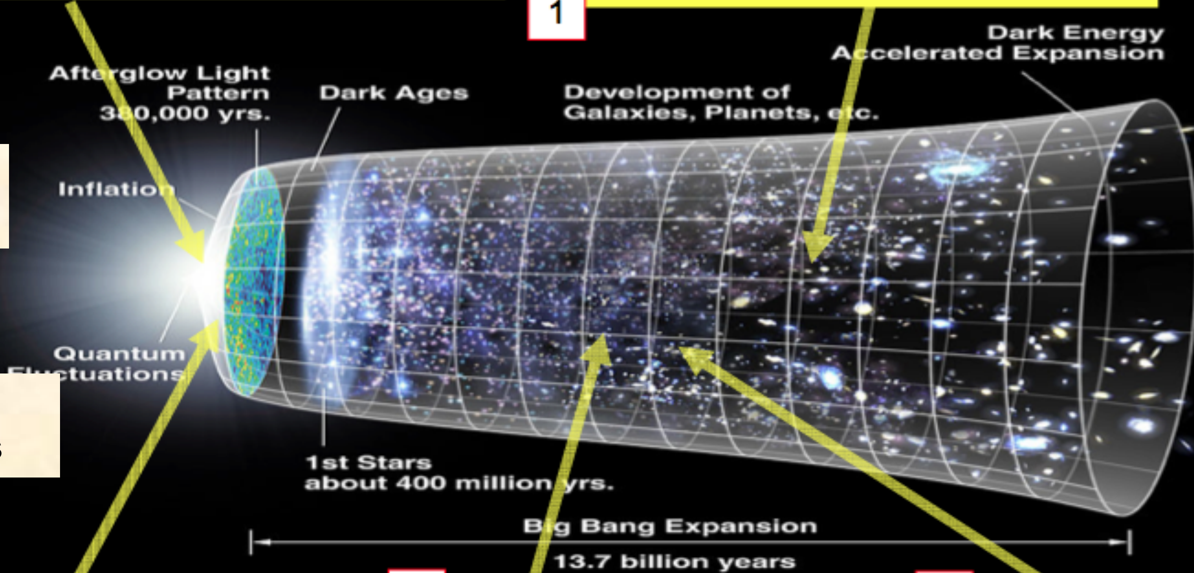


Courtesy P. de Bernardis

6 — A complete survey of the interstellar medium in the Milky way : dust, molecular lines, magnetic field, …

4 — Probe epochs before recombination and new physics using CMB spectral distortion measurements

3 — Map the gravitational potential all the way to z=1100 through CMB lensing

2 — Probe early star formation and its evolution through precision characterization of the Cosmic Infrared Background (CIB)

# CORE (ESA M5 Call) channels and sensitivity

| Channel [GHz] | Beam [arcmin] | $N_{\rm det}$ | $\Delta T$ [$\mu$K.arcmin] | $\Delta P$ [$\mu$K.arcmin] | $\Delta I$ [$\mu K_{\rm RJ}$.arcmin] | $\Delta I$ [kJy/sr.arcmin] | $\Delta y \times 10^6$ [$y_{\rm SZ}$.arcmin] | PS ($5\,\sigma$) [mJy] |
|---|---|---|---|---|---|---|---|---|
| 60 | 17.87 | 48 | 7.5 | 10.6 | 6.81 | 0.75 | −1.5 | 5.0 |
| 70 | 15.39 | 48 | 7.1 | 10.0 | 6.23 | 0.94 | −1.5 | 5.4 |
| 80 | 13.52 | 48 | 6.8 | 9.6 | 5.76 | 1.13 | −1.5 | 5.7 |
| 90 | 12.08 | 78 | 5.1 | 7.3 | 4.19 | 1.04 | −1.2 | 4.7 |
| 100 | 10.92 | 78 | 5.0 | 7.1 | 3.90 | 1.20 | −1.2 | 4.9 |
| 115 | 9.56 | 76 | 5.0 | 7.0 | 3.58 | 1.45 | −1.3 | 5.2 |
| 130 | 8.51 | 124 | 3.9 | 5.5 | 2.55 | 1.32 | −1.2 | 4.2 |
| 145 | 7.68 | 144 | 3.6 | 5.1 | 2.16 | 1.39 | −1.3 | 4.0 |
| 160 | 7.01 | 144 | 3.7 | 5.2 | 1.98 | 1.55 | −1.6 | 4.1 |
| 175 | 6.45 | 160 | 3.6 | 5.1 | 1.72 | 1.62 | −2.1 | 3.9 |
| 195 | 5.84 | 192 | 3.5 | 4.9 | 1.41 | 1.65 | −3.8 | 3.6 |
| 220 | 5.23 | 192 | 3.8 | 5.4 | 1.24 | 1.85 | ... | 3.6 |
| 255 | 4.57 | 128 | 5.6 | 7.9 | 1.30 | 2.59 | 3.5 | 4.4 |
| 295 | 3.99 | 128 | 7.4 | 10.5 | 1.12 | 3.01 | 2.2 | 4.5 |
| 340 | 3.49 | 128 | 11.1 | 15.7 | 1.01 | 3.57 | 2.0 | 4.7 |
| 390 | 3.06 | 96 | 22.0 | 31.1 | 1.08 | 5.05 | 2.8 | 5.8 |
| 450 | 2.65 | 96 | 45.9 | 64.9 | 1.04 | 6.48 | 4.3 | 6.5 |
| 520 | 2.29 | 96 | 116.6 | 164.8 | 1.03 | 8.56 | 8.3 | 7.4 |
| 600 | 1.98 | 96 | 358.3 | 506.7 | 1.03 | 11.4 | 20.0 | 8.5 |
| Array | | 2100 | 1.2 | 1.7 | | | 0.41 | |

**Table 1.** Proposed *CORE* frequency channels. The sensitivity is calculated for a 4-year mission, assuming $\Delta\nu/\nu = 30\%$ bandwidth, 60% optical efficiency, total noise of twice the expected photon noise from the sky and the optics of the instrument being cooled to 40 K. This configuration has 2100 detectors, about 45% of which are located in CMB channels between 130 and 220 GHz. Those six CMB channels yield an aggregate CMB sensitivity in polarisation of 2 $\mu$K.arcmin (1.7 $\mu$K.arcmin for the full array).

**J. Delabrouille et al. arXiv:1706.04516**

# CORE in a global framework

**CMB S4**
Ground-based Imager
1-2' in atmospheric windows
$\nu$ = 40, 95, 150, 220
Good on small scales

High angular resolution

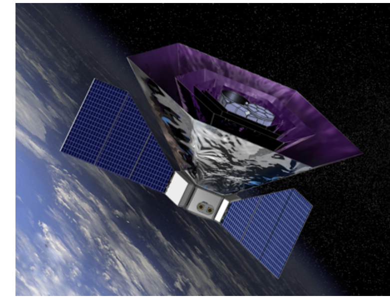

**PIXIE (+)**
Absolute measurement
1-2° in many bands
Clean large scales

**A high resolution (1-2') absolute ($10^{-8}$) imaging spectrophotometer ($N_{freq}$>20)**

**Cosmic Origins Explorer**
Space-borne Imager, many frequencies
1-2' at high frequency ($\nu \geq 300$)
4'-6' at CMB frequencies
Clean large scales

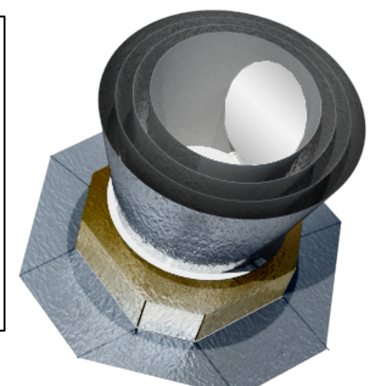

Absolute calibration & zero-level of maps

# CORE scanning strategy & typical sensitivity map

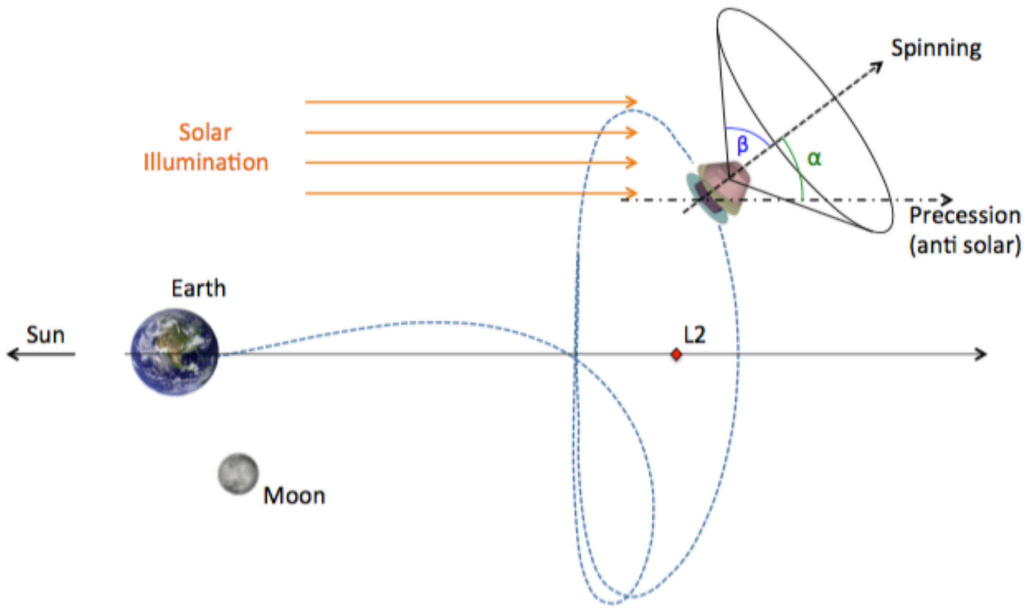


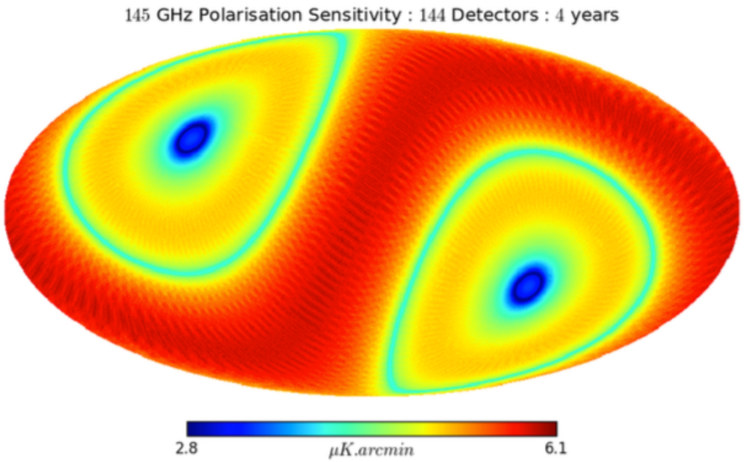


**Figure 3.** On an orbit around the Sun-Earth L2 Lagrange point, 1.5 million kilometre away from the Earth, the spacecraft scans the sky with three modulations of the pointing direction on various timescales. The spacecraft spins at a rate of order $f_{\rm spin} \simeq 0.5\,{\rm RPM}$, so that the line of sight scans the sky on quasi-circles of opening angle $\beta$ with a period of about 2 minutes. The circles are not perfectly closed by reason of a slower precession, with a period of $T_{\rm prec} \simeq 4\,{\rm days}$, with precession angle $\alpha$. The precession axis is kept anti-solar, so that the symmetric spacecraft always receives the same amount of illumination from the Sun, ensuring hence the thermal stability of the payload. The last modulation is provided by the slow revolution of the whole system around the Sun with a period of one year.

Aimed at optimizing polarization reconstruction through many different beam orientations

**J. Delabrouille et al.
arXiv:1706.04516**

# CORE alone

## Delensing through arcmin resolution

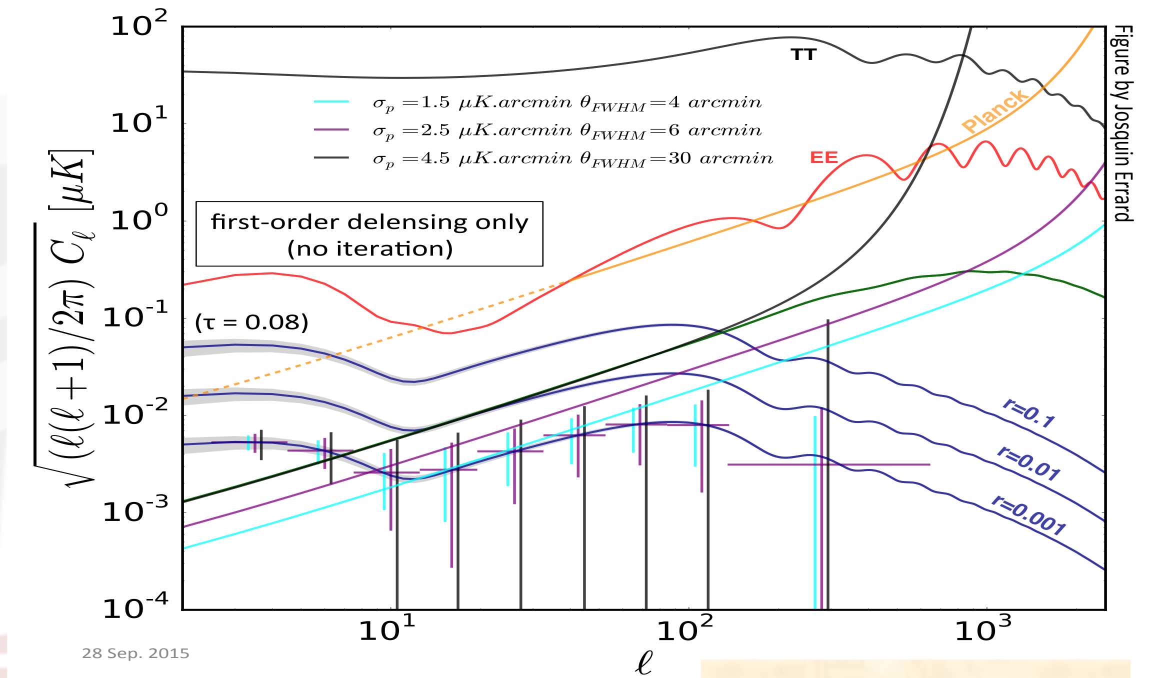


Courtesy J. Delabrouille

## Foreground cleaning through wide multifrequency

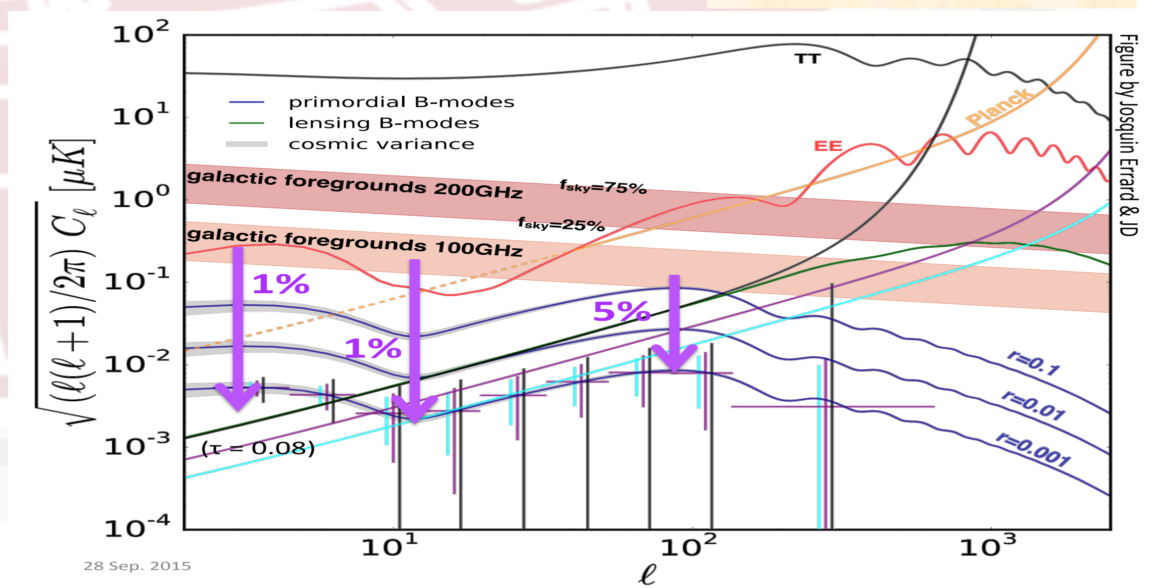

# Future CMB - Ex: cosmological parameters with CORE

| Parameter | Description | Current results (Planck 2015+Lensing) | CORE expected uncertainties |
|---|---|---|---|
| ΛCDM | | | |
| $\Omega_b h^2$ | Baryon Density | $\Omega_b h^2 = 0.02226 \pm 0.00016$ (68 % CL) [12] | $\sigma(\Omega_b h^2) = \mathbf{0.000037}$ {4.3} |
| $\Omega_c h^2$ | Cold Dark Matter Density | $\Omega_c h^2 = 0.1193 \pm 0.0014$ (68 % CL) [12] | $\sigma(\Omega_c h^2) = \mathbf{0.00026}$ {5.4} |
| $n_s$ | Scalar Spectral Index | $n_s = 0.9653 \pm 0.0048$ (68 % CL) [12] | $\sigma(n_s) = \mathbf{0.0014}$ {3.4} |
| $\tau$ | Reionization Optical Depth | $0.063 \pm 0.014$ (68 % CL) [12] | $\sigma(\tau) = \mathbf{0.002}$ {7.0} |
| $H_0$ [km/s/Mpc] | Hubble Constant | $H_0 = 67.51 \pm 0.64$ (68 % CL) [12] | $\sigma(H_0) = \mathbf{0.11}$ {5.8} |
| $\sigma_8$ | r.m.s. mass fluctuations | $\sigma_8 = 0.8150 \pm 0.0087$ (68 % CL) [12] | $\sigma(\sigma_8) = \mathbf{0.0011}$ {7.9} |
| Extensions | | | |
| $\Omega_k$ | Curvature | $\Omega_k = -0.0037^{+0.0083}_{-0.0069}$ (68 % CL) [12] | $\sigma(\Omega_k) = \mathbf{0.0019}$ {4} |
| $N_{\rm eff}$ | Relativistic Degrees of Freedom | $N_{\rm eff} = 2.94 \pm 0.20$ (68 % CL) [12] | $\sigma(N_{\rm eff}) = \mathbf{0.041}$ {4.9} |
| $M_\nu$ | Total Neutrino Mass | $M_\nu < 0.315\,\mathrm{eV}$ (68 % CL) [12] | $\sigma(M_\nu) = \mathbf{0.043}$ eV {7.3} |
| $(m_s^{eff}, N_s)$ | Sterile Neutrino Parameters | $(m_s^{eff} < 0.33\mathrm{eV}, N_s < 3.24)$ (68 % CL) [12] | $\sigma(m_s^{eff}, N_s) = (\mathbf{0.037}eV, \mathbf{0.053})$ {8.9, 4.5} |
| $Y_p$ | Primordial Helium abundance | $Y_p = 0.247 \pm 0.014$ (68 % CL) [12] | $\sigma(Y_p) = \mathbf{0.0029}$ {4.8} |
| $Y_p$ | Primordial Helium (free $N_{eff}$) | $Y_p = 0.259^{+0.020}_{-0.017}$ (68 % CL) [12] | $\sigma(Y_p) = \mathbf{0.0056}$ {3.2} |
| $\tau_n$ [s] | Neutron Life Time | $\tau_n = 908 \pm 69$ (68 % CL) [167] | $\sigma(\tau_n) = \mathbf{13}$ {5.3} |
| $w$ | Dark Energy Eq. of State | $w = -1.42^{+0.25}_{-0.47}$ (68 % CL) [12] | $\sigma(w) = \mathbf{0.12}$ {3} |
| $T_0$ | CMB Temperature | Unconstrained [12] | $\sigma(T_0) = \mathbf{0.018}$ K |
| $p_{ann}$ | Dark Matter Annihilation | $p_{ann} < 3.4 \times 10^{-28}$ $cm^3/GeV/s$ (68 % CL) [12] | $\sigma(p_{ann}) = \mathbf{5.3 \times 10^{-29}}$ $cm^3/GeV/s$ {6.4} |
| $g^4_{\rm eff}$ | Neutrino self-interaction | $g^4_{\rm eff} < 0.22 \times 10^{-27}$ | $\sigma(g^4_{\rm eff}) = 0.34 \times 10^{-28}$ {6.4} |
| $\alpha/\alpha_0$ | Fine Structure Constant | $\alpha/\alpha_0 = 0.9990 \pm 0.0034$ (68 % CL) | $\sigma(\alpha/\alpha_0) = \mathbf{0.0007}$ {4.8} |
| $\Sigma_0 - 1$ | Modified Gravity | $\Sigma_0 - 1 = 0.10 \pm 0.11$ (68 % CL) [53] | $\sigma(\Sigma_0 - 1) = \mathbf{0.044}$ {2.5} |
| $A_{2s1s}/8.2206$ | Recombination 2 photons rate | $A_{2s1s}/8.2206 = 0.94 \pm 0.07$ (68 % CL) [12] | $\sigma(A_{2s1s}/8.2206) = \mathbf{0.015}$ {4.7} |
| $\Delta(z_{reio})$ | Reionization Duration | $\Delta(z_{reio}) < 2.26$ (68 % CL) [35] | $\sigma(\Delta z_{reio}) = \mathbf{0.58}$ {3.9} |

**From E. Di Valentino et al. arXiv:1612.00021**

**Table 34.** Current limits from Planck 2015 and forecasted CORE-M5 uncertainties. The first 6 rows assume a ΛCDM scenario while the following rows give the constraints on single parameter extensions. In the fourth column, numbers in curly brackets {...} give the improvement in the parameter constraint when moving from Planck 2015 to CORE-M5, defined as the ratio of the uncertainties $\sigma^{Planck}/\sigma^{CORE}$.

# $n_s$ – r ; improvement from COrE

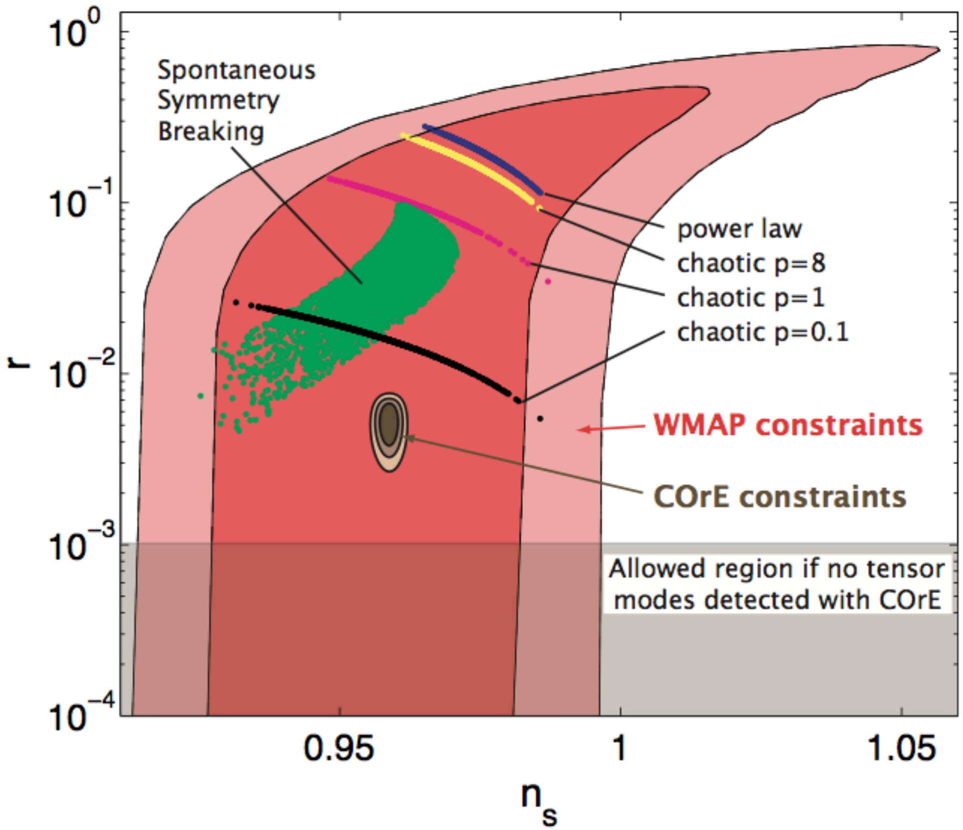


Courtesy M. Bucher

$r = 10^{-3}$ at $3\sigma$ at least.

**Characterization of tensor perturbations, ex.: in single field or slow-roll inflation:**

$$|n-1| = |2\eta - 6\varepsilon| << 1; \quad n_T = 2\varepsilon \qquad \varepsilon \equiv \frac{1}{16\pi G}\left(\frac{V'}{V}\right)^2, \ \eta \equiv \frac{1}{8\pi G}\frac{V''}{V}$$

# Reionization beyond simple tau-approximation
# Extension to all modes – EE & BB modes

$$\tau = \int \chi_e n_e \sigma_T c dt$$

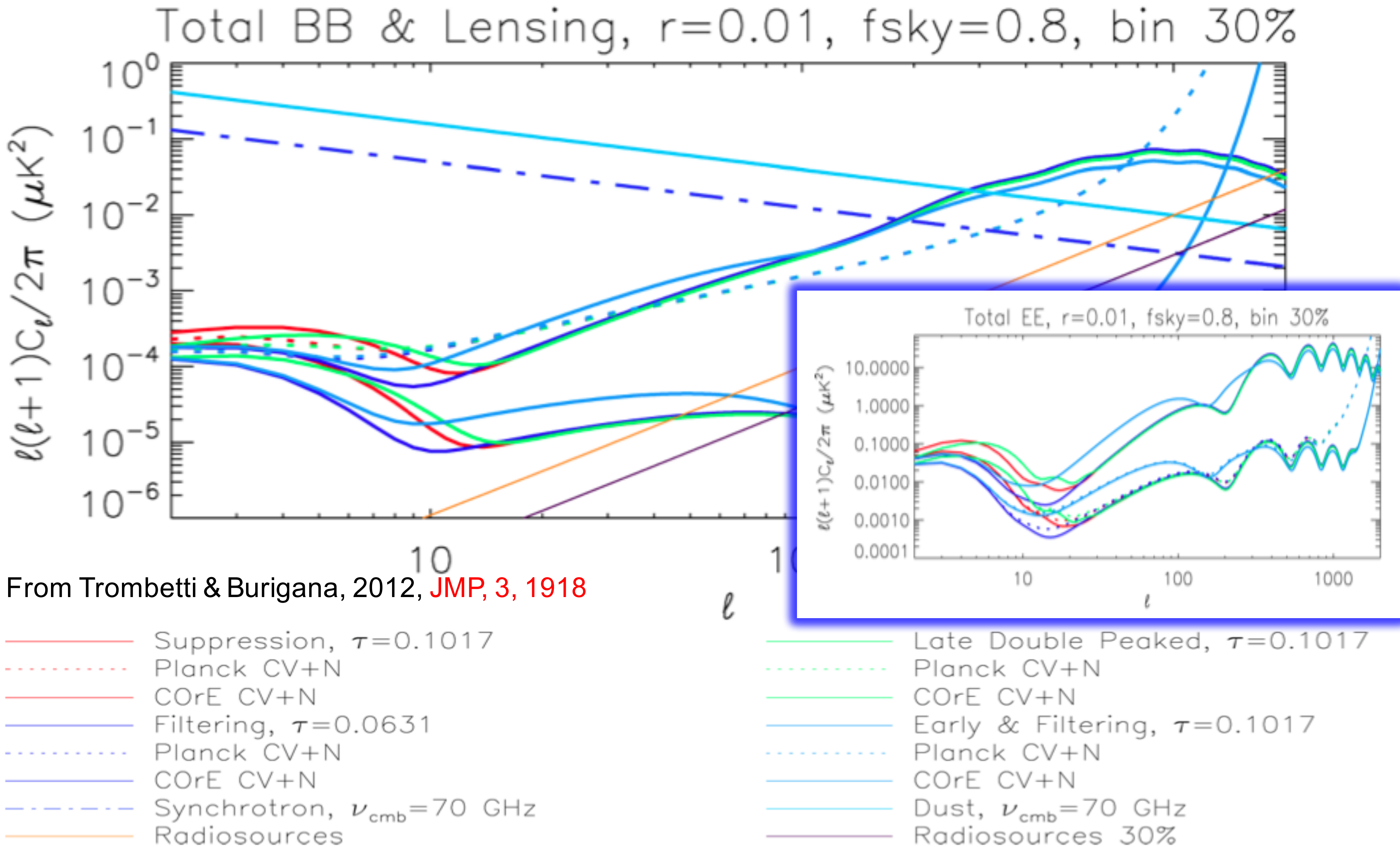


From Trombetti & Burigana, 2012, JMP, 3, 1918

# Y map gives us lots of clusters

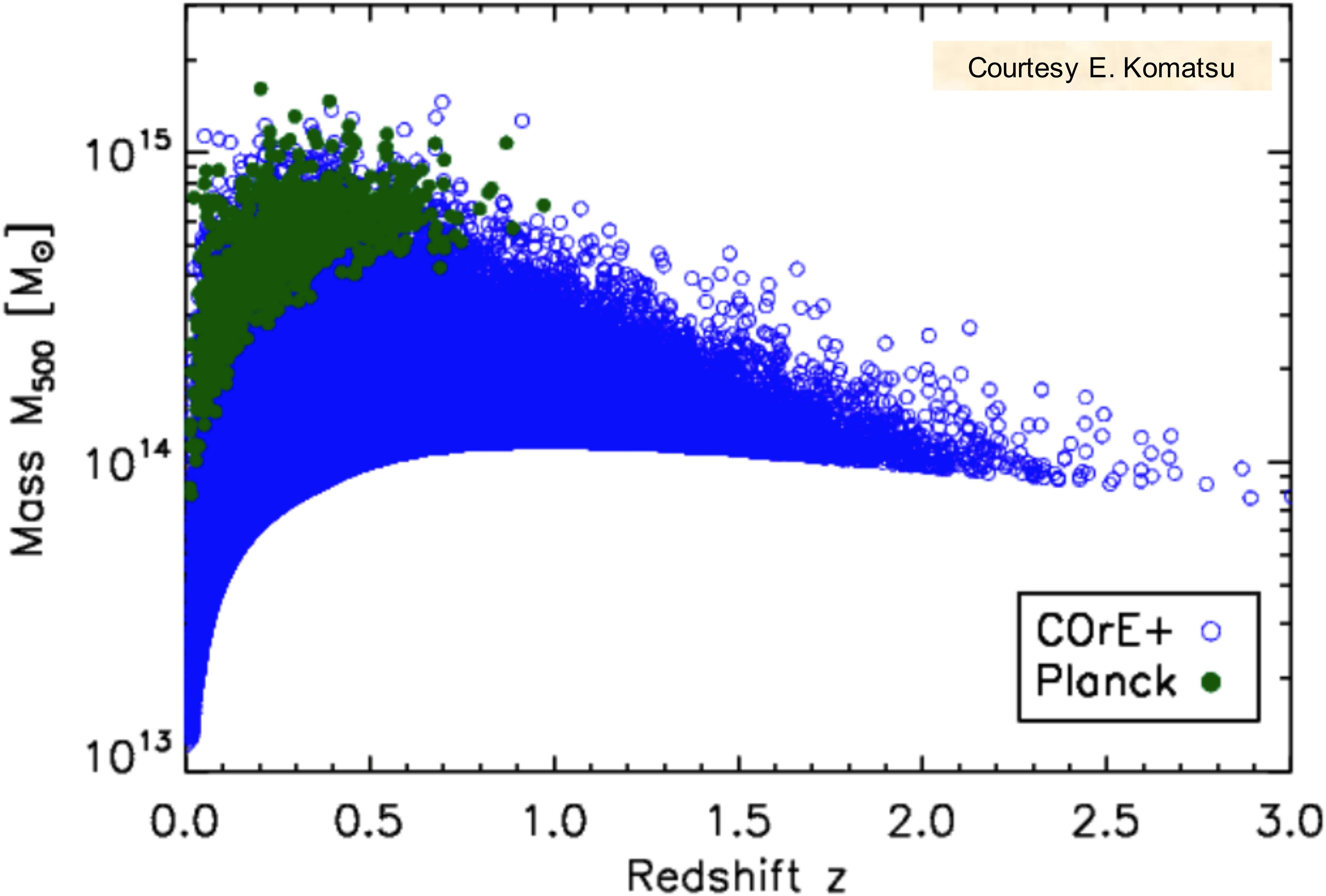

# Detection limits for a diffraction-limited survey

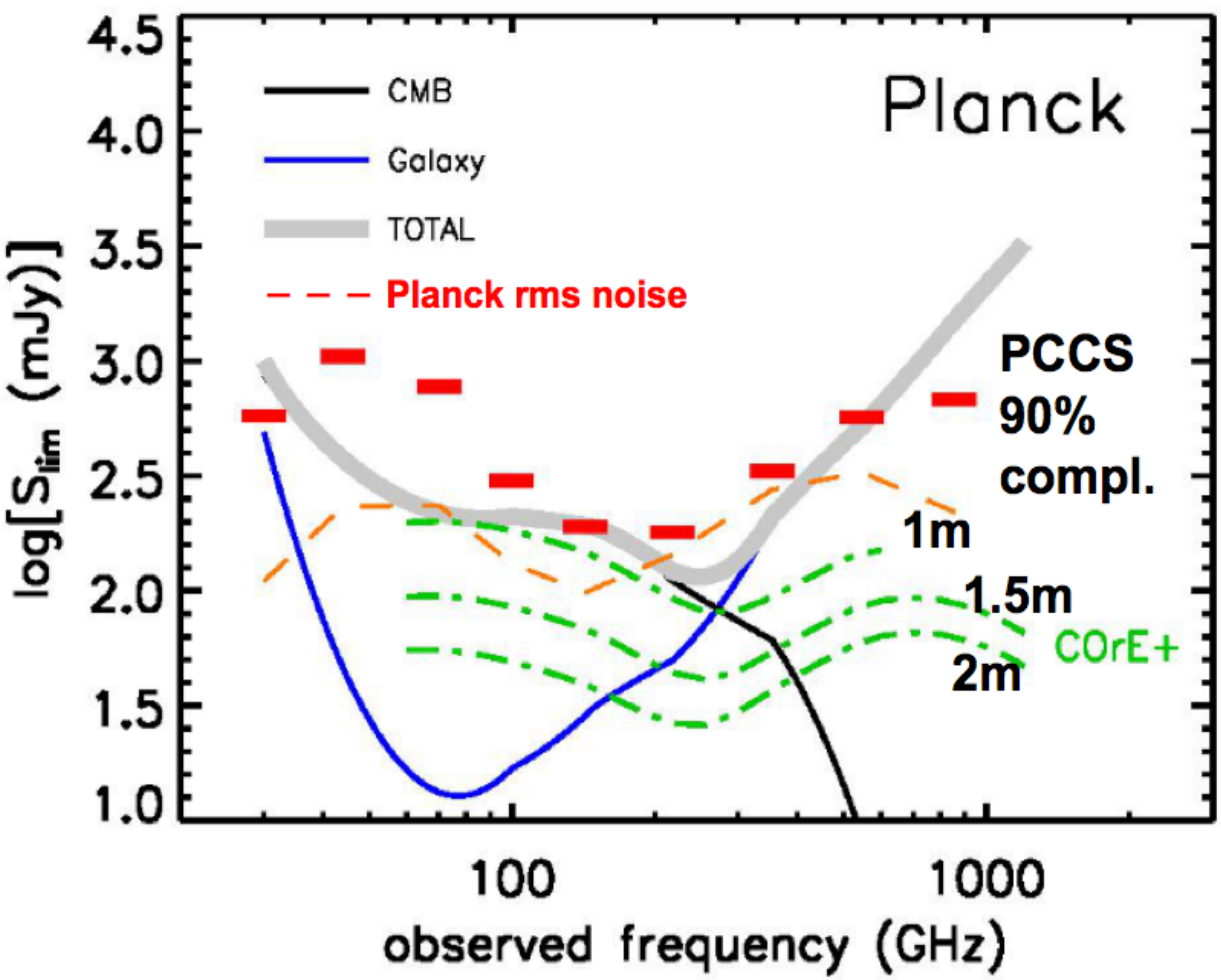


**In total intensity:**

Given current sensitivities, confusion dominates detection limits

→ **Angular resolution critical**

*Planck* HFI worse than diffraction limited

**Improvements** expected even with *smaller telescope* but *diffraction-limited*

# Effect of CORE detection limit for extragalactic source counts

- Extragalactic **radio-sources** almost dominated by **blazars**, that is also dominating population in gamma-rays

- *Planck* data crucial to characterize their **synchrotron peak** and understanding their physics (Giommi et al. 2012)

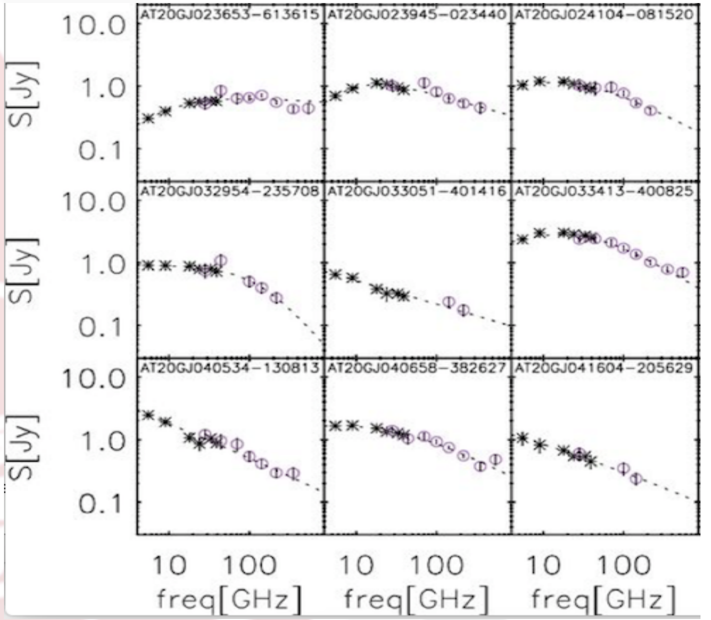


Extracted from Massardi et al. 2016

- **Galaxies with active star formation**
  - starlight absorbed by circumstellar dust grains and re-emitted in far-IR/sub-mm
  - **CORE will fill gap** between Planck flux limit and Herschel flux range, a gap where
    - ✓ **cosmological evolution** appears and thus particularly important for evolutionary models
    - ✓ it is easier to identify extreme cases of flux **gravitational amplification**

# Predicted counts in polarization for a 1m telescope

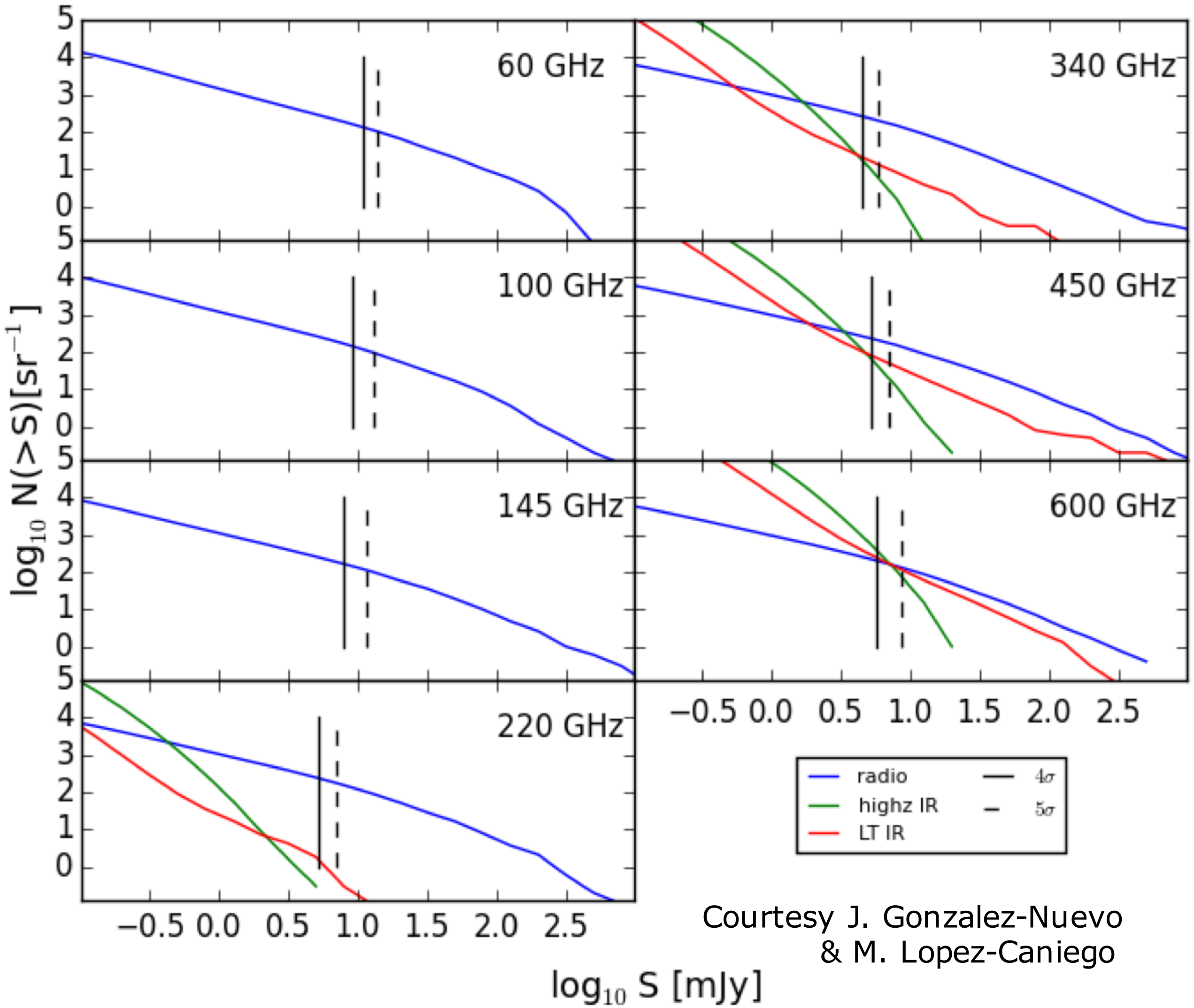


**Complete samples in polarization are currently limited to:**

- ✓ **some tens of radio-sources (microwaves/mm)**
- ✓ **negligible number (sub-mm)**

**COrE-M5 high sensitivity in polarization open a new window**

**Simulations for COrE-M5 suggest:**

- ❖ **detection of:** **thousands of sources in its whole frequency range**
- ❖ **for the first time:** **hundreds of galaxies with intense star formation with polarized signal by dust grains**

**→ Unique information on:**

- ➢ **their magnetic fields**
- ➢ **unknown origin of tight correlation between IR and radio luminosities of these objects**

# Future of CMB spectrum

C. Burigana – Varenna 6/7/2017

# CMB spectrum: current status

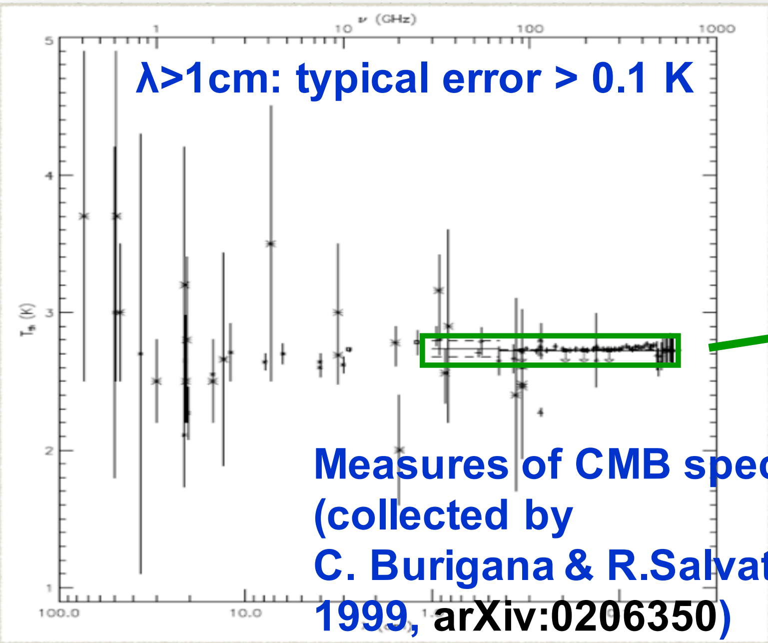


λ>1cm: typical error > 0.1 K

Measures of CMB spectrum
(collected by
C. Burigana & R.Salvaterra,
1999, arXiv:0206350)

$T_0 = 2.725$
$\pm\, 0.002$ °K

Mather, J.C.,
et al., 1999,
ApJ, 512, 511

FIRAS
measures:
typical error
±0.0001 K

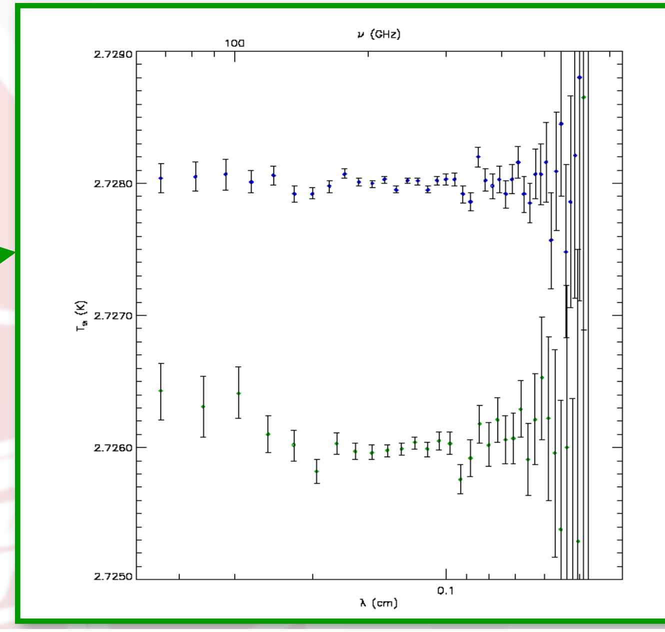


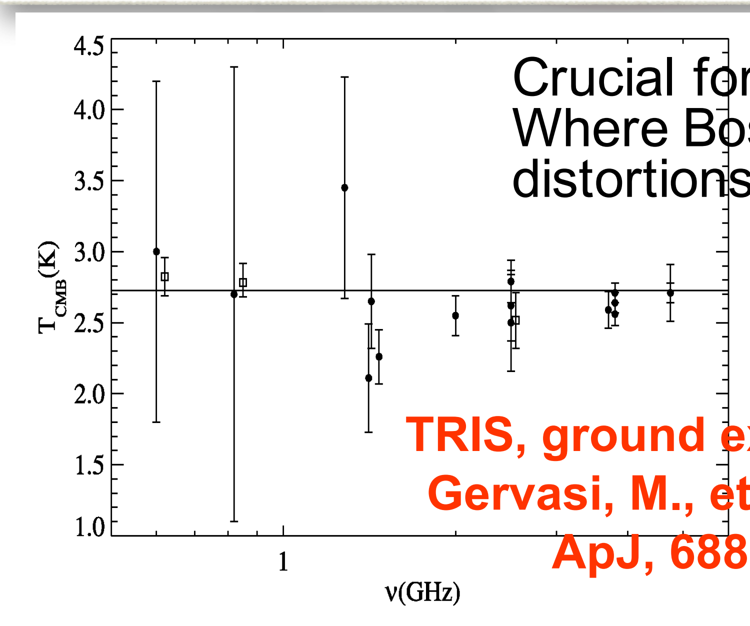


Crucial for free-free distortions
Where Bose-Einstein like
distortions are more prominent

TRIS, ground experiment
Gervasi, M., et al. 2008,
ApJ, 688, 24

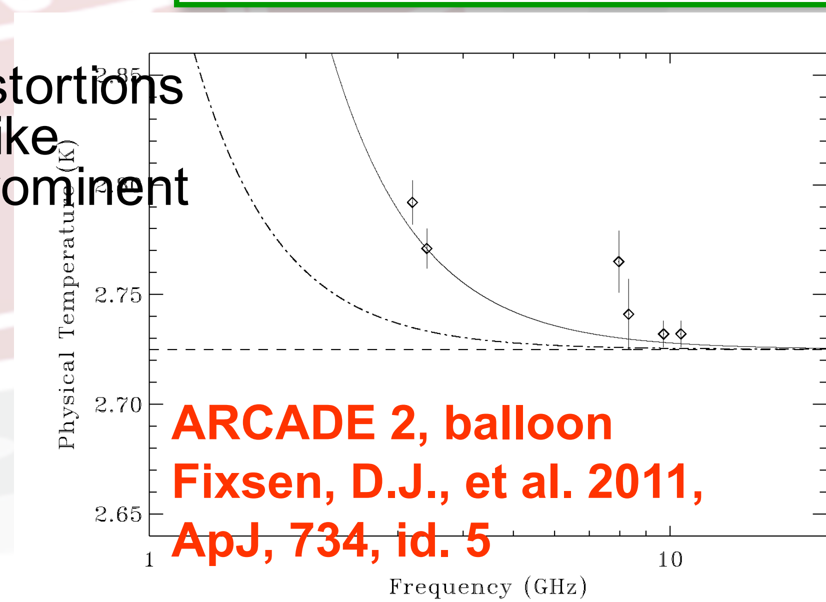


ARCADE 2, balloon
Fixsen, D.J., et al. 2011,
ApJ, 734, id. 5

Fig. 5 —CMB thermodynamic temperature measured at low frequencies (see

# CMB distortions @ different cosmic times

BIG BANG

Blackbody Photosphere

**Current accurate & general numerical codes, able to ingest many kinds of source terms: KYPRIX: P. Procopio & C. Burigana 2009, A&A, 507, 1243; CosmoTherm: J. Chluba & R.A. Sunyaev, 2012, MNRAS, 419, 1294**

Zeldovich & Sunyaev 1969; Illarionov & Sunyaev 1974; Danese & de Zotti 1977; Burigana et al. 1991; Hu & Silk 1993

**Intermediate distortions**

today

$z_{thermalization}$ — $z_{BE}$ — $z$ — $z_{recombination}$ — $z$

**Primordial distortions**

Bose-Einstein like

$$\eta_\nu = \frac{1}{e^{(h\nu/kT)+\mu} - 1}$$

**Late distortions**

Superposition of black bodies

$$\eta(x, y^*) \simeq (4\pi y^*)^{-1/2} \int_0^\infty \eta_0(x') \exp\left[ - \frac{(\ln(x/x') + 3y^*)^2}{4y^*} \right] \frac{dx'}{x'}$$

with μ function of x $\mu(x) \simeq \mu_0 \, e^{(-x_C/x)}$

where $y^* = \int \frac{k_B(T_e - T_r)}{m_e c^2} d\tau$

**+ Free-free distortions** → $y_B \simeq x^2 \left( \frac{T_{br} - T_r \phi_i}{T_r} - 2u\phi_i \right)$

**$\mu \sim 1.4 \, \Delta\varepsilon/\varepsilon_i$**

**$y \sim (1/4) \, \Delta\varepsilon/\varepsilon_i$**

**Late distortions** → **Related (mainly) to the reionization history of the universe**

**To firmly observe such small distortions the Galactic and extragalactic foreground contribution should be accurately modelled and subtracted.**

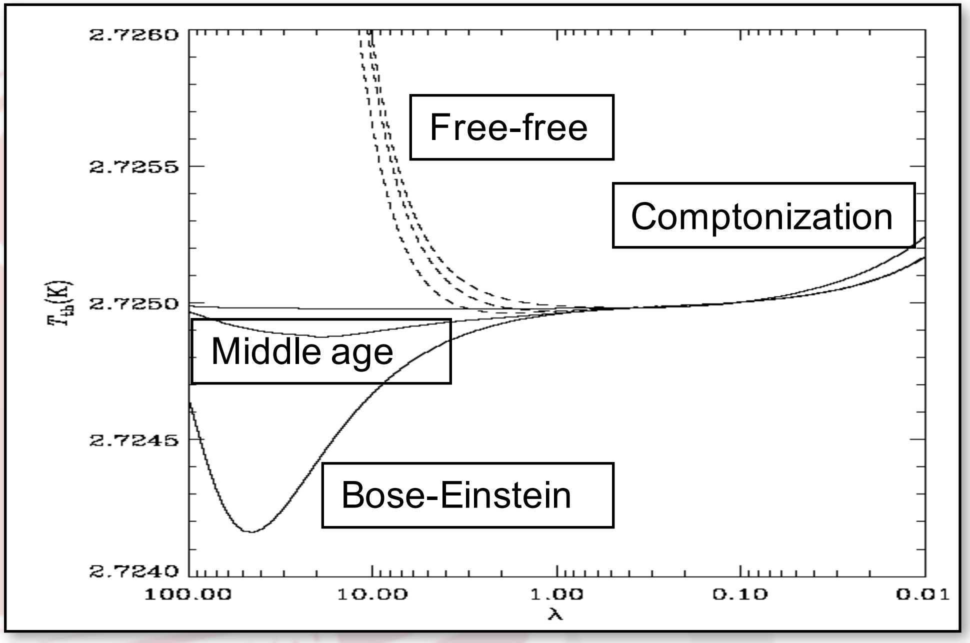


**CMB distorted spectra as functions of the wavelength λ (in cm) in the presence of a late energy injection with $\Delta\varepsilon/\varepsilon_i \simeq 4y = 5 \times 10^{-6}$ plus an early/intermediate energy injection with $\Delta\varepsilon/\varepsilon_i = 5 \times 10^{-6}$ occurring at the "time" Comptonization parameter $y_h$ = 5, 1, 0.01 (from the bottom to the top; in the figure the cases at $y_h = 5$ – when the relaxation to a Bose-Einstein modified spectrum with a dimensionless chemical potential given, in the limit of small distortions, by $\mu \simeq 1.4\Delta\varepsilon/\varepsilon_i$ is achieved – and at $y_h = 1$ are extremely similar at short wavelengths; solid lines) and plus a free-free distortion with $y_B = 10^{-6}$ (dashes). From Burigana et al. '04.**

# Ideas of the future of CMB spectrum from space

- The current limits on CMB spectral distortions and energy dissipation processes in the plasma, $|\Delta\varepsilon/\varepsilon_i|\leq 10^{-4}$, are mainly set by the NASA COBE/FIRAS experiment.

- High accuracy CMB spectrum experiments from space, like DIMES at $\lambda \geq 1$ cm (Kogut 1996) and FIRAS II at $\lambda \leq 1$ cm (Fixsen & Mather 2002), have been proposed to constrain (or probably detect) energy exchanges 10–100 times smaller than the FIRAS upper limits possibly generated by heating (but also by cooling) mechanisms at different cosmic epochs.

- These perspectives have been recently renewed:
  - in the context of a new CMB space mission like PIXIE (Kogut et al. 2011) proposed to NASA
  - in the possible inclusion of spectrum measures in the context of a polarization dedicated CMB space mission, of high sensitivity and up to arcmin resolution, like PRISM proposed to ESA in 2013
  - exploting differential approaches in anisotropy missions (CORE)

# Probing primordial power spectrum on very small scales using spectral distortion

- Current constraints on the power spectrum (and the spectral index $n_s$) are limited by the size of current horizon (CMB quadrupole) on large scales, and by nonlinearity and Silk damping on small scales.
- Little improvement can be expected from galaxy surveys and SKA because of these fundamental limitation.
- The small scale primordial power dissipated by Silk damping does not disappear completely, but leaves its imprint in **spectral distortions** from the perfect CMB blackbody spectrum. **Important target for the PRISM spectrometer.**

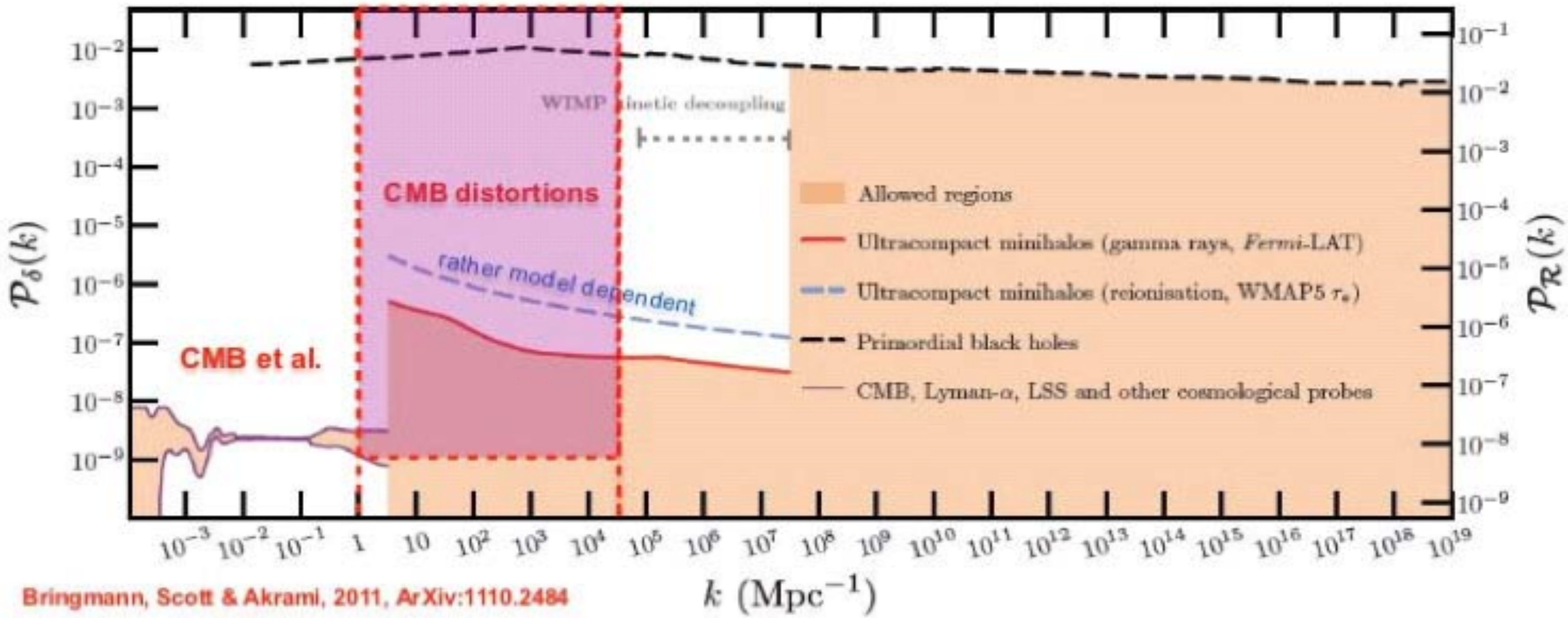


Bringmann, Scott & Akrami, 2011, ArXiv:1110.2484

# Adiabatic cooling (BE condensation) vs perturbation dissipation

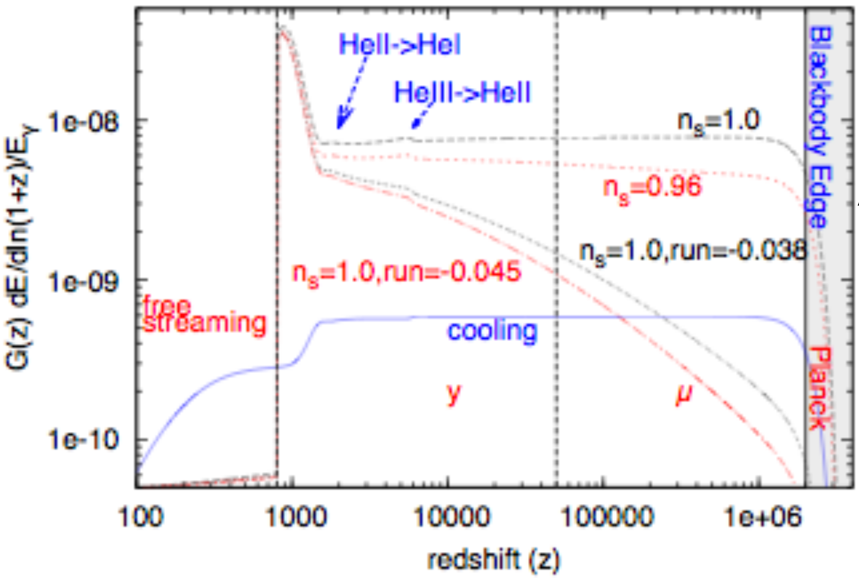


Sketch of fractional rate of energy release due to Silk damping and free streaming for different initial power spectra.
Also shown for comparison is the rate of energy loss due to adiabatic cooling of baryonic matter.

*Energy injection in μ distortions during $5 \times 10^4 < z < 2 \times 10^6$ for different initial power spectra without running compared with energy losses due to Bose-Einstein condensation.*

| $n_s$ | $\Delta E/E$ |
|---|---|
| 1.07 | $6.8 \times 10^{-8}$ |
| 1.04 | $4.7 \times 10^{-8}$ |
| 1.0 | $2.9 \times 10^{-8}$ |
| 0.96 | $1.8 \times 10^{-8}$ |
| 0.92 | $1.1 \times 10^{-8}$ |
| BEC | $-2.2 \times 10^{-9}$ |

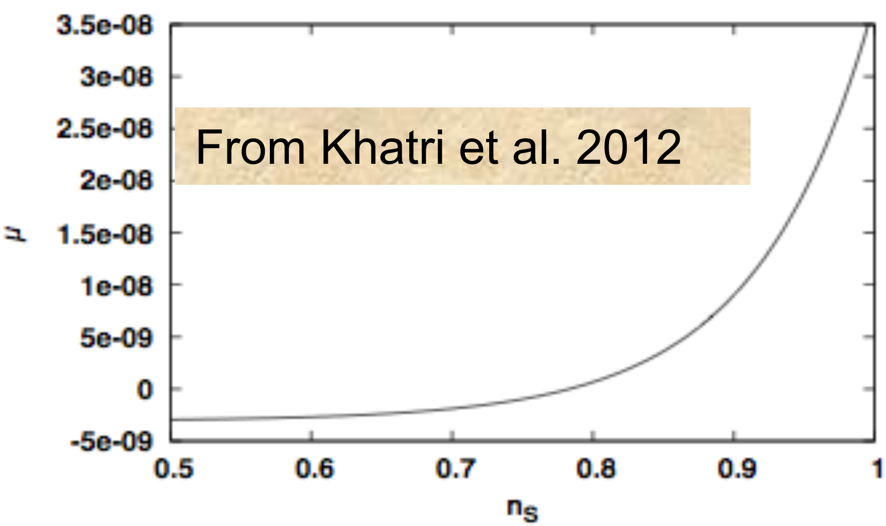


From Khatri et al. 2012

$\mu \sim 1.4\, \Delta\varepsilon/\varepsilon_i$ as a function of spectral index $n_s$ (without running)

**Chluba et al. 2012: also amplitude unknown @ small scales → larger range of μ**

# “Exotic” spectral distortions

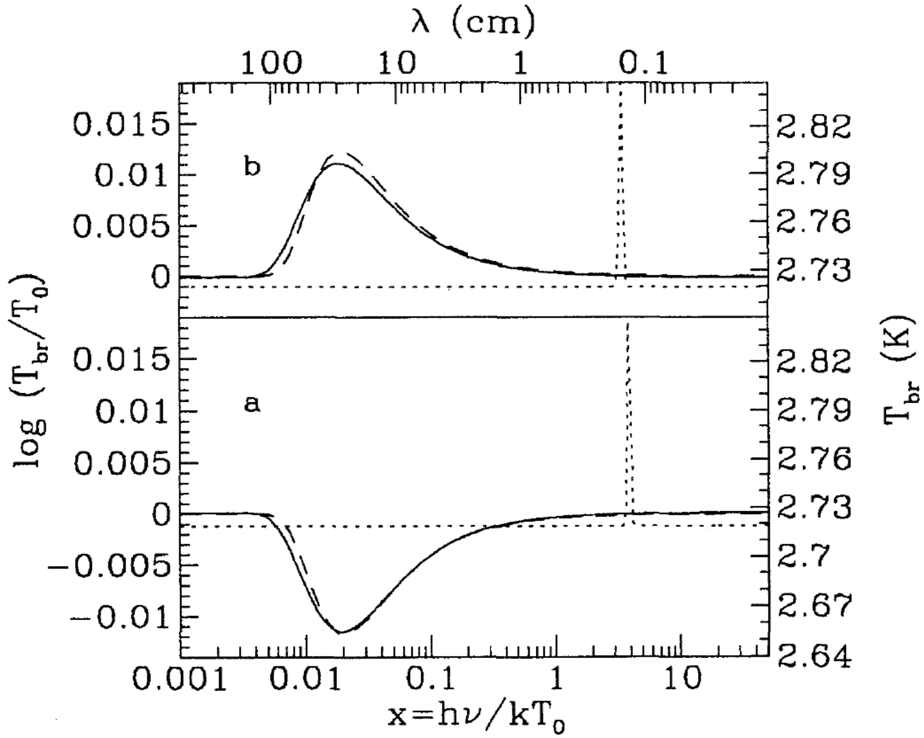


**Fig. 4.** Relaxation to a Bose–Einstein like spectrum of early distortions in presence of radiative decay with $\Delta n_\gamma/n_i = 7.5\,10^{-3}$ and $\Delta\epsilon/\epsilon_i$ such that $\mu = 10^{-3}$ (a) and $\mu = -10^{-3}$ (b) (see eq. (28), $\Delta\epsilon/\epsilon_i \simeq 0.01$). The initial spectrum is a black–body plus a “line” due to the radiative decay (dotted lines). The numerical results for the present spectrum (solid lines) and the approximation of Burigana et al. (1991a) (dashed lines) are showed. The agreement results to be quite good ($\Omega_b = 0.1$, $H_0 = 50$, $\Omega_T = 1$).

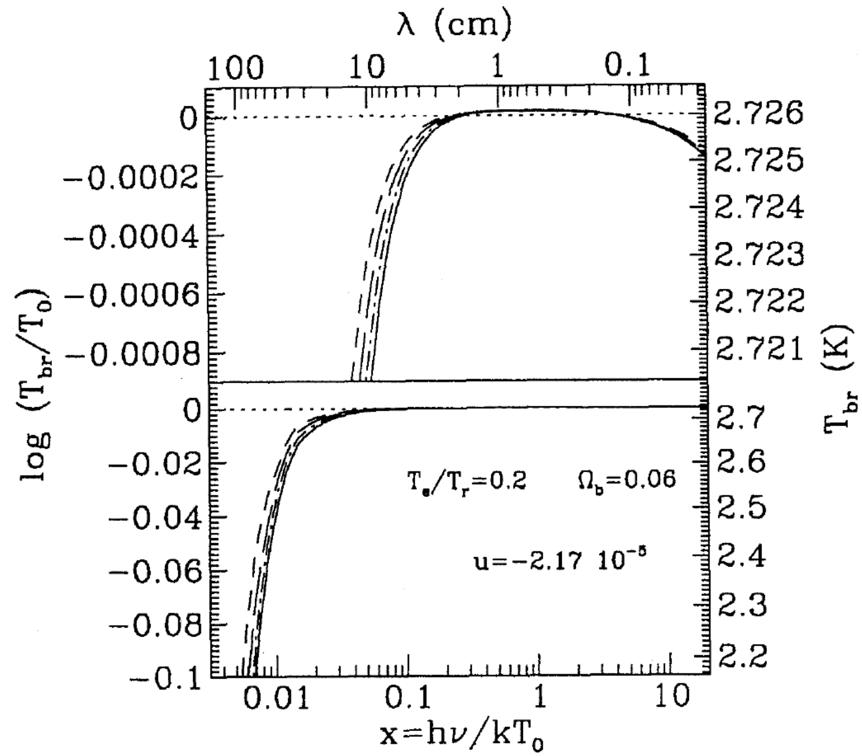


**Fig. 13.** Evolution of a BB spectrum since $z = 1500$ (dotted line) for the case of ionized matter with a constant ratio $T_e/T_r = 0.2$ between the matter and radiation temperature. The spectrum at several times is showed: $z = 749$ (dashed line), 499 (long dashes), 245 (dots plus dashes) and present time (solid line) ($H_0 = 50$, $\Omega_T = 1$). The distorted spectrum is characterized by negative values of $u$ and $y_B$ as a consequence of the assumption on the ratio $T_e/T_r$ (see eqq. (35) and (46)). Of course at very long wavelengths, where bremsstrahlung is very efficient, the spectrum approaches to that of a black–body with temperature $T = T_e$. The top panel is only a blow–up of a part of the bottom one for sake of comparison between the distortions at submillimetric and RJ spectral regions.

$$\mu \simeq 1.4 \left( \frac{1 + \Delta\epsilon/\epsilon_i}{(1 + \Delta n_\gamma/n_i)^{\frac{4}{3}}} - 1 \right) = 1.4 \left( \frac{1 + R_X B_\gamma x_X / \bar{x}_{CMB}}{(1 + R_X B_\gamma)^{\frac{4}{3}}} - 1 \right)$$

$R_x = (3/8)(g_f/X)$

*$g_f$ is the number of states per momentum mode and X is the effective number of relativistic interacting species at the decay epoch*

**Danese & Burigana ’94, Lecture Notes Phys., 429, 28**

# Summary of CMB spectral distortions in intensity

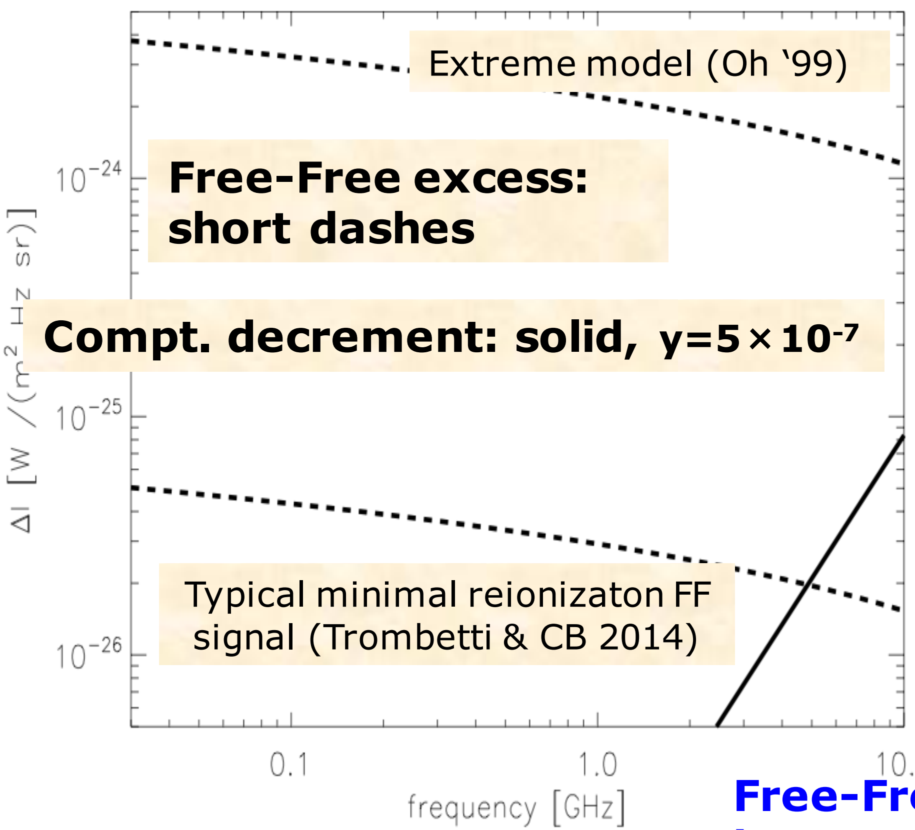


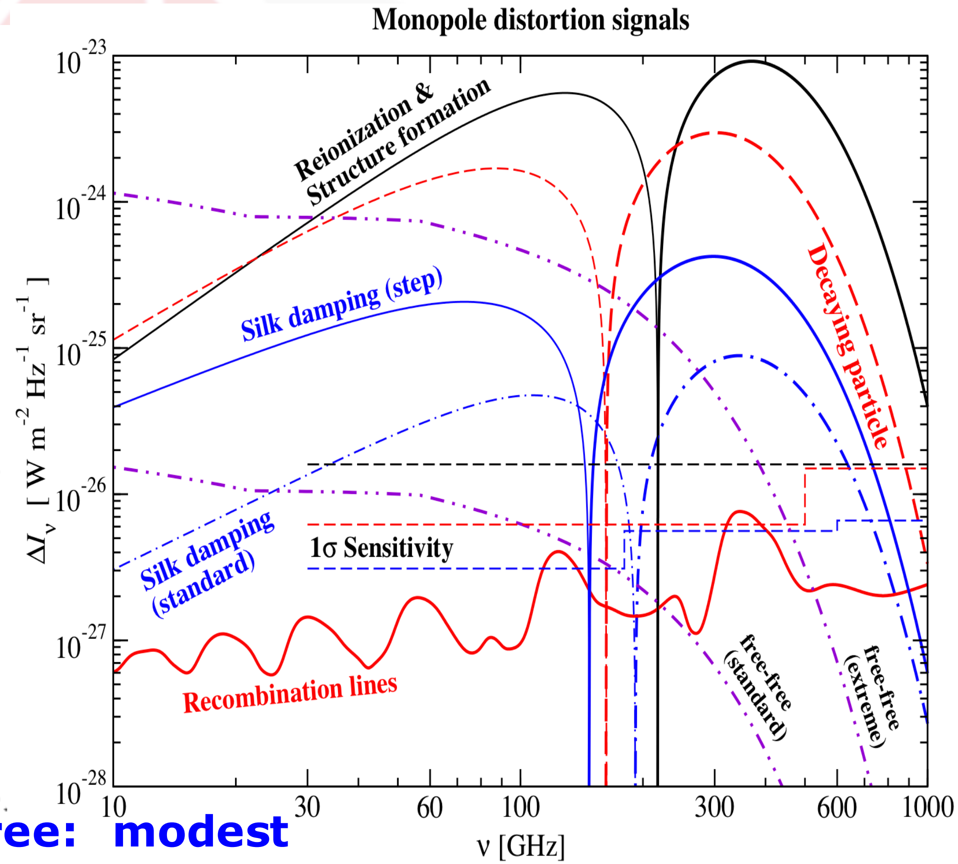


**Free-Free: modest but not negligible impact for CMB space missions, main target for ground-based observations.**

## Low freqs.

**Ground experiments, DIMES, ARCADE 2, SKA & its precursors**

## High freqs.

**FIRAS II, Pixie, PRISM**

**From PRISM studies**

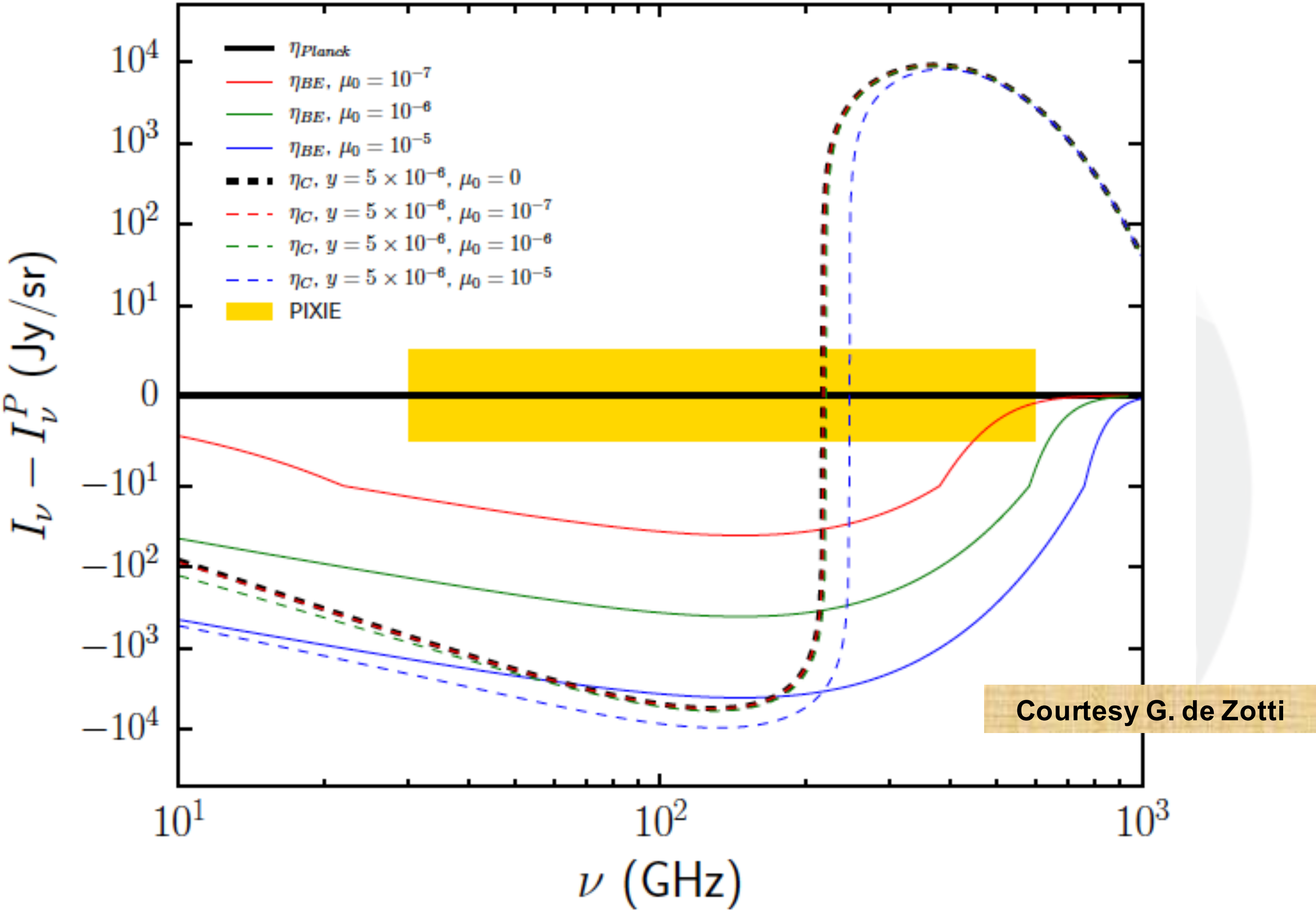
$\eta_{Planck}$
$\eta_{BE},\ \mu_0 = 10^{-7}$
$\eta_{BE},\ \mu_0 = 10^{-6}$
$\eta_{BE},\ \mu_0 = 10^{-5}$
$\eta_C,\ y = 5\times10^{-6},\ \mu_0 = 0$
$\eta_C,\ y = 5\times10^{-6},\ \mu_0 = 10^{-7}$
$\eta_C,\ y = 5\times10^{-6},\ \mu_0 = 10^{-6}$
$\eta_C,\ y = 5\times10^{-6},\ \mu_0 = 10^{-5}$
PIXIE
$10^4$
$10^3$
$10^2$
$10^1$
0
$-10^1$
$-10^2$
$-10^3$
$-10^4$
$I_\nu - I_\nu^P$ (Jy/sr)
$10^1$
$10^2$
$10^3$
$\nu$ (GHz)
Courtesy G. de Zotti

# Dipole spectrum: CMB distortions and CIB

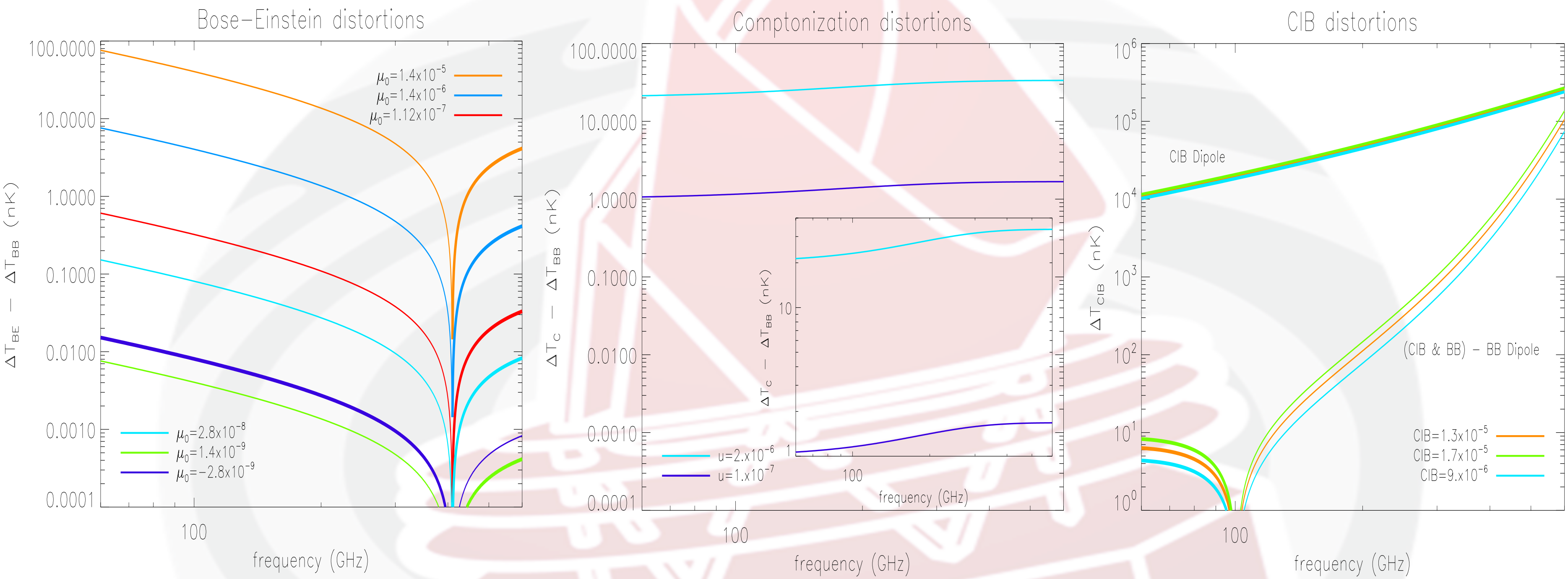


Original idea by Danese & de Zotti 1981;
rediscussed in 2016 by de Zotti et al. and Balashev et al.

Courtesy T. Trombetti & C.B. 2016

- **Without absolute calibration, but with only accurate relative & interfrequency calibration CORE will have the chance to detect CIB & reonization (& others?) distortions through low multipole pattern**

→ **Global & (almost) model independent constraints on energy dissipations**

# From dipole to higher multipoles

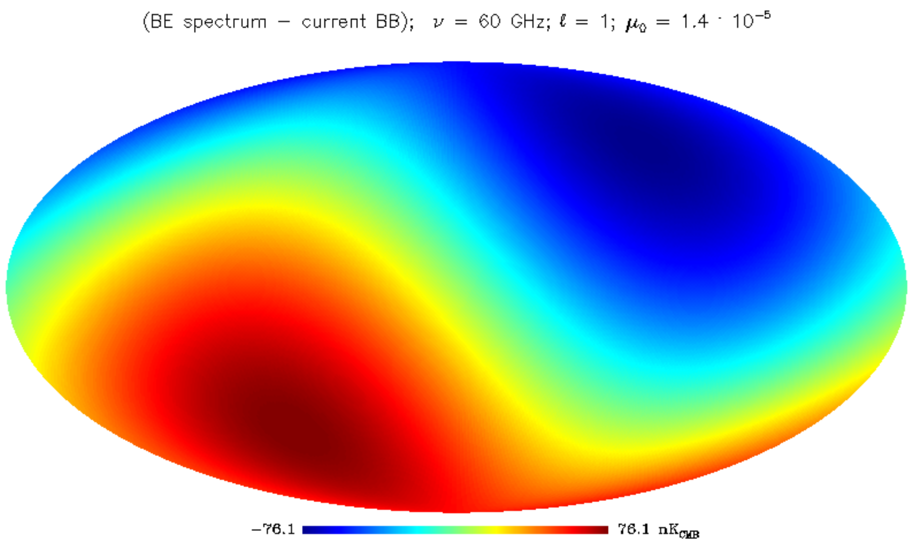


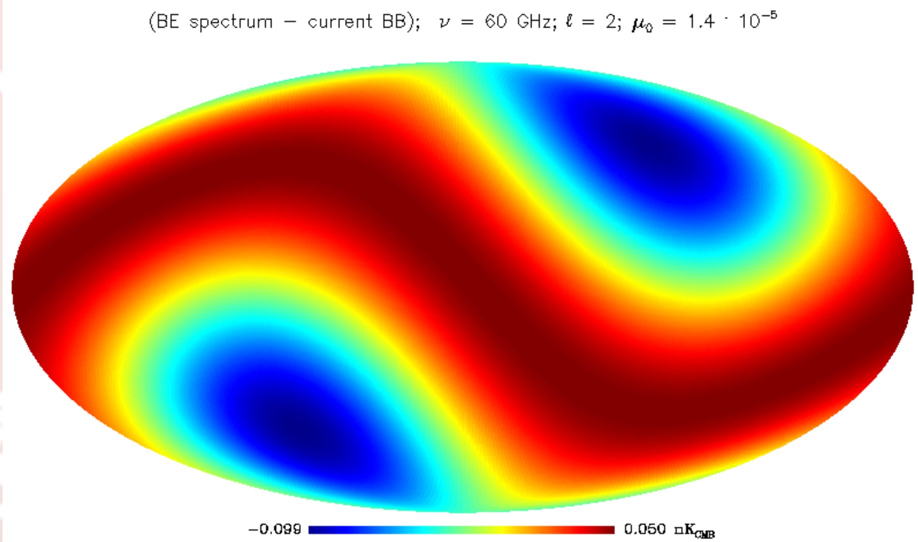


**Courtesy T. Trombetti & C.B. 2016**

**Compute full effect → maps**
**Harmonic expansion →**
**Computations of all multipole components at each frequency for each type of signal**

Great hopes from PIXIE absolute spectrum measurements (Kogut et al. 2011) to constrain (or detect) energy exchanges 1000 times smaller than the FIRAS upper limits

## Angular power spectrum of the dipole map difference between distorted spectra and current blackbody spectrum vs CORE (black) & LiteBIRD (red) white noise power spectrum

From Burigana, Carvalho, Trombetti et al. arXiv:1704.05764

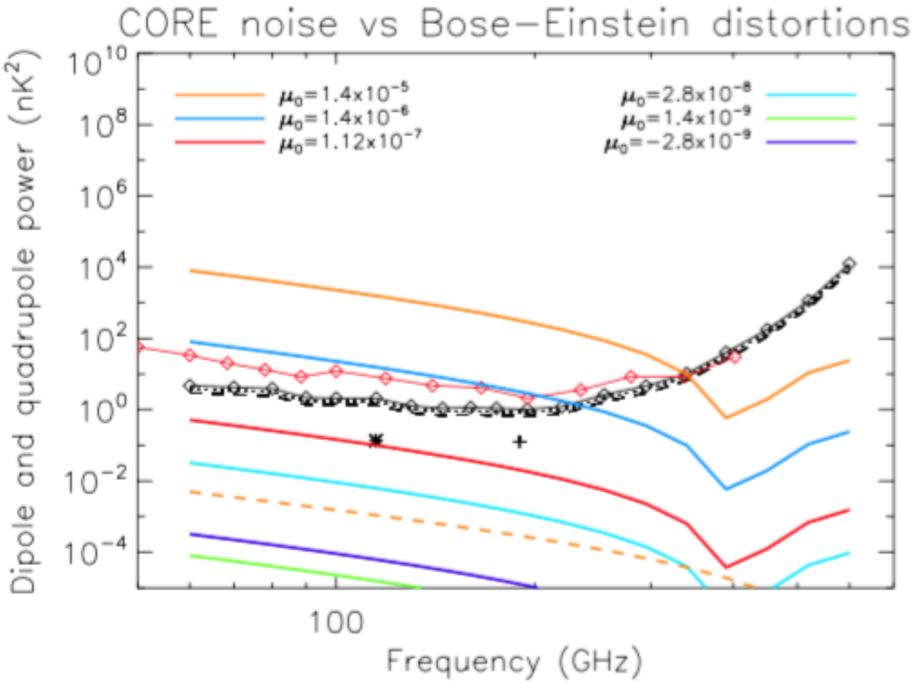


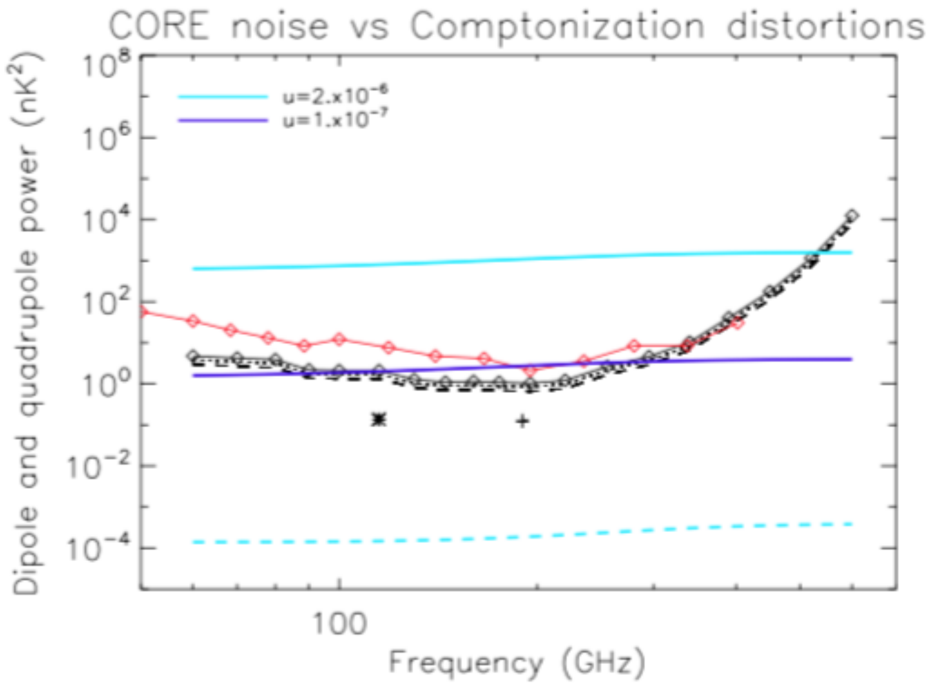

# Recovery dipole amplitude

1 Bose Einstein, 60 GHz, Ns 1024, no noise, no mask, no cal, no sky

**Courtesy G. De Gasperis, A. Buzzelli, N. Vittorio 2016**

**From Burigana, Carvalho, Trombetti et al. arXiv:1704.05764**

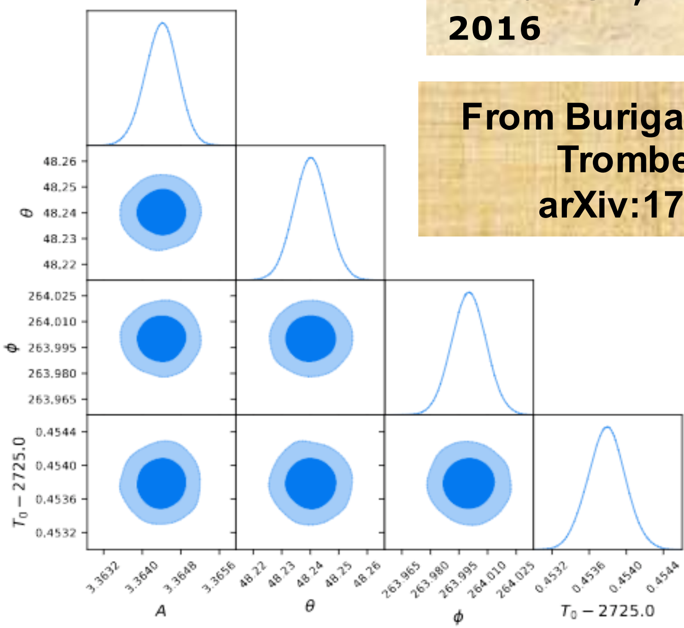


Fig: Likelihoods of the parameters $A$, $\theta$, $\phi$ and $T_0$.

| | $A(mk)$ | $\theta(°)$ | $\phi(°)$ | $T_0(mK)$ |
|---|---|---|---|---|
| 68% CL | $3.36440 \pm 0.00034$ | $48.2402 \pm 0.0059$ | $264.0002 \pm 0.0090$ | $2725.45379 \pm 0.00020$ |
| 95% CL | $3.36440^{+0.00065}_{-0.00068}$ | $48.240^{+0.012}_{-0.012}$ | $264.000^{+0.018}_{-0.018}$ | $2725.45379^{+0.00040}_{-0.00039}$ |
| 99% CL | $3.36440^{+0.00084}_{-0.00089}$ | $48.240^{+0.015}_{-0.016}$ | $264.000^{+0.023}_{-0.023}$ | $2725.45379^{+0.00052}_{-0.00051}$ |

Tab: 68, 95 and 99% confidence level of the parameters $A$, $\theta$, $\phi$ and $T_0$.

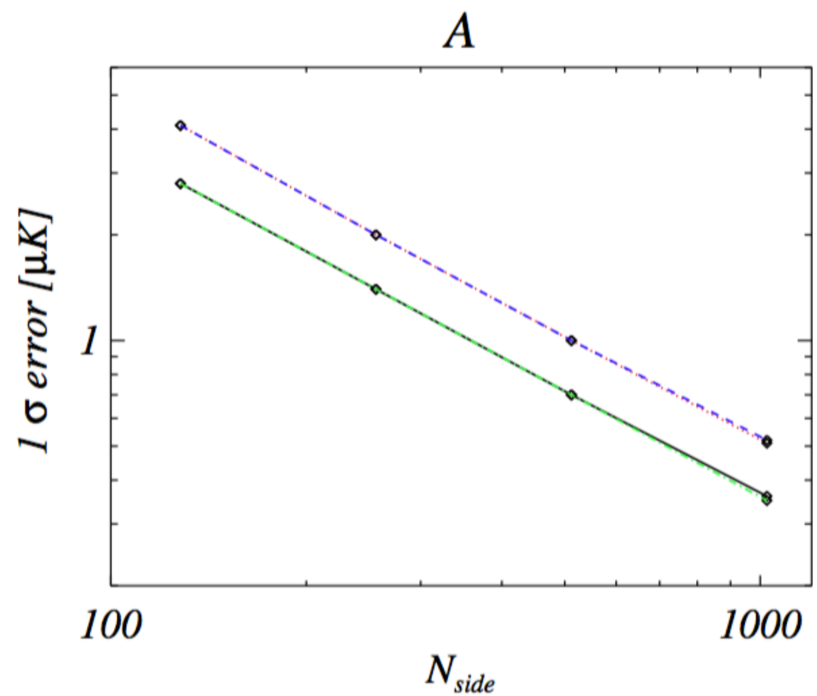


Scaling with sampling of dipole recovery uncertainty

| | $E_{\rm cal}$ (%) | $E_{\rm for}$ (%) | CIB amplitude | Bose-Einstein | Comptonization |
|---|---|---|---|---|---|
| Ideal case, all sky | - | - | $\simeq 4.4 \times 10^3$ | $\simeq 10^3$ | $\simeq 6.0 \times 10^2$ |
| All sky | $10^{-4}$ | $10^{-2}$ | $\simeq 15$ | $\simeq 42$ | $\simeq 18$ |
| P76 | $10^{-4}$ | $10^{-2}$ | $\simeq 19$ | $\simeq 42$ | $\simeq 18$ |
| P76ext | $10^{-2}$ | $10^{-2}$ | $\simeq 17$ | $\sim 4$ | $\sim 2$ |
| P76ext | $10^{-4}$ | $10^{-2}$ | $\boxed{\simeq 22}$ | $\boxed{\simeq 47}$ | $\boxed{\simeq 21}$ |
| P76ext | $10^{-4}$ | $10^{-3}$ | $\boxed{\simeq 2.1 \times 10^2}$ | $\boxed{\simeq 2.4 \times 10^2}$ | $\boxed{\simeq 1.1 \times 10^2}$ |
| P76ext | $10^{-3}_{(\leq 295)}$–$10^{-2}_{(\geq 340)}$ | $10^{-2}$ | $\boxed{\simeq 19}$ | $\boxed{\simeq 26}$ | $\boxed{\simeq 11}$ |
| P76ext | $10^{-3}_{(\leq 295)}$–$10^{-2}_{(\geq 340)}$ | $10^{-3}$ | $\boxed{\simeq 48}$ | $\boxed{\simeq 35}$ | $\boxed{\simeq 15}$ |
| P76ext, $N_{\rm side} = 128$ | $10^{-3}_{(\leq 295)}$–$10^{-2}_{(\geq 340)}$ | $10^{-2}$ | $\simeq 38$ | $\simeq 51$ | $\simeq 23$ |
| P76ext, $N_{\rm side} = 128$ | $10^{-3}_{(\leq 295)}$–$10^{-2}_{(\geq 340)}$ | $10^{-3}$ | $\simeq 43$ | $\simeq 87$ | $\simeq 39$ |
| P76ext, $N_{\rm side} = 256$ | $10^{-3}_{(\leq 295)}$–$10^{-2}_{(\geq 340)}$ | $10^{-2}$ | $\simeq 76$ | $\simeq 98$ | $\simeq 44$ |
| P76ext, $N_{\rm side} = 256$ | $10^{-3}_{(\leq 295)}$–$10^{-2}_{(\geq 340)}$ | $10^{-3}$ | $\simeq 85$ | $\simeq 1.6 \times 10^2$ | $\simeq 73$ |

**Table 11.** Predicted improvement in the recovery of the distortion parameters discussed in the text with respect to FIRAS for different calibration and foreground residual assumptions. This table summarizes the results derived with approach (c). "P06" stands for the *Planck* common mask, while "P06ext" is the extended P06 mask. When not explicitly stated, all values refer to $E_{\rm cal}$ and $E_{\rm for}$ at $N_{\rm side} = 64$.

**From Burigana, Carvalho, Trombetti et al. arXiv:1704.05764**

# Hierarchy of issues vs type of signal

- From a wide set of simulations with different residual levels

→ following hierarchy

| Calibration | Foregrounds |
|---|---|
| Bose-Einstein | CIB |
| Comptonization | Comptonization |
| CIB | Bose-Einstein |

Decreasing relevance

# Free-free distortions from cosmological reionization vs SKA

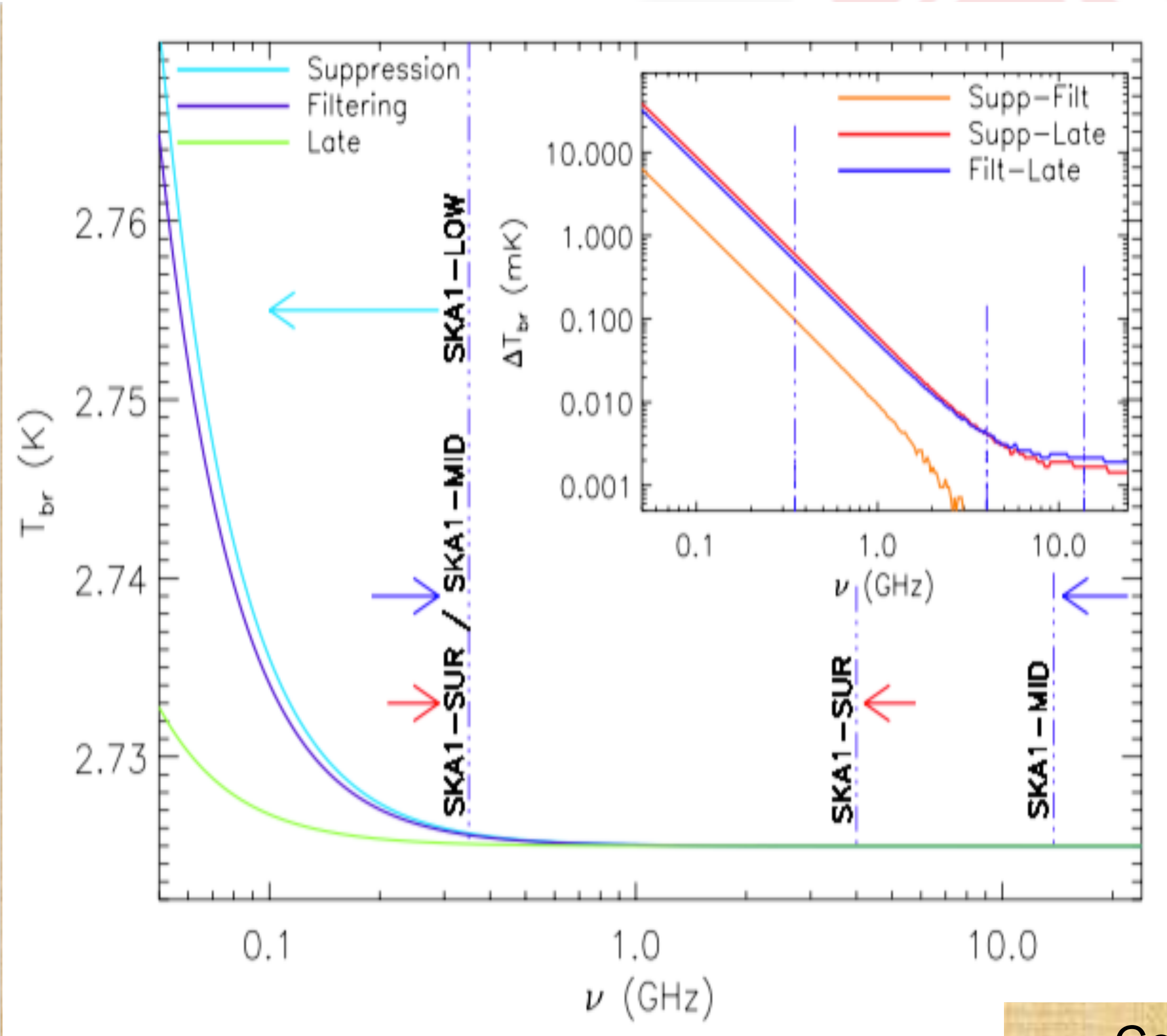


Global distortions

FF produces global & local spectral distortions

$$\frac{T_{br}(x)}{T_r} \simeq \frac{y_B(x)}{x^2} - 2u\phi_i + \phi_i$$

$$u \simeq 1/4(\Delta\varepsilon/\varepsilon_i)$$

Courtesy T. Trombetti 2015

# Radiosource confusion noise – I

To observe tiny CMB sp distortions .... control of Galactic emission & xGal foreground

XGal sources below obs threshold appear as diffuse isotropic radio background

Galaxy not isotropic signal ➧ used spatial separation techniques Gal-CMB

SKA will obs sources down 2 very faint fluxes (few tens nJy) ↠ reduces confusion noise & background

Integrating differential # counts in flux densities ↦ source confusion noise contribution & $T_b$ due 2 background of xGal sources

After removing sources brighter than few tens nJy ↦ $T_b$ is found 2 be ↠

≲ 1 mK @ ν ≳ 1 GHz

≳ 10 mK @ ν ≲ 0.3 GHz

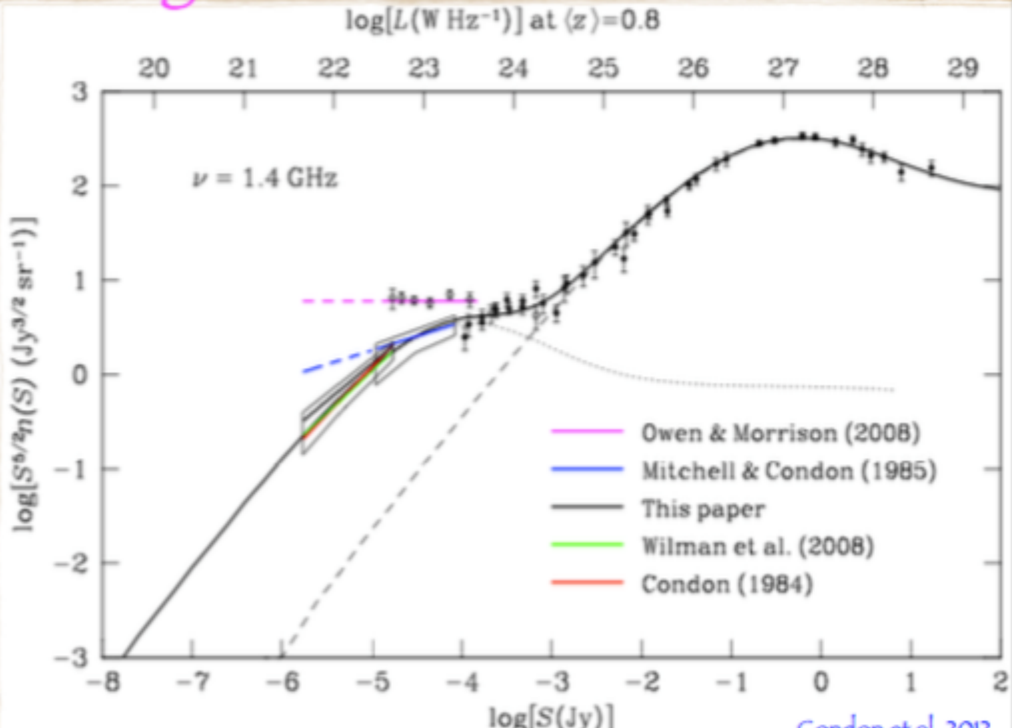


Condon et al. 2012

**Courtesy T. Trombetti 2015**

# Radiosource confusion noise – II

Comparison of source detection threshold from instrumental noise & source confusion noise ⇝ @ 1.4 GHz sky fluctuations due to xGal sources are (Condon et al. 2012)

$$5\sigma_{conf} \simeq 5 \times 1.2(\nu / 3\mathrm{GHz})^{-0.7} (\theta / 8'')^{10/3} \mu\mathrm{Jy}$$

res ~ 1''

Thus ... for deep surveys @ $\nu$ ~ few GHz ...

source confusion noise is not a limit

& ...

@ 1 GHz ≲ $\nu$ ≲ some GHz ($\lambda \approx$ 1 dm)

signal amplitude for CMB distorted spectra

»

background from xGal sources

$\lambda \approx$ 1 dm ⇝ max BE signal & good enough FF signal

@ lower freq source confusion noise too big

↝ GOAL of SKA excellent imaging capabilities

Courtesy T. Trombetti 2015

# Temperatures:[kinetic, CMB, spin (21 cm)]

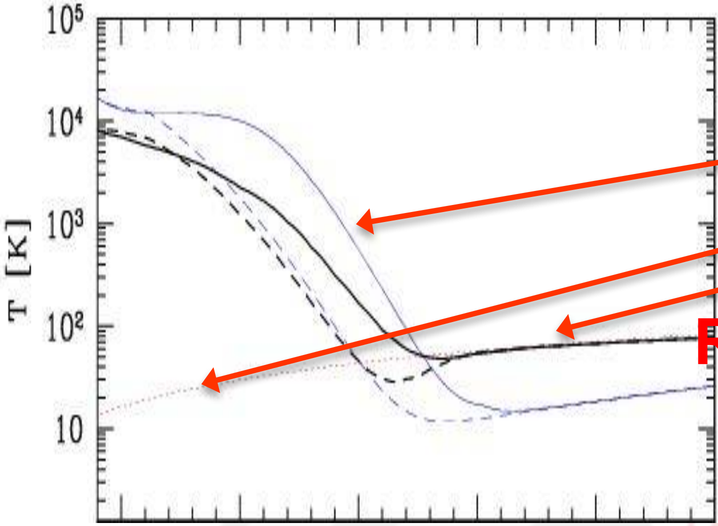


## Reionization: synergy CMB-21cm

**From Schneider et al. 2008, MNRAS, 384, 1525**

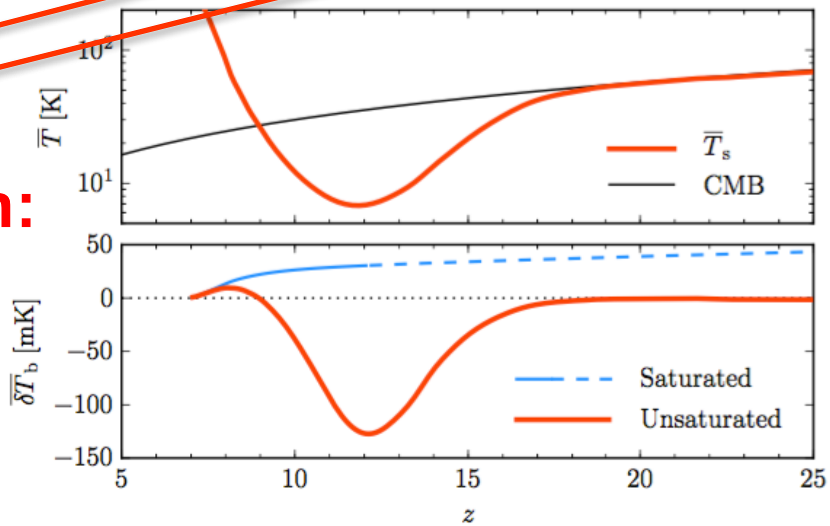


**From Geil et al et al. 2017 (Mesinger et al 2016)**

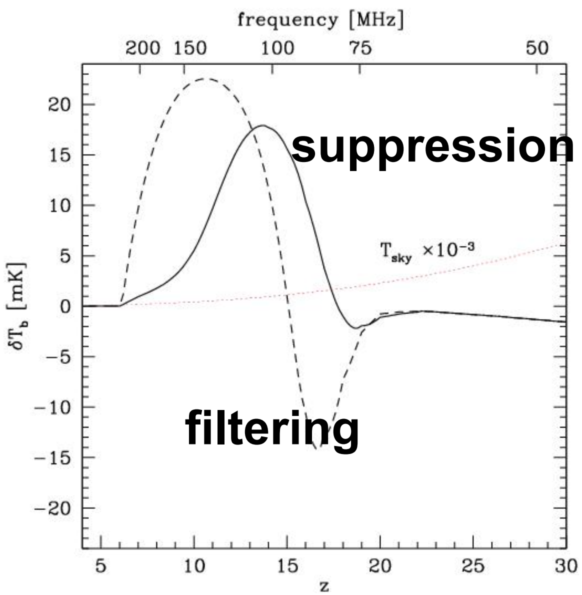


Planck Collaboration: Planck constraints on reionization history

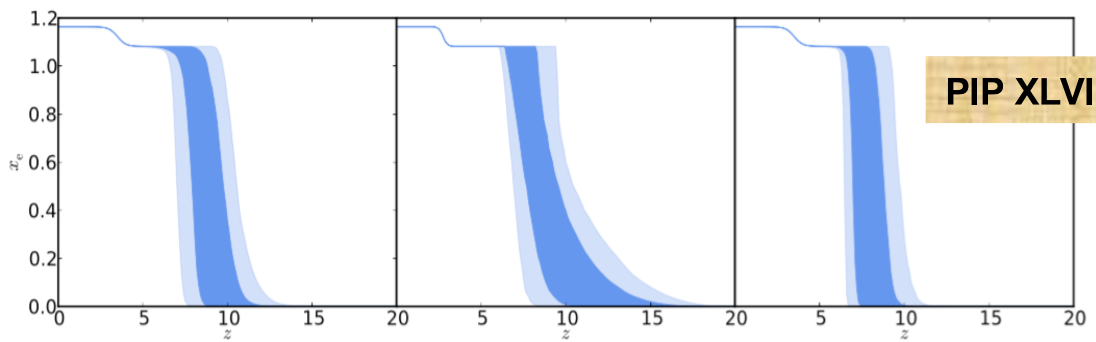


**Fig. 18.** Constraints on ionization fraction during reionization. The allowed models, in terms of $z_{re}$ and $\Delta z$, translate into an allowed region in $x_e(z)$ (68 % and 95 % in dark blue and light blue, respectively), including the $z_{end} > 6$ prior here. *Left*: Constraints from CMB data using a redshift-symmetric function ($x_e(z)$ as a hyperbolic tangent with $\delta z = 0.5$). *Centre*: Constraints from CMB data using a redshift-asymmetric parameterization ($x_e(z)$ as a power law). *Right*: Constraints from CMB data using a redshift-symmetric parameterization with additional constraints from the kSZ effect.

**PIP XLVII, 2016**

**21cm require removal of foreground at a few x $10^{-3}$ level**

# Conclusion - I

- *Planck* legacy will set the scene for many years
- **Time is appropriate for new CMB missions/projects**, from both scientific expertise and technological development
- **CMB science** (“primary” & “secondary”) **essential** for early Universe and cosmic evolution
- **Competition/<u>synergy</u> between ground & space projects**

- **While achieving Higgs/Starobinsky limit ($r \sim 0.004$) is the minimum goal of a future CMB polarization mission …**
- **for “ultimate” polarization mission targeted to *characterize, not only detect* B-modes down to $r \cong 10^{-3}$, or even lower,**
- **other key scietific goals are “automatically” assured**

# Conclusion - II

- Astrophysical foregrounds: ***limitation*** & ***opportunity***

- We need to map & understand them with high accuracy in order to properly extract CMB maps and spectrum
  - This is crucial in polarization and for B-modes for low *r* values
  - This is crucial for spectral distortions

- Microwave sky complexity calls for many frequency channels (e.g. 15 or more in about one decade in frequency, for polarization), related to the global number of foreground parameters

- Spectrum is currently as anisotropy before COBE/DMR
- → A new window!
- Huge synergy with radio observations in particular for reionization

# Conclusion - III

❖ **Legacy science of a future CMB mission potentially immense, e.g.:**

- **all-sky → essential for Galactic studies, extragalactic samples, high-z studies, rare phenomena**
- **polarization: even *Planck* is only at the beginning (ex.: 2 Galactic components, about $10^2$ sources)**
- **products: mapping all Solar System & Galactic components, identify fine features, producing sample of thousands of galaxies**
- **cross-product: "absolute" calibration → legacy data for calibrating ground observations**

# Thanks for the attention!